STRUCTURE AND FUNCTION OF RAT SUPRAOPTIC NUCLEUS NEURONS IN VITRO

by

John C.R. Randle
Department of Physiology
McGill University, Montreal

September, 1985

A thesis submitted to the
Faculty of Graduate Studies and research
McGill University

In partial fulfillment of the requirements for the Degree
of
Doctor of Philosophy

ABSTRACT

Supraoptic nucleus (SON) neurosecretory neurons were examined in perfused explants of rat hypothalamus. Intracellular injections of lucifer yellow revealed ovoid somata, 1-3 unbranched dendrites with numerous spiny processes and a single axon with no obvious collaterals.

SON neurons displayed both spontaneous and electrically-evoked hyperpolarizing, chloride-dependent inhibitory post-synaptic potentials that were reduced by bicuculline (1-100 μM) and prolonged by pentobarbital (100 μM). In 60% of neurons, low concentrations of γ-aminobutyric acid (GABA; 10-100 μM) and muscimol (0.3-3 μM) also induced a chloride-dependent conductance (2-20 nS) and hyperpolarization. At higher drug concentrations, a profound conductance increase was accompanied by a biphasic voltage response. The remaining cells responded only to high concentrations of GABA with a modest conductance increase and membrane depolarization.

At the cellular level, norepinephrine (10-200 μM), acting via α_1-adrenoreceptors, induced bursting activity, membrane depolarization and increased firing. Norepinephrine also stimulated the release of vasopressin and oxytocin into the perfusion medium.

RESUME

Les neurones neurosécréteurs du noyau supraoptique (NSO) ont été étudiés in vitro en utilisant l'hypothalamus perfusé. L'injection intracellulaire de 'lucifer yellow' a révélé la présence de corps cellulaires ovoïdes dont les dendrites (1 à 3 par cellule) se divisent peu et dont l'axone est unique sans collatérale.

Les neurones du NSO génerent des potentiels post-synaptiques inhibiteurs (p.p.s.i.) spontanés ou induits par stimulation électrique. Ces p.p.s.i. requiérent la présence d'ions chlore, sont réduits par la bicuculline (1-100 µM) et prolongés par le pentobarbital (100 µM). L'acide gamma-aminobutyrique (GABA) à faible concentration (10-100 µM) ainsi que le muscimol (0.3-3 µM) induisent une conductance (2-20 nS) dépendante d'ions chlores et une hyperpolarisation chez 60% des cellules étudiées. Des concentrations plus élevées de ces substances donnent lieu à une forte augmentation de la conductance membranaire accompagnée de changements de voltage biphasiques. Les autres cellules ne répondent qu'à de fortes concentrations de GABA, démontrant une faible augmentation de conductance accompagné d'une dépolarisation membranaire.

La noradrénaline (10-200 µM), agissant sur les récepteurs adrénergiques de type 'α_1', induit une dépolarisation membranaire ainsi que des potentiels d'action. La noradrénaline provoque également une forte libération de vasopressine et d'oxytocine.

PUBLICATIONS ORIGINATING FROM THIS RESEARCH

Papers:

Randle, J.C.R., Bourque, C.W. and Renaud, L.P. α-Adrenergic activation of rat hypothalamic supraopt neurons maintained in-vitro. Brain Research 307: 374-378 (1984).

Randle, J.R.C., Bourque, C.W. and Renaud, L.P. Serial reconstruction of supraoptic nucleus neurons in perfused rat hypothalamic explants. Neuroscience, In press.

Day, T.A., Randle, J.C.R. and Renaud, L.P. Opposing alpha- and beta-adrenergic mechanisms mediate dose-dependent actions of noradrenaline on supraoptic vasopressin neurons in vivo. Brain Res, in press.

Bourque, C.W., Randle, J.C.R. and Renaud, L.P. A calcium-dependent potassium conductance in rat supraoptic nucleus neurosecretory neurons. J. Neurophysiol. (in press)

Review Chapters:

Renaud, L.P., Bourque, C.W., Day, T.A., Ferguson, A.V. and Randle, J.C.R. Electrophysiology of mammalian hypothalamic supraoptic and paraventricular neurosecretory cells. in: The Electrophysiology of the Secretory Cell. A.M. Poisner & J. Trifaro (eds.). Elsevier Science Publ. B.V. Amsterdam (1985), pp 165-194.

Renaud, L.P., Day, T.A., Randle, J.C.R. and Bourque, C.W. In vivo and In vitro electrophysiological evidence that central noradrenergic pathways enhance the activity of hypothalamic vasopressinergic neurosecretory cells. In: Vasopressin. R.W.Schrier (ed.) Raven Press, New York (1985). pp. 385-393.

Renaud, L.P., Day, T.A., Randle, J.C.R., Bourque, C.W. and Ferguson, A.V. Characterization of noradrenergic afferents to hypothalamic magnocellular neurons. In: Endocrinology, F. Labrie and L. Proulx (eds). Elsevier Science Publ. B.V., Amsterdam (1984) pp 1015-1019.

Abstracts:

Randle, J.C.R., Bourque, C.W. and Renaud, L.P. Norepinephrine enhances excitability and burst discharges in rat supraoptic neurosecretory neurons maintained in vitro. Proc. Can. Fed. Biol. Soc. 26: 115 (1983).

Randle, J.C.R., Bourque, C.W. and Renaud, L.P. α-adrenergic activation and induction of phasic and bursting activity patterns in hypothalamic supraoptic nucleus neurons recorded in vitro. Soc. Neurosci. Abstr. 9: 1120, (1983).

Bourque, C.W., Day, T.A., Randle, J.C.R. and Renaud, L.P. In vivo and in vitro evidence that noradrenaline activates putative vasopressinergic neurones in the rat supraoptic nucleus. J. Physiol. 345:118P, 1983.

Randle, J.C.R., Bourque, C.W. and Renaud, L.P. A comparison of the effects of norepinephrine and glutamate on electrical properties of neurosecretory neurons of the supraoptic nucleus. Physiology Canada 14: 137, (1984).

Randle, J.C.R., Bourque, C.W. and Renaud, L.P. Complete serial reconstruction of lucifer yellow-filled supraoptic nucleus (SON) neurosecretory neurons. Soc. Neurosci. Abstr. 10: 209, (1984).

Day, T.A., Randle, J.C.R. and Renaud, L.P. Dose-dependent actions of noradrenaline on the activity of putative vasopressin neurons of the supraoptic nucleus. Soc. Neurosci. Abstr. 10: 90, (1984).

Randle, J.C.R., Bourque, C.W. and Renaud, L.P. Calcium-activated potassium conductance in rat supraoptic nucleus neurosecretory neurons. Canad. J. Physiol. Pharmacol. 63: A xxiv-xxv (1985).

Randle, J.C.R., Bourque, C.W. and Renaud, L.P. Spontaneous and evoked IPSPs in rat supraoptic nucleus (SON) neurosecretory neurons in vitro. Proc. Can. Fed. Biol. Soc. 28: 93 (1985).

Randle, J.C.R., Bourque, C.W. and Renaud, L.P. GABA-mediated synaptic inhibition in rat supraoptic nucleus (SON) neurosecretory neurons in vitro. Soc. Neurosci. Abstr. 11, 150 (1985).

Mazurek, M.F., Randle, J.C.R., Kneifel, D. and Renaud, L.P. α-1 adrenoreceptor mediated release of arginine vasopressin (AVP) and oxytocin (OXY) from perfused rat hypothalamo-neurohypophysial explants. Soc. Neurosci. Abstr. 11: 1057, (1985).

"What wisdom can you find
that is greater than
kindness?"

Jean-Jacques Rousseau

(1712-1778)

ACKNOWLEDGEMENTS

The three years working in Dr. Leo P. Renaud's lab were not only stimulating and productive, but also a lot of fun. Dr. Renaud has been an encouraging and cheerful supervisor and an expert mentor. Thanks Leo! Very special thanks to Dr. Charles Bourque who not only taught me many of the techniques used in this work, but is a good friend and correspondent. Thanks also to Jean Dufresne, Dorli Knieffel, and François Grondin who contributed tremendously to the hormone release studies, to Dr. Mike Mazurek who performed the radioimmunoassays, to Serge Lafontaine who coordinated the computer services, to Joanne Rogers for her electron micrographs, to Arlene Berg and Gwen Peard for their help in typing this thesis, and to Dr. Sue Keirstead for her efforts. Also, I wish to thank the F.R.S.Q. for their support.

And thank you Andrea, for the enormous amount of effort that you put into preparing this thesis, for all the sunshine that you missed ... and for kindness, given and received.

TABLE OF CONTENTS

PAGE

PAGE

ABBREVIATIONS

BMI	bicuculline methiodide
E_{EPSP}	equilibrium potential of the EPSP
$E_{IPSP\ (e,s)}$	equilibrium potential of the IPSP (evoked, spontaneous)
EPSP	excitatory post-synaptic potential
ΔG	change in input conductance
GABA	γ-aminobutyric acid
G_{in}	input conductance
$G_{IPSP\ (e,s)}$	change of input conductance associated with IPSP (evoked or spontaneous)
G_{TOT}	input conductance during IPSP or drug response
IPSP	inhibitory post-synaptic potential
LY	lucifer yellow
MOXY	methoxamine
NE	norepinephrine
PHE	phenylephrine
PHEN	phentolamine
PHOXY	phenoxybenzamine
PSP	post-synaptic potential
PVN	paraventricular nucleus
R_{in}	input resistance
R_{TOT}	input resistance during IPSP or drug response
SON	supraoptic nucleus

CHAPTER 1

INTRODUCTION

1.1 Preface

Neurophysiologists interested in the mammalian central nervous system are accustomed to relying on data from "model systems" for an understanding of the fundamental properties governing the excitability of neurons. Over the past 50 years, the giant axon (e.g. Hodgkin and Huxley, 1952a,b,c) and synapse (Katz and Miledi, 1967a,b,1968) of the squid, the neuromuscular junction (Katz and Miledi, 1965), spinal motoneurons (Eccles, 1961; Rall, 1959,1960) and various giant ganglion neurons of mollusks and crustaceans (see Kandel, 1976) have yielded information vital to conceptual and technological advances in neurobiology. Although, findings from these systems were sometimes not generally applicable to the central nervous systems of mammals, they did expedite the exploration of other, less accessible systems. However, technical advances of the past decade have permitted access to the central nervous system for more direct and detailed electrophysiological investigation. In particular, *in vitro* techniques have provided a means to obtain stable intracellular recordings from spinal neurons in culture (Barker and Ransom, 1978), autonomic ganglia cells in explants (Adams and Brown, 1975; McAfee and

Yarowsky, 1979), and a variety of neuronal types in brain slices (Hillman et al., 1963; Yamamoto and McIlwain, 1966).

For more than 20 years, the magnocellular neurosecretory neurons of the hypothalamic supraoptic nucleus (SON) and paraventricular nucleus (PVN) have been the subject of intense electrophysiological investigation. Owing to their location deep in the brain and adjacent to major blood vessels, most of the earlier data was derived from extracellular recording in vivo (see review by Poulain and Wakerley, 1982). However, in vitro slice and explant techniques, perfected in the past five years (Brimble et al., 1978; Haller et al., 1978; Hatton et al., 1978; Bourque and Renaud, 1983) have permitted more detailed analysis of the electrophysiological properties of these neurosecretory neurons by intracellular recording (cf. Mason, 1980; Andrew and Dudek, 1984a,b; Bourque and Renaud, 1985a,b).

SON and PVN magnocellular neurosecretory neurons synthesize either of the hormones vasopressin or oxytocin which they secrete from axon terminals in the neurohypophysis. As neurosecretory neurons, they occupy a middle ground between central nervous system neurons, whose processes and secretions are restricted to the brain, and endocrine cells which are located in many (if not all) parts of the body, and whose secretions often have actions throughout the body. They can be considered as autonomic motoneurones whose neurotransmitter acts through the

bloodstream rather than across a synaptic cleft. Alternatively, they can be considered as unusual endocrine cells that are located in the brain and have a morphology typical of neurons.

While these properties are true of many neurosecretory cells, the compactly arranged and relatively homogeneous SON neurosecretory neurons (see Section 1.2.1) are most amenable to both biochemical and electrophysiological experimentation. As a result, vasopressin was the first peptide hormone whose amino acid sequence was elucidated (du Vigneaud, 1954) and much is known about the processes governing its biosynthesis, intracellular packaging, transport and, ultimately, secretion (Section 1.3). Electrophysiological studies *in vivo* have characterized the electrical activity patterns that are associated with autonomic reflexes governing the release of vasopressin and oxytocin (Section 1.4.1). Intracellular recordings obtained from SON neurons maintained *in vitro* have revealed many of the membrane properties responsible for their characteristic firing patterns (Section 1.4.2). *In vitro* studies of the release of vasopressin from isolated neural lobes were seminal to the theory of stimulus-secretion coupling (Section 1.4.3). The great value of the SON neurosecretory neurons as a model system for CNS neurons is, therefore, the comparative ease with which all levels of their cellular function can be studied.

1.2 The Supraoptic Nucleus (SON) of the hypothalamus

1.2.1 Organization of the rat SON.

The supraoptic nuclei (SON) of the rat are well-defined elongated groupings of magnocellular neurons located on the ventral surface of the brain along the lateral borders of the optic tract. The SON is filled with an extensive network of capillaries (Finley, 1939) from branches of the anterior and retrochiasmatic arteries, which penetrate the hypothalamus, and also supply several "accessory" nuclei composed of neurosecretory neurons (Vandesande & Dierickx, 1975; Sherlock et al., 1975; Sofroniew and Glassman, 1981).

In Nissl preparations, the SON appears as a dense aggregation of between 5,000-10,000 homogeneous intensely stained cells (Leranth et al., 1975). In the rat, a rostrocaudal progression in their morphology is revealed in serial coronal sections (see Armstrong et al., 1982). Rostrally, the SON forms a thin layer of cells on the ventral surface of the brain. Medially, the SON profile is triangular as SON neurons line the entire lateral edge of the optic tract. Caudally, where the optic tract penetrates the temporal lobe, SON neurons form a narrow vertically oriented band of cells lining its lateral border. An additional group of neurosecretory neurons located caudal and medial to the optic tract forms the retrochiasmatic portion of the SON (Sherlock et al., 1975).

Following injection into the neurohypophysis, retrogradely transported horseradish peroxidase (HRP) reaction product is evident in almost all SON neurons (Sherlock, 1975). Similarly, most (greater than 85%) SON neurons are immunoreactive for vasopressin or oxytocin and their associated neurophysins (Vandesande and Dierickx, 1975; Swaab et al., 1975; and section 1.3). Only a small number of non-neurosecretory neurons have been observed within the confines of the nucleus (Dyball and Kemplay, 1980). Leranth et al. (1975) estimate that interneurons account for approximately 6-7% of neurons in the SON.

At the electron microscope level, glia are seen to be interposed between the somata and dendrites of neurosecretory neurons, particularly in the "ventral glial lamina" (VGL). The VGL lines the ventral surface of the SON and is composed of glial cells surrounding the dendrites of SON neurons and axons afferent to the SON (Armstrong et al. 1981; McNeill and Sladek, 1980; Sofroniew and Glassman, 1981). These glia show a great deal of plasticity related to the functional state (i.e. parturition, lactating, dehydrated) of the animal (Perlmutter et al., 1984).

1.2.2 SON neurosecretory neuron morphology and ultrastructure

SON neurosecretory neurons are apparently resistant to silver impregnation (LuQui and Fox, 1976), thus few studies

of their morphology have used the Golgi technique (Leontovich, 1969; LuQui and Fox, 1976; Felten and Cashner, 1979; Armstrong et al., 1982; Dyball and Kemplay, 1982). Immunocytochemistry performed on thick sections of hypothalamus now provide a more reliable means of staining SON neurons and has contributed tremendously to our knowledge of their light microscopic morphology (Armstrong et al., 1982; Sofroniew and Glassmann, 1981; Silverman et al., 1980). There are a comparatively large number of electron microscopic studies (e.g. Rechardt, 1969; Ifft and McCarthy 1974; Tweedle et al., 1977; Armstrong et al., 1982; Yulis et al., 1984) of SON neuronal ultrastructure and interrelations.

The somata of rat SON neurons are round or elongated, with dimensions of approximately 15 x 20-30 μm (Dyball and Kemplay, 1982) and give rise to 1-3 ventrally directed dendrites (Armstrong et al., 1982; Dyball and Kemplay, 1982). The somata contain a large, eccentrally located nucleus with one or more nucleoli (Rechardt, 1969). The cytoplasm is typical of secretory cells in that it contains mitochondria and stacks of rough endoplasmic reticulum, golgi apparatus and dense-core vesicles.

The dendrites of SON neurons are irregular in diameter

(<2 μm) and taper gradually. They branch sparingly but possess spines (Silverman et al., 1980; Armstrong et al., 1982; Felten and Cashner, 1979; Dyball and Kemplay, 1982) which form synaptic contacts (Ifft and McCarthy, 1974). Many dendrites of SON neurons course extensively in the ventral glial lamina (Armstrong et al., 1982) where they are enveloped by glial processes (Perlmutter et al., 1984, Yulis et al., 1984).

The axons of SON neurons are beaded in appearance due to numerous rounded enlargments or varicosities (Sofroniew and Glasmann, 1981). They course dorsally from the nucleus and then into the basal hypothalamus to form the supraoptico-neurohypophysial tract (cf. Luqui and Fox, 1976). Axons of SON neurons proceed to the internal zone of the median eminence and, infundibular stalk and terminate as large granule-filled dilatations (cf. Pickering, 1978) throughout the neurohypophysis (Vandesande and Dierickx, 1975; Alonso and Assenmacher, 1981). Although axon collaterals have been reported in the region dorsal to the SON (Mason et al., 1984) other studies suggest that they are infrequent (Sofroniew and Glasmann, 1981; Dyball and Kemplay, 1982; Armstrong et al., 1982).

1.2.3 Immunohistochemical localization of peptide hormones in SON neurons

Immunohistochemical staining for vasopressin and oxytocin provided the first direct proof that the SON contains separate populations of neurons that synthesize the two peptides (Vandesande and Dierickx, 1975; Swaab et al., 1975; Sokol et al., 1976). In the rat, a spatial segregation exists such that oxytocin neurons are more numerous in rostral and dorsal parts of the SON and vasopressin neurons are more numerous caudally and ventrally (Vandesande and Dierickx, 1975; McNeill and Sladek, 1982).

Several other peptides have been observed histochemically in SON neurosecretory neurons. The opioid peptide dynorphin co-exists in vasopressin neurons (Watson et al., 1982a,b; Weber et al., 1982). Leu-enkephalin (Martin and Voigt, 1981) and α-neo-endorphin (Ito et al., 1981; Millan et al., 1983) are found in vasopressin terminals in the neurohypophysis as is met-enkephalin in oxytocin terminals (Martin et al., 1983; Martin and Voigt, 1981). Corticotropin-releasing factor (CRF) (Sawchenko et al., 1984) and cholecystokinin (Martin et al., 1983) are also found in some oxytocin neurons of the SON. The function of these peptides is still unknown but evidence is accumlating that the opioid peptides may modulate the release of oxytocin and vasopressin (Bicknell et al., 1985; Clarke et al., 1979; Iversen et al., 1980).

1.2.4 Synapses and afferent fibers in the SON

Quantitative electron microscopical studies by Leranth et al. (1975) revealed that each SON neuron receives approximately 600 synapses distributed on its soma, dendrites, dendritic spines and axon. Remarkably, only 30% of these synapses are sensitive to lesions or knife cuts that isolate the SON from surrounding tissues, indicating that the remaining 70% of synapses arise from cells located within or near the SON (Leranth et al., 1975; Zaborsky et al., 1975). Contacts between neurosecretory cells account for a portion of the intranuclear synapses (cf. Theodosis, 1985). The small number of putative interneurons present in the SON likely account for another portion although Leranth et al. (1975) have calculated that each of these neurons would be required to form 6000 synapses if they alone are to account for all the synapses of intranuclear origin. Therefore, a more reasonable proposal is that neurons located adjacent to the SON contribute a prominent portion of their afferent innervation.

γ-Aminobutyric acid (GABA): The SON and adjacent structures contain a plexus of GABAergic fibers (Perez de la Mora et al., 1981) that make synaptic contacts with SON neurons (Tappaz et al., 1982). Lesion studies indicate that approximately 60% of this GABA innervation is of local origin (Meyer et al., 1980). Neurons containing glutamate

decarboxylase (GAD) and GABA-transaminase (GABA-T), the GABA synthesizing and metabolizing enzymes, respectively, are located around the periphery of the SON (Tappaz et al., 1982) and in the lateral hypothalamus and substantia inominata, structures dorsal to the SON (Nagai et al., 1983) However, the remaining GABA innervation is thought to originate in the region anterior to the third ventrical (Meyer et al., 1980). The diagonal band of Broca and lateral septum both contain many GABA neurons (Nagai et al., 1983; Pannula et al., 1984) and are possible sources of this innervation.

This hypothesis is supported by lesion (Carithers et al., 1980; Powell and Rorie, 1967; Zaborsky et al., 1975) and retrograde HRP tracing studies (Oldfield et al., 1985; Tribollet et al., 1985) which suggest that the neurons in the diagonal band of Broca and the septum project to the SON or nearby structures. However, these studies indicate that septal projections terminate dorsal to the SON and may contact interneurons which, in turn, innervate SON neurons (Tribollet et al., 1985). Nevertheless, these fibers also form synapses with dorsally directed processes (possibly axons) of SON neurons (Oldfield et al., 1985). Unfortunately, the identity of the transmitter contained in these terminals has not been ascertained.

Norepinephrine: Early histofluorescence studies showed that the SON contains one of the most dense catecholaminergic

innervations in the brain (Carlsson et al., 1962) which is primarily noradrenergic (Palkovits et al., 1974) and originates in the A1 cell group of the ventrolateral medulla (Sawchenko and Swanson, 1981). The nucleus of the tractus solitarius and locus ceruleus contribute only a small number of noradrenergic fibers to the SON (Sawchenko and Swanson, 1982; Jones and Moore, 1977). The noradrenergic plexus is most dense ventrally and is thus in closest contact with vasopressin-containing SON neurons (McNeill and Sladek, 1980). Large numbers of axo-dendritic noradrenergic contacts have been identified in the ventral glial lamina underlying the SON although a lesser number of axosomatic contacts occur throughout the nucleus (Alonso and Assenmacher, 1984; McNeill and Sladek, 1980). Thus, the ventrally directed dendrites of SON neurons appear to be critical to the cell's contact with the noradrenergic innervation (Sawchenko and Swanson, 1982; Alonso and Assenmacher, 1984).

Acetylcholine: Deafferentiation of the SON has little effect on its content of choline acetyltransferase, a specific marker for cholinergic neurons (Meyer and Brownstein, 1980). Thus, as with GABA, the cholinergic innervation of the SON appears to originate locally. Mason et al. (1983) used immunocytochemical and histochemical techniques to identify a diffuse group of cholinergic

neurons dorsolateral to the SON whose processes enter the nucleus and appear to be responsible for its cholinergic innervation.

Other Brain Regions: A number of other brain regions contribute afferents to the SON. Neurons of the subfornical organ which project heavily to the SON (Miselis et al., 1979; Lind et al., 1980; Renaud et al., 1983; Tribollet et al., 1985) may contain angiotensin II (Lind et al., 1984).

A projection from the amygdala (Zaborsky et al., 1975) probably terminates primarily dorsal to the SON (Tribollet et al., 1985; Oldfield et al., 1985). Although this input is reported to be inhibitory (see section 1.4.3) the transmitter mediating this effect is unknown at present.

1.3 Synthesis, Processing, Transport and Secretion of Vasopressin and Oxytocin

Since du Vigneaud (1956) deduced the primary structure of the cyclic neuropeptide vasopressin, the neurohypophysial hormones have been a model system for the study of the synthesis, processing, transport and secretion of peptide hormones (see reviews by Brownstein 1980; Pickering, 1978; Pickering et al., 1983). Vasopressin and oxytocin can be studied with relative ease because large amounts of the hormones that are synthesized and secreted and the sites of synthesis, transport and secretion are physically separated.

1.3.1 Synthesis and Processing of Vasopressin and Oxytocin

Sachs and coworkers were the first to suggest that vasopressin and the associated protein, neurophysin, are synthesized from a high molecular weight precursor (see Sachs et al., 1969). Ultimate proof of this theory was obtained recently when the sequence of a complimentary DNA (cDNA) for messenger RNA coding for vasopressin was determined (Land et al., 1982). The primary sequence of "pre-provasopressin-neurophysin" was deduced from the cDNA sequence and revealed that the precursor contains (in order from N- to C-terminus) a signal peptide, vasopressin, neurophysin, and a glycoprotein. Similarly, Land et al. (1983) determined the primary structure of pre-prooxytocin-neurophysin and showed that it is homologous to pre-provaso-

pressin-neurophysin except for the absence of a glycoprotein from the C-terminus.

The pre-prohormones are processed to their respective hormones by removal of the N-terminal signal peptide and, in the case of vasopressin, the C-terminal glycoprotein. Thus pro-oxytocin-neurophysin and pro-vasopressin-neurophysin are composed of oxytocin and vasopressin attached to their respective neurophysin by the tripeptide glycine-lysine-arginine (Land et al., 1982,1983). The paired basic amino acids serve as a site for the enzymatic cleavage of the prohormones. The remaining C-terminal glycine probably donates its amino group in the C-terminal amidation of vasopressin and oxytocin (Land et al., 1983). Finally, a disulfide linkage forms between cysteine residues in positions 1 and 6 of both hormones (cf. du Vigneaud, 1956) to form the characteristic 6-amino acid ring structure.

1.3.2 Transport of Vasopressin and Oxytocin

Information concerning the sites of synthesis and processing of vasopressin and oxytocin has been obtained in pulse-chase experiments. ^{35}S-cysteine or ^{35}S-methionine injected near the SON was rapidly incorporated into proteins by neurosecretory cells. Following synthesis on ribosomes in the somata of SON neurons, the prohormones are packaged in granules and transported to the neurohypophysis (See

Brownstein et al., 1980). Radioactivity associated with vasopressin is present in the neurohypophysis within 1½ hours of injection in the SON (Sachs et al., 1969; Heap et al., 1974). This indicates that the granules are conducted over the 3 mm distance by fast axonal transport at a rate estimated to be greater than 200 mm/day (Brownstein et al., 1980).

Radioactivity found in the neurohypophysis within several hours of injection of tritiated amino acids into the SON is mostly associated with large molecular weight proteins, probably the precursors of vasopressin and oxytocin (Brownstein et al., 1980). These radioactive protein species disappear over several days until most of the radioactivity can be associated with vasopressin, oxytocin and their neurophysins. Since autoradiographic studies confirm that this radioactivity is confined to secretory granules (Kent and Williams, 1974) Brownstein et al. (1980) concluded that the granules must contain, not only the hormones bound to their neurophysins, but also the enzymes and other factors necessary for their processing. Thus, processing of the hormone precursors appears to occur during and following axonal transportation from the SON to the neurohypophysis.

Heap et al. (1975) traced the progress of radiolabelled neurosecretory granules through the neurohypophysis using autoradiography. Labelled neurosecretory granules were

observed in three sites: 1) axons, 2) small axonal dilatations, in which small granules were present, termed "endings" and 3) larger dilatations in which large granules were present, termed "swellings" and resembled Herring bodies (Herring, 1908). Based upon the time-course of their appearance at, and disappearance from each site, Heap et al. (1975) concluded that granules containing newly-synthesized material proceed from axons to "endings" and thereafter to "swellings". The possible significance of these data is discussed below (Chapter 1.3.3) as it applies to secretion of newly synthesized hormone.

1.3.3 Secretion of Vasopressin and Oxytocin

Experiments with isolated neurohypophysis *in vitro* (Douglas, 1963; Douglas and Poisner, 1964) were important to the formulation of the theory of stimulus-secretion coupling (see Douglas, 1968). According to this theory, vasopressin and oxytocin are released in response to calcium flux into nerve terminals provoked by membrane depolarization. Experimentally, depolarization was induced by electrical stimulation of the isolated glands or exposure to medium containing an elevated concentration of potassium. *In vivo*, depolarization is presumed to be due to invasion of the neurohypophysial terminals by action potentials generated in the somata of SON neurons. The correlation between electrical activity of neurosecretory neurons and secretion

of vasopressin and oxytocin supports this hypothesis (see Poulain and Wakerley, 1982) and Section 1.4.4).

Secretion of neurophypophysial hormones is thought to occur by exocytosis (See review by Pickering, 1978). Thus, according to the scheme of Palade (1975), secretory granules fuse with the plasma membrane and discharge their contents into the extracellular space where it eventually enters the portal circulation. Details of the mechanism of exocytosis are lacking. For example, the role of calcium in this process, although critical, is still obscure.

Several interesting observations have been made concerning the "pools" of vasopressin available for release. Experiments performed both in vivo and in vitro showed that high levels of release of vasopressin are not maintained or repeatable (Sachs et al., 1967; Sachs and Haller, 1968; Thorn, 1966; Ingram et al., 1982). The release of oxytocin may undergo a lesser degree of "fatigue" (Bicknell et al., 1984). Sachs and Haller (1968) proposed the existence of a readily "releasable pool" of vasopressin which comprises no more than 10-20% of the total content of the neurophypophysis. It might be separated from "unreleasable" vasopressin either: 1) morphologically in different dilations, 2) extragranularly as opposed to intragranularly, or 3) within active as opposed to inactive neurons. No evidence is available to support the latter possibility.

The second possibility is unlikely in view of evidence supporting exocytotic release of vasopressin (see above). An argument in support of the first hypothesis can be formulated based upon studies that show that newly-synthesized vasopressin is preferentially released by neurohypophyses in vitro (Sachs and Haller, 1968; Nordmann and Labouesse, 1981). Taken together, this physiological evidence and the morphological data of Heap et al. (1975) suggest that newly synthesized vasopressin contained in granules is briefly available for release from terminals before being transported to swellings for storage. However, failure of the calcium signal, either through reduction of its influx or its intracellular effects, could also account for the fatigue of vasopressin release (See consideration in Section 1.4.4).

1.4 Electrophysiology of SON neurons

Kandel (1964) demonstrated that neurosecretory neurons have electrical properties similar to other central nervous system neurons in his studies of the preoptic nucleus of teleost fish. Following confirmation of this finding in mammals (Yagi et al., 1966; Ishikawa et al., 1966) the electrical activity of mammalian neurosecretory neurons became a subject of intense investigation (see reviews by Poulain and Wakerley, 1982; Renaud et al., 1985). These studies have provided information which now allows identification of SON neurons according to their firing patterns, both spontaneous and stimulus or reflex-evoked (Section 1.4.1 and 1.4.3). Intracellular recordings provide insight into the membrane properties of SON neurons responsible for generation of these characteristic firing patterns (Section 1.4.2) and their relevance to secretion of hormones (Section 1.4.4).

1.4.1 Identification of SON neurosecretory neurons

Antidromic activation: The axons of SON neurons project uniformly to the neurohypophysis (Section 1.2). Yagi et al. (1966) showed that antidromically conducted action potentials can be recorded in the mammalian SON following electrical stimulation of the neurohypophysis. This procedure has since been used routinely to identify SON neurosecretory neurons during electrical recordings (eg.

Dyball and Koizumi, 1969; Yamashita et al., 1970; Poulain et al., 1980; Armstrong and Sladek, 1982; Bourque and Renaud, 1983; Day and Renaud, 1984; Barker et al., 1971; Harris, 1979; Koizumi and Yamashita, 1972; Wakerley et al., 1975). Three criteria verify the antidromic nature of the evoked action potential: 1) all-or-nothing, constant latency spike, which 2) follows high frequency (larger than 100 Hz) stimulation, and is 3) cancelled by 'collision' with a spontaneous orthodromic action potential (See detailed explanation in Poulain and Wakerley, 1982). Latencies for somatic invasion of the antidromic spike are typically 8-20 msec indicating that SON neuron axons have conduction velocities of approximately 0.5-1 m/sec (Yagi et al., 1966; Yamashita et al., 1970; Koizumi and Yamashita, 1972).

Intracellular Injection of Marker Dye: During intracellular recordings from SON neurons in vitro in brain slices or explants, antidromic activation is often impractical. Although in vitro recording systems ease visual positioning of micro-pipettes in the SON (Andrew et al., 1981; Bourque, 1984) confirmation of recording sites by intracellular injection of a marker dye (cf. Thomas and Wilson, 1966) is essential. Several groups (Andrew et al., 1981; Reaves et al., 1982; Yamashita et al., 1983; Bourque, 1984) have accomplished this using the fluorescent naphthalimide dye, lucifer yellow introduced by Stewart

(1978). Histological examination of the lucifer yellow-filled SON neuron not only confirms its identity but opens the experimental avenues discussed below.

Spontaneous Action Potential Firing Patterns: SON neurons identified by antidromic activation demonstrate three broadly-defined catagories of spontaneous activity patterns (Poulain et al., 1977; Wakerley et al., 1978):

1) slow, irregular - characterized by low mean firing rate (0-3 spikes/sec) and frequent silent periods,
2) fast, continuous - characterized by uninterrupted firing at a mean rate of 3-15 spikes/sec, and
3) phasic - described in the rat by Wakerley and Lincoln (1971) and characterized by alternating 10-90 sec periods of action potential firing ($\geq$5 Hz) and quiescence.

Individual neurons sometimes exhibit more than one of these firing patterns during prolonged recording sessions, particularly during responses to some of the manipulations to be described below. Nevertheless, the pattern of firing is an indication of the hormone content of the neuron and the rate of release of that hormone (Section 1.4.4).

Autonomic reflexes and the identification of vasopressin and oxytocin neurons: The release of oxytocin and vasopressin is governed by autonomic reflexes. Most notably, suckling leads to oxytocin release and milk

ejection (Lincoln and Wakerley; 1974, 1975) and vasopressin release is closely regulated by plasma osmolality and blood volume (Dunn et al., 1973). Since vasopressin and oxytocin are contained in separate neurons in the SON (Vandesande and Digrickx, 1975; Swaab et al., 1975) it was anticipated that these populations of neurons would respond differently during autonomic reflexes.

Lincoln and Wakerley (1974, 1975) showed that about half of SON neurons fire a synchronous, high frequency burst of action potentials 10-15 seconds before milk ejection. The spontaneous activity pattern of these neurons was usually "continuous" or "slow, irregular" prior to the burst: "phasic" neurons rarely fired a burst prior to milk ejection. Therefore "phasic" neurons were deemed to be vasopressin-secreting while continuously firing cells were likely to be oxytocin-secreting.

This relationship was affirmed by experiments that tested the responses of "continuous" and "phasic" SON neurons to manipulations known to alter vasopressin secretion. Thus, hemorrhage increased the firing of "phasic" SON neurons (Wakerley et al., 1975) while baro-receptor activation (increased blood pressure) abruptly halted firing of SON neurons (Yamashita, 1977; Kannan and Yagi, 1978) an effect reported to be restricted to "phasic" neurons (Harris, 1979). Responses to changes in plasma osmolality were not restricted to one category of SON

neuron (Brimble and Dyball, 1977).

Conclusive proof that "phasic" SON neurons contain vasopressin could best be obtained by coupling intracellular recording of phasic activity followed by injection of lucifer yellow (see above) with immunocytochemical staining for vasopressin and oxytocin. Studies using this approach confirmed that most phasic SON neurons are immunoreactive for vasopressin but not oxytocin (Yamashita et al., 1983). However, 30% of phasic SON neurons were unstained in these studies, leaving an element of doubt concerning the hormonal content of "phasic" SON neurons.

1.4.2 Intrinsic electrical properties of SON neurons

Intracellular recordings from rat (Andrew and Dudek, 1982,1983,1984,a,b; Mason, 1983a; Bourque, 1984; Bourque and Renaud, 1985a,b; Bourque et al., 1985) and guinea pig (Abe and Ogata, 1982; Abe et al., 1983) SON neurons in vitro have begun to provide a description of the intrinsic electrical properties that underly their firing patterns.

Properties of the "Resting" Membrane: SON neurons maintain resting membrane potentials of 50-70 mV (Andrew and Dudek, 1982; Bourque and Renaud, 1985; Mason, 1983a). In keeping with their small size, input resistance is high (100-400 MΩ) and cell-time constants are long (8-20 msec). The voltage-current relationship is linear for hyperpolarizing pulses (Mason, 1983a) but depolarizing

pulses are subject to strong rectification (Bourque, 1984). This rectification is reduced by calcium channel blockers such as cobalt (Bourque and Renaud, 1985b) indicating that it is due in part to the voltage-dependent activation of a calcium current. These passive electrical properties, when considered with the simple dendritic morphology of SON neurons (Section 1.2), predict efficient conduction and summation of synaptic and non-synaptic voltage transients (see below).

Action Potentials: Overshooting action potentials in SON neurons attain amplitudes up to 100 mV with durations of 1.0 - 3.5 msec (Mason, 1983a; Bourque and Renaud, 1985a,b; Andrew and Dudek, 1984). Blockade of Na^+ channels with tetrodotoxin (TTX) raises the threshold for firing of a TTX-resistant spike (Andrew and Dudek, 1983; Bourque and Renaud, 1985) which is reversibly abolished when $CaCl_2$ is replaced by equimolar EGTA, Cd^{++}, Co^{++} or Mn^{++}. Thus, both Na^+ and Ca^{++} currents contribute to action potentials in SON neurons. Both ions also contribute to compound action potentials recorded optically in neurohypophysial axon terminals (Salzberg et al., 1983).

Prolongation of action potentials by tetraethylammonium (TEA) indicates that potassium currents contribute to action potential repolarization in SON neurons (Bourque and Renaud, 1984). Enhanced Ca^{++} entry consequent to blockade of voltage and/or Ca^{++}-dependent potassium currents likely

accounts for the increase in spike duration.

Action potential duration also varies as a function of spontaneous firing frequency and is maximal at 10-20 Hz (Bourque and Renaud, 1985b). Furthermore, dynamic broadening of action potentials occurs at the onset of spontaneous phasic bursts; spike duration is increased as much as 100%. The changes in duration are blocked by Ca^{++} channel blockers indicating they result from enhancement of the Ca^{++} component of the action potential, perhaps as a consequence of gradual inactivation of the potassium currents that terminate the spike. Similarly, increased entry of calcium in neurohypophysial axon terminals during rapid or phasic firing might increase release of vasopressin and oxytocin (See section 1.5).

Hyperpolarizing After-Potentials and antidromic inhibition: Action potentials in SON neurons are followed by a hyperpolarizing after-potential (Andrew and Dudek, 1984; Koizumi and Yamashita, 1972; Mason, 1983). A similar hyperpolarization follows high frequency trains of spikes induced by repetitive antidromic stimulation or intracellular current injection (Andrew and Dudek, 1984). These potentials result primarily from activation of a Ca^{++} dependent K^{+} current following influx of Ca^{++} during action potentials (Bourque et al., 1985) and function to limit action potential firing frequency.

The existence of a recurrent inhibiting mechanism has

been inferred from the period of reduced excitability that follows antidromic activation (Barker et al., 1971b; Dreifuss and Kelly, 1972). The hyperpolarizing after-potential that follows antidromic spikes is of similar duration (Koizumi and Yamashita, 1972) but is not graded by stimulus intensity and disappears below threshold for antidromic activation (Bourque and Renaud, 1983). These data indicate that most of what has been termed as "post-antidromic inhibition" does not result from synaptic activation of a recurrent collateral pathway, but rather from an intrinsic inhibitory mechanism, i.e. a calcium-activated potassium conductance (Andrew and Dudek, 1984; Bourque et al., 1985).

Depolarizing after-potential and spontaneous phasic activity: Repetitive antidromic (Dreifuss et al., 1976) or orthodromic (Thompson, 1982) activation can induce premature onset of phasic bursts. This effect appears to be dependent upon periodic fluctuations in the excitability or refractoriness of phasic SON neurons since the effectiveness of these stimuli is low immediately following a spontaneous burst but increases progressively with time. Intracellular recordings have shown that the periodicity of phasic firing can be modified by small adjustments of membrane potential with current injection (Andrew and Dudek, 1983, 1984a) and that spontaneous synaptic input to SON neurons is

unpatterned (Andrew and Dudek, 1984a; Bourque, 1984). Therefore, in agreement with extracellular observations (Hatton, 1982) phasic firing reflects an intrinsic property of SON neurons (see Renaud et al., 1985).

Andrew and Dudek (1983, 1984a) made several salient observations which provide an explanation for the ability of SON neurons to generate repetitive burst firing. Single action potentials, or brief current-evoked bursts, are followed by a late 2-5 mV depolarizing after-potential that lasts 1-2 msec and persists in the absence of synaptic transmission. Therefore, when action potentials occur in succession (as at the beginning of a phasic burst) their depolarizing after-potentials summate and may eventually reach threshold. Repetitive firing ensues and is sustained by summation of depolarizing after-potentials into a "plateau" potential (Andrew and Dudek, 1984a). According to these authors, termination of the phase cannot be explained by synaptic inhibitory drive or active repolarization (eg: by calcium-dependent potassium current). Characteristically, action potential firing slows and fails at the end of a phase although the plateau potential is maintained. The cell then hyperpolarizes and begins a depolarizing drift that culminates in a subsequent phase (Bourque, 1984).

Large, calcium-dependent plateau potentials in cultured fetal hypothalamic neurons resemble phasic bursts in adult neurons in many respects (Legendre et al., 1982; Theodosis

et al., 1983). Although the amplitude is far greater than that observed in adult neurons, the voltage-dependence of plateau duration is very similar to that of phasic burst duration (cf. Andrew and Dudek, 1984a). Similar calcium-dependent plateau potentials are observed in adult SON neurons when potassium channels are blocked by intracellular injection of cesium (Bourque et al., submitted). However, plateau durations are increased tremendously by replacing medium calcium with barium. Barium carries Ca^{++} currents but does not mimic the intracellular actions of calcium such as Ca^{++}-dependent activation of K^{+} currents and Ca^{++}-dependent inactivation of Ca^{++} currents (See Eckert and Chad, 1984). Thus plateau termination appears to depend not only on potassium currents that hyperpolarize the cell, but also upon Ca^{++}-dependent inactivation of the calcium current underlying the plateau. While plateaus of this size do not occur in untreated adult SON neurons, the underlying current(s) may be responsible for the depolarizing after-potential and plateau potential. Accumulation of intracellular calcium during a phasic burst may lead to the calcium-dependent inactivation of the plateau current and burst termination.

Synaptic and Non-Synaptic spontaneous potentials:

Several groups have reported the existence of spontaneous excitatory and inhibitory synaptic potentials in SON neurons

which are abolished by tetrodotoxin or Ca^{++} channel blockers (Andrew and Dudek, 1984a,b; Bourque, 1984; Mason, 1983). No detailed study of the potentials has been reported, although inhibitory post-synaptic potentials are reported to reverse polarity upon membrane hyperpolarization (Andrew and Dudek, 1984a) and to be sensitive to intracellular injection of chloride ions (Bourque, 1984; Mason, 1983). Spontaneous post-synaptic potentials occur randomly and do not appear to participate in phasic burst generation (Andrew and Dudek, 1984a).

A second class of brief, sub-threshold, depolarizing potentials have been indentified in SON neurons (Bourque, 1984). These "fast-depolarizing potentials" can be distinguished from post-synaptic potentials by their insensitivity to Ca^{++} channel blockers, their small amplitude (1-4 mV), their symmetrical shape, and pronounced voltage-dependence. Their voltage dependence and sensitivity to tetrodotoxin indicate that fast-depolarizing potentials may arise from the activation of small numbers of cation channels. The high input resistance of SON neurons may permit resolution of the current (50 pS) flowing through single or clusters of cation channels in a manner similar to that proposed for pituitary cells (See Vincent and Dufy, 1982).

Osmosensitivity of SON neurons: SON neurons respond to an increase in plasma osmotic pressure by increasing their

electrical activity (Brimble and Dyball, 1977) and hormone output (Dunn et al., 1973). Neurons in many central (Iovino et al., 1983; Mangiapane et al., 1983; Sladek and Johnson, 1983; Yamashita and Kannan, 1976) and peripheral (Baertschi and Vallet, 1981) locations undoubtedly contribute to this neuroendocrine reflex. However, recent electrophysiological experiments in vivo (Leng, 1980) and in vitro (Abe and Ogata, 1982; Bourque and Renaud, 1984; Mason, 1980) suggest that SON neurons are endogenously osmosensitive. Synaptic input to SON neurons serves to increase the sensitivity of the response or to amplify the output (see Renaud et al., 1985).

The mechanism of the response to osmotic stimuli has been studied using intracellular recordings in vitro (Abe and Ogata, 1982; Mason, 1980). Increasing the osmotic pressure of the bathing medium with NaCl, mannitol or sucrose induces a membrane depolarization and enhanced action potential firing as a result of inactivation of a potassium conductance (Abe and Ogata, 1982). The frequency of spontaneous post-synaptic potentials also enhanced in hyper-osmotic solutions. Thus the output of SON neurons depends upon intrinsic and extrinsic factors responding to osmotic stimuli.

1.4.3 Synaptic and Drug Responses of SON neurons

Electrophysiological studies of the past 20 years have

identified several areas of the brain that influence the activity of SON neurons. This section reviews these reports and, where anatomical, physiological and pharmacological studies are available, portrays the role that various brain regions may play in neuroendocrine control.

A1 Noradrenergic input: The function of the dense noradrenergic input to the SON (Carlsson et al., 1962; Palkovitz et al., 1974) from the A1 cell group of the ventrolateral medulla (Sawchenko and Swanson, 1981,1982) has long been a source of controversy.

Secretion of vasopressin, usually indicated by a change in diuresis, is generally enhanced by central administration of norepinephrine (Bhargava et al., 1972; Bridges et al., 1976; Kuhn, 1974; Milton and Paterson, 1974; Morris et al., 1976; Olsson, 1969; Stutinsky, 1974; Urano and Kobayashi, 1978; Vandeputte-Van Messon and Peeters, 1975; Willoughby et al., 1985) and diminished following destruction of central catecholamine pathways (Everitt et al., 1983; Lightman et al., 1984; Miller et al., 1979; Milton and Patterson, 1973). Similarly, oxytocin release, as evidenced by milk ejection, is stimulated by central administration of norepinephrine or the α-adrenoreceptor agonist, phenylephrine (Clarke et al., 1979) and reflex milk ejection is delayed by administration of α-antagonists (Moos

and Richard, 1975; Clarke et al., 1979; Tribollet et al., 1978).

In contrast, iontophoretic application of norepinephrine is reported to inhibit firing of SON neurons (Arnauld et al., 1983; Barker et al., 1971; Moss et al., 1971, 1972) an effect apparently mediated by β-adrenoreceptors (Barker et al., 1971). In hypothalamic organ cultures, vasopressin release (Armstrong et al., 1982) and neurosecretory cell firing (Sakai et al., 1974) are inhibited by norepinephrine. Furthermore, reflex milk ejection is depressed by β-adrenoreceptor activation (Moos and Richard, 1979; Tribollet et al., 1978).

Despite this controversy, two recent studies support a facilitatory role of noradrenergic afferents in the release of vasopressin: (a) First, electrical stimulation of the A1 cell group enhances the activity of SON and PVN vasopressin neurons (Day and Renaud, 1984a,b). (b) Second, pressure ejection of norepinephrine at concentrations of 50-150 μM excites SON neurons via α-adrenoreceptors whereas concentrations of norepinephrine in excess of 1 mM induce a β-adrenoreceptor- mediated inhibition (Day et al., 1985). These findings suggest that iontophoretic application of norepinephrine (see above) results in exposure of the neurons to high concentrations of the drug (cf. Armstrong-James and Fox, 1983).

A contradictory report by Blessing et al. (1982) that

lesions encompassing the A1 cell group are followed by a brief rise in plasma vasopressin levels may have been misinterpreted as indicating that A1 neurons reduce SON neuron activity. A recent report (Blessing and Willoughby, 1985b) now suggests the contrary, i.e. that micro-injection of glutamate in the caudal ventrolateral medulla increases plasma vasopressin, presumably by activating A1 neurons which, in turn, activate SON vasopressin neurons. Furthermore, microinjections of muscimol, a GABA agonist, in this same region, block the hemorrhage-induced increase in plasma vasopressin (Blessing and Willoughby, 1985a). These observations confirm the electrophysiologic impression (Day and Renaud, 1984a,b) that A1 neurons are an important excitatory link in the central nervous system pathways that transmit cardiovascular information to hypothalamic vasopressin neurons.

The role of noradrenergic afferents, particularly the A1 cell group, in control of oxytocin neurons is less well established. Putative oxytocin-secreting neurons in the SON or PVN do not demonstrate an increase in excitability after electrical stimulation of the A1 cell group (Day and Renaud, 1984) and are far less responsive (compared with putative vasopressin neurons) to pressure ejection of norepinephrine (Day et al.,1985). However, evidence for the participation of α-adrenergic receptors in the milk ejection reflex is compelling (see above), raising the possibility that

oxytocin neurons of lactating rats are more responsive to norepinephrine and noradrenergic afferents than they are at other times in the reproductive cycle. Another possibility is that dopamine, which increases SON neuron firing (Mason, 1983) and oxytocin release (Bridges et al., 1976; Clarke et al., 1978) may be the catecholamine regulating oxytocin secretion. Dopamine antagonists administered intravenously block suckling-induced oxytocin secretion and milk ejection (Clarke et al., 1979).

Limbic afferents: Anatomical studies have revealed a modest projection from the septum and amygdala to the region of the SON and PVN (Zaborsky et al., 1975; Oldfield et al., 1985; Tribollet et al., 1985). Alterations in neurohypophysial hormone release caused by emotional or stressful stimuli (Mirsky et al., 1954; Cross, 1955; Taleisnik and Deis, 1964; Keil and Severs, 1977) are likely mediated by these limbic regions.

Two groups have independently observed that electrical stimulation of the lateral septum produces predominantly inhibitory responses in SON neurons (Cirino and Renaud, 1985; Poulain et al., 1980) with both continous and phasic firing neurons affected. Similar responses of SON neurons to amygdala stimulation are reported (Hanamura et al., 1980; Cirino and Renaud, 1985; Ferreyra et al., 1983; Thompson, 1982). Septal stimulation has inconsistent effects on the basal release of vasopressin and oxytocin (Aulsebrook

and Holland, 1969). However, repetitive septal stimulation inhibits suckling-induced release of oxytocin (Lebrun et al., 1983) and osmotically-induced increase in SON neurosecretory neuron firing (Yamashita and Kannan, 1976). Furthermore, septal lesions abolish the reflex release of vasopressin in response to bilateral carotid occlusion (Harris et al., 1984) and induce chronic polydipsia and polyuria associated with decreased vasopressin secretion (Iovino et al., 1983).

The results indicate that limbic structures modulate neuroendocrine reflexes involving the SON. No direct evidence is available concerning the transmitter substances present in these afferent systems. However, the fact that a potent inhibitory influence of septal and amygdalar stimulation is observed on SON neural excitability allows speculation that GABA is the transmitter underlying these effects. This hypothesis is supported by the observation that inhibitory post-synaptic potentials in neurosecretory neurons of the paraventricular nucleus follow septal stimulation (Koizumi and Yamashita, 1972). Further investigation is required to clarify the role of these limbic structures and the nature of the transmitter mediating their influence.

Subfornical Organ: Anatomical studies at both the light (Miselis et al., 1979; Lind et al., 1982) and electron microscope level (Renaud et al., 1983) reveal that the SON

receives a direct innervation from the subfornical organ. This circumventricular structure is thought to be important to drinking behavior and mediates the stimulation of vasopressin release by circulating angiotensin II (Simpson et al., 1978; Eng and Miselis, 1981; Knepel et al., 1982; Iovino and Steardo, 1984). Electrical stimulation of the subfornical organ produces a prolonged (up to 500 msec) excitation of the majority of SON neurons of both classes i.e. putative oxytocin and vasopressin-secreting cells (Sgro et al., 1984). Thus, although direct evidence is lacking, it is proposed that stimulation of the subfornical organ will promote the release of both vasopressin and oxytocin.

Several structures located rostral to the third ventricle appear to participate in autonomic responses consequent to central administration of angiotensin II (Brody and Johnson, 1980). However, the subfornical organ has angiotensin II-containing neurons whose fibers project to the PVN and SON (Lind et al., 1984). Also, angiotensin II receptors have been localized in the SON (Mendelsohn et al., 1984). In light of the ability of angiotensin II to induce phasic firing in cultured hypothalamic neurons (Gahwiler and Dreifuss, 1980), it is tempting to speculate that centrally administered angiotensin II stimulates vasopressin secretion via a direct action on neurosecretory neurons.

Cholinergic control: The earliest studies of the control of vasopressin secretion suggest a stimulatory role for acetylcholine (Abrahams and Pickford, 1956). Subsequent studies are unanimous in their conclusion that central administration of acetylcholine stimulates secretion of vasopressin (Bhargava et al., 1972; Bridges et al., 1976; Kuhn, 1974; Milton and Paterson, 1973,1974; Stutinsky, 1974; Vandeputte-Van Messom and Peeters, 1974) and oxytocin (Bridges et al., 1976). Similar responses are observed in vitro in hypothalamo-neurohypophysial explants (Bridges et al., 1976; Sladek and Knigge, 1977; Sladek and Joynt, 1979). Furthermore, since the electrical activity of SON neurons is enhanced by acetycholine administered by iontophoresis in vivo (Arnauld et al., 1983; Barker et al, 1971; Moss et al.,1971,1972) or bath application in vitro (Bioulac et al., 1978; Gahwiler and Dreifuss, 1980; Hatton et al., 1983; Ogata and Matsuo, 1984; Sakai et al., 1974), there is little doubt that acetylcholine enhances SON neuronal functi

Mason et al. (1983) recently identified a diffuse group of cholinergic neurons located in the lateral hypothalamus, dorsolateral to the SON, whose processes appear to penetrate the SON. Excitatory post-synaptic potentials can be recorded in phasic SON neurons following electrical stimulation of this region in hypothalamic slices (Hatton et al., 1983). This excitation is blocked by the nicotinic receptor antagonist, hexamethonium, but not the muscarinic

receptor antagonist, atropine. Therefore, these cholinergic neurons located dorsolateral to the SON may influence vasopressin secretion.

1.4.4 Relevance of SON neuron firing patterns to stimulus-secretion coupling

The majority of *in vitro* studies of the release of vasopressin and oxytocin have utilized isolated neural lobes impaled upon platinum electrodes. Hormone release evoked by repetitive electrical stimulation depolarizes axon terminals, mimicking the effect of action potentials propagated to the neurohypophysis from somata in the supraoptic and paraventricular nuclei. Early studies showed the amount of hormone released into the bathing medium was dependent upon the number and frequency of the applied stimuli, and the presence of calcium in the bathing medium (Dreifuss et al., 1971; Ishida, 1967) in a manner compatible with Douglas' model (1966) of "stimulus-secretion coupling".

Subsequent studies have shown that the efficiency of release of vasopressin (Bicknell and Leng, 1981; Dutton and Dyball, 1979) and oxytocin (Bicknell et al., 1982), on a "per stimulus" basis, is greatly increased if electrical stimulation is administered phasically rather than continuously, with pre-recorded phasic activity used to trigger the electrical stimulation. The high frequency of short interspike intervals during phasic firing is thought

to facilitate hormone release (Dutton and Dyball, 1979). Bourque and Renaud's (1985b) observation of activity-dependent changes in action potential duration provide one explanation for this phenomenon, assuming that the changes observed in somata of SON neurons also occur in axon terminals in the neurohypophysis. Enhanced calcium entry during action potentials occuring at short intervals can be expected to increase hormone release.

However, Bicknell and Leng (1981) argued that the silent period between phasic bursts might also contribute to the efficiency of this stimulation pattern, by relieving the fatigue of hormone release associated with prolonged stimulation (See Section 1.3.3 and Ingram et al., 1982). Recent experiments by Bourque et al. (submitted) suggest that plateau potentials underlying phasic activity (cf. Andrew and Dudek, 1984b) in SON neurons result from a calcium-current that inactivates when calcium accumulates intracellularly. Conceivably, calcium entry that underlies the plateau potential and is critical to stimulus-secretion coupling is impaired during prolonged electrical stimulation. This would result in a fall in hormone secretion.

1.5 Originality, Objectives and Overview

As our familiarity with the SON neuron increases, it becomes important to adopt a holistic approach to further investigation. Thus, morphological features of SON neurons must be related to their membrane properties and afferent inputs. The membrane properties and the neuropharmacology of SON neurons must be studied simultaneously since neither can be fully understood individually. Finally, firing patterns gain significance primarily when correlated with a measurement of the output of the neurons, ie: release of vasopressin and oxytocin.

The results described in this thesis derive from experiments performed using the perfused hypothalamic explant (cf. Bourque & Renaud, 1983). The findings are original and except for parts of Chapters 3 and 6, have not appeared previously. In general terms, the objective of my studies was to apply this preparation to the study of many aspects of SON neuronal function. The projects undertaken are described as follows.

In CHAPTER 2, "Materials and Methods", the preparation of the perfused hypothalamic explant is described. Details of the modifications of the basic preparation necessary to perform each kind of experiment are given along with the techniques used in analysis of the data.

In CHAPTER 3 "Serial Reconstruction of Lucifer Yellow-Filled SON Neurons" details of the stereotyped morphology of individual SON neurons are revealed more completely than is possible with Golgi or immunocytochemical techniques.

In CHAPTER 4 "Characterization of Spontaneous and Evoked Post-Synaptic Potentials (PSPs) in SON Neurons", evidence is presented that inhibitory PSPs (IPSPs) in SON neurons are mediated by a GABA-activated chloride conductance. CHAPTER 5 "The Effects of GABA on the Membrane Properties of SON neurons" is a sequel to CHAPTER 4. The effects of exogenous GABA on the membrane properties of SON neurons are shown to resemble those of the IPSPs. These findings support the hypothesis that GABA mediates spontaneous and evoked IPSPs in the SON (cf. Werman, 1969).

CHAPTER 6 "α-Adrenergic Activation of SON Neurons" describes a neuropharmacological study of the function of the dense noradrenergic innervation of the SON. Norepinephrine is shown to excite SON neurons and induce a bursting firing pattern via activation of α-adrenoreceptors. The mechanism of action of norepinephrine is investigated and data is presented that support a recent report (Aghajanian 1985) that α_1-adrenoreceptors modulate the voltage-dependent, transient potassium current known as I_A.

In CHAPTER 7 "Norephinephrine-Induced Release of Vasopressin and Oxytocin from the Hypothalamic Explant", a neuroendocrinological study reveals that norepinephrine acting on α_1-adrenoreceptors stimulates vasopressin and oxytocin release from the hypothalamic explant.

In CHAPTER 8 "Discussion", the results of these and other recent studies are incorporated in a model of the neural circuitry mediating reflex secretion of vasopressin and oxytocin. The model focuses on the possible role of GABAergic and noradrenergic afferents to the SON.

CHAPTER 2

MATERIALS AND METHODS

The experiments described in this thesis were all performed *in vitro* using perfused explants of rat hypothalamus, prepared in a manner similar to that described previously (Bourque, 1984; Bourque and Renaud, 1983).

2.1 Hypothalamic Explant Chamber

Hypothalamic explants were incubated in a twin-chambered cylindrical bath (Figure 2-1) whose outer chamber (Figure 2-1,no.6) contained distilled water maintained at 35 ^{0}C thermostatically. The inner chamber (Figure 2-1A) consisted of a perspex disc with a central well filled to within 1-2 mm of the top with Sylgard elastomer (Corning Ltd.), thereby providing a shallow depression in which the explant could be fixed (see below).

Perfusion media (contents described below) were stored at room temperature under a 95% O_2: 5% CO_2 atmosphere in reservoirs located approximately 1.5 meters above the bath. These were gravity-fed through PE-120 polyethylene tubing to a series of solenoid-controlled 3-way valves (General Valves Inc.) which allowed selection of control medium, or one to four other media containing test substances. The selected medium then flowed through a 30-40 cm segment of PE tubing

contained within the outer bath where it was heated to 35 ^{0}C. The PE tubing was led through a hole in the top of the outer chamber and connected to a pipette (Figure 2-1B) whose tip diameter of 100-200 μm permitted medium flow rates of 0.6-1.5 mL/min. This pipette was fitted to a micromanipulator to allow positioning in the stump of the internal carotid or anterior cerebral artery.

In order to avoid possible loss of CO_2 by diffusion from medium while in transit from reservoir to the bath, the PE-120 tubing carrying the media from the reservoirs to the valves were surrounded by Tygon tubing through which a 95% O_2: 5% CO_2 gas mixture was passed. This gas was directed into the outer bath for humidification and then to the vicinity of the inner bath via holes drilled in the plate covering the outer bath so as to provide a warm, humidified, oxygenated environment for the explant. A fibreoptic illuminator positioned immediately below the inner bath provided heat-free transillumination of the explant.

2.2 Preparation for Electrophysiology

All experiments utilized a perfused basal forebrain explant from male Sprague-Dawley rats (150-300 g, Canadian Breeding Farm Laboratories). Following decapitation, bones forming the roof of the skull were rapidly removed and the olfactory tubercles and optic nerves were severed. The brain was gently removed and attached by its dorsal surface

to the base of an inverted petri dish using cyanoacrylate glue. An explant of the basal forebrain measuring approximately 10x10x3 mm and including the hypothalamus, pituitary and parts of the temporal and frontal cortex, optic nerves and chiasm and mesencephalon (Figure 2-2) was cut carefully with razor blades to preserve the entire vasculature of the Circle of Willis.

Following transfer to the inner bath described above (Section 2.1) this brain explant was fixed in place with four insect pins inserted into the Sylgard. A micro-manipulator-mounted perfusion pipette with medium flowing was then inserted into the right internal carotid artery and the pipette tip advanced to the bifurcation of the anterior and middle cerebral arteries. This caused the tissue to blanch rapidly. Clotted blood was removed from arteries and veins with jeweler's forceps and the optic nerves were trimmed to the level of the optic chiasm, avoiding damage to surrounding tissues.

To facilitate entry of recording electrodes in the SON (Chapters 3-6) the arachnoidal and pial membranes as well as small caliber arteries and veins were removed from the ventral surface of the nucleus. The level of the fluid covering the area of the supraoptic nucleus was kept to a minimum (~200 μm) by careful positioning of "wicks" of filter paper or gauze to break the fluid surface tension. Explants were allowed 2-4 hours of "equilibration" prior to

recording, during which time the tissue swelled some 10-15% but remained stable thereafter. Explants were viable for at least 12 hours as judged by the ability to obtain stable recordings from SON neurons (see below).

2.3 Preparation for Hormone Release Studies

A series of experiments was performed to evaluate control and drug-induced release of vasopressin and oxytocin from perfused explants (Chapter 5). Samples of effluent perfusion medium were collected for radioimmunoassay of vasopressin and oxytocin (see section 2.9).

The explant was prepared as described above but with several precautions and modifications (see Figure 2-3). The usual perfusion medium was supplemented with bovine serum albumin (0.1%, to serve as a carrier protein) and phenol red (10 mg/l, a pH indicator). To minimize damage to the hypothalamo-neurohypophysial tracts during removal of the brain from the skull, the diaphragma sella was torn using a hooked 24-gauge hypodermic needle to free the pituitary from the sella turcica. Damaged preparations were discarded.

In these experiments, optimal perfusion of the entire explant was assured when both internal carotid arteries were cannulated (Figure 2-3). Blood clots were removed from blood vessels and the optic nerves were cut as described above, but the membranes overlying the SON were not disturbed. Also, instead of positioning filter paper wicks

to regulate fluid level, the medium was allowed to collect and cover the explant to a depth of approximately 1 mm. Excess fluid was then drawn off via a suction pipette positioned caudal to the pituitary and powered by a peristaltic pump (see Figure 2-3). Finally, the pars distalis of the pituitary (anterior pituitary) was removed using the hooked hypodermic needle and fine scissors, leaving the partes nervosa and intermedia (neurointermediate pituitary) intact so as to ease diffusion of secretory products of the neurohypophysis into the medium. Explants were incubated for 1 hour prior to collection of medium.

During the 1-3 hour experiments, 1 or 2 minute fractions of effluent medium were collected in 16x100 mm polystyrene test tubes. Samples were immediately transferred to ice, and later frozen (-20^0 C) and lyophilized for shipment.

2.4 Perfusion Media and Drug Application

The "control" perfusion medium consisted of a modified Yamamoto's solution (cf. Yamamoto and McIlwain, 1966) and contained (in mM) NaCl (124), KCl (3), KH_2PO_4 (1.25), $MgCl_2 \cdot 2H_2O$ (1.30), $CaCl_2 \cdot 2H_2O$ (2.4), $NaHCO_3$ (26), Glucose (10.0). The osmolality of the medium was determined by freezing-point osmometry (Advanced instruments micro-osmometer OSM) and adjusted when necessary, to 295 ± 2 mOsm usually by the addition of 10-50 ml of water. The medium

was equilibrated with a 95% O_2: 5% CO_2 gas mixture as described above (section 2.1).

Modifications of the ionic composition of the medium were made by equimolar replacement of NaCl with KCl or $MgCl_2 \cdot 2H_2O$ so as to obtain media containing 2-10 mM K^+, or 10-15 mm Mg^{++}. Medium containing 10.4-78 mM Cl^- was obtained by equiosmolar replacement of NaCl with NaGlucuronate. Replacement of KCl with KH_2PO_4 and $MgCl_2$ with $MgSO_4$, lowered medium Cl^- to 4.8 mM (contributed by $CaCl_2$).

These media were stored in separate reservoirs, equilibrated with 95% O_2: 5% CO_2 and selected using the remote-controlled solenoid valves (Figure 2-1). Pharmacological antagonists (phenoxybenzamine, phentolamine, prazosin, yohimbine, bicuculline methiodide and strychnine sulphate) and pentobarbitol were dissolved in 200-500 ml of perfusion medium and administered by switching from control to test medium as described above. Because of its poor solubility in aqueous solutions, prazosin was first dissolved in dimethylsulfoxide (DMSO) and then diluted to the desired concentration. In these experiments, an equivalent amount of DMSO (not exceeding 0.005%) was added to all media. Due to the "dead space" of the tubing supplying the chamber, medium changes began after a delay of 1-2 minutes, depending upon the flow rate, but then proceeded rapidly over 30-60 seconds.

In order to test the effects of pharmacological agents (especially agonists) on steady-state phenomena (membrane potential, firing rate, input resistance) two methods of rapid and brief drug application were used. A 30-gauge hypodermic needle was inserted into the perfusion line as shown in Figure 2-1 (#1) and connected via PE10 tubing to a syringe containing a concentrated solution of drug dissolved in control medium. Delivery of the drug was controlled by a syringe pump (Hamilton) in the range 12-240 µl/min. Using the measured flow rate, the dilution (and thus concentration) of drug was calculated. In control experiments, administration of hyperosmotic or dye-containing solutions confirmed the accuracy of the dilution calculation. Following a short delay which depended upon flow rate and pump speed (see Figure 2-3), the concentration of the substance rose to its maximum within 5-30 seconds and fell to less than 10% within 30-60 seconds of termination of the administration. In all figures, symbols (usually bars) indicate the actual timing of drug administration. No correction was made for dead space delay.

For extracellular recordings from SON neurons, it was also possible to use pressure to eject small pulses of drug from pipette barrels attached to the recording electrode (Figure 2-5). Three pieces of fibre-filled glass tubing (100 mm long, outer diameter = 1.5 mm, inner diameter =

0.9 mm, W-P Instruments, Cat# 1B150F) were attached together using heat-shrink tubing and dental cement or epoxy. The tubes were heated, twisted and then pulled on a Narashige vertical pipette puller yielding two triple-barrel micropipettes. The micropipettes were broken back to a tip diameter of 2-10 µm and then bent using a deFonbrune Microforge and a small flame. They were then attached to a recording electrode (5-20 MΩ) using cyanoacrylate glue and dental cement (see Figure 2-5).

The barrels of the ejection pipettes were then filled with medium containing drugs at known concentrations and connected via Tygon tubing to a pressure ejection system (Picospritzer, General Valves Inc). Pressures of 3-40 psi were used with 10 msec-10 sec pulses, depending upon the concentration of drug used and the patency of the ejection barrels. This method yielded results similar to those obtained with bath application but provided less control over local drug concentrations.

2.5 Extracellular Recording

In certain experiments, extracellular recordings were obtained using glass micropipettes (1.5 mm OD., with microfilament) filled with 2 M NaCl (5-20 MΩ). Positioning of the recording electrode was achieved with an LPC micromanipulator. Signals were amplified conventionally (WPI M-707 preamplifier and an operational amplifier, total

10,000x AC, bandwith 0.5-5 kHz), displayed on an oscilloscope, stored on magnetic tape (JVC KD-D20 casette deck), and led through a variable voltage gate to the interrupt bus of a PDP 11/23+, computer for spike train analysis (rate-meter, time interval histograms, post-stimulus histograms; Figure 2-6). In addition, a concentric bipolar stimulating electrode (diameter 0.2 mm) was placed on the pituitary stalk to allow identification of SON neurons by antidromic activation. The stimulating electrode was connected to an isolated stimulating unit (Digitimer DS2) which was controlled by an external clock (Digitimer 4030) to deliver current pulses (50 μsec, 0.1-1 mA).

2.6 Intracellular Recording

Intracellular recordings were obtained using glass micropipettes made by pulling 10 cm sections of capillary tubing (containing a microfilament, OD = 1.2 mm, ID = 0.6 mm, Fredrick Haer) on a Brown and Flaming (P-77A) pipette puller. Micropipettes filled with either 3M-Potassium chloride (KCl) or 3M-Potassium acetate (KAc) had tip resistances of 70-300 MΩ. Electrodes were connected via an Ag-AgCl electrode to the input stage of a Mentor N-950 pre-amplifier using 5 kHz low pass filtering (see Figure 2-7). A separate Ag-AgCl wire inserted into the inner bath provided the floating reference ground necessary for the Mentor pre-amplifier. High resistance electrodes must be

used to obtain good quality impalements from SON neurons. Therefore, capacitance compensation was applied at the input to avoid attenuation of high frequency components of the voltage signal. Capacitance compensation was adjusted prior to impalement of a cell by "squaring" the voltage response to a current pulse applied through the unbalanced bridge circuit. The bridge circuit was then balanced by eliminating the time-independent voltage deflection induced by a similar current pulse. The remaining capacitive artifacts at the beginning and end of such pulses had durations of <0.2 msec. Bridge balance was monitored closely during recording and adjusted when necessary. This was important because the accuracy of measurements of membrane potential and input resistance (section 2.7) are dependent upon precise balancing of the bridge circuit. Current pulses were supplied by isolated stimulating units (Digitimer DS2) controlled by a programmable clock (Digitimer 4030). Voltage and current signals from the pre-amp as well as trigger pulses from the clock were stored on magnetic tape (7.5 i.p.s.) with an FM recorder (RACAL) and monitored on an oscilloscope (Figure 2-7).

Impalement of SON neurons were obtained by advancing the electrode by 4 μm steps with a piezoelectric micropositioner (Burleigh) and applying 2-10 nA depolarizing pulses (40-50 msec) of current through the electrode. Overcompensation ("buzzing") of the capacitance compensation

of the preamplifier was less effective. Impalements were improved by applying .05-.2 nA of hyperpolarizing ("holding") current for the first 1-2 minutes following penetration of a cell. In "well impaled" neurons, this current could be removed within 3-4 minutes. Criteria for determining the quality of impalement included (1) resting membrane potential of 50 mV or more, 2) overshooting action potentials of amplitude at least 70 mV, 3) input resistance greater than 75 MΩ, 4) strong inward rectification of the voltage response to depolarizing current pulses, and 5) spontaneous activity patterns that were similar to those noted in vivo.

Data processing and analysis was performed 'off-line' following the experiments. Recorded signals were played back on the Racal recorder and led to either a storage oscilloscope (Tektronix R5103N), a digital oscilloscope (Data Precision, model Data 6000) or to a pen plotter (Gould Instrument 2200S) as shown in Figure 2-7. The storage oscilloscope was used primarily to make manual measurements of membrane potential, particularly for construction of current-voltage plots and analysis of responses to drugs. Traces displayed on the oscilloscope were photographed with a rack-mounted 35 mm camera (Pentax) using Kodak Technical-Pan film processed for maximum contrast.

Analog signals fed into the digital oscilloscope were digitized at 1-20 kHz depending upon the nature of the

signal to be analyzed. Digitized data were either plotted directly (Hewlett-Packard 7470A plotter) or were processed using the system programs of the Data 6000 (especially signal averaging) or programs supplied by the user. In particular, semi-log plots of the decay of voltage transients (current pulses, IPSPs) were obtained in this way.

Traces of duration 1 sec or more were plotted on the Gould pen recorder from taped signals using playback speeds of 1/8 or 1/16 the recording speed (frequency response DC-1kHz at 1/16).

2.7 Measurement of Input Resistance and Conductance

Input resistance (R_{in}) was estimated based upon the amplitude of the membrane voltage deflection (ΔVm) in response to intracellular injection of current pulses (ΔI). Thus:

$$R_{in} = \Delta Vm / \Delta I \qquad (1)$$

Similarly, R_{in} can be determined as the slope of a plot of ΔVm as a function of ΔI when a series of current pulses of varying amplitude is applied. Input conductance (G_{in}) is defined as the reciprocal of R_{in}:

$$G_{in} = 1/R_{in} \qquad (2)$$

The accuracy of these measurements is critically dependent upon precise adjustment of the bridge circuit (section 2.6). Analysis of the synaptically-induced changes in input

resistance (ΔR_{in}) and input conductance (G_{IPSP}) can be performed with consideration of the equivalent circuit for a synaptic conductance in parallel with the resting membrane conductance (Figure 2-8)(cf. Ginsborg, 1983; Choi and Fischbach, 1981). Total input conductance during an IPSP (G_{TOT}) is related to resting membrane conductance (G_{in}) and the synaptically-activated conductance (G_{IPSP}) by the equation:

$$G_{TOT} = G_{in} + G_{IPSP} \qquad (3)$$

This relationship can be rearranged to:

$$G_{IPSP} = 1/R_{TOT} - 1/R_{in} \qquad (4)$$

where R_{in} is the resting input resistance and R_{TOT} is the input resistance measured at the peak of the IPSP. This approach is suitable for the determination of G_{IPSP} for the evoked IPSP (G_{eIPSP}). The membrane voltage response to 150-300 msec intracellular current pulses can be measured under "resting" conditions and at the peak of the evoked IPSP. Plots of the voltage-current (V-I) relationships can be constructed as in Figures 4-3 and 4-5, and R_{in} and R_{TOT} determined as the slope of the linear portion of the V-I plot (generally between -70 and -120 mV). If short (i.e. 10 msec) current pulses are applied before, during or after the evoked IPSP (Figure 4-4), both R_{in} and R_{TOT} are underestimated because voltage response does not equilibrate due to the relatively long membrane time constant of SON neurons (~8-15

msec). As a result, G_{eIPSP} is overestimated. However the % change from R_{in} to R_{TOT} appears to be similar to that observed with the long pulse format (compare results of Figures 4-3 and 4-4).

Alternatively, since the amplitude of an IPSP (voltage deflection, ΔV) is related to G_{IPSP}, G_{IPSP} can be calculated as follows if membrane potential (V_m), resting input conductance (G_{in}) and IPSP reversal potential (E_{IPSP}) are known. Thus:

$$\Delta V = R_m \times I_{IPSP} \quad (5)$$

or

$$I_{IPSP} = G_m(V_m - V_{IPSP}) \quad (6)$$

where I_{IPSP} is the synaptic current, V_{IPSP} is the membrane potential of the peak of the IPSP and R_m and G_m are the resting resistance and conductance, respectively of the non-synaptic membrane. Also:

$$I_{IPSP} = G_{IPSP}(V_{IPSP} - E_{IPSP}) \quad (7)$$

so by combining equations (6) and (7):

$$G_{IPSP} = G_m(V_m - V_{IPSP}/V_{IPSP} - E_{IPSP} \quad (8)$$

SON neurons appear to be adequately "space-clamped" during intracellular current injection (Bourque, 1984). Therefore, G_{in} can be substituted for G_m in equation 8 as a reasonable approximation since intracellular and extracellular resistivity can be assumed to be low compared to the membrane resistance.

Values of G_{eIPSP} calculated using equation 8

agree to within ±5% of those obtained by the analysis of equation 4. This method of analysis was better for spontaneous IPSPs because considerable membrane potential fluctuations sometimes occurred during the long periods of current passage (several seconds) necessary to observe enough of these randomly occurring events and because of the considerable variation in spontaneous IPSP amplitude.

Analysis of the effects of exogenously applied substances (GABA, Muscimol, Norepinephrine) was also performed using equation 4.

2.8 Lucifer Yellow Injections and Reconstruction of SON neurons

Intracellular recordings were obtained from SON neurons with glass micropipettes filled with 4-6% aqueous solution of the trilithium salt of lucifer yellow (Sigma). The electrodes were constructed as described in section 2.6 except that thin-walled capillary tubes (1.2 mm OD, 0.9 mm ID, Frederick Haer) were used. Typical tip resistances were between 200-400 MΩ. Dye injection was achieved by iontophoresis with 0.5-1.0 nA of constant and pulsed hyperpolarizing current for 5-10 minutes with occasional oscillation of the capacitance compensation to clear the electrode tip (Figure 2-9). Usually only one cell was injected in each SON (but see Figure 3-2).

Within 15 minutes of injection, explants were fixed by

immersion in cold 4% formaldehyde in isotonic phosphate buffer (pH 7.4) where they remained for 1-3 days at 4^0 C. The tissue was transferred to 4% formaldehyde plus 10% sucrose for 2 hrs. prior to sectioning in order to reduce artifact due to swelling, shrinking or freezing. The tissue was then embedded in Tissue-tek, and frozen in 2-methylbutane chilled to -80^0 C in liquid nitrogen. Horizontal or coronal 40 µm sections were cut on a cryostat at -25^0 C. Sections were mounted on gelatin-coated slides, dried, processed through phosphate buffer and graded alcohols, cleared with methyl salicylate and coverslipped. Following photography of the labelled neurons (see below), sections were rehydrated through graded alcohols, and stained with 3% cresyl violet to allow verification of the location of the injected neuron in the SON (Figure 2-10).

Lucifer yellow fluorescence was visualized with a Leitz Ortholux microscope using ploem filter pair H_2. Cells were photographed at 64X or 320X magnification using Kodak Tri-X Pan (black and white) or VR1000 (colour) negative film. Since the depth of field of the objective lenses was usually insufficient to simultaneously focus on all segments of a dendrite or an axon passing through a 40 µm histological section, exposures were made in different focal planes so as to achieve an accurately focused record of all segments of the neurone. To compensate for the variation in intensity of fluorescence between soma and distal axon or dendritic

spine, the camera's (Leitz-ortholux) automatic exposure was used with metering restricted to the center of the field. Thus, by centering the desired object (soma, dendritic spine, etc.) in the microscope field an appropriate exposure time (range 0.1-10 sec) was obtained. This reduced the halo around intensely fluorescent parts of the cell and allowed for a more accurate determination of soma and dendrite dimensions.

Cell reconstructions were made from prints by apposing portions of the labelled neuron found in adjacent histological sections (Figure 2-11). Where adjacent segments of a process were more sharply in focus at different exposures, or focal planes, appropriate parts of the prints were inserted into the reconstruction.

Drawings were made from projected negative images using a microfilm viewer (Zeiss). Measurements of the lengths of processes were made from these drawings. Since dendrites penetrated as many as 10 histological sections and axons penetrated as many as 25 sections, the following correction of the length of each process was applied to account for the number of histological sections through which it passed (Length of the hypotenuse of a right triangle):

$$\text{real length} = [\text{measured length}^2 + (\#\ \text{sections} \times 40\ \mu\text{m})^2]^{1/2}.$$

Somata were examined for size, shape, location and the presence of spines. Measurements were made of the lengths of dendrites, the position of branches and number and

frequency of spines. The axon, identified on the basis of its origin (soma or dendrite) and trajectory was carefully examined for the presence of collaterals or spines. Spinous processes on somata, dendrites and axons were counted by direct observation of the cell with a 100X oil immersion objective lens. No attempt was made to distinguish quantitatively between spinous processes of various length and shape.

2.9 Radioimmunoassay of Arginine-Vasopressin (AVP) and Oxytocin (OXY)

Vasopressin and oxytocin in the samples of effluent perfusion medium were measured by radioimmunoassay (RIA) by Dr. Michael F. Mazurek (Massachusetts General Hospital, Boston, Mass.). Antibodies were raised in New Zealand white rabbits against synthetic peptides (Bachem) conjugated with thyroglobulin. Synthetic peptides were used as standard and for iodinated (^{125}I) tracer. These assays were highly sensitive (0.2 pg/tube) and were characterized for specificity by high pressure liquid chromatography (HPLC) and serial dilution curves (Figure 7-1). Cross-reaction of AVP in the OXY-RIA and of OXY in the AVP-RIA was less than 0.2%. Results were expressed as pg of AVP- or OXY-like immunoactivity released per minute (pg AVP-LI/min or OXY-LI/min).

Figure 2-1 Diagram of the perfusion apparatus. The perfusion (inner) chamber consisted of a well drilled into a thick perspex disc (A). The bottom of the chamber was filled with Sylgard elastomer into which pins were inserted to stabilize the explant. The right internal carotid artery of the explant was cannulated with a glass pipette (B). The entire perfusion system is schematized in (C): 1) infusion lines; 2) thermostatic temperature regulator; 3) fiberoptic light source 4) micromanipulator and perfusion pipette; 5) perfusion chamber; 6) water jacket; 7) pressurized 95% O_2/ 5% CO_2 source; 8) ACF reservoir; 9) jacketed perfusion line; 10) pressurized outflow of the perfusion line jackets; 11) selected ACF output perfusion line; 12) solenoid valve assembly; 13) waste drain. (From Bourque (1984), with permission.)

A PERFUSION CHAMBER

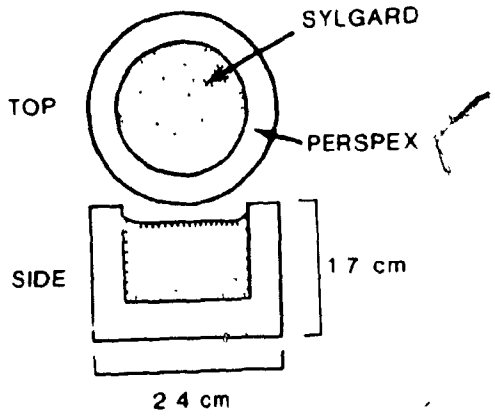

B PERFUSION PIPETTE

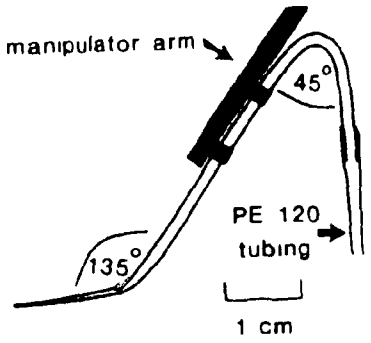

C BATH

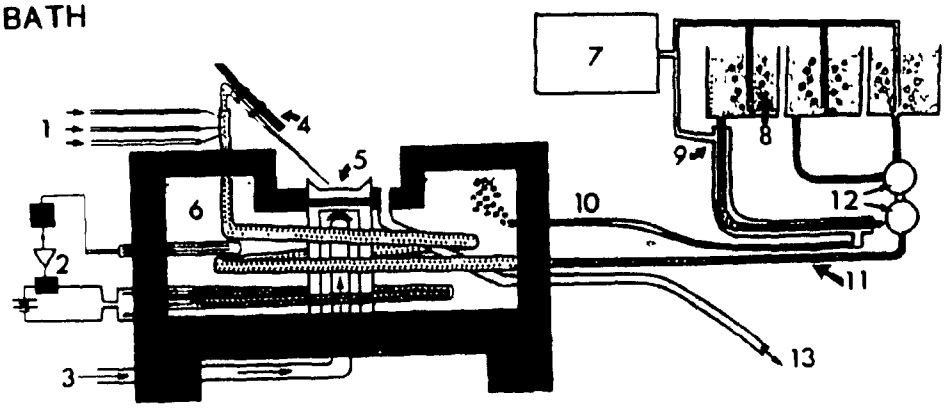

Figure 2-2 Drawing of the perfused hypothalamic explant. MCA, middle cerebral artery; ACA, anterior cerebral artery; PCA, posterior communicating artery; ICA, internal carotid artery; DBB, diagonal band of Broca; OC, optic chiasm; ME, median eminence; Pit, pituitary gland; PP, perfusion pipette; SON, supraoptic nucleus. (Drawing by Jean Dufresne.)

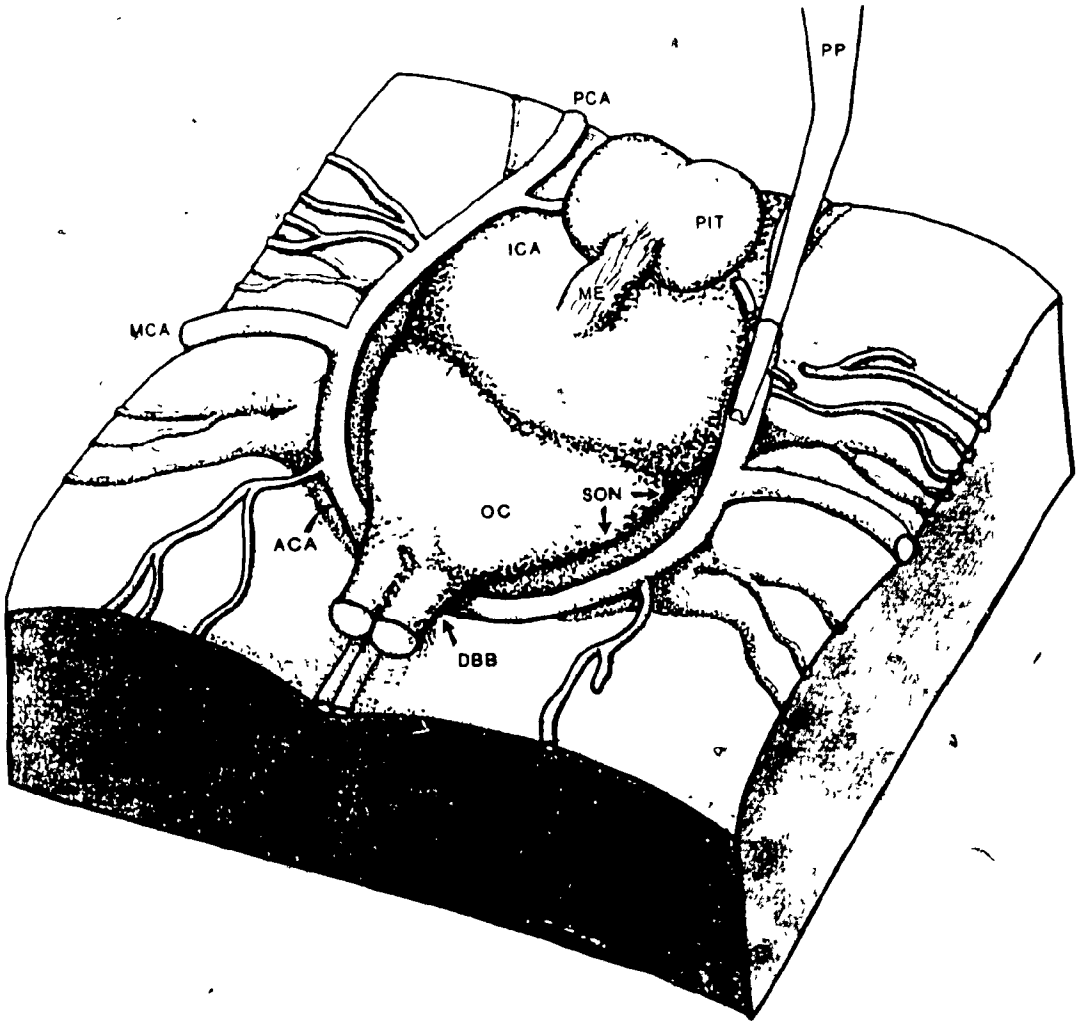
PP
PCA
PIT
ICA
ME
MCA
SON
OC
ACA
DBB

Figure 2-3 Experimental set-up for collection of perfusion medium for hormone assay. Both internal carotid arteries are cannulated and the anterior pituitary is removed. Medium was removed by a suction pipette positioned caudal to the neurointermediate lobe, PE100 polyethylene tubing and a peristaltic pump for collection in polystyrene test tubes. Vasopressin and oxytocin were determined by radioimmunoassay.

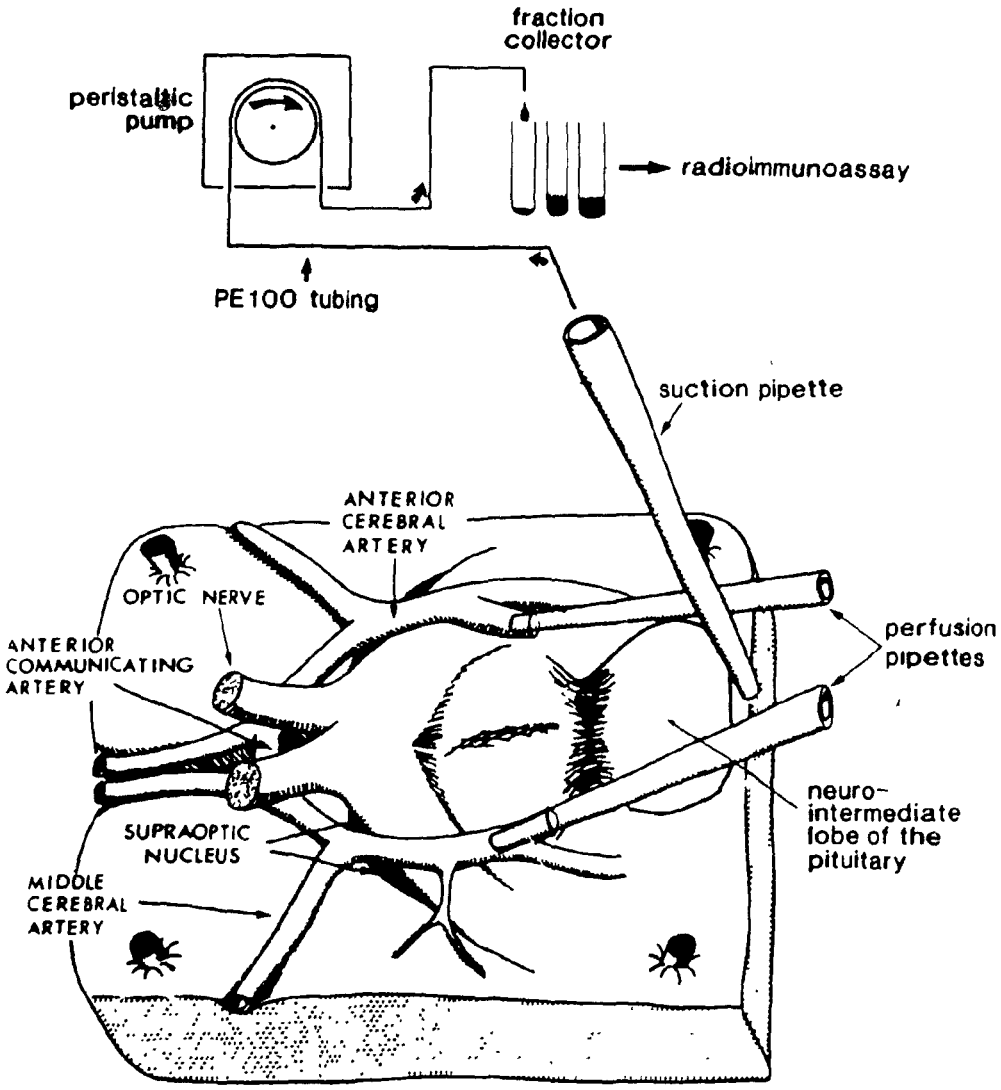
fraction collector
peristaltic pump
radioimmunoassay
PE100 tubing
suction pipette
ANTERIOR CEREBRAL ARTERY
OPTIC NERVE
ANTERIOR COMMUNICATING ARTERY
perfusion pipettes
neuro-intermediate lobe of the pituitary
SUPRAOPTIC NUCLEUS
MIDDLE CEREBRAL ARTERY

Figure 2-4 Time-course of the appearance in, and disappearance from, the bath of a hyperosmotic solution (1000 mOsm/L) administered using the infusion pump. Infusion rate was 55 µl/min and pipette flow rate was 0.7 ml/min. Pump was turned on for 5 sec (circle), 10 sec (triangle), or 20 sec (square) and samples of medium in the bath were drawn every 10 sec for measurement of the osmolarity by freezing point depression (Advanced Instruments Microosmometer OSM). Medium osmolality reached the maximum expected level within 15-20 seconds. Shorter administrations of hyperosmotic solution produced submaximal changes in osmolarity.

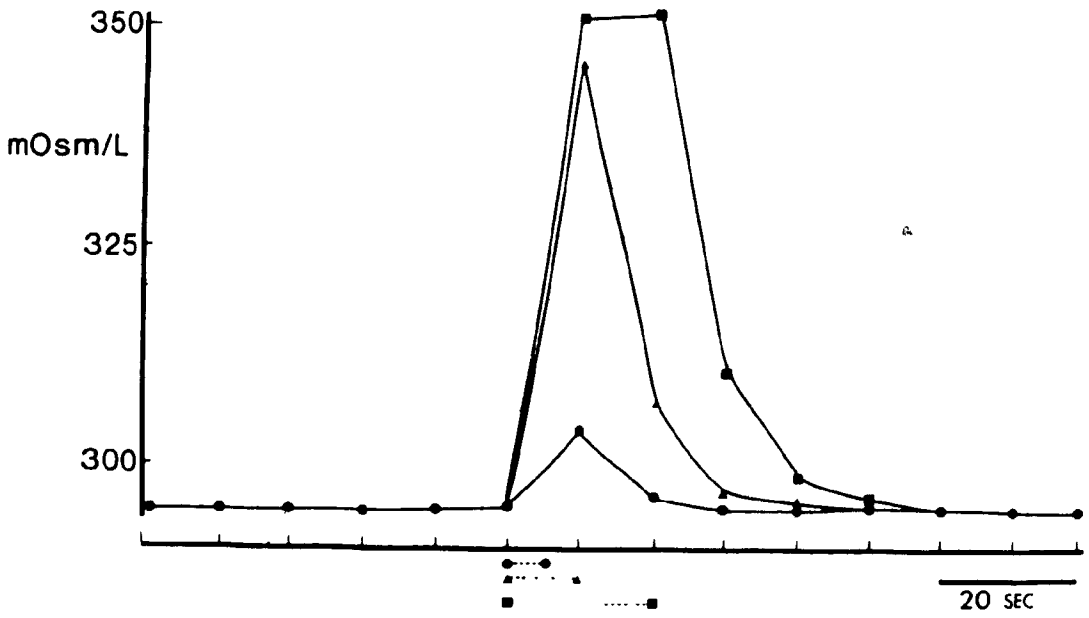
350
mOsm/L
325
300
20 SEC

Figure 2-5 Multibarrel pipettes used for pressure ejection of drugs during extracellular recording. Top: low power photo showing the 3-barrel ejection pipette attached to a recording electrode. Bottom: Photomicrograph showing 3-barrel pipette (tip diameter 5 µm) positioned approximately 30 µm back from the tip of the recording electrode.

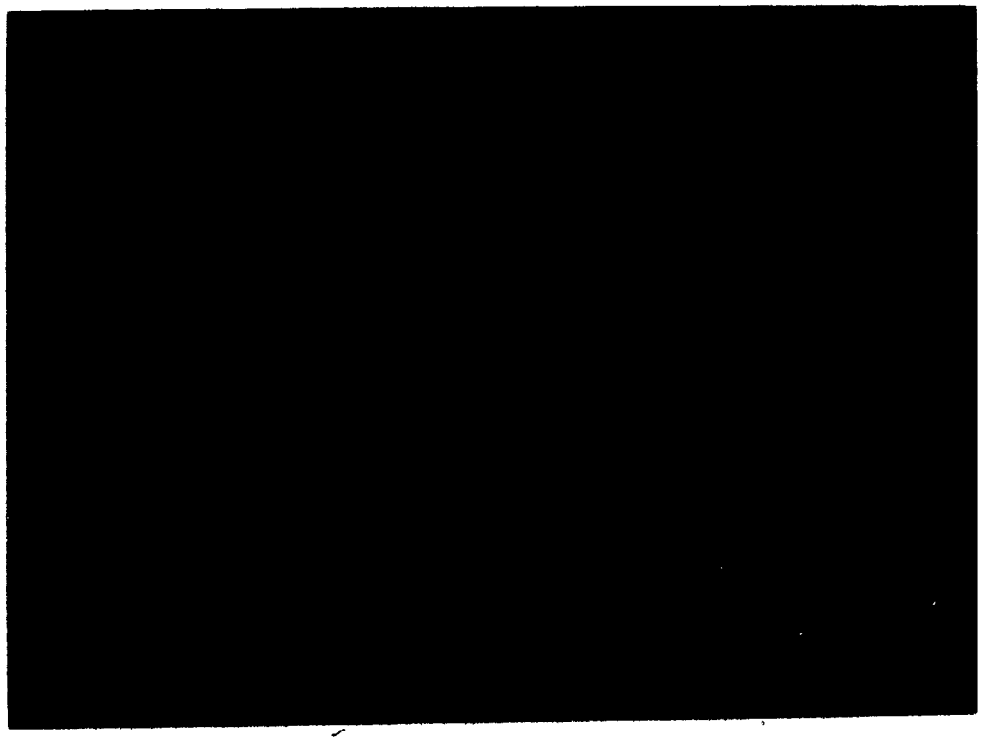

50 um

Figure 2-6 Block diagram of the experimental set-up used fo extrcellular recording experiments. Modified from Bourque (1984).

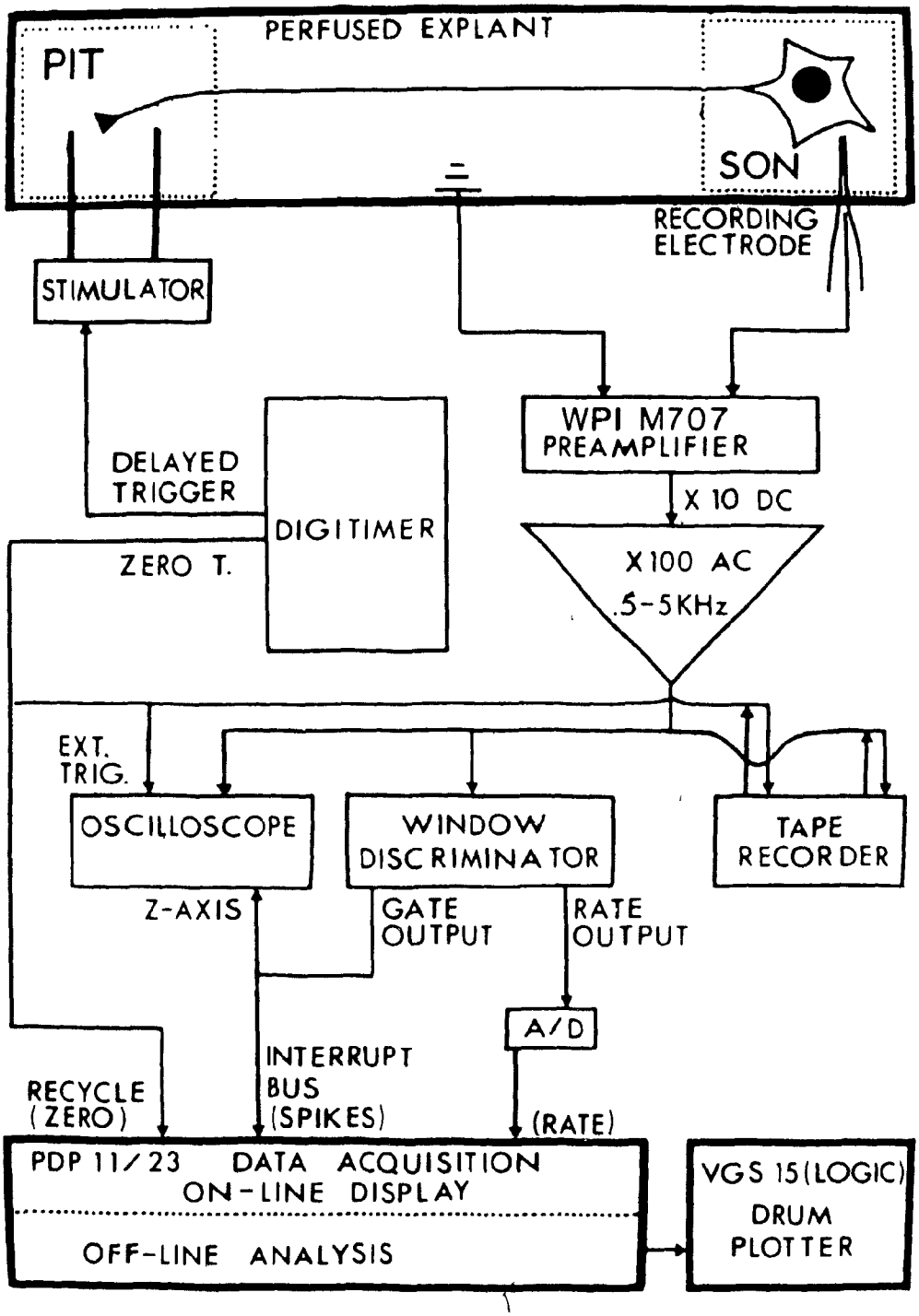
PERFUSED EXPLANT
PIT
SON
RECORDING ELECTRODE
STIMULATOR
DELAYED TRIGGER
DIGITIMER
ZERO T.
WPI M707 PREAMPLIFIER
X 10 DC
X100 AC
.5-5KHz
EXT. TRIG.
OSCILLOSCOPE
WINDOW DISCRIMINATOR
TAPE RECORDER
Z-AXIS
GATE OUTPUT
RATE OUTPUT
A/D
INTERRUPT BUS (SPIKES)
RECYCLE (ZERO)
(RATE)
PDP 11/23 DATA ACQUISITION
ON-LINE DISPLAY
OFF-LINE ANALYSIS
VGS 15 (LOGIC)
DRUM PLOTTER

Figure 2-7 Block diagram of the experimental set-up used for intracellular recording experiments. Modified from Bourque (1984).

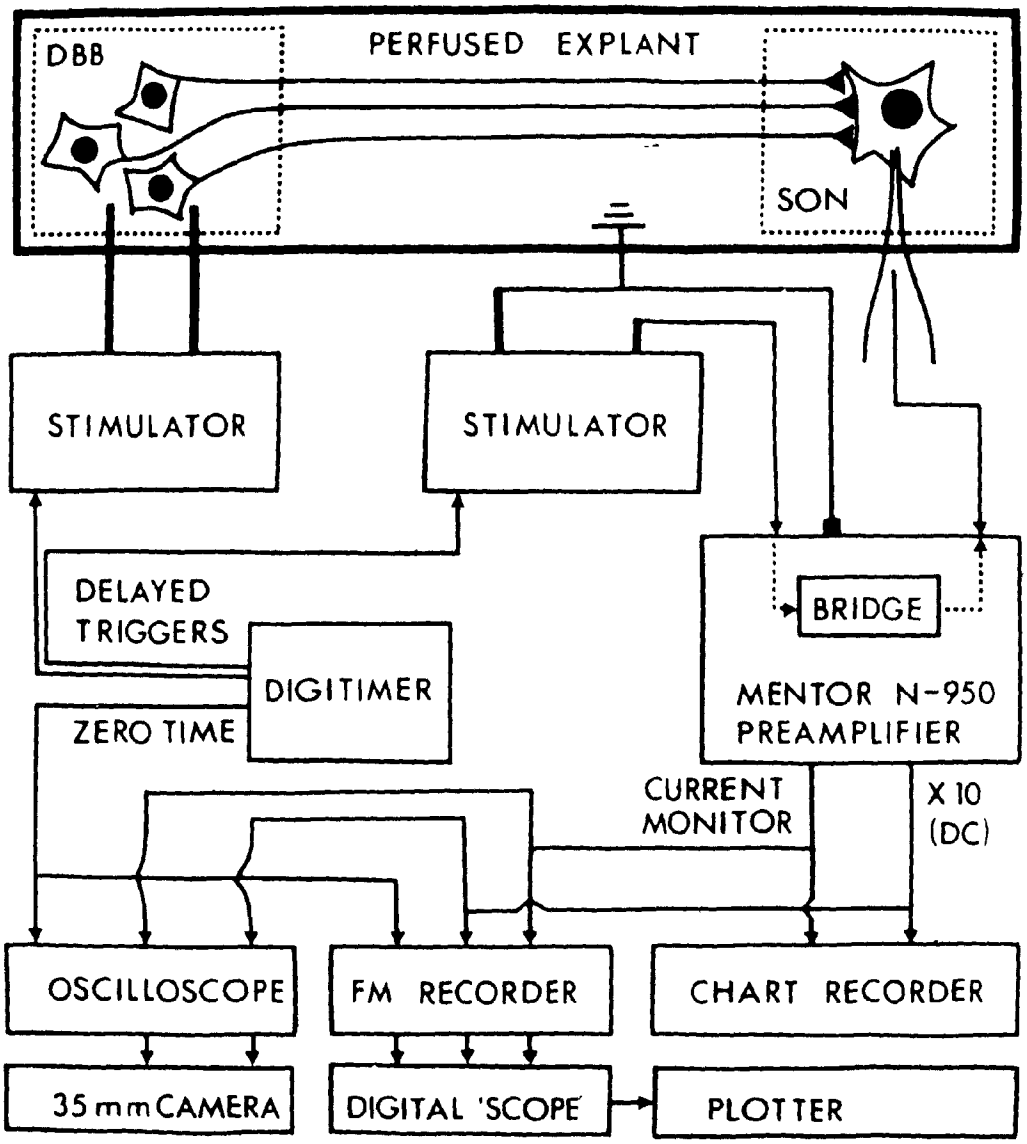
DBB
PERFUSED EXPLANT
SON
STIMULATOR
STIMULATOR
DELAYED
TRIGGERS
DIGITIMER
ZERO TIME
BRIDGE
MENTOR N-950
PREAMPLIFIER
CURRENT
MONITOR
X 10
(DC)
OSCILLOSCOPE
FM RECORDER
CHART RECORDER
35 mm CAMERA
DIGITAL 'SCOPE
PLOTTER

Figure 2-8 Equivalent circuit of an inhibitory synapse. The non-synaptic membrane is represented as an ionic battery (E_m) for the resting membrane potential (V_m) in series with the resting membrane resistance (R_m). The synaptic membrane is represented in parallel with the non-synaptic membrane as an ionic battery for the IPSP (E_{IPSP}) in series with a resistance (R_{IPSP}). The action of a transmitter during an IPSP is equivalent to closing the switch.

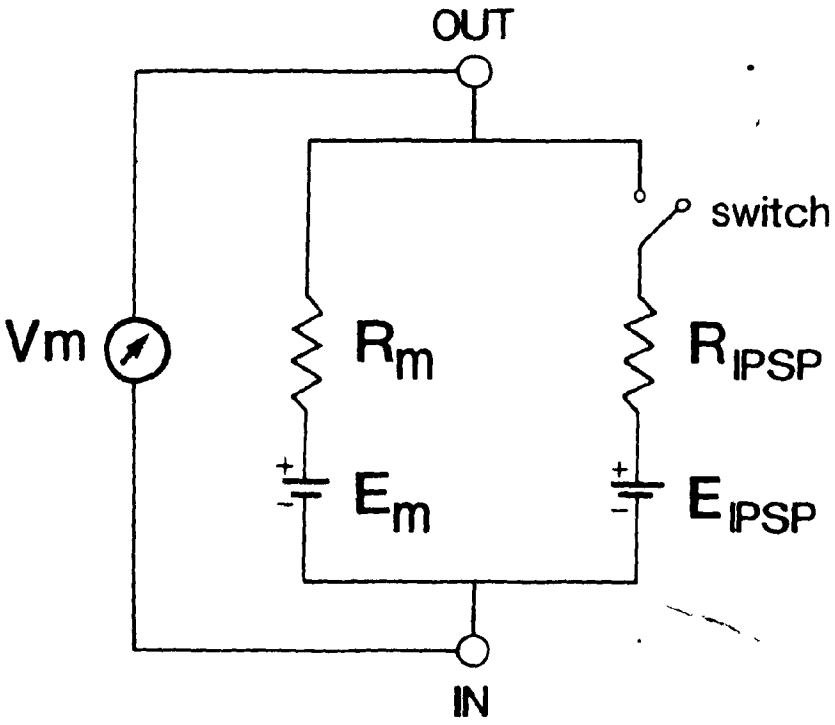
OUT
switch
Vm
R_m
R_{IPSP}
E_m
E_{IPSP}
IN

Figure 2-9 The schematic in the lower part of the picture depicts the approximate dimensions of the rat hypothalamic explant and pituitary (PIT). Orientation is indicated on the lower right. A recording micropipette filled with Lucifer yellow is directed towards the supraoptic nucleus (SON), along the lateral edge of the optic chiasm (OC). Planes of horizontal and coronal sections are indicated by interrupted lines. During intracellular injection in a typical cell, the voltage (upper) and current (lower) traces at the top of the figure indicate that hyperpolarizing current is injected continuously (0.5 nA) and also intermittently (as an additional 0.3 nA pulse). Note the presence of occasional 'anode break' action potentials in the voltage trace.

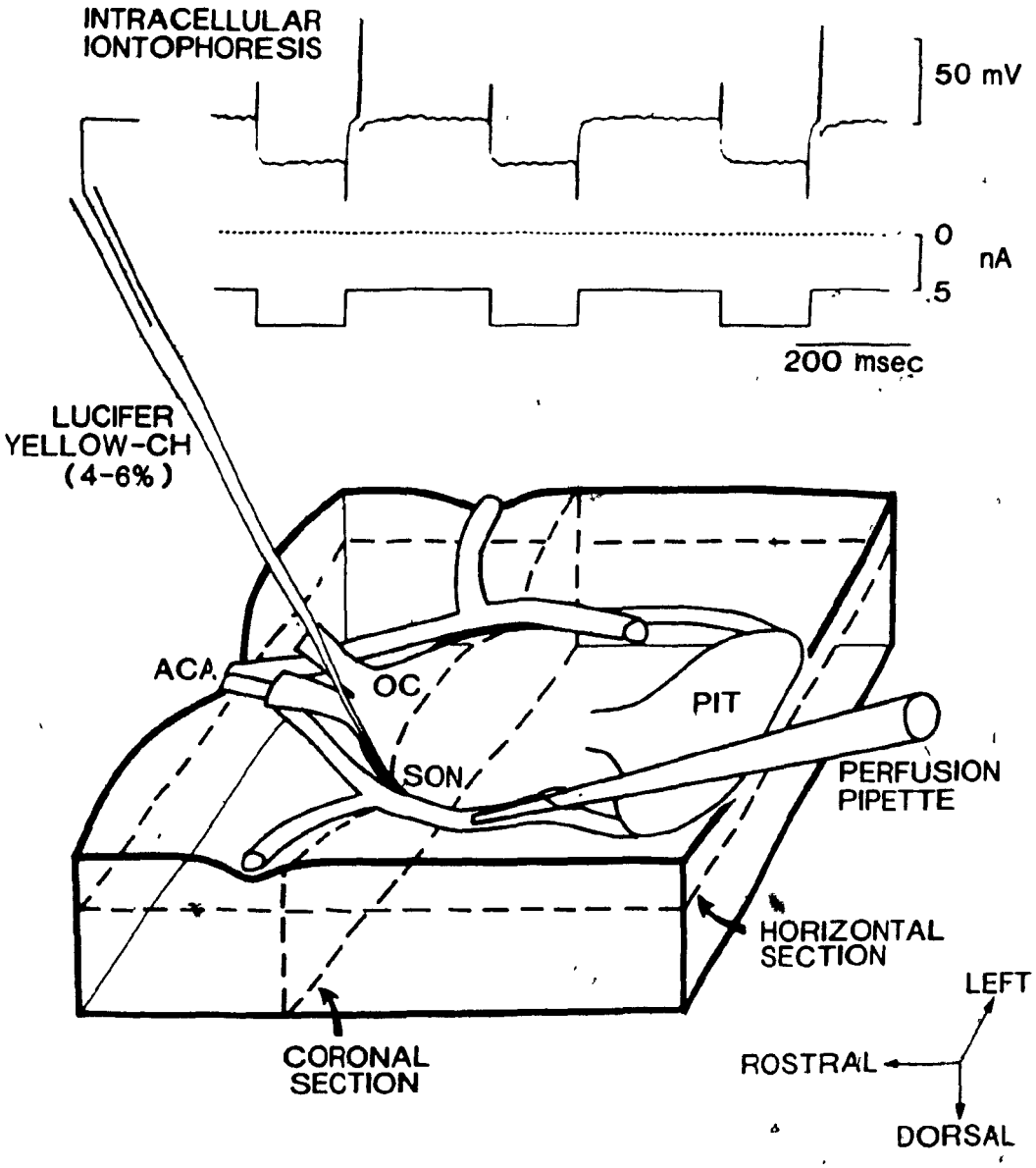
INTRACELLULAR
IONTOPHORESIS
50 mV
0
nA
.5
200 msec
LUCIFER
YELLOW-CH
(4-6%)
ACA
OC
PIT
SON
PERFUSION
PIPETTE
HORIZONTAL
SECTION
CORONAL
SECTION
LEFT
ROSTRAL
DORSAL

Figure 2-10 Cresyl violet stained coronal (a-b) and horizontal (c) sections from hypothalamic explants that were fixed by immersion after 8 hrs. of intra-arterial perfusion with artificial cerebrospinal fluid. Vertical arrows indicate the changing profile of the SON from a rostral position (a) along the lateral edge of the optic chiasm (OC) to a more caudal position (b) along the lateral border of the optic tract (OT). In the horizontal plane the SON is identified by oblique arrowsheads placed along its medial and lateral borders. The interrupted lines identify the approximate plane of section of the respective coronal sections. Calibration bar 500 µm. Abbreviations: 3V, third ventricle; SCN, suprachiasmatic nucleus; SON, supraoptic nucleus.

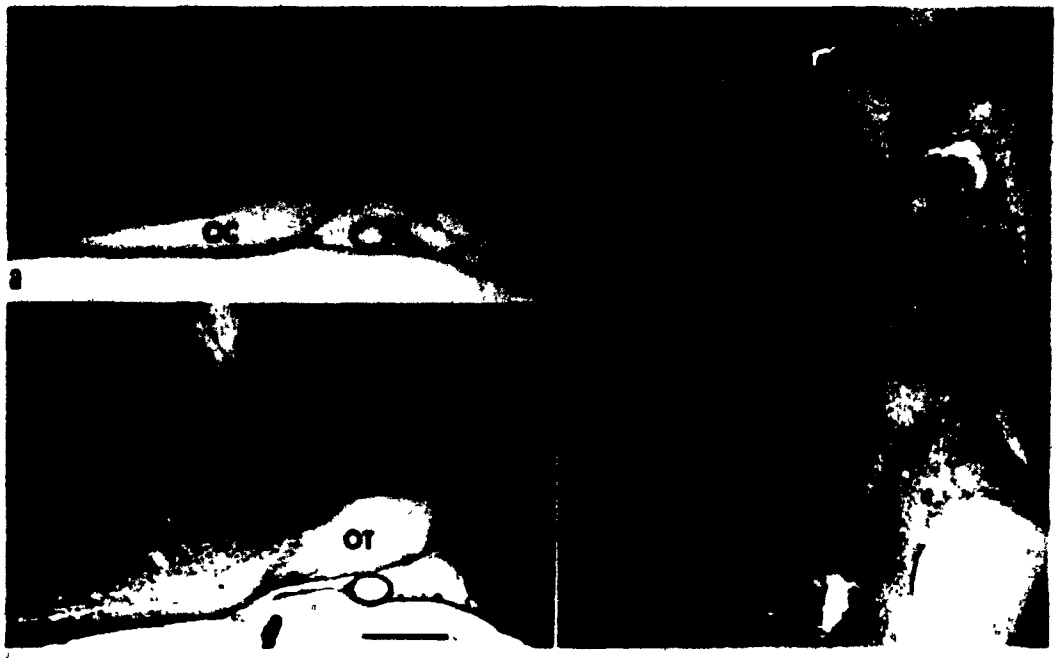
OC
OT

Figure 2-11 Reconstruction of Lucifer yellow-filled SON neurons. Top: Photographic reconstructions of neurons were made by apposing segments of neuronal processes found in adjacent histological sections. This example shows low power photographs of the soma and dendrites of a neuron in horizontal section. Bottom: Drawings were made by tracing the negative image on a microfilm projector. In this example, high power negatives of a dendrite taken in different focal planes are combined to illustrate dendritic spines.

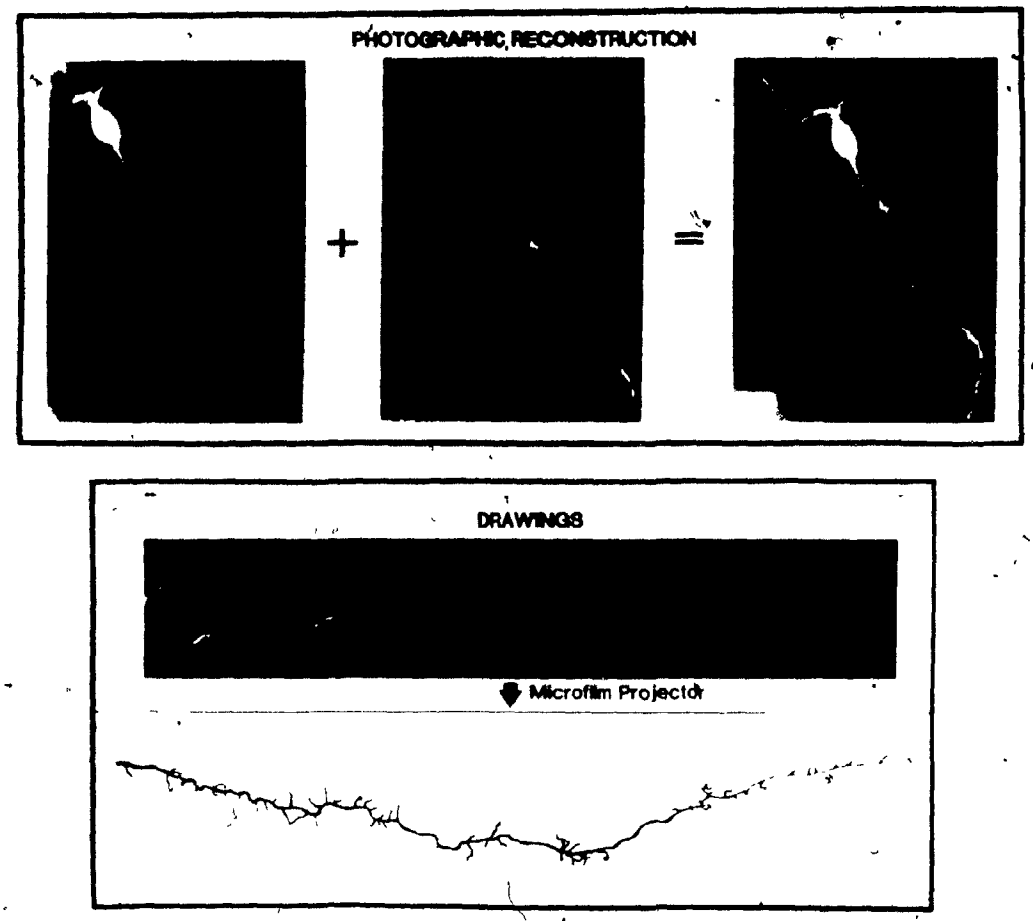
PHOTOGRAPHIC RECONSTRUCTION
DRAWINGS
Microfilm Projector

CHAPTER 3

SERIAL RECONSTRUCTION OF LUCIFER YELLOW-FILLED SON NEURONS

3.1 Introduction

Early studies on the light microscopic morphology of SON neurosecretory neurons were hampered by the resistance of these neurons to Golgi stains (see Chapter 1). Immunocytochemical approaches (Swaab et al., 1975; Vandersande and Dierickx, 1975) have not only circumvented this problem but also enabled the distinction between neurons that synthesize either vasopressin or oxytocin. Nevertheless, one of the drawbacks of successful Golgi and immunocytochemical experiments is the multiplicity of neurons that are stained, making it is difficult to follow the processes of a single neuron in order to obtain whole-cell reconstructions. The latter is an important step in the characterization of neuronal cytoarchitecture relative to surrounding structures or afferent fibers.

When situations permit stable intracellular recordings, a suitable alternative is whole-cell reconstruction after injection of a diffusable marker (Preston et al., 1980). In the hypothalamus, in vitro intracellular recordings and labelling of neurosecretory neurons with the fluorescent naphthalamide dye, lucifer yellow, has recently been

achieved in tissue slices (Andrew et al., 1981) and perfused explants (Bourque and Renaud, 1983). Both preparations offer excellent stability and quality of recordings. However, in slice preparations, SON neurons are likely to lose a part of their dendritic tree and/or axon. In contrast, entire SON cells are likely to remain intact in perfused hypothalamic explants. This chapter reports on the morphological features of SON neurons in hypothalamic explants as revealed by whole-cell reconstruction following intracellular lucifer yellow injection.

3.2 Results

Forty-nine injections were made in 27 explants, yielding 57 LY labelled cells; the sample included cells located throughout the rostrocaudal extent of the nucleus and situated at various depths within its dorsoventral boundaries. Fifteen were chosen for complete analysis, including 4 in the horizontal plane (Figures 3-1, 3-3) and 11 in the coronal plane (Figure 3-2). Criteria for selection included their apparent completeness when assembled from consecutive histological sections and the presence of intense fluorescence in distal dendrites, an indication that all parts of the cell were likely to have been filled. On four occasions, more than one cell was labelled by a single injection (see consideration in Section 3.3 and Figure 3-10). Such neurons demonstrated traits

similar to those reported below but were excluded from analysis owing to the difficulty of assigning a given process to a given soma.

Somata: The somata of LY-filled SON cells were occasionally round but most often (80%) elongated with a mean long axis of 25.4 µm and a shorter diameter of 12.5 µm (Table 1). Spine-like protuberances arose from the soma of 50% of the cells; some of these processes achieved lengths up to 15 µm (Figure 3-4).

Dendrites: Each SON cell contained one to three primary dendrites, readily recognized by their numerous spiny processes (24.6 per 100 µm of dendrite). The latter varied widely in length (up to 15 µm), thickness and direction, and ended in filamentous, club-like and grape cluster-like dilatations (Figure 3-5). Individual primary dendrites ranged in length between 68 and 725 µm, tapering gradually and branching sparingly (Table 3.1). The combined length of all dendrites of an individual neuron ranged between 536 and 1456 µm with a mean of 880 µm. In the rostrocaudal direction, a given cell's dendritic tree extended from 22 to 56% of the extent of the nucleus. Most dendrites of SON cells remained entirely within the confines of the nucleus. The majority (95%) eventually entered the glial lamina immediately ventral to the nucleus (Figure 3-2). On rare

occasions dendrites were observed to course beyond the nuclear boundary in the ventral glial lamina, either laterally towards the temporal lobe or medially along the ventral surface of the optic tract (Figure 3-2). No dendrite was observed to extend beyond the dorsal border of the nucleus.

Axons: Axons were distinguishable by their smaller diameter, paucity of spinous processes, and beaded varicose appearance due to large rounded swellings (Figure 3-6a,b). In 40% of cells the axon arose directly from the soma (Figures 3-4a, 3-7, 3-8): when this occurred, the initial 50-100 µm segment of the axon usually resembled a dendrite by virtue of the presence of short spiny processes (Figures 3-7, 3-8). In the remaining cells the axon appeared to originate from a proximal portion of a dendrite (Figures 3-3, 3-4b); such axons possessed few or no spinous processes and immmediately developed varicosities.

Axons from all labelled cells initially coursed dorsally then caudally over the optic tract, after which they turned sharply in the medial and ventral direction to enter the mediobasal hypothalamus. Axons were followed for up to 2100 µm. No axon collaterals of a similar magnitude were observed. However, an occasional short spine-like process (Figure 3-6c,d) could be visualized on many of the axons as they coursed in the lateral hypothalamic area

dorsal to the SON. Two axons possessed clusters of spine-like processes (Figure 3-6e,f) and one axon displayed a bouton-like structure (Figure 3-6g).

3.3 Discussion

Intracellular staining with horseradish peroxidase is usually viewed as superior to LY in terms of stability of the labelled product. However, the disadvantage of fading LY fluorescence in studies on SON neurons is balanced by the relative ease with which impalements can be maintained during dye injection with hyperpolarizing current pulses. In the present circumstances, the depolarizing current pulses required to eject horseradish peroxidase and the need to have somewhat large electrode tips to prevent blockage would clearly impede progress in the study of SON cells in view of their small size, high membrane resistance (Mason, 1983b; Renaud et al., 1985) and general resistance to stable impalements.

Details visualized with LY injections include spine-like processes arising from somatic and dendritic surfaces. At the ultrastructural level, many of these are sites of synaptic contact (Ifft and McCarthy, 1974; Leranth et al., 1975; see also Figure 3-9). The more prominent and elongated structures protruding from somata (Figure 3-4) may in fact be cilia which have been reported previously in fish preoptic neurons (Palay, 1961; Scharrer, 1962; Vigh-

Teichmann et al., 1976a,b), reptile (Vigh-Teichmann et al., 1976) and neonatal rat (Lafarga et al., 1980) SON and paraventricular neurons (see also Figure 3-9d). As one proceeds distally towards the endings of dendrites, an abundance of different hair-like processes may be indicative of their specialized function, perhaps to act as an anchor for axons 'en passage' (cf. Ifft and McCarthy, 1974), or as a sensing device, e.g. for plasma or extracellular osmotic pressure. In agreement with earlier data (Armstrong et al., 1982; Dyball and Kemplay, 1982) is the observation that one or more of the dendrites of SON cells extend to and end within the ventral glial lamina. It is also apparent from whole cell reconstructions that the dendritic tree of an individual SON neuron may extend over 40% of the nucleus. Therefore, on a strictly morphological basis, it would seem reasonable to exercise caution in ascribing importance to rostrocaudal or dorsoventral distributions of afferent fibers with respect to the position of immunoreactive vasopressin or oxytocin cell somata. More specifically, the predominantly ventral catecholamine innervation of the SON (McNeill and Sladek, 1980; Sawchenko and Swanson, 1982; Swanson and Sawchenko, 1983) may not only contact the predominantly ventrally located vasopressinergic neurons; dendrites of the more dorsally located oxytocinergic neurons are equally likely to extend into this region. However, in this particular instance, recent electrophysiological data

(Day and Renaud, 1984) have in fact corroborated impressions based on double labelling anatomical studies (McNeill and Sladek, 1980; Sawchenko and Swanson, 1982; Swanson and Sawchenko, 1983) that noradrenergic afferents originating in the ventrolateral medulla selectively innervate vasopressinergic SON neurons.

In comparison with the experience of other investigators (Andrew et al., 1981; Mason, 1983) who have reported that dye coupling between LY labelled magnocellular neurons is a common occurrence, our experience would indicate quite the contrary. When we note that two (or more) neurons fluoresced after a single LY injection, both cells were closely apposed, one was more intensely labelled than the other and fluorescent material could usually be seen in an apparent extracellular location (Figure 3-10). It was our impression that the injected cell was either injured and leaked the dye, or that a part of the injection was delivered into the extracellular space. Of potential significance is the difference between hypothalamic slices and hypothalamic explants. In hypothalamic slices, where dye coupling is most often seen, axotomy (or dendritic severance) is inevitable and may contribute to an enhanced capacity for dye coupling among mammalian magnocellular neurosecretory cells, similar to that reported between abdominal ganglion cells in the snail Helisoma (Murphy et al., 1983). The prevalence of LY dye

coupling between magnocellular neurons in hypothalamic slice preparations is influenced by the animal's hydration state and osmotic pressure of the perfusion media (Cobbett and Hatton, 1984). It would also be interesting to explore the influence of steroid hormone levels and the reproductive state, so that an understanding of the significance of dye coupling might become more obvious. Evidently this issue deserves further study.

These data confirm that the axons of SON cells course dorsomedially as they leave the nucleus, pass over the optic tract and descend ventrally (Alonso and Assenmacher, 1981; Dyball and Kemplay, 1982). Once the axon has exited from the nucleus, distinctions between dendrites and axons become obvious with the axons bearing frequent large varicosities and few spinous processes. Exceptions were the few large spines noted on axons in the region dorsal and medial to the SON (Figures 3-6, 3-7, 3-8), the only observations that approximated the 'axon collaterals' reported in a recent HRP tracer study (Mason et al., 1983) to arise from SON axons in this vicinity. At this time we cannot confirm the existence of 'true' axon collaterals in SON cells; however, our sample size is relatively small. It is also possible that LY, which spreads by diffusion, does not enter axon collaterals. This would seem unlikely in view of the excellent filling of axons up to 2100 μm from the soma (i.e. 1500 μm beyond the anticipated location of collaterals) and

the ability for LY to fill tiny spines and branches within distal dendritic trees (Figure 3-5). Therefore, it would seem that axon collaterals are not a prominent feature of the axons of the SON, and that alternative explanations (cf. Andrew and Dudek, 1984a; Bourque et al., 1985; Leng and Dyball, 1983; Leng and Dyball, 1984) must be sought to explain 'recurrent inhibition' (Barker et al., 1971; Dreifuss and Kelly, 1972) in the supraoptico-neurohyopophysial pathway.

As noted previously (Dyball and Kemplay, 1982), axons of SON neurons may arise from either the soma or a dendrite. Based on our sample, almost two thirds of SON axons appear to arise from a dendrite, sometimes as far as 32 μm from the soma. In the other instances where the axons appears to arise directly from the cell soma, the presence of spinous processes and lack of typical varicosities on the initial 50-100 μm of the axon bears a striking resemblance to a dendritic profile and may, in fact, be dendritic in nature. The initial segment has not been described in ultrastructural studies of SON neurons, perhaps because it is remotely located from the soma in all SON cells. It remains to be defined at the ultrastructural level whether the initial part of the presumed axon in SON neurons such as those in Figures 3-4a, 3-7 and 3-8 is really 'axonal' or 'dendritic' in nature. These data will have a bearing on our understanding of the generation of propagated action potentials in SON neurons.

TABLE 3-1

Summary of the morphological features of 15 LY filled SON neurons. The column to the right refers to the site of origin of the axon as dendritic (D), somatic (S) or unknown (?); when dendritic in origin, numbers in brackets refer to the distance (in microns) from the soma to the apparent site of origin of the axon.

Cell	Soma Size (um)	# of Dendrites	(lengths) (um)	# of branches	(lengths) (um)	Total dendritic length (um)	Spine density (#/100 um)	Axon origin*
1	12 x 30	2	357 316	2 2	(266,90) (36,27)	1092	37.5	D(12)
2	10 x 25	2	445 291	3 1	(38,25,10) (251)	1060	27.4	S
3	11 x 18	3	160 430 320	0 0 0		910	17.7	D(32)
4	11 x 20	3	220 255 61	0 0 0		536	27.1	D(32)
5	7 x 23	1	625	1	(17)	642	30.1	S
6	21 x 35	3	68 390 315	0 0 1	 (215)	988	n.d.	S
7	16 x 25	2	328 410	2 0	(100,28)	866	31.7	D(8)
8	12 x 23	2	175 655	0 0		830	36.1	S
9	15 x 20	2	445 162	0 0		607	23.4	S
10	14 x 25	2	604 725	0 1	 (70)	1399	18.0	D(10)
11	14 x 30	2	467 443	0 1	 (267)	1177	17.8	D(9)
12	16 x 32	2	274 467	0 0		741	17.8	?
13	11 x 25	3	573 378 505	0 0 0		1456	18.5	D(6)
14	9 x 24	2	430 480	0 0		910	14.2	?
15	11 x 24	2	315 360	0 0		675	22.6	D(18)

Figure 3-1 Reconstruction of 4 SON neurons in the horizontal plane. The solid line depicts the lateral edge of the optic tract; the interrupted line represents the lateral edge of the nucleus. Orientation: C, caudal; R, rostral; L, lateral; M, medial. Note that presumptive dendritic processes remain within the confines of the nucleus, whereas single unbranched axons arise from either the soma (cells 4 and 6) or a proximal dendritic profile (cells 1 and 7) and course caudomedially over the optic tract.

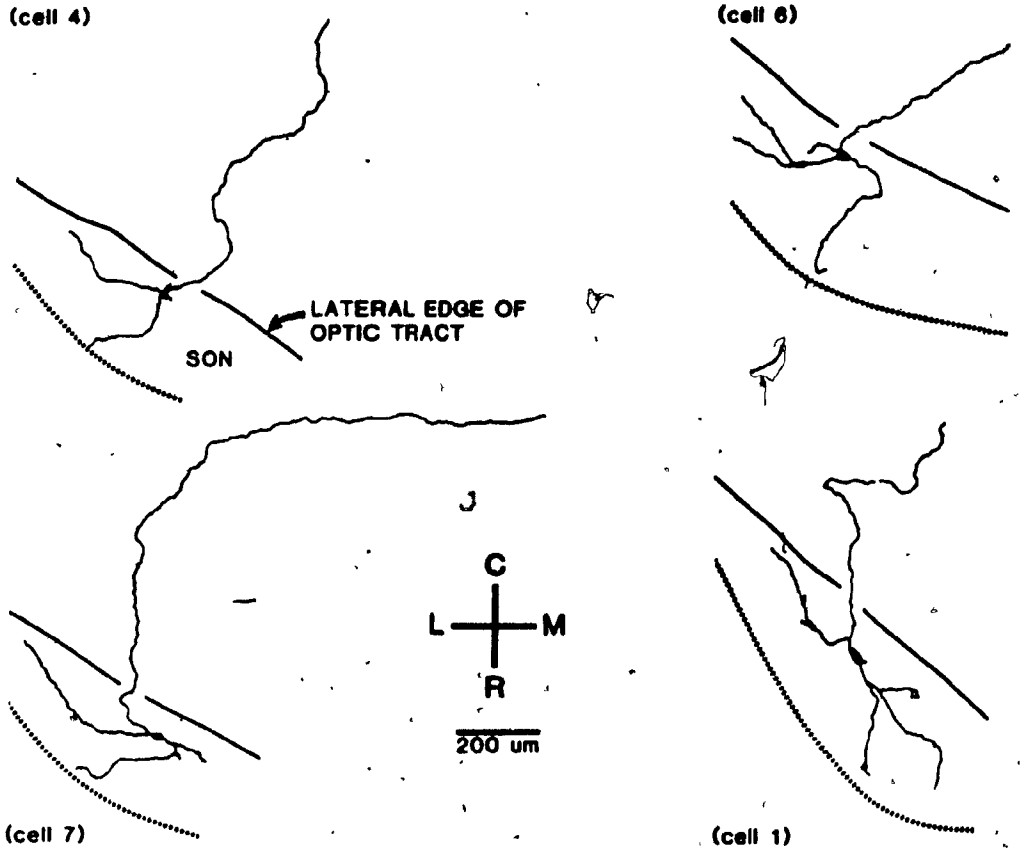
(cell 4)
LATERAL EDGE OF
OPTIC TRACT
SON
(cell 6)
C
L
M
R
200 um
(cell 7)
(cell 1)

Figure 3-2 Reconstructions of 5 SON neurons in the coronal plane. The shaded area depicts the cut end of the optic tact. Most dendrites eventually course towards the ventral surface. The dendrites of cell 10 were rare in that they extended laterally beyond the confines of the SON (filled star) while those of cell 11 course onto the ventral surface of the optic tract (open star). The single axon follows a tortuous dorsomedial and caudal trajectory.

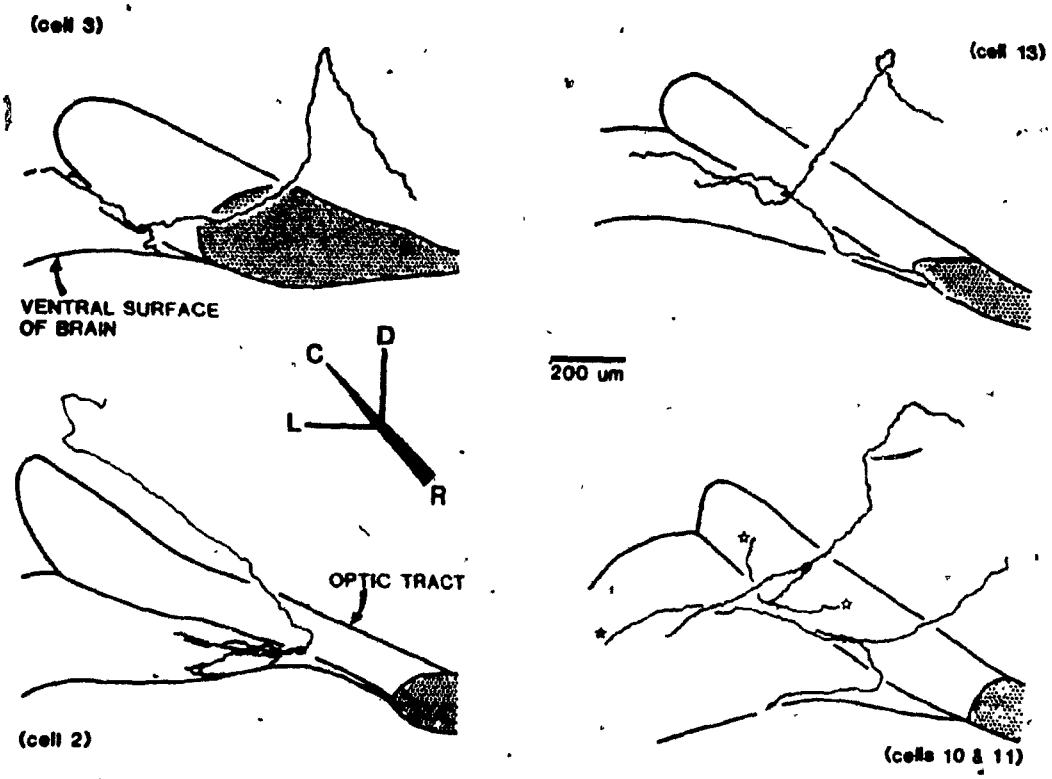
(cell 3)
VENTRAL SURFACE
OF BRAIN
C
D
L
R
(cell 13)
200 um
OPTIC TRACT
(cell 2)
(cells 10 & 11)

Figure 3-3 More details of cell 1 (cf Figure 3-1) are illustrated in a photomontage (above) and the composite reconstructed from negatives obtained at 320 X magnification (below). Presumptive dendrites contain numerous spinous processes and eventually taper to a fine termination within the nucleus, usually along the ventral glial lamina (VGL). The axon is recognized by its varicosities, extranuclear destination and lack of collaterals.

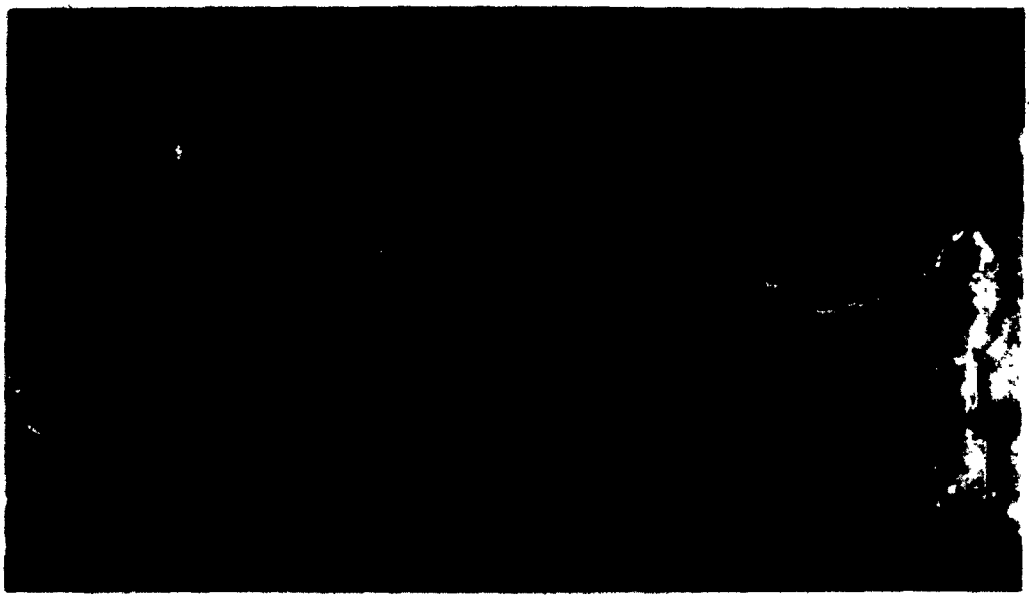

(cell 1)

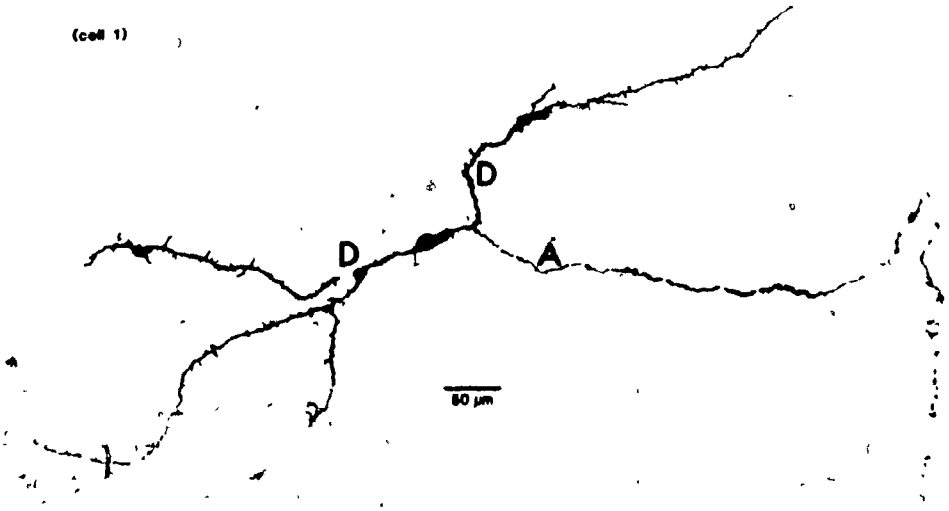

Figure 3-4 Montages of the somata of two LY-filled SON magnocellular neurons reconstructed from photographs taken in several focal planes of a single 40 µm histological section. The cell in (a), (Cell 8 in Figure 3-7 has several somatic spines (arrowheads), the origin of a ventrally directed dendrite (D) and a dorsally directed axon (A). In (b), (cell 1 in Figures 3-1 and 3-3) note the particularly prominent somatic spine along with several smaller spines. Spines are present on two dendrites (D) originating at opposite poles of this cell. The axon (A) originates from the caudally-directed dendrite but was visible for only a short distance in this section. The apparent diameter of the soma and dendrites are increased by the overexposure of the original negative necessary to visualize the less intensely fluorescent spines. Scale bar = 15 µm.


a
b
D

Figure 3-5 High power photomontages illustrate features typically associated with dendrites. In (a), a segment of dendrite located 50 µm from the soma (curved arrow points towards the soma) reveals numerous club and grape cluster-like (arrow) spinous processes proximal to a branch point and filamentous (arrowhead) processes beyond the branch point. Processes contain numerous constrictions and angular enlargements. In (b), the distal segment of a dendrite located 300 µm from the soma displays a complex array of spines. Scale bar = 15 µm.

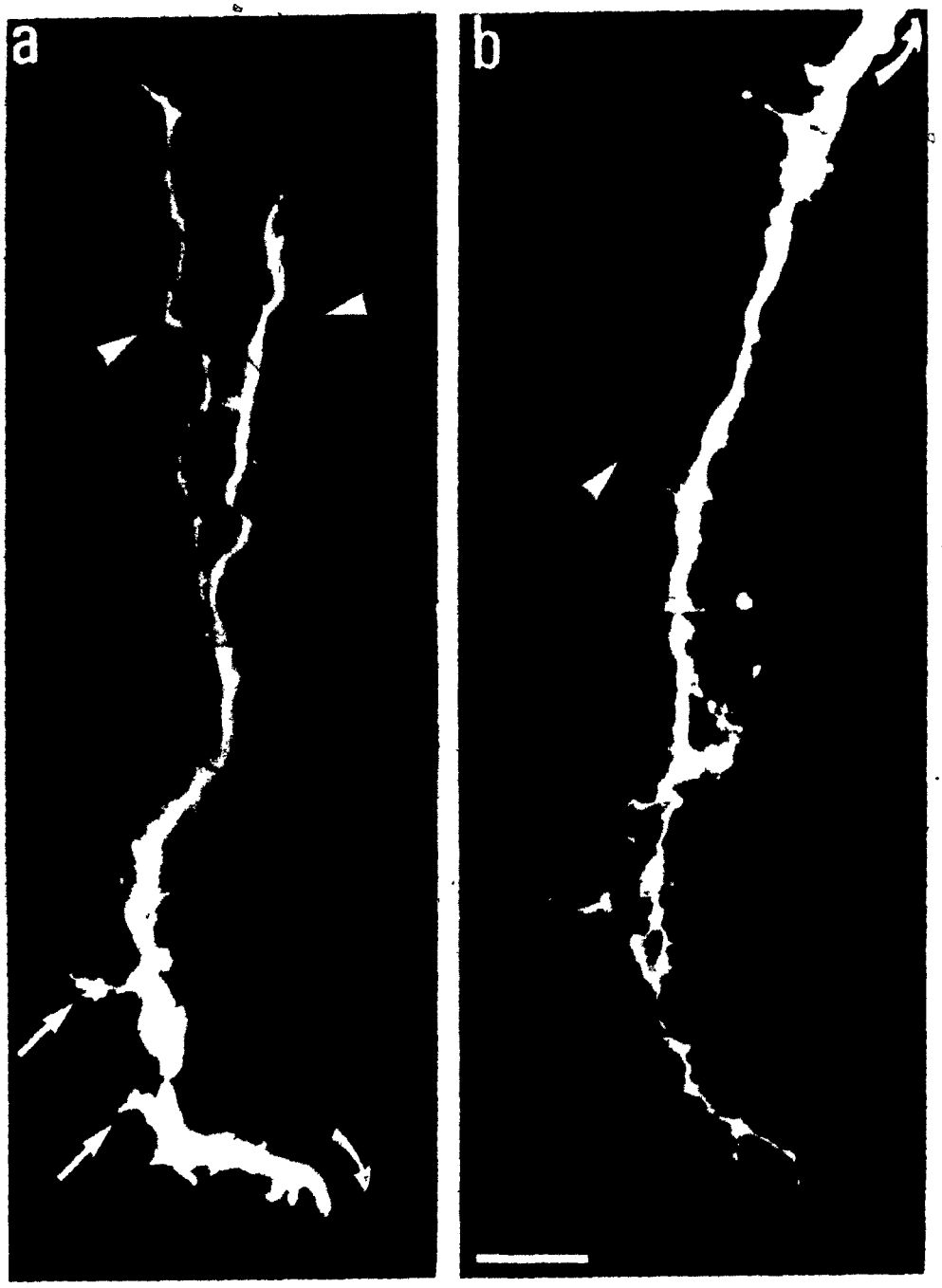
a
b

Figure 3-6 High power photomontages reveal details of the axons of different LY-filled SON neurons. In (a), note the typical varicose appearance. The remaining pictures demonstrate specializations associated with that portion of the axon located dorsomedial to the SON, as it courses over the optic tract. (b), a large varicosity (arrowhead) situated 500 µm from the soma. (c), a small secondary axonal process (arrow) found 700 µm from the soma. (d), an unusually large secondary axonal process (arrow) detected 200 µm from the soma. (e,f), areas of specialization (between arrows) in two different axons (approximately 400 µm from soma) where spine-like processes are visible. In (f) one varicosity yields 5 short secondary processes with bouton-like endings; another is surrounded by extremely fine processes that are poorly resolved in this focal plane. (g), a secondary process (arrow) with a large bouton-like ending that approaches but does not touch the parent varicosity. Scale bar = 15 µm.

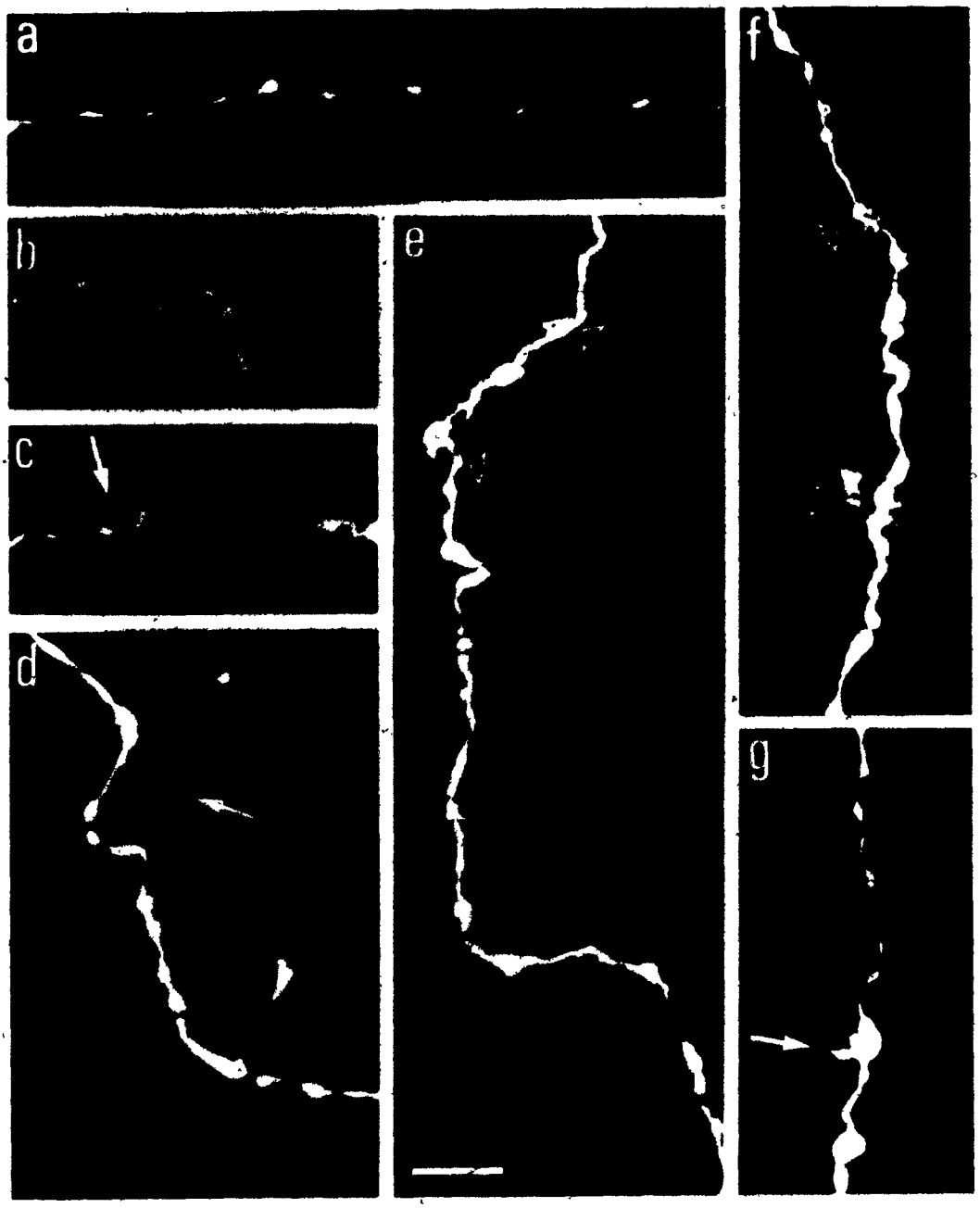
a
b
c
d
e
f
g

Figure 3-7 Drawings of a SON neuron whose axon originates on the soma. This cell possessed two ventrally directed dendrites with the usual complement of spines (see the inset labelled 'D'). The third, dorsally directed process is clearly the axon as judged by its trajectory. Note, however, that its initial 200 µm segment (A1) has numerous spines similar to those observed on dendrites. As the axon leaves the SON, it becomes thinner and devoid of spines (A2). In the region dorsal to the optic tract, the axon displays a region of many large thickenings and a few spines (A3). The axon then becomes thinner and less varicose as it continues on its trajectory into the basal hypothalamus. Reconstruction from coronal sections; same cell as Figures 3-4a. Scale bar is 50 µm for main drawing, 10 µm for insets.

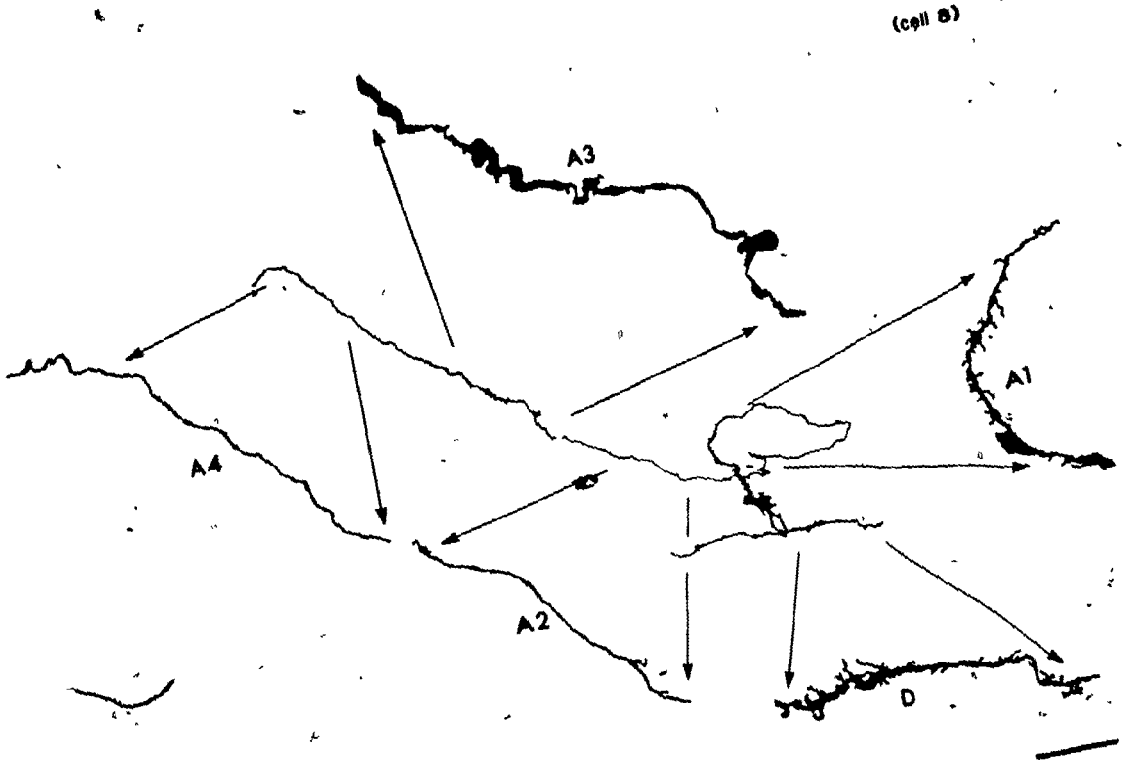
(cell 8)
A3
A1
A4
A2
D

Figure 3-8 Drawings of a SON neuron whose axon originates on the soma. This cell possessed a single dendrite, directed ventrally and caudolaterally, with the usual complement of spines (see inset labelled D). The second process, directed dorsally and medially is clearly the axon as judged by its trajectory. Note, however, that its initial 100 µm segment (A1) has numerous spines similar to those observed on dendrites. As it leaves the SON, the axon has fewer spines but displays large varicosities (A2). Reconstruction from coronal sections. Scale bar is 50 µm for main drawing; 10 µm for insets.

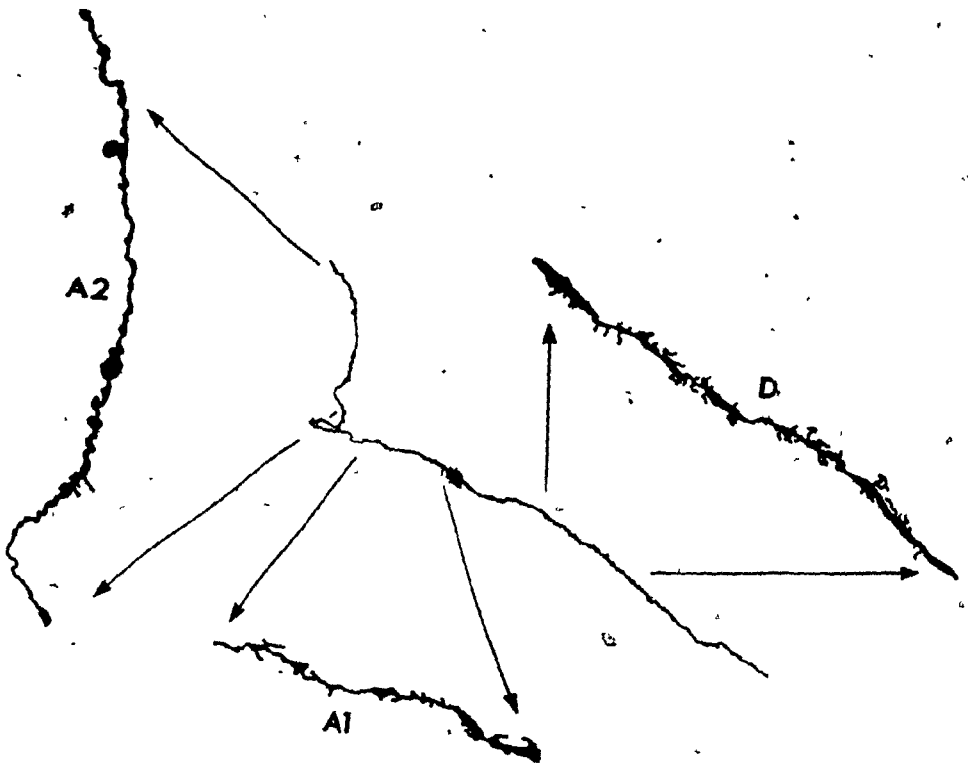

(cell 5)

Figure 3-9 Electron micrographs of spines and cilia on SON neurons. (a-c) Spines (arrowheads) were commonly observed on dendritic (D) or somatic (S) profiles. Presynaptic elements (stars) containing synaptic vesicles were located adjacent to spines. Synaptic specializations (membrane thickening) were often evident either on the spine or on the dendritic (D) or somatic (S) membrane at its base. As in (C), one or a pair of spines sometimes appeared to surround a presynaptic element as if to secure it against a segment of dendritic or somatic membrane where a synapse was formed. In (d) a cilium arises from the soma of an SON neuron (arrowhead) and projects a considerable distance out of the plane of section (arrow). Inset is a cilium cut in cross-section. Magnification: a,c and d (inset) 34,000x; b and d 18,000x. Courtesy of Joanne Rogers.

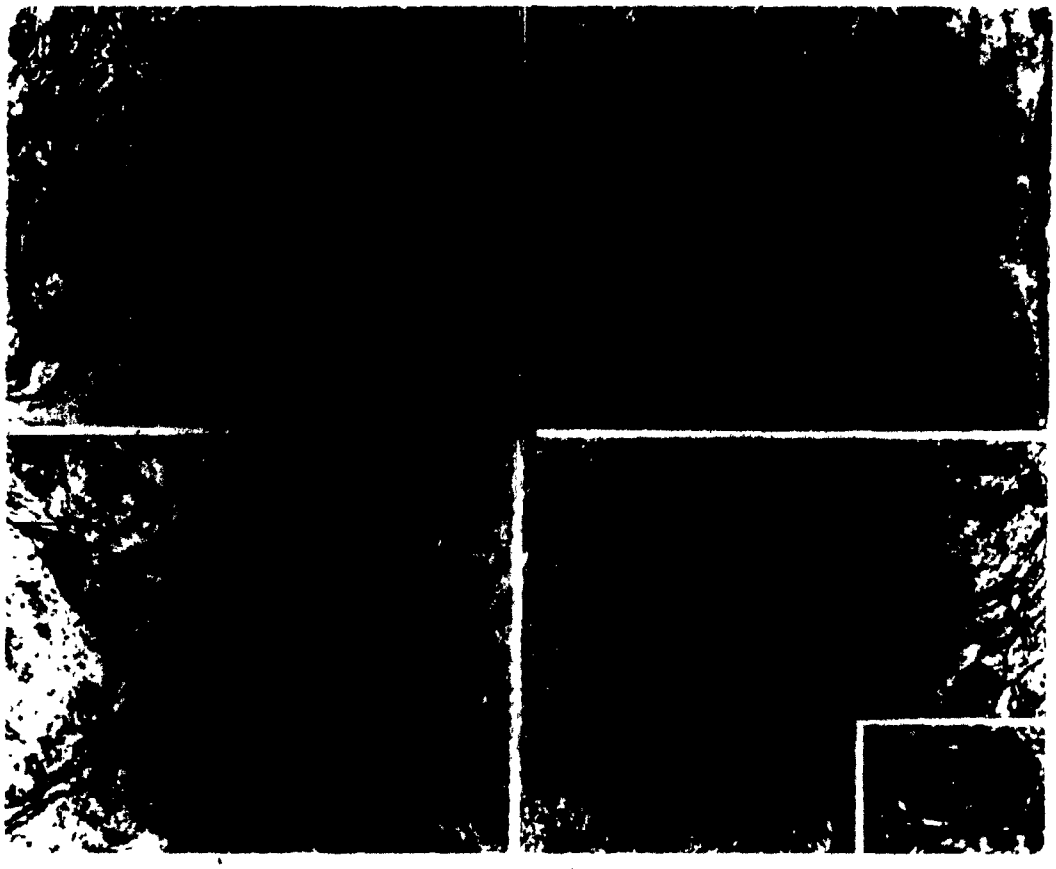

Figure 3-10 On four occasions, more than one cell was labelled by a lucifer yellow injection. In (a), at least 3 SON neurons and perhaps a glial cell were labelled; in this coronal section, two axons follow the normal course dorsal to the optic tract (ot). Inset shows somata photographed with shorter exposure. In (b), at least 4 neurons were labelled following this lucifer yellow injection. In this horizontal section, several dendrites and a blood vessel (star) are visible. Scale bar = 50 µm.

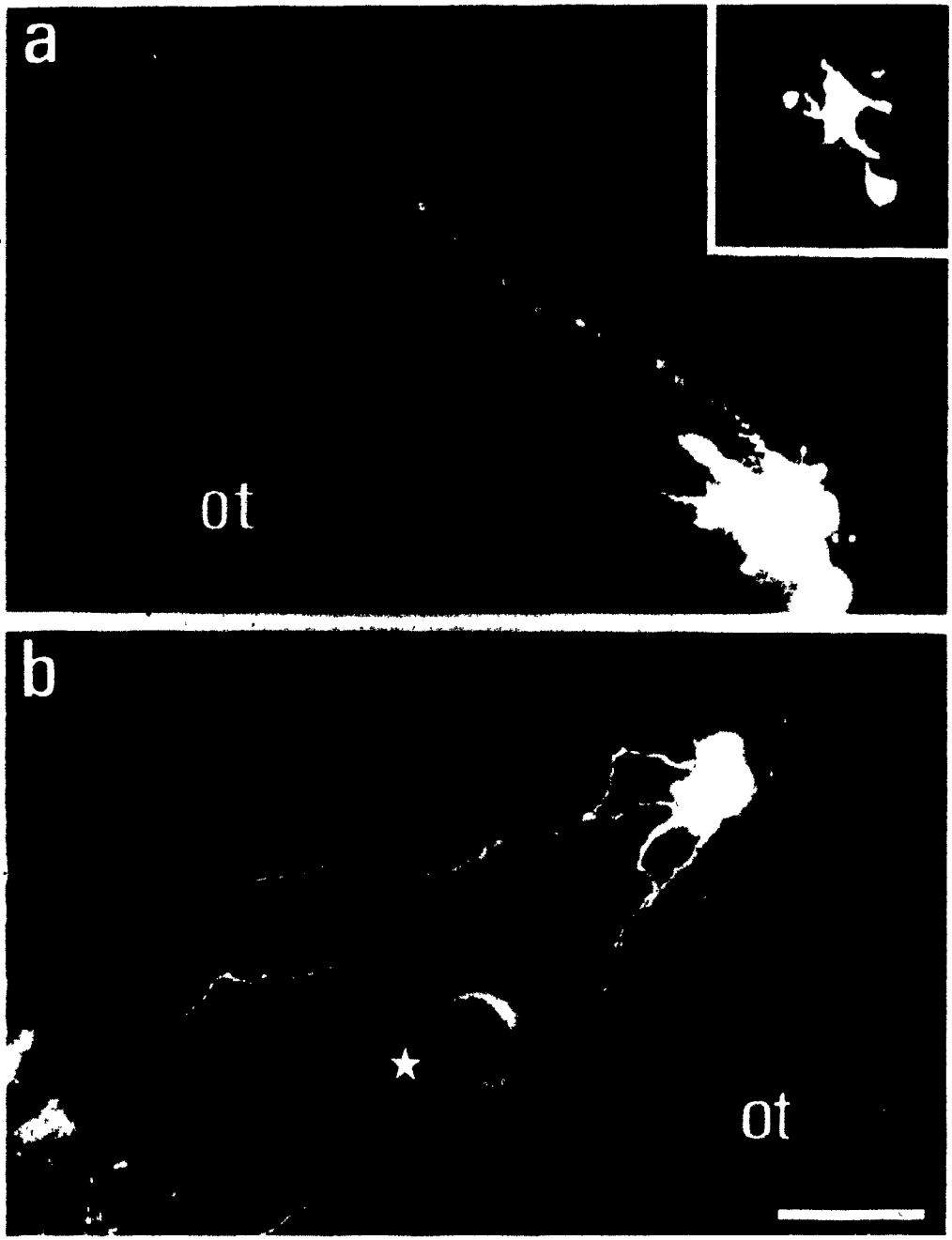
a
ot
b
ot

CHAPTER 4

CHARACTERISATION OF SPONTANEOUS AND EVOKED POST-SYNAPTIC POTENTIALS (PSPs) IN SON NEURONS

4.1 Introduction

As recently as a decade ago it was stated that neurosecretory neurons had few afferent connections (cf. Cross et al., 1975). With the advent of improved retrograde and anterograde anatomical tracer techniques, it is now evident that this is not the case. In fact, SON neurons receive afferents from several parts of the brain including the septum, anteroventral third ventricular area, diagonal band of Broca, lateral hypothalamus, amygdala, subfornical organ, and brainstem (Carithers et al., 1980, 1981, 1984; Miselis et al., 1979; Powell and Rorie, 1967; Renaud et al. 1983; Swanson and Sawchenko, 1983; Tribollet et al., 1985; Zaborsky et al., 1975).

To date, electrical stimulation in a number of these regions has been shown to alter the electrical activity of SON neurons recorded *in vivo* (Cirino and Renaud, 1985; Day and Renaud, 1984; Ferreyra et al., 1983; Hamamura et al., 1982; Sgro et al., 1984; Poulain et al., 1980). Furthermore, several of these regions appear to participate in or influence neuroendocrine reflexes that govern the release of vasopressin and oxytocin (Aulsebrook and Holland, 1969;

Iovino et al., 1983; Lebrun et al., 1983; Mangiapane et al. 1983; Sladek and Johnson, 1983; Thornton et al., 1984; Woods et al., 1969; Yamashita, 1977). For example, synaptic inhibition appears to be important in the control of SON neuron action potential firing (Poulain et al., 1980; and reflex oxytocin (Lebrun et al., 1983) and vasopressin secretion (Knepel et al., 1980).

In keeping with the notion that SON neurons do receive afferent impulses is the observation from intracellular recordings that SON neurons have both spontaneous and evoked post-synaptic potentials (PSPs; Andrew and Dudek, 1983; 1984a,b; Bourque, 1984; Hatton et al., 1983; Koizumi and Yamashita, 1972; Mason, 1983,1984). In the hypothalamic explant, inhibitory PSPs (IPSPs) are the predominant form of spontaneous synaptic input and electrical stimulation rostromedial to the SON also evokes a powerful compound IPSP (Bourque, 1984). Therefore, it is important to understand how individual PSPs alter the membrane properties of SON neurons. This chapter describes the results of experiments performed to characterize the IPSPs in terms of the magnitude and specificity of the underlying current, and the transmitter responsible for their activation.

4.2 Results

4.2.1 Spontaneous IPSPs

During intracellular recordings in SON neurons using KAc-filled micropipettes, an abundance of spontaneous hyperpolarizing potentials were observed (Figure 4-1A). The frequency of these events varied between cells. In cells in which they were most common, 3-10 spontaneous potentials might be observed over a period of 100-200 msec. Their sensitivity to tetrodotoxin and high concentrations of Mg^{++} attest to their synaptic nature. Their reduction and ultimate reversal consequent to membrane hyperpolarization, and their ability to delay action potential firing (Bourque, 1984) is typical of inhibitory post-synaptic potentials (IPSPs). These IPSPs exhibited durations of 30-50 msec, rising to peak in 3-5 msec and then decaying exponentially with a mean time constant for the decay (τ_{sIPSP}) of 20.2 msec. This was 1.6-fold greater than the membrane time constant for the decay of hyperpolarizing pulses (τ_m; mean 13.8 msec, n = 9 cells). Spontaneous IPSP amplitudes ranged between 1 and 20 mV. When IPSPs occurred in rapid succession, summation resulted in greater voltage deflections (Figures 4-3 and 4-5).

4.2.2 Evoked IPSPs

Current pulses (50-500 μA, 50 μsec) administered through a concentric bipolar electrode placed on the ventral

surface of the explant in the region of the diagonal band of Broca (rostromedial to the SON) evoked a compound hyperpolarizing PSP in almost all SON neurons impaled with KAc electrodes (Figure 4-1B). This evoked IPSP occurred with a latency of 4-12 msec (mean 6.8 msec), rose to a peak in 3-10 msec (mean 5.7 msec) and decayed exponentially over 60-100 msec. The mean time constant of decay of the evoked IPSP (τ_{eIPSP}) was 37.0 msec, 2.6-fold greater than τ_m (15.1 msec) for the same cells (n = 16) (Figure 4-2). Action potentials were absent during the evoked IPSP (Figure 4-1B,C). In the majority of cells, a period of increased neuronal excitability followed the inhibitory period (Figures 4-1B,C).

4.2.3 Reversal Potential of the IPSPs

The voltage dependence of the IPSPs was apparent during intracellular current injection (Figure 4-3). Membrane hyperpolarization to -70 to -75 mV, reduced the amplitudes of both the spontaneous and the evoked IPSPs. Further hyperpolarization caused the IPSPs to become depolarizing and of increasing amplitude. The membrane potential at which the IPSP amplitude was reduced to zero, i.e. the "reversal potential" or "equilibrium potential" (E_{IPSP}) was -72.4 mV (range -62 to -82 mV, n = 24) in SON cells recorded with KAc electrodes. The reversal potentials for both spontaneous and evoked IPSPs were

usually identical (see Figure 4-3) with the E_{IPSP} always negative to the resting potential (mean -15.2 mV; range 5-32 mV).

4.2.4 Evoked IPSP conductance measurements

The mean input resistance of 24 SON neurons recorded with KAc electrodes was 264 ± 25 MΩ (SEM). During the evoked IPSP, R_{in} was reduced by between 23 and 83% (mean 91 MΩ). Thus mean resting input conductance (G_{in}) was 3.78 nS and mean input conductance at the peak of the IPSP (G_{TOT}) was 10.97 nS. Using equation 4 (Chapter 2.6), the evoked IPSP-induced conductance, G_{eIPSP} was estimated as 7.19 nS (range 0.79 to 22.03 nS). Clearly, considerable shunting of the membrane resistance occurred during the evoked IPSP, even though the magnitude of the synaptically evoked conductance varied 20-fold between the neurons in this study. No correlation between the quality of impalement (resting potential, spike amplitude, input resistance) and G_{eIPSP} could be found. The amplitude of the maximal evoked IPSP conductance under control conditions was constant for each cell (independent of membrane potential) whereas the amplitude of the IPSP voltage deflection was closely correlated to the membrane potential (Figures 4-3, 4-5).

4.2.5 Spontaneous IPSPs conductance measurements

Spontaneous IPSPs were smaller than evoked IPSPs (mean spontaneous IPSP-induced conductance (G_{IPSP-S}) of 0.56 nS) and displayed a much greater variation in their amplitude at all membrane potentials (Figures 4-3,4-5). Accordingly, G_{sIPSP} varied between 0.17 and 3 nS (Figure 4-9B). Since spontaneous IPSP amplitude was fairly constant between cells, the ratio G_{eIPSP} : G_{sIPSP} showed tremendous variation between cells (mean 13.1, range 1.6 to 43.7).

4.2.6 Dependence of IPSP Reversal Potential on chloride ion gradient

<u>KCl in recording micropipettes:</u> Following impalement of SON neurons with KCl-filled micropipettes, spontaneous and evoked PSPs were initially hyperpolarizing at resting membrane potential, but rapidly (within 1-5 minutes) became depolarizing due to diffusion and/or iontophoresis of chloride ions from the electrode tip into the neuron. The voltage-dependence of IPSP amplitude under these conditions differed considerably from that observed with KAc-filled micropipettes. Membrane hyperpolarization increased, and depolarization decreased the amplitude of both spontaneous and evoked IPSPs (Figure 4-5).

Because of action potential firing and rectifying currents within the depolarized range, (cf. Bourque, 1984

and Figure 6-9) it was rarely possible to reverse the IPSPs recorded with KCl electrodes. For this reason E_{IPSP} was estimated under these conditions by extrapolation of the plot of IPSP amplitude versus membrane potential. In 22 cells, the mean E_{IPSP} was -43.2 mV (range -30 to -53 mV) with identical reversal potentials for spontaneous and evoked IPSPs. There was no significant difference in any other properties of spontaneous or evoked IPSPs when recorded with KCl electrodes as compared to KAc electrodes. In particular, mean G_{eIPSP} in cells recorded with KCl electrodes was only slightly (not statistically significant) higher than in cells with KAc electrodes (Table 4-1), and the distribution of G_{eIPSP} was similar (Figure 4-6). This small difference may be accounted for by a contribution of voltage-dependent inward currents activated at the peak of depolarizing IPSPs recorded with KCl electrodes, where action potentials are often observed (See Figure 4-10A, top trace).

Alterations in extracellular chloride concentration: A second approach to the examination of the chloride dependence of the IPSP involved alteration of the concentration of chloride in the perfusion medium; i.e. the extracellular fluid ($[Cl^-]_o$). Perfusion with low chloride medium caused a positive shift of E_{IPSP} (Figure 4-7) such that a 10-fold change in $[Cl^-]_o$ caused a 42 mV shift in

E_{IPSP} (Figure 4-8A). This change was considerably less than the 61 mV/decade predicted by the Nernst equation. Accompanying the shift of E_{IPSP} was a 50-90% decrease in G_{IPSP} (Figure 4-8b) such that G_{IPSP} was roughly proportional to $[Cl^-]_o$. As a result, spontaneous IPSPs were rarely observed in medium containing less than 40 mM Cl^-.

An additional observation was that the input resistance of SON neurons was increased (although somewhat inconsistently) up to 50% during perfusion with low Cl^- medium. This would imply the existence of a resting chloride conductance in SON neurons.

4.2.7 Influence of Bicuculline Methiodide and Strychnine Sulfate

Bicuculline methiodide is a potent antagonist of the actions of γ-aminobutyric acid (GABA) in the central nervous system (Enna and Gallagher, 1983). Perfusion of the SON with bicuculline methiodide (BMI, 1-100 μM) reversibly reduced the amplitude of both spontaneous and evoked IPSPs (Figures 4-9, 4-10). The concentration of BMI which reduced G_{IPSP} to 50% of control (IC_{50}) was approximately 1.5 μM for spontaneous IPSPs, and 2.2 μM for evoked IPSPs (Figure 4-11). At 100 μM BMI, spontaneous PSPs were infrequent and of small amplitude (1-3 mV) and the G_{IPSP-E} was reduced by 90-100%. However, a majority of cells now displayed a residual PSP,

whose voltage-dependence was markedly different from that of the IPSP (E_{PSP} = -20 to +20 mV), and was associated with an input conductance change of 0.1-0.6 nS (Figure 4-12). In certain of these cells, this residual PSP could evoke action potentials at short latency (Figure 4-13) suggesting that in some SON neurons an excitatory PSP (EPSP) concealed by the powerful evoked IPSP was unmasked by treatment with BMI. It is important to note that in such cells, E_{IPSP} for spontaneous and evoked IPSPs differed slightly (Figure 4-12). BMI had no consistent effect on input resistance. Strychnine is a convulsant that antagonizes glycine and GABA binding to synaptic receptors in the central nervous system (DeFeudis et al., 1977) and blocks synaptic transmission mediated by GABA (Choi et al., 1981; Piggott et al., 1977; Scholfield, 1980,1982). Strychnine sulfate (5-50 μM) reduced or abolished spontaneous and evoked synaptic activity (data not shown). Lower concentrations (0.5 μM) were ineffective.

4.2.8 Influence of Pentobarbital on the IPSPs

Barbiturate anaesthetics prolong IPSPs (Nicoll et al. 1975) presumably due to their ability to facilitate the actions of GABA (Barker and Ransom, 1978a) by increasing the mean open time of GABA activated chloride channels (Mathers and Barker, 1980; Barker and McBurney, 1979). Addition of pentobarbital (10^{-5} to 10^{-4} M) to the perfusion medium

reversibly prolonged both spontaneous and evoked IPSPs (Table 4-1). Both the period of reduction in excitability (Figure 4-14) and the IPSP (Figure 4-15) that followed diagonal band of Broca stimulation, were prolonged by pentobarbital from 50-100 msec to 300-800 msec (Figure 4-14). The time constant of decay of the IPSPs (τ_{IPSP}) was increased on average 5-fold. Thus, for spontaneous IPSPs, τ_{IPSP} = 20.2 msec under control conditions and τ_{IPSP} = 116.7 msec in the presence of 10^{-4} M pentobarbital. For evoked IPSPs, control τ_{IPSP} = 37 msec and in pentobarbital (10^{-4}M) τ_{IPSP} = 204.8 msec (5 cells, Table 4-1 and Figure 4-15). No effect of pentobarbital on E_{IPSP} or G_{IPSP} was detected.

4.3 Discussion

4.3.1 GABA mediated IPSPs in SON neurons

These observations indicate that spontaneous and evoked IPSPs in SON neurons both result from activation of a chloride ion conductance which is blocked by bicuculline and prolonged by pentobarbital. Their sensitivity to bicuculline methiodide is typical of putative γ-aminobutyric acid (GABA)-mediated synaptic events (Alger and Nicoll, 1980, 1982; Okamoto, 1984; Scholfield, 1980). For these and the additional reasons mentioned in the following paragraph it is proposed that the majority of IPSPs observed in SON

neurons is mediated by GABA.

The sensitivity of the IPSPs to strychnine may be held as evidence of their mediation by glycine (Curtis et al., 1971; Choi and Fischbach, 1981). However, three lines of evidence argue against this conclusion. First, at the concentrations used in this study (5-50 μM), strychnine is not selective, and can serve as an effective antagonist of GABA-mediated synaptic and exogenously induced inhibition (Choi et al., 1981; Scholfield 1980,1982; Piggott et al., 1977). Furthermore, strychnine can displace both GABA and glycine specifically bound to receptors at all levels of the central nervous system (DeFeudis, 1977). Second, pentobarbital is selective in its facilitation of the actions of GABA; it does not alter the effects of glycine (Barker and Ransom, 1978b). Third, glycine is at least 10-fold less potent than GABA in its effects on SON neurons (Chapter 5) suggesting that SON neurons contain few receptors for glycine.

Bicuculline methiodide (1-100 μM) reduced or abolished IPSPs with an approximate IC50 (dose at which G_{IPSP} is reduced by 50%) of 1.5 μM for spontaneous, and 2.2 μM for evoked IPSPs. In view of the greater conductance associated with evoked IPSPs (and presumably, greater amount of GABA released) this slight difference is to be anticipated. Based on biochemical studies of GABA-receptor binding (see review, Enna and Gallagher, 1983) the potency with which BMI

blocks the IPSPs suggests that synaptic GABA concentrations are in the range of 100 nM to 10 μM.

4.3.2 Sources of GABAergic projections to the SON

GABA is synthesized from glutamate by the enzyme glutamate decarboxylase (GAD). Biochemical studies indicate the presence of moderate levels of GAD and GABA in the SON (Tappaz et al., 1977). However, immunocytochemical studies reveal that GAD is contained only in terminals in the SON at both the light (Perez de la Mora et al., 1981; Tappaz et al., 1982) and electron microscope level (R. Buijs, personal communication). Lesions placed rostral and medial to the SON reduced the GAD content of the SON by 40%, indicating that a significant proportion of the GABAergic input to the SON originates in areas located rostral to the third ventricle (Meyer et al., 1980).

Immunocytochemical studies show that the diagonal band of Broca and the lateral septum both contain numerous GABA neurons (Perez de la Mora et al., 1981; Panula et al., 1984; Nagai et al., 1983). Since these regions are intact in the hypothalamic explant, they would be likely sources of the GABAergic input responsible for the evoked IPSP, and at least a portion of the spontaneous IPSPs in SON neurons. This hypothesis is supported by observations made <u>in vivo</u> that electrical stimulation of the diagonal band or lateral septum inhibits SON neurons (Koizumi and Yamashita, 1972;

Poulain et al., 1980; Cirino and Renaud, 1985; Jhamandas and Renaud, 1985). Furthermore, neurons in this region can be activated antidromically by electrical stimulation of the SON (Poulain et al., 1981; Shibuki, 1984). Experiments using a variety of anatomical techniques indicated that neurons from these regions project to the SON and surrounding regions (Carithers et al., 1980; Miselis et al., 1979; Tribollet et al., 1985; Oldfield et al., 1985; Powell and Rorie, 1967; Zaborsky et al., 1975).

According to Zaborszky et al. (1975), SON neurons receive the majority of their synaptic input from neurons located within or nearby the nucleus. Sixty percent of the GAD content of the SON remains after lesions which isolate the SON from nearby structures (Meyer et al., 1980). Thus, GABA-containing neurons located adjacent to the SON (Tappaz et al., 1982) and in the lateral hypothalamus and substantia inominata, dorsal to the SON (Nagai et al.,1983) may be the source of much of the afferent GABAergic innervation. Indeed, electrical stimulation dorsal to the SON in hypothalamic slices can evoke IPSPs in certain SON neurons (Andrew and Dudek, 1984). A dense projection of septal neurons to this area (Oldfield et al., 1985; Tribollet et al., 1985) raises the possibility that inhibition of SON neurons evoked by stimulation of the septum may be mediated disynaptically by GABA neurons of the lateral hypothalamus.

The amygdala is a third possible source of the GABAergic input to the SON. Electrical stimulation of the amygdala, which contains numerous GABAergic neurons (Nagai et al., 1983), inhibits SON neurons (Hamamura et al., 1982; Ferreyra et al., 1983). Axons of these neurons probably follow the ventral amygdalofugal pathway to the SON (Hamamura et al., 1982) and are not likely to contribute to the evoked IPSP following diagonal band of Broca stimulation.

4.3.3 Synaptically activated conductances

The spontaneous synaptically activated conductances (0.5-3 nS) are smaller than those observed in hippocampal pyramidal cells (5-9 nS, Miles and Wong, 1984). However, because of the low input conductance of SON neurons (3-10 nS), these IPSPs represent an important shunting of the membrane resistance and attain amplitudes of up to 10 mV.

Estimates of the conductances of GABA channels in other neurons range between 14-20 pS (Gold and Martin, 1984; Barker et al., 1980; Segal and Barker, 1984). The present data indicate that as few as 25-35 channels may be activated at the peak of a unitary synaptic event in a SON neuron. Larger spontaneous IPSPs probably result from simultaneous release of several quanta of transmitter causing activation of an estimated 100-200 channels. An alternative explanation of the variability in amplitude of spontaneous

IPSPs is that they result from activation of synapses located at different distances from the recording electrode (Rall, 1967). This is unlikely since spontaneous IPSPs of all sizes have similar time courses (i.e. fast rise times and exponential decay at ~ 1.5 x τ_m).

4.3.4 Time course of the IPSPs: Effects of Pentobarbital

The rapid 3-5 msec rise of the IPSPs is indicative of their electrotonic proximity to the somatic recording site (Rall, 1967). It is notable that the decay of spontaneous and evoked IPSPs resembled a single exponential whose time constants exceeded that of the cell membrane by 1.4-fold and 2.3-fold, respectively. This is evidence that the current underlying the IPSP persists briefly, possibly due to the kinetics governing either the inactivation of the receptor-channel complex, or the disposition of transmitter.

Pentobarbital delays current inactivation by increasing the mean open time of GABA-activated chloride channels (Barker and McBurney, 1979) resulting in a prolongation of GABA-mediated synaptic potentials (Nicoll et al., 1975; Barker and McBurney, 1979; Alger and Nicoll, 1980; Scholfield, 1978a). The 2-8 fold prolongation of spontaneous and evoked IPSPs in SON neurons by pentobarbital (10^{-5} to 10^{-4} M) is similar to that observed in cultured spinal cord neurons (Barker and McBurney, 1979) and in hippocampal neurons (Alger and Nicoll, 1980).

4.3.5 Specificity of the GABAergic innervation of SON neurons

According to Miles and Wong (1984) the ratio $G_{eIPSP} : G_{sIPSP}$ in a cell can be taken as an estimate of the number of inhibitory afferent fibers that project to that cell. In the present study, this value widely varied from 1.6 to 43.7, indicating that certain SON neurons receive a greater density of inhibitory input than others. Since the SON contains primarily two populations of neurons (ie: those that synthesize vasopressin or oxytocin), it is tempting to speculate that one population of SON neurons might receive this input specifically.

In vivo, spontaneous firing patterns and responses to physiological stimuli such as suckling or changes in blood pressure, provide a means of tentative identification of SON cell type (Poulain and Wakerly, 1982; Day and Renaud, 1984). This permits some degree of correlation of cell type (eg: vasopressin-secreting cells) with sensitivity to electrical stimulation (cf. Day and Renaud, 1984; Cirino and Renaud, 1985). It may now be possible to obtain direct confirmation of this neural circuitry in vitro by combining the techniques of identification of afferents during intracellular recording, cell marking by injection of lucifer yellow and subsequent immunocytochemical staining (cf. Yamashita, et al., 1983).

4.3.6 Chloride dependence of the GABA-activated conductance

According to the Nernst equation, the reversal potential of an IPSP (E_{IPSP}) can be considered an approximation of the equilibrium potential of the ionic conductance which underlies the IPSP (assuming that there is a single permeant ion species). The sensitivity of E_{IPSP} to manipulations which alter the transmembrane Cl^- gradient (intracellular Cl^- iontophoresis; removal of extracellular Cl^-) indicates that chloride is the permeant ion of the synaptically activated channel. Furthermore, reduced IPSP-associated conductance changes (G_{IPSP}) in solutions deficient in Cl^- is evidence that chloride is the permeant ion (Takeuchi and Takeuchi, 1967).

Under these recording conditions, the Nernst equation predicts an internal free Cl^- concentration of 6-10 μM when KAc electrodes are used. This is less than would be expected if Cl^- is passively distributed across the plasma membrane according to its electrical charge. This suggests the existence in SON neurons of a chloride pumping mechanism (cf. Lux, 1970, 1971; Llinas et al., 1974; Meyer and Lux, 1974; Gallagher, 1983) or a mechanism for intracellular sequestration and subsequent extrusion of Cl^- (Ascher et al., 1976). E_{IPSP} was altered by 40 mV for a 10-fold change in $[Cl^-]_o$, 35% less than the 61 mV/decade predicted by the Nernst equation. This can be explained by the existence of a chloride extrusion mechanism and the high

level of spontaneous synaptic activity in SON neurons which cause depletion of intracellular chloride when extracellular chloride is removed (Meyer, 1976; Matthews and Wickelgren, 1979; Motozikawa et al., 1969; Newberry and Nicoll, 1985), and prevent the reversal of the chloride gradient necessary to obtain the predicted shift of E_{IPSP}. Indeed, it could be anticipated that at equilibrium (after perhaps 30 min to 1 hr in low Cl^- medium) there would be no shift in E_{IPSP} from its control values, but that G_{IPSP} would be decreased in proportion to $[Cl^-]_o$ (Takeuchi and Takeuchi, 1967). In these experiments, measurements of E_{IPSP} and G_{IPSP} were made after 5-10 minutes in low Cl^- medium. Therefore, the deviation of the reversal potential data from Nernstian predictions and the variability of changes in G_{IPSP} with $[Cl^-]_o$ can be explained based on gradual depletion of intracellular chloride.

A contribution of another ionic species to G_{IPSP} (eg. K^+) is unlikely in view of the almost complete abolition of G_{IPSP} in medium containing 4.8 mM Cl^-. However, some neurons demonstrated an evoked EPSP that was insensitive to $[Cl^-]_o$ and probably mediated by another ion (see below), thereby complicating measurements of G_{IPSP}. This event may account for the deviation of some observations from the predictions of Takeuchi and Takeuchi (1967).

4.3.7 Existence of an underlying EPSP

In many cells there was an evoked PSP that was resistant to BMI (100 μM) and appeared to be excitatory. This EPSP exhibited voltage dependence that allowed estimation of E_{EPSP} in the range -20 to +20 mV and G_{EPSP} of 0.1 - 0.6 nS. The contamination of the evoked IPSP with a second synaptic conductance has several important implications in the interpretation of the IPSP data. Figure 4-12 illustrates an example of how E_{eIPSP} can be underestimated relative to E_{sIPSP}, presumably due to contamination of the evoked IPSP by the EPSP. Similarly, G_{eIPSP} may be overestimated in solutions containing BMI due to the EPSP-associated conductance. Finally, the EPSP may interfere with estimates of E_{eIPSP} and G_{eIPSP} in experiments with low chloride medium (see above).

While no studies have been done to characterise the source of such EPSPs in detail, previous studies in vivo have indicated that SON neurons do receive an excitatory input from areas rostral to the third ventricle (Koizumi and Yamashita, 1972; Sgro et al., 1984; Cirino and Renaud, 1985). Some of these afferents are proposed to participate in the release of oxytocin and vasopressin (Woods et al., 1969; Aulsebrook and Holland, 1969; Sladek and Johnson, 1983). Preliminary data reported here (cf. Figure 4-13) indicate that the EPSP results from the activation of an

ionic conductance (possibly Na^+ or Ca^{++}) whose equilibrium potential is positive to the membrane potential. Such a conductance might be activated by activation of glutamate or acetylcholine receptors (Krnjevic, 1973) and deserves more detailed consideration.

Table 4-1 Properties of IPSPs in SON neurons. Values are means ± standard error of the mean, or when more appropriate, means and range. The number of cells is indicated in the brackets. Abbreviations are defined in the text except for "ΔR_{in}" which represents the IPSP-induced reductions in input resistance.

Latency	6.8 msec (range 4-12 msec, 45 cells)
Rise time	5.7 msec (range 3-10 msec, 45 cells)
Fall time	60-100 msec (45 cells)

	Control	Pentobarbital (10^{-4}M)
τ_m	15.1±1.0 msec (16)	16.1±0.6 (5)
τ_{eIPSP}	37.0±2.8 msec (16)	204.8±61.1 (5)
τ_e/τ_m	2.57±0.2 (16)	14.4±4.7 (5)
τ_{sIPS}	20.2±1.9 msec (9)	116.7±44.9 (5)
τ_s/τ_m	1.56±0.1 (9)	8.5±3.3 (5)

	KAcetate electrodes	KCl electrodes
E_{eIPSP}	-67.4±1.2 mV (24)	-43.2±1.4 mV (21)
E_{sIPSP}	-72.4±1.1 mV (14)	-42.7±1.2 mV (16)
$E_e - E_s$	+3.2 mV (13)*	-0.2 mv (13)
G_{eIPSP}	7.18 (0.79-22.0) nS (23)	8.82 (0.79-19.6) nS (21)
G_{sIPSP}	0.56 (0.17-3.0) nS (16)	0.78 (0.28-3.0) nS (17)
G_e / G_s	7.23 (1.6-43.7) (14)	13.88 (1.9-36.9) (17)
R_{in}	264±20 MΩ (24)	194±14 MΩ (21)
ΔR_{in}	-51±4 % (24)	-54±5 % (21)

*For $E_e - E_s$, values were: 0, 0, 0, +20, 0, 0, +9, +4, 0, 0, +1, +7, and 0. Note that cells in which this value ≠ 0, had bicuculline-resistant evoked PSPs.

Figure 4-1 Intracellular recordings with a KAc-filled microelectrode reveal spontaneous and evoked IPSPs in a SON neuron.

A) A series of single sweeps illustrates action potentials interspersed with frquently occurring spontaneous hyperpolarizing synaptic potentials.

B) 15 superimposed oscilloscope sweeps illustrate the absence of action potentials during the IPSP evoked by electrical stimulation of the diagonal band of Broca (arrow).

C) Peristimulus histogram constructed during 150 cycles of the activity shown in (B) reveal that a reduction in neuronal excitability during the IPSP is followed by a period of enhanced excitability lasting approximately 100 msec.

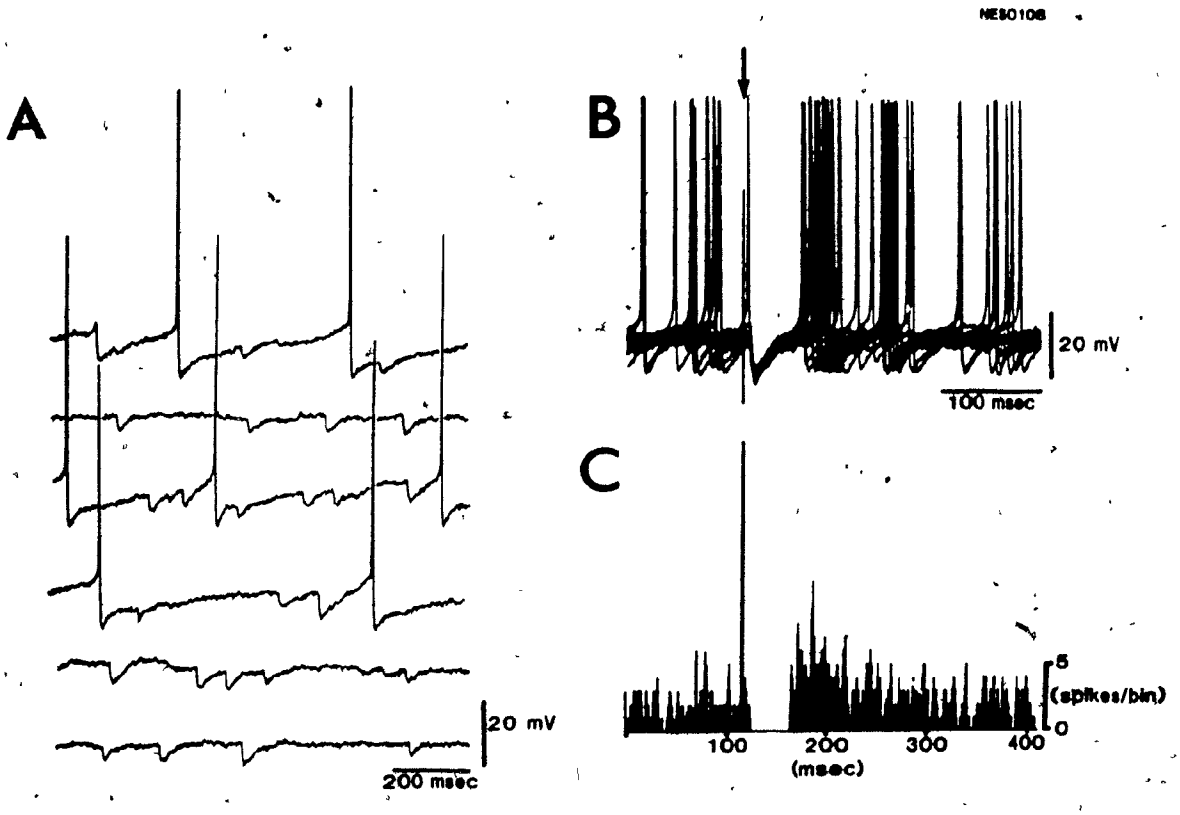
NES010B
A
20 mV
200 msec
B
20 mV
100 msec
C
5
(spikes/bin)
0
100
200
300
400
(msec)

Figure 4-2 Computer plots of the exponential decay of the IPSP evoked by electrical stimulation of the diagonal band of Broca (arrow) after the saturation of a hyperpolarizing pulse of intracellularly injected current (see inset; average of 32 sweeps).

A) IPSP and pulse are superimposed to allow comparison of voltage decay. B) Semilogarithmic plots of the IPSP and hyperpolarizing pulse can be approximated by single exponentials having time constants (arrow) of 31.6 msec (IPSP) and 11.3 msec (hyperpolarizing pulse) estimated as the time required for the decay from $V_t - V_\infty$ to 1/e x $(V_t - V_\infty)$.

NESO 108

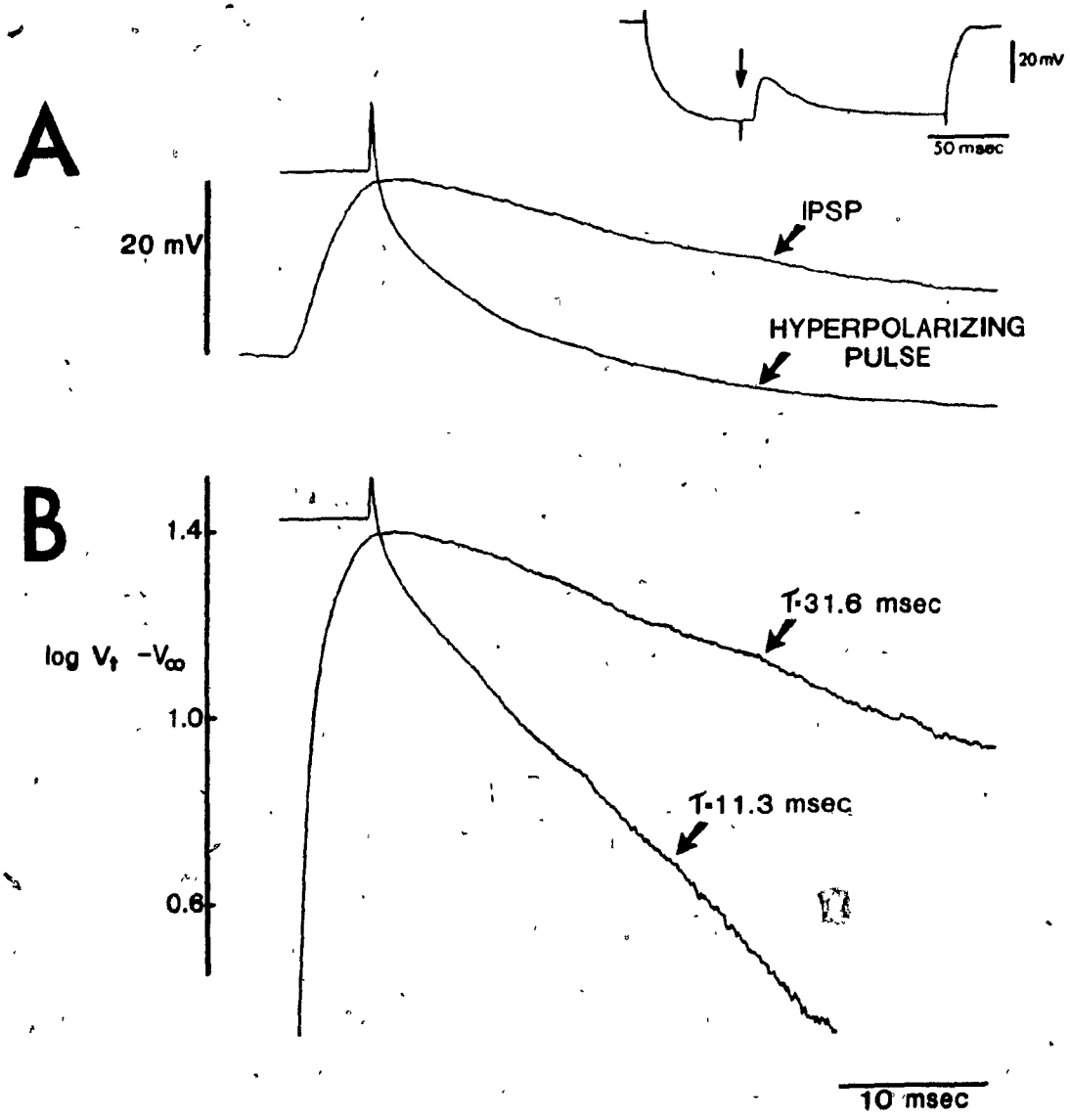
A
20 mV
20 mV
50 msec
IPSP
HYPERPOLARIZING
PULSE
B
1.4
log $V_t - V_\infty$
1.0
0.6
T-31.6 msec
T-11.3 msec
10 msec

Figure 4-3 Voltage-dependence and membrane conductance of spontaneous and evoked IPSPs in a SON neuron recorded with a KAc electrode.

A) IPSP is evoked (arrow) at the peak of voltage response to injection of current pulses. The evoked IPSP is hyperpolarizing at membrane potentials (Vm) in the range of -50 to -75 mV, and depolarizing at Vm = -80 mV.

B) Spontaneous IPSPs display a similar voltage-dependence during constant injection of hyperpolarizing current.

C) Current-voltage plot constructed from the data in (A). Baseline voltage measurements (filled squares) made immediately before the IPSP are compared with measurements made at the peak of the IPSP (open squares). Input resistance (R_i), estimated as the slope of the linear portion of the plot (from -80 to -120), was reduced by 71% during the evoked IPSP. A corresponding increase in input conductance (G_i) from 4.39 nS to 15.38 nS indicates a membrane shunt of 10.99 nS associated with the evoked IPSP (G_{IPSP}).

D) Plots of amplitude of spontaneous and evoked IPSPs vs. Vm. Note that these each have identical reversal potentials (E_{IPSP}) of approximately -77 mV. Note also that while maximal evoked IPSP shows little variation at a given Vm, the amplitude of spontaneous IPSPs is quite variable. Accordingly, from this plot (Equation 6, Section 2.6) estimated evoked G_{IPSP} = 11.23 nS while spontaneous GIPSP ranges from 0.42 - 1.91 nS.

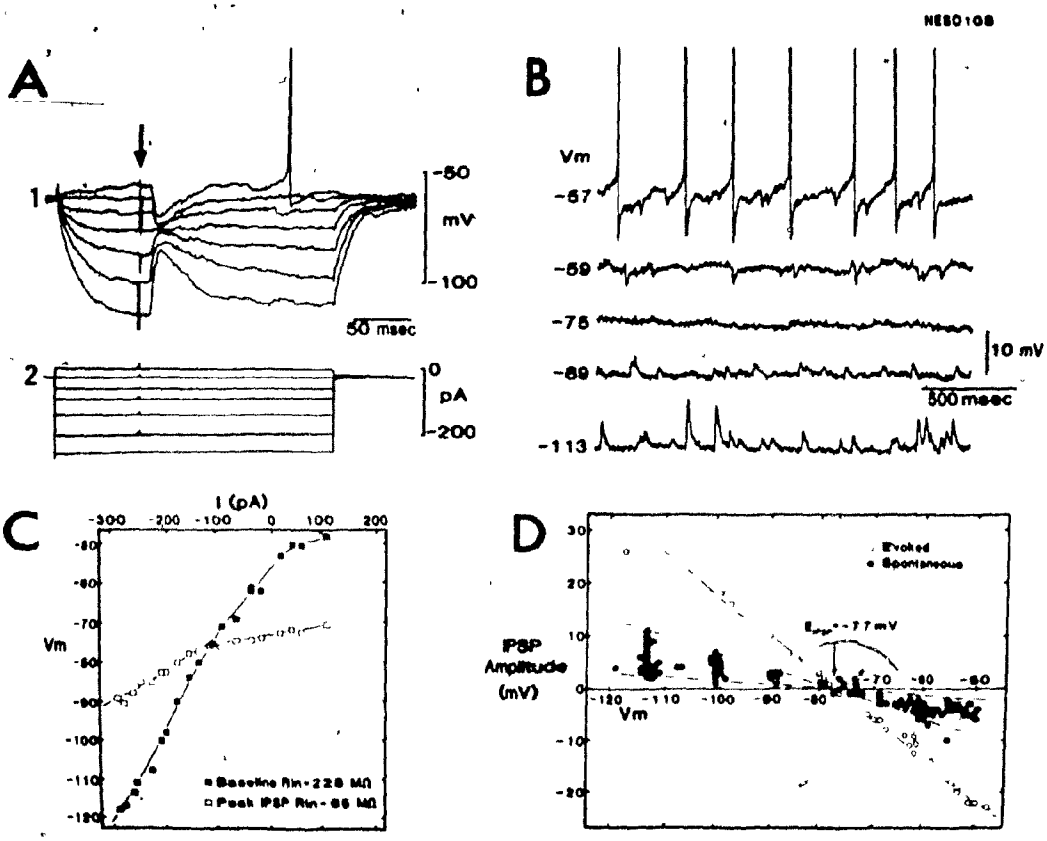
A
1
-50
mV
-100
50 msec
2
0
pA
-200
B
NES0108
Vm
-57
-59
-75
-89
-113
10 mV
500 msec
C
I (pA)
-300
-200
-100
0
100
200
Vm
Baseline Rin = 228 MΩ
Peak IPSP Rin = 86 MΩ
D
Evoked
Spontaneous
IPSP
Amplitude
(mV)
Vm
-120
-110
-100
-90
-80
-70
-60
-50
30
20
10
0
-10
-20

Figure 4-4 Change in input resistance associated with the Evoked IPSP. Short pulse experiment; same cell as Figure 4-3.

A) 1) At resting potential, diagonal band of Broca stimulation (arrow) evokes a hyperpolarizing IPSP. 2) Steady application of 90 pA of hyperpolarizing current adjusts Vm to near E_{IPSP} (-75 mV). 3 & 4) Voltage response to 10 msec current pulses applied before (a,b) during (c) and after (d,e) the IPSP. Note the diminished amplitude of the current-induced voltage deflection during the IPSP.

B) Current-voltage plot of data in $A_{3\&4}$. Voltage measurements were made immediately prior to the capacitive artifact that occurs at the end of each current pulse. Note that the voltage response to these brief current pulses did not saturate due to membrane capacitance (τ_m = 11.8 msec) so R_i is underestimated. Nevertheless, the 74% decrease in R_i during the IPSP determined in this way agrees closely with the decrease measured in the same cell using 200 msec current pulses (Figure 4-3).

C) Data from (B) plus two additional determinations having current pulses delayed 3 and 6 msec, demonstrate the rapid decay of the conductance change underlying the IPSP.

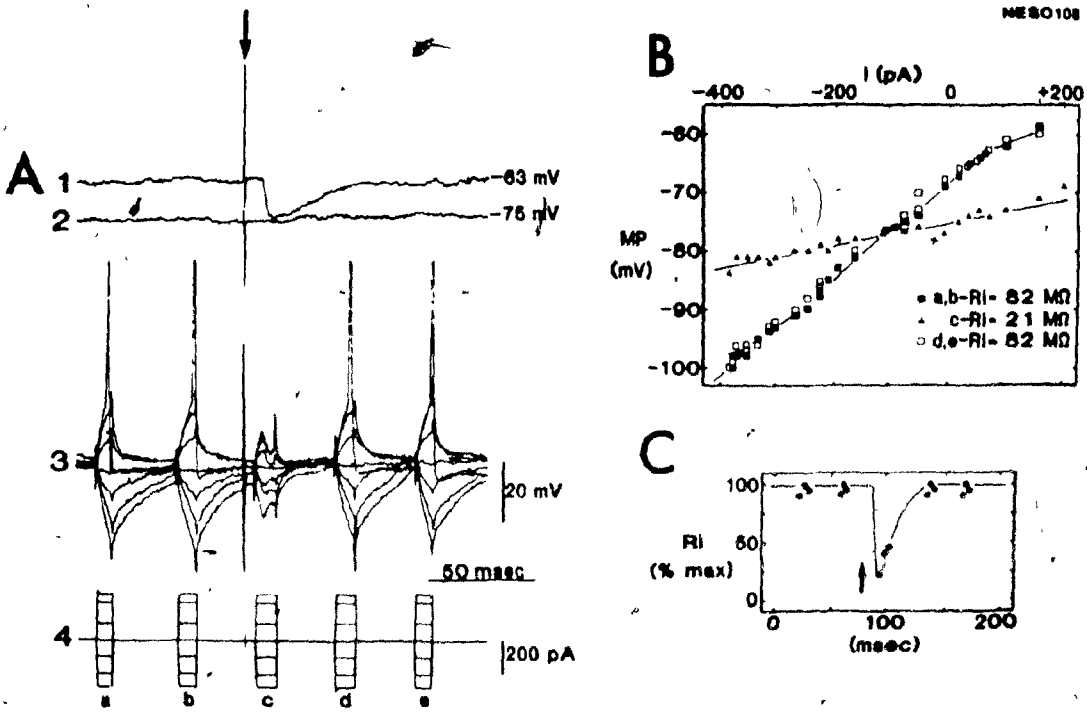
A
1
2
-63 mV
-75 mV
3
20 mV
50 msec
4
200 pA
a
b
c
d
e
B
I (pA)
-400
-200
0
+200
-60
-70
-80
-90
-100
MP
(mV)
• a,b-RI- 82 MΩ
▲ c-RI- 21 MΩ
○ d,e-RI- 82 MΩ
C
100
50
0
RI
(% max)
0
100
200
(msec)

Figure 4-5 Voltage-dependence and membrane conductance of spontaneous and evoked IPSPs in a SON neuron recorded with a KCl electrode.

Analysis is identical to that of Figure 4-3. Note the strongly depolarizing evoked (A) and spontaneous (B) IPSPs that increase in amplitude with hyperpolarization. Action potentials are evoked at the peak of the evoked IPSPs.

C) Current-voltage plot reveals an 82% decrease in input resistance (R_i) during the IPSP. Baseline input conductance (G_i; 4.35 nS) rises to 23.81 nS at the peak of the IPSP. The evoked G_{IPSP} is estimated at 19.46 nS although this value may be contaminated with a contribution of voltage-dependent inward currents.

D) Plot of IPSP amplitude vs. membrane potential (Vm) yields an extrapolated IPSP reversal potential (E_{IPSP}) of -44 mV. As in Figure 4-3, evoked IPSP amplitudes vary little at a given Vm, in comparison with spontaneous IPSP amplitudes. From this plot (Equation 6, Section 2.6) estimated evoked G_{IPSP} = 19.1 nS while spontaneous G_{IPSP} ranges between 0.25 and 3.26 nS.

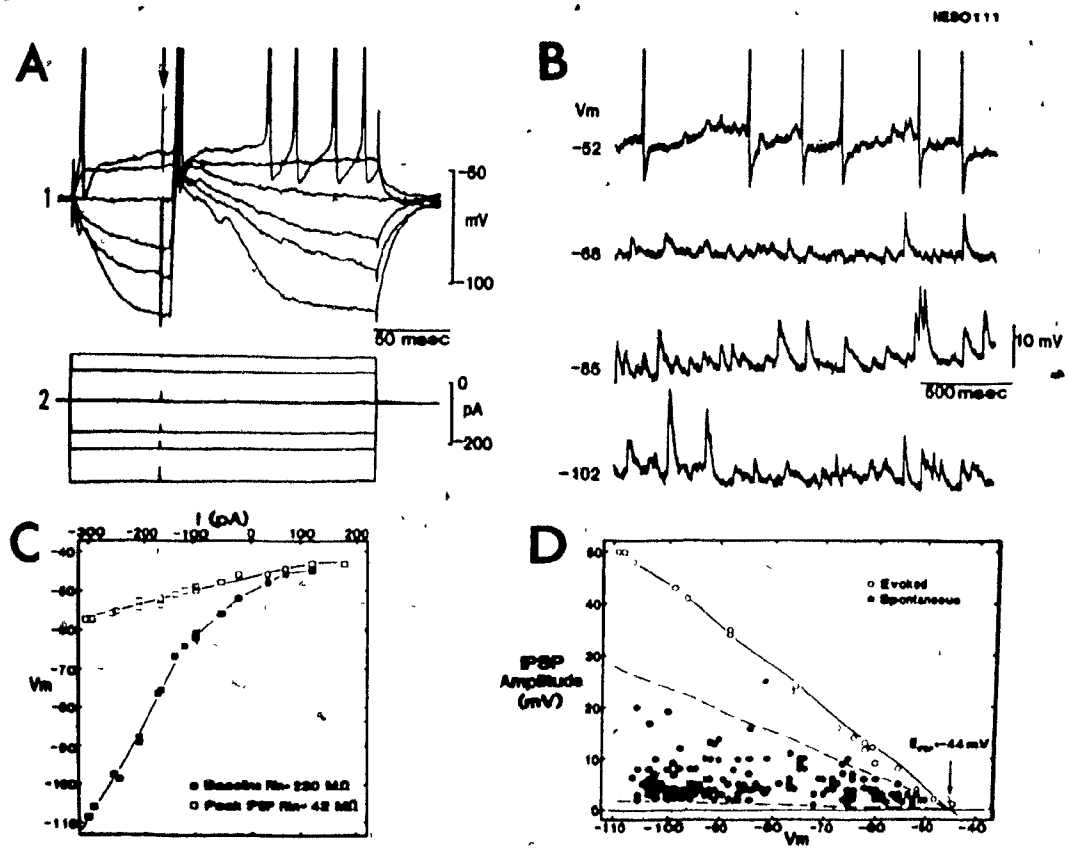
A
1
-60
mV
-100
50 msec
2
0
pA
-200
B
NEBO111
Vm
-52
-68
-85
-102
10 mV
500 msec
C
I (pA)
Vm
D
Evoked
Spontaneous
IPSP Amplitude (mV)
Vm

Figure 4-6 Histogram of the distribution of conductance associated with the evoked IPSP (G_{IPSP-E}) in cells recorded with potassium acetate (KAc, closed bars) and potassium chloride (KCl, open bars) electrodes. There was no significant difference between data obtain with KAc and KCl electrodes; the data are superimposed.

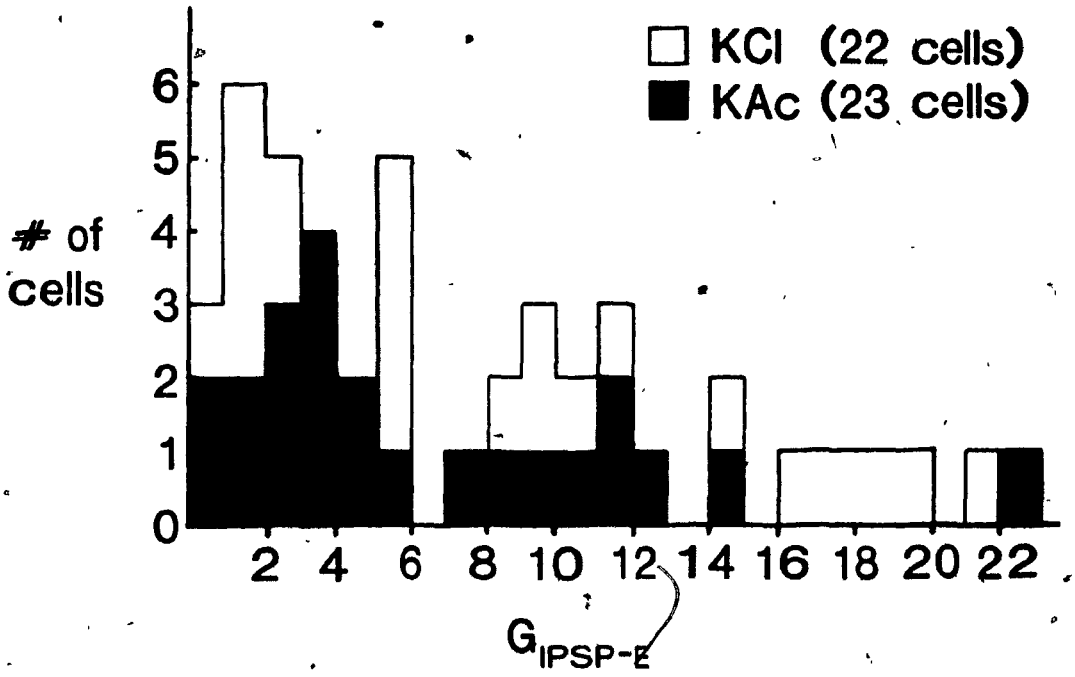
KCl (22 cells)
KAc (23 cells)
# of cells
0
1
2
3
4
5
6
2 4 6 8 10 12 14 16 18 20 22
G IPSP-E

Figure 4-7 Effect on the evoked IPSP of altering the concentration of chloride in the perfusion medium.

A) Voltage-dependence of the diagonal band of Broca evoked IPSP (arrow) in normal (134 mM Cl^-) medium where the IPSP reverses at approximately -79 mV.

B) In low chloride medium (10.4 mM), the IPSP is positive-going at all membrane potentials and evokes an action potential at depolarized levels.

C) Plot of IPSP amplitude versus membrane potential. The IPSP reverses at -79 mV in normal medium (circle). In low chloride medium (triangle) an extrapolated reversal potential of -30 mV is estimated. The reduced slope of the line drawn through the data obtained in low chloride is indicative of the reduced IPSP conductance.

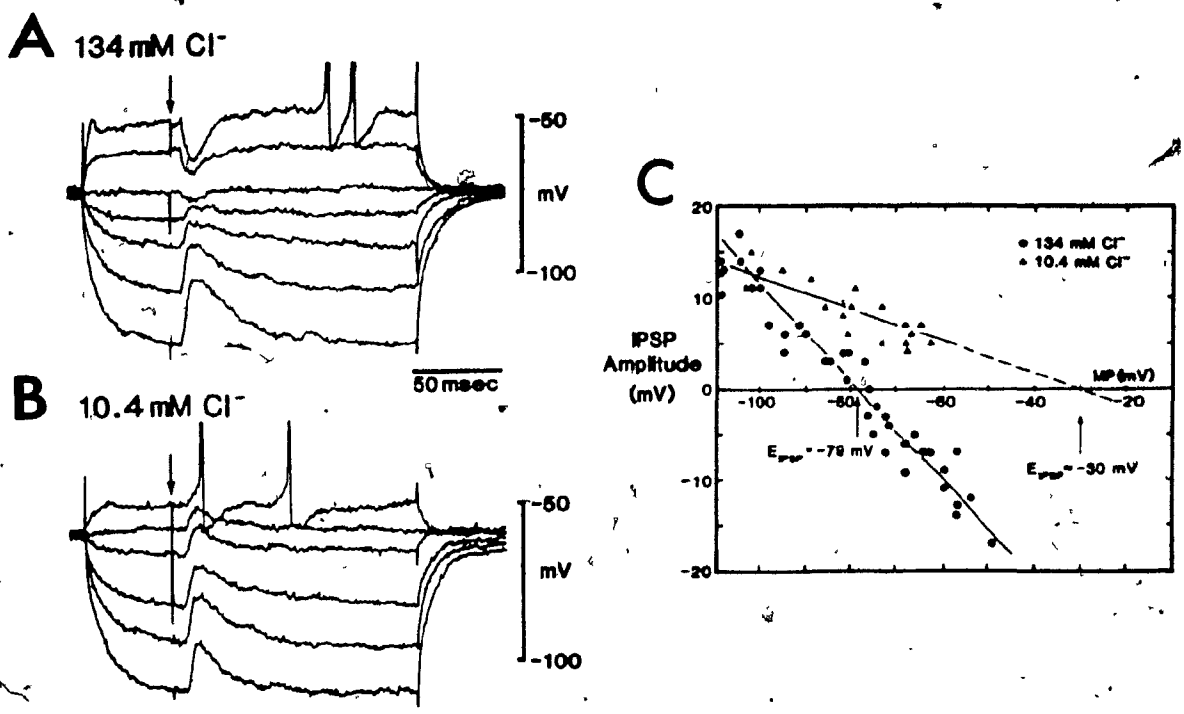
A
134 mM Cl⁻
-50
mV
-100
50 msec
B
10.4 mM Cl⁻
-50
mV
-100
C
IPSP Amplitude (mV)
MP (mV)
20
10
0
-10
-20
-100
-80
-60
-40
-20
• 134 mM Cl⁻
▲ 10.4 mM Cl⁻
E_IPSP = -78 mV
E_IPSP = -30 mV

Figure 4-8 Effect of altering the concentration of chloride in the perfusion medium on the evoked IPSP reversal potential (E_{IPSP}) and the associated conductance (G_{IPSP}). $[Cl^-]_o$ is assumed to be equal to the concentration of chloride in the perfusion medium.

A) Semi-log plot of evoked IPSP reversal potential (E_{IPSP}) as a function of extracellular chloride concentration $[Cl^-]_o$. The line drawn through the data (fitted by eye) has a slope of 42 mV/ten-fold change in $[Cl^-]_o$.

B) Linear plot of the IPSP-associated conductance (G_{IPSP}) as a function of $[Cl^-]_o$. The line represents the theoretical dependence of channel conductance on $[Cl^-]_o$ (see text). Each symbol represents a different cell (n = 7). The star in (B) represents data from all cells in 134 mM $[Cl^-]_o$ where G_{IPSP} is normalized to 100%.

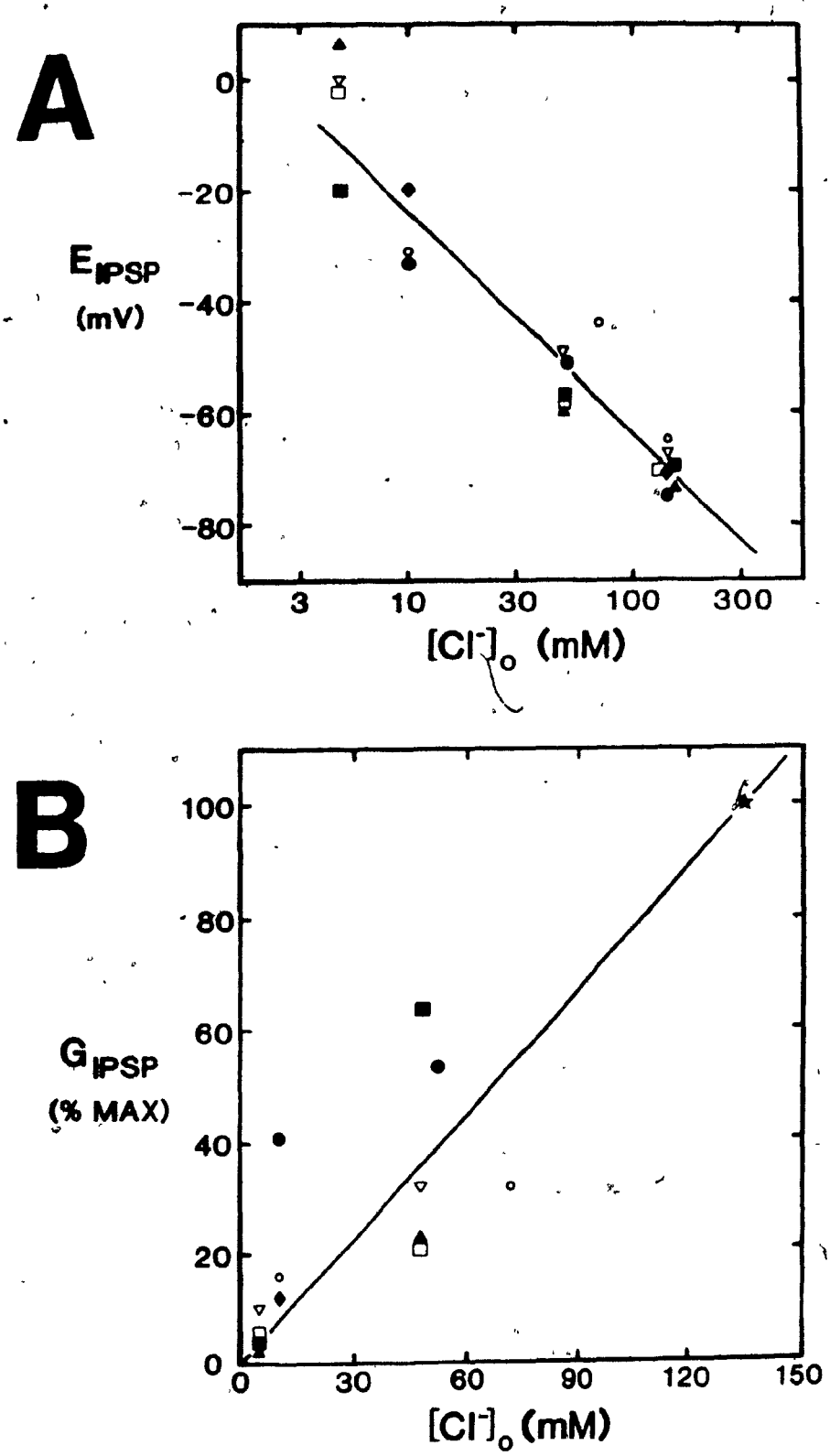
A
0
-20
-40
-60
-80
E_{IPSP}
(mV)
3
10
30
100
300
$[Cl^-]_o$ (mM)
B
100
80
60
40
20
0
G_{IPSP}
(% MAX)
0
30
60
90
120
150
$[Cl^-]_o$ (mM)

Figure 4-9 Sensitivity of spontaneous IPSPs to bicuculline methiodide (BMI).

A) Spontaneous IPSPs occurring in a SON neuron recorded with a KCl electrode and held at a Vm of -95 mV. BMI (1-100 µM) reduces or abolishes the IPSPs.

B) Histogram of distribution of G_{IPSP} for IPSPs observed in control medium and BMI (1-100 µM). G_{IPSP} was calculated as described in section 2.6. BMI (1 µM) reduces the amplitude of the IPSPs but does not noticeably alter their frequency. Higher concentrations of BMI (10-100 µM) reduce the amplitude of the IPSP voltage deflections sufficiently that only infrequently can events be clearly distinguished from background noise (same cell as Figure 4-10).

NESO111

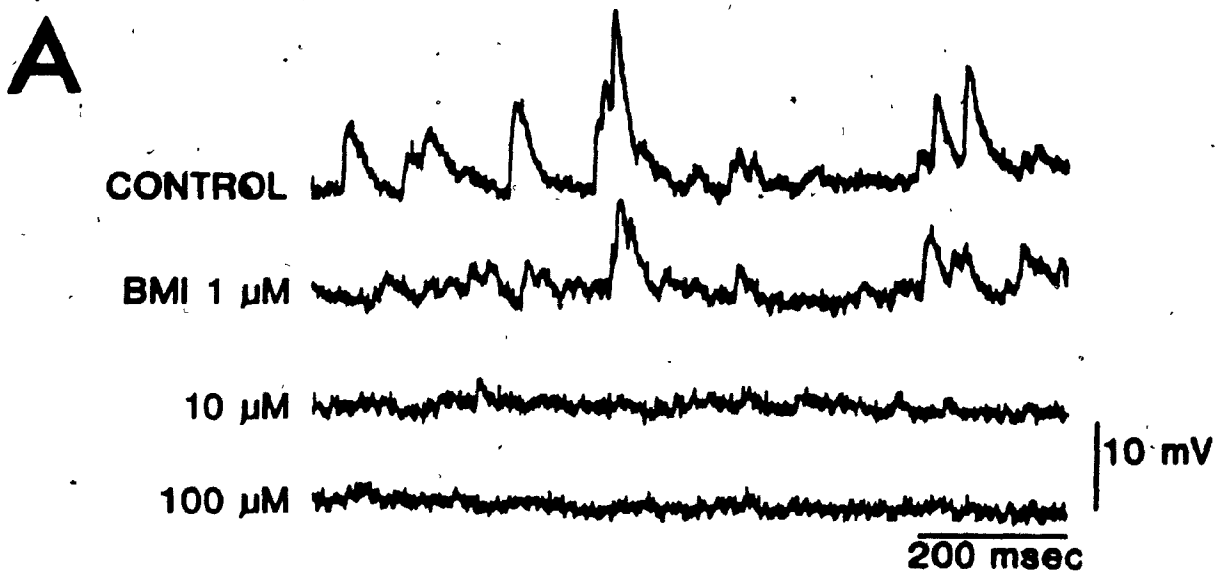
A
CONTROL
BMI 1 µM
10 µM
100 µM
10 mV
200 msec

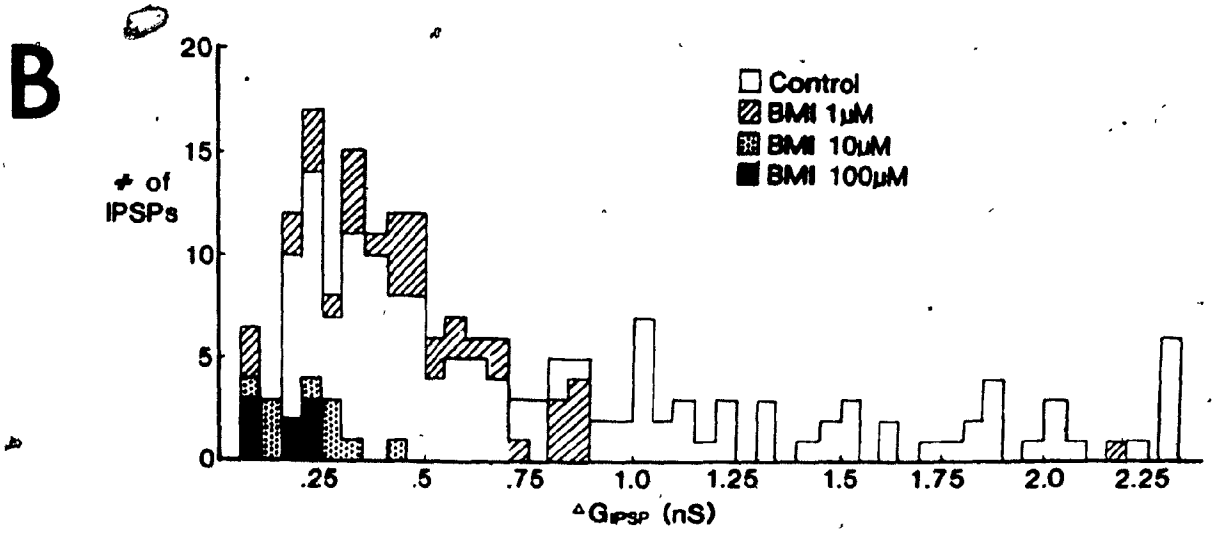
B
# of IPSPs
20
15
10
5
0
Control
BMI 1µM
BMI 10µM
BMI 100µM
.25
.5
.75
1.0
1.25
1.5
1.75
2.0
2.25
ΔGIPSP (nS)

Figure 4-10 Sensitivity of evoked IPSP to BMI

A) Evoked IPSP in a SON neuron recorded with a KCl electrode and held at a Vm of -105 mV. BMI (1-100 μM) reduces or abolishes the evoked IPSP. Note the action potentials at the peak of the IPSP under control conditions.

B) Plot of IPSP amlitude versus membrane potential (Vm). BMI (10 μM) reduces IPSP considerably and causes a slight positive shift of the E_{IPSP}. BMI (100 μM) virtually abolishes G_{IPSP} but leaves a small residual PSP whose reversal potential (extrapolated) differs considerably from E_{IPSP} under control conditions. This phenomenon is more pronounced in the cell illustrated in Figure 4-12. Same cell as Figure 4-9.

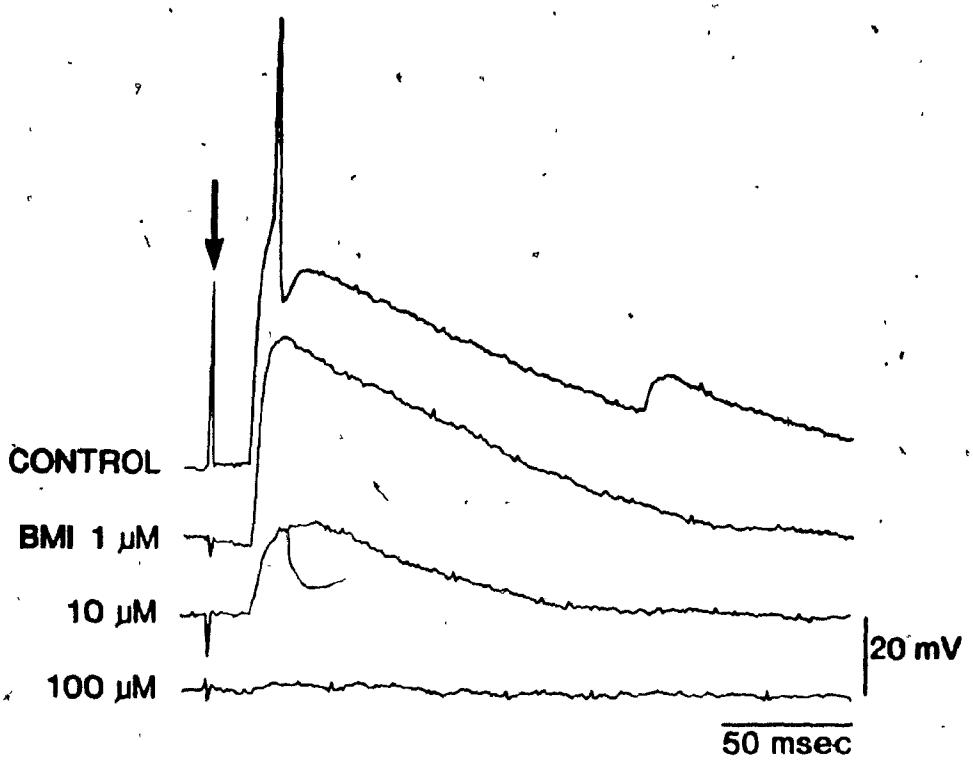
CONTROL
BMI 1 µM
10 µM
100 µM
20 mV
50 msec

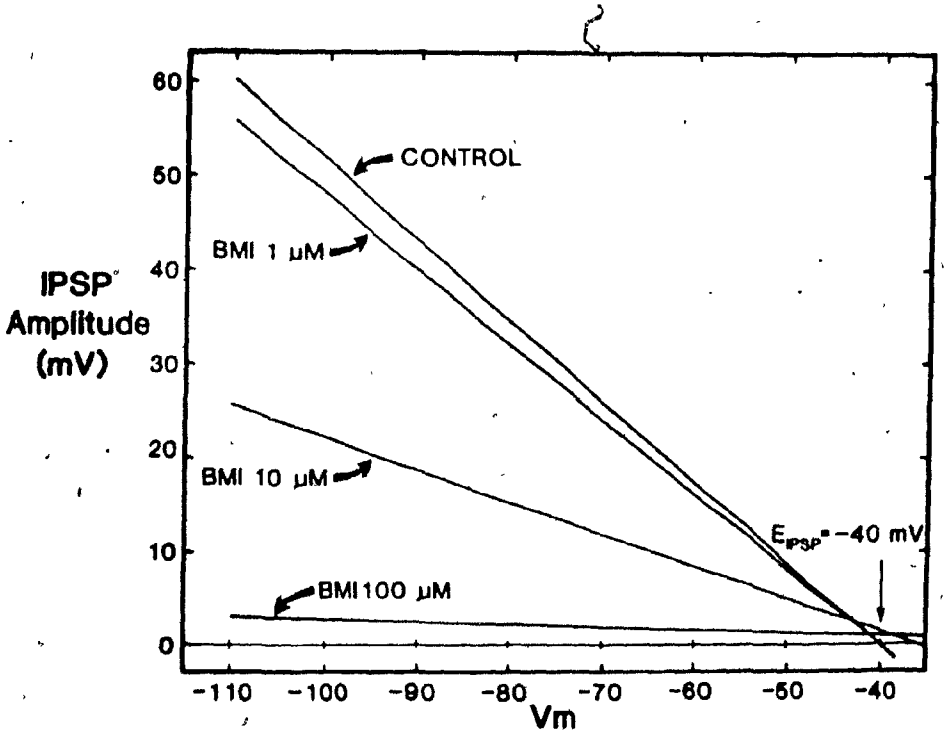
IPSP Amplitude (mV)
60
50
40
30
20
10
0
CONTROL
BMI 1 µM
BMI 10 µM
BMI 100 µM
E_{IPSP} = -40 mV
-110
-100
-90
-80
-70
-60
-50
-40
Vm

Figure 4-11 Dose-dependence of effects of BMI on a conductance induced during spontaneous and evoked IPSPs. Data from 12 cells. Spontaneous (closed triangles) IPSPs appear to be slightly more sensitive to BMI than evoked (open triangles) IPSPs; the concentrations of BMI necessary to reduce G_{IPSP} by 50% (IC50) is approximately 1.5 μM for spontaneous IPSPs and 2.2 μM for evoked IPSPs.

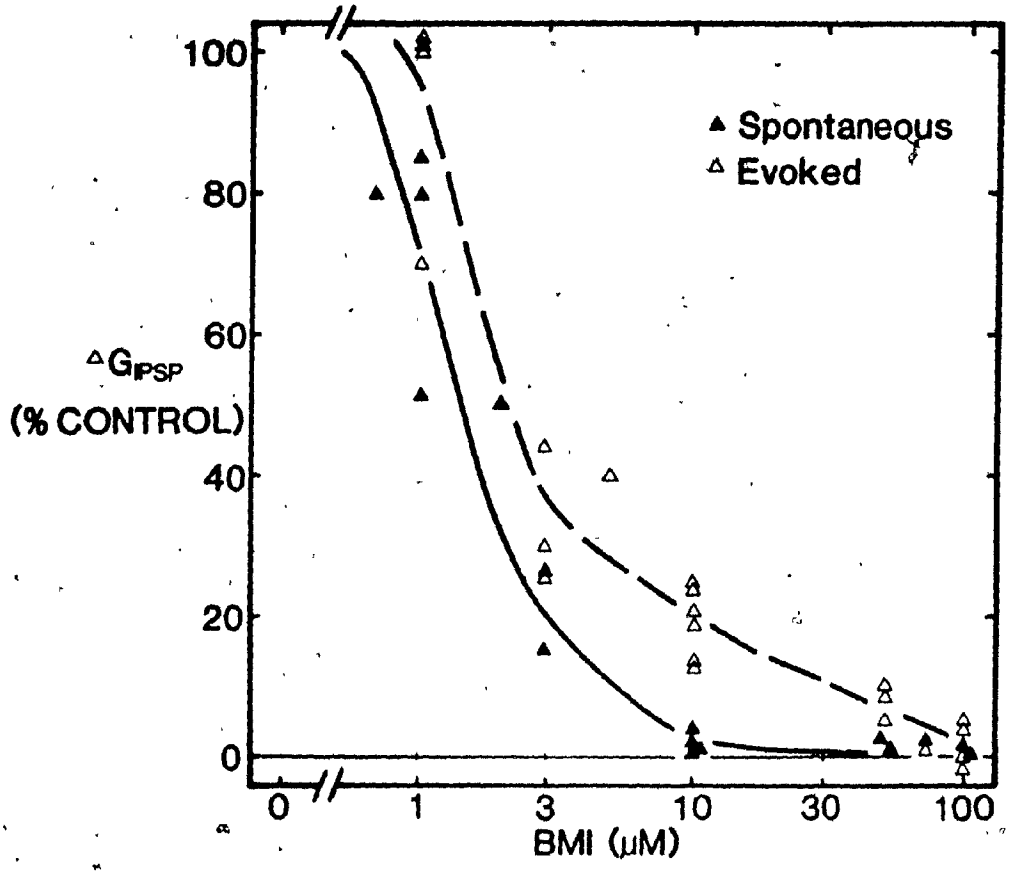
100
80
60
40
20
0
0
1
3
10
30
100
BMI (μM)
ΔGIPSP
(% CONTROL)
Spontaneous
Evoked

Figure 4-12 Evidence for the existence of an evoked EPSP in a SON neuron.

A) Under control conditions, the neuron has an evoked IPSP which is hyperpolarizing at resting membrane potential and reverses normally with hyperpolarization.

B) In the presence of BMI (100 μM) the PSP is depolarizing, evokes a spike at resting membrane potential, and is slightly increased in amplitude by hyperpolarization.

C) Plot of PSP amplitude as a function of membrane potential (Vm) under control conditions and in the presence of BMI. E_{IPSP-E} (arrow) obtained in control conditions was near -64 mV. The extrapolated E_{EPSP} (curved arrow) obtained in BMI was near $^{+}$20 mV. Note that the evoked G_{IPSP} = 25.08 nS while the evoked G_{EPSP} = 0.63 nS. Despite the relatively small conductance increase associated with the EPSP, its presence undoubtedly caused an underestimation of the E_{IPSP} for the evoked IPSP. Indeed, E_{IPSP-S} (arrow) of spontaneous IPSPs in this cell was estimated to be -77 mV. Same cell as Figure 4-13.

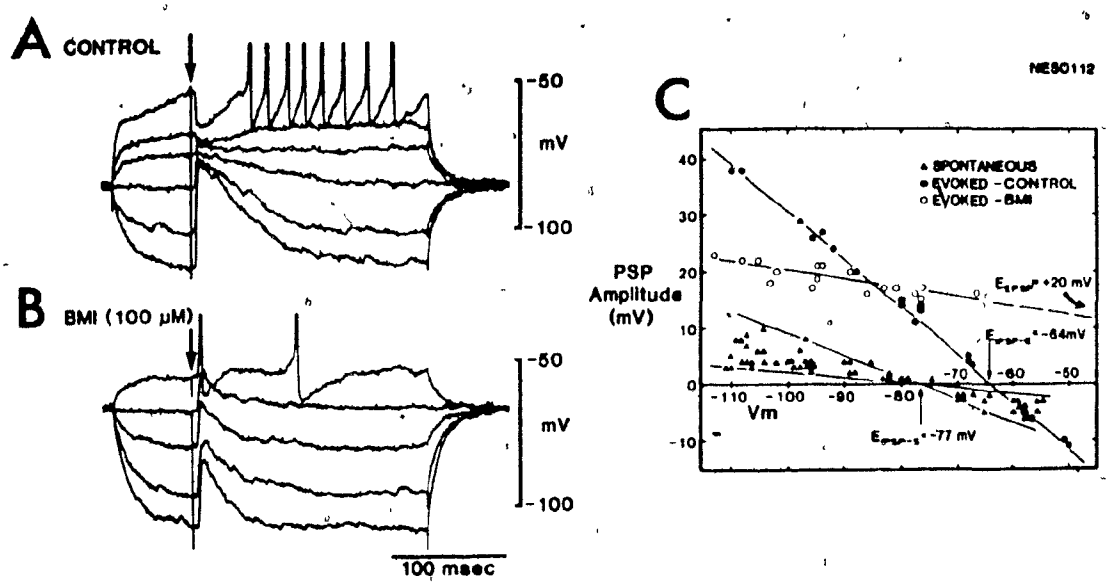
A
CONTROL
-50
mV
-100
B
BMI (100 μM)
-50
mV
-100
100 msec
C
NE80112
▲ SPONTANEOUS
● EVOKED - CONTROL
○ EVOKED - BMI
PSP Amplitude (mV)
40
30
20
10
0
-10
+20 mV
-64mV
-70
-60
-50
-110
-100
-90
-80
Vm
-77 mV

Figure 4-13 Evidence for the existence of an evoked EPSP in a SON neuron.

A) 1) 10 superimposed oscilloscope sweeps showing IPSP evoked by diagonal band of Broca stimulation (arrow) during spontaneous actvity in control medium. 2) Peristimulus histogram (PSH) collected during 40 cycles of the activity shown in A1.

B) 1) In the presence of BMI (100 μM), DBB stimulation evokes an EPSP which faithfully induces an action potential and prolonged period of increased excitability. 2) PSH of activity in B1. Same cell as in Figure 4-12.

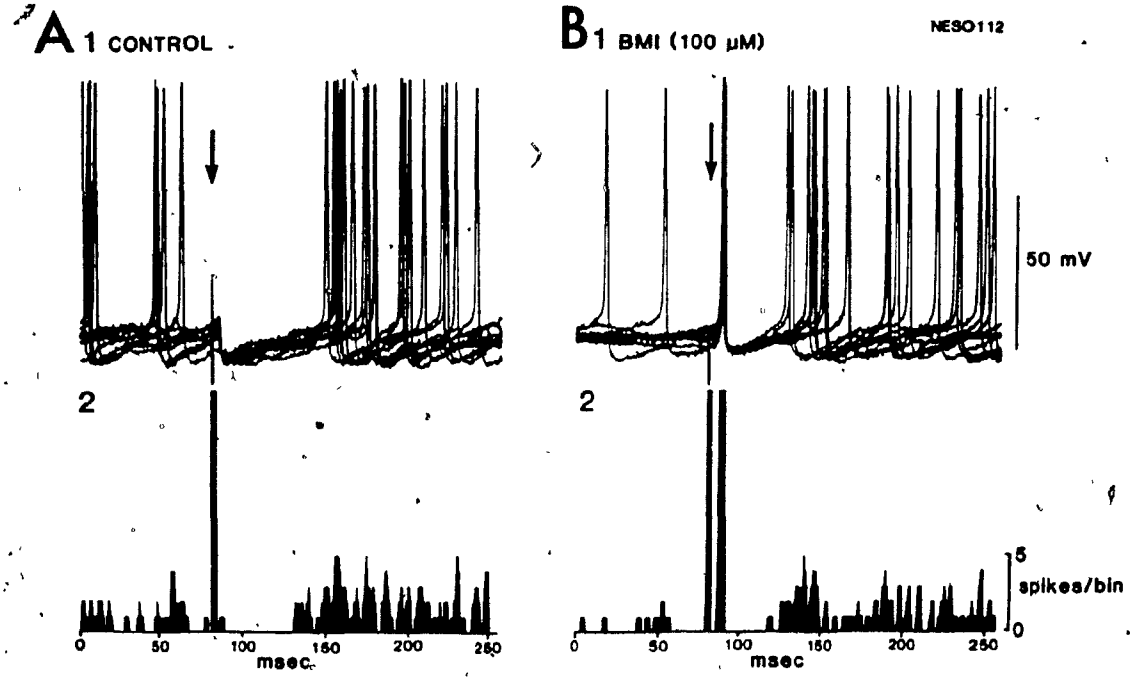
A 1 CONTROL
B 1 BMI (100 μM)
NESO112
50 mV
2
2
5
spikes/bin
0
0
50
100
150
200
250
msec
0
50
100
150
200
250
msec

Figure 4-14 Pentobarbital prolongs the evoked IPSP.
A) 1) 10 superimposed oscilloscope sweeps showing IPSP evoked by diagonal band of Broca stimulation during spontaneous activity in control medium. 2) Peristimulus histogram (PSH) collected during 40 cycles of activity shown in A1.
B) 1) In the presence of pentobarbital (100 μM), the IPSP induced by the diagonal band of Broca stimulation is markedly prolonged. 2) PSH of the activity in B1.

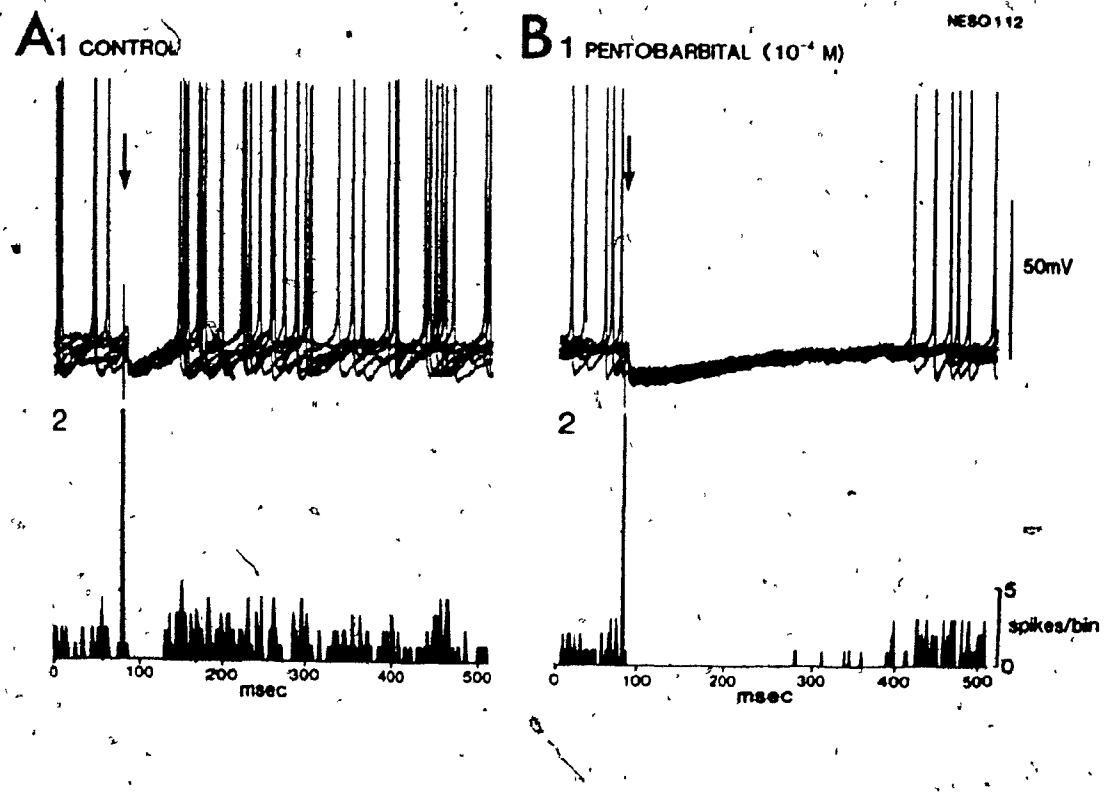
A1 CONTROL
B1 PENTOBARBITAL (10^{-4} M)
NESO112
50mV
2
2
0
100
200
300
400
500
msec
5
spikes/bin
0

Figure 4-15 Pentobarbital prolongs the evoked IPSP. Analysis similar to that in Figure 4-2.

A) Averaged record of 16 cycles with membrane potential held near -95 mV (KAc electrode) and IPSP evoked at 0.5 Hz under control conditions or in the presence of pentobarbital (PB, 10^{-4} M).

B) Semilogarithmic plot of the data in A. τ_{IPSP} is increased 2.1-fold by pentobarbital.

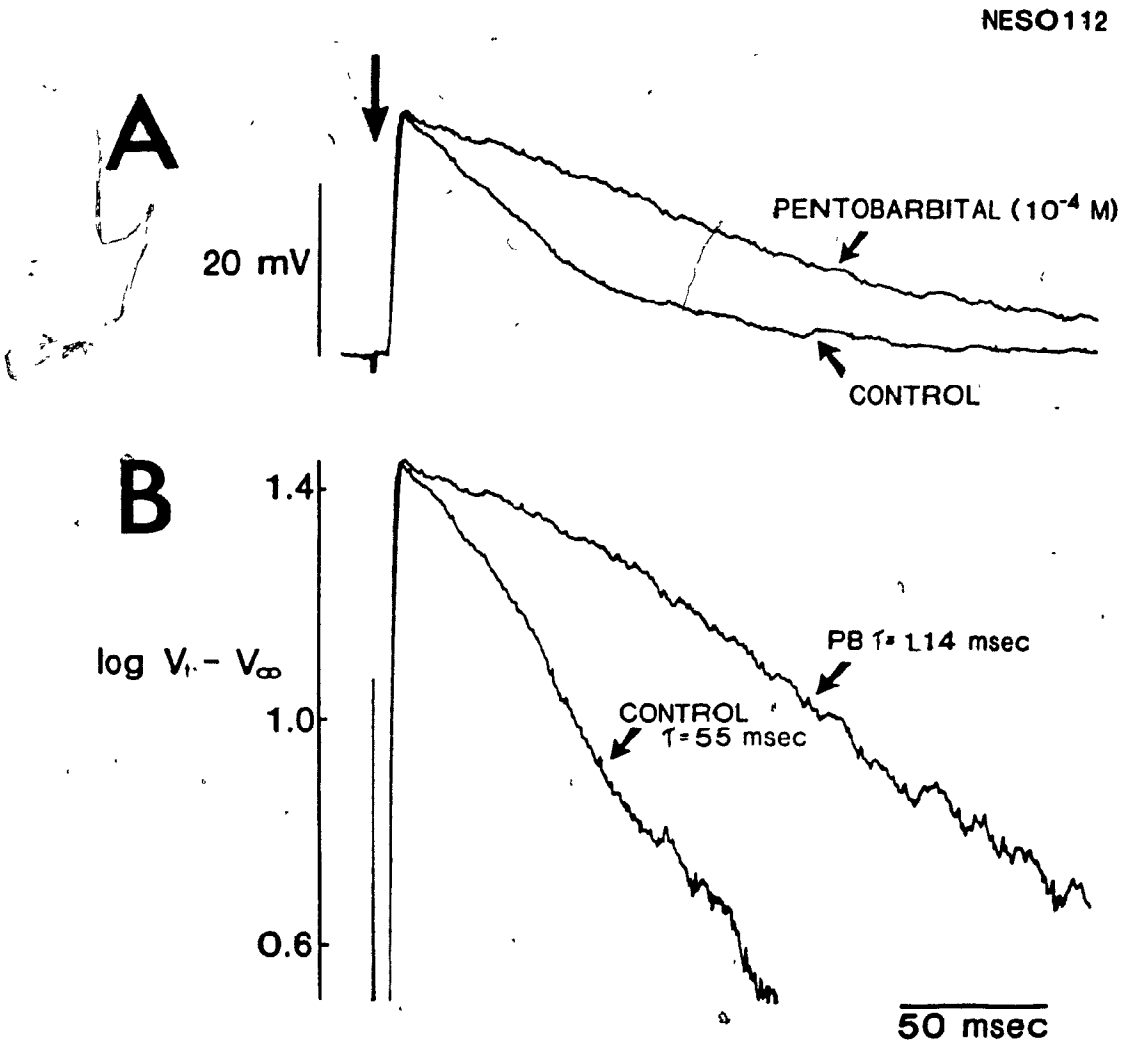
NESO112
A
20 mV
PENTOBARBITAL (10^{-4} M)
CONTROL
B
1.4
log $V_t - V_\infty$
1.0
0.6
PB τ = 114 msec
CONTROL
τ = 55 msec
50 msec

CHAPTER 5

THE EFFECTS OF GABA ON THE MEMBRANE PROPERTIES OF SON NEURONS

5.1 Introduction

SON neurons receive a powerful and active inhibitory input that appears to be mediated by the amino acid γ-aminobutyric acid (GABA) (see Chapter 4). Werman (1966) has outlined criteria which should be satisfied in order to identify the transmitter at a given synapse. In the case of GABAergic transmission in the SON, several have already been satisfied as morphological and biochemical studies that GABA, and the enzymes responsible for its synthesis and degradation, are present in the SON (Tappaz et al., 1977; Meyer et al., 1980; Perez de la Mora et al., 1981; Nagai et al., 1983). Two important criteria have yet to be satisfied: 1) Exogenous application of the putative transmitter must mimic the actions of the endogenous transmitter and 2) both of these effects must demonstrate sensitivity to a specific antagonist.

Iontophoretic studies on SON neurons in vivo have confirmed that GABA prompts a reduction in their excitability (Arnauld et al., 1983; Bioulac et al., 1978; Moss et al., 1972). There have also been reports involving the intracellularly recorded responses of SON neurons to

GABA (Abe and Ogata, 1983; Ogata et al., 1984) but none have described its actions in any detail. In order to confirm that GABA is the transmitter mediating most of the IPSPs observed in SON neurons, exogenous GABA must be shown to have effects similar to synaptic events on their membrane properties. This chapter reports observations on the actions of GABA and analogous compounds on SON neurons.

5.2 Results

5.2.1 Effects of GABA, Muscimol and Glycine

GABA (10 μM-1 mM) was applied in the perfusion medium for periods of 3-30 seconds. Its effects on action potential firing, membrane potential and input resistance were observed in 23 SON neurons in 15 explants. GABA (50μm) consistently inhibited spontaneous firing, but induced either a hyperpolarization (Fig. 5.1A) or a depolarization (Fig. 5.1B) in different cells. This response was resistant to synaptic blockade using tetrodotoxin (10^{-6} M, Figure 5-1B) or 15 mM Mg^{++}, indicating that GABA action is postsynaptic. Muscimol, a potent GABA-A receptor agonist, also induced similar effects but at a much lower range of concentrations (0.3-30μM). The responses to muscimol were 2-3 times longer than the responses to GABA (Fig. 5.1A). Glycine (1-10 mM) also mimicked the effects of GABA, but at concentrations at least 10-fold greater than those of GABA (Figure 5-1C).

5.2.2 GABA-induced conductance

GABA and muscimol induced dose-related decreases of input resistance (R_{in}; Figures 5-2, 5-3). Cells varied considerably in their sensitivity to GABA: cells which responded to 10-100 μM GABA usually underwent a 90-100% decrease in R_{in} in response to high doses of GABA (100 μM; Figure 5-2); cells sensitive to 0.1-1 mM GABA reduced R_{in} by a maximum of 50-80% of control values (Figure 5-3). These changes in R_{in} corresponded to GABA-induced conductances (ΔG) of 10-50 nS (mean 42 nS; see analysis in Chapter 2.7). Despite their differing sensitivities to GABA, all cells had sigmoidal dose-response relationships (ΔG vs. log [GABA]; Figure 5-4A) and the critical slope of the log-log plot of the dose-response relationship was 1.7 (Figure 5-4B). A similar variablity of the response to muscimol was observed (Figure 5-5) but the dose-response relationships (ΔG vs. log [muscimol]) were sigmoidal and the critical slope of the log-log plot was 1.6 (Figure 5-4).

5.2.3 Effects of Bicuculline Methiodide

Bicuculline can be viewed as a specific inhibitor of the effects of GABA in mammalian brain (Curtis et al., 1971b). The dose-response relationships for the conductance induced by GABA and muscimol were shifted to the right by

bicuculline methiodide (BMI, 100 μM, Figure 5-3). This effect of bicuculline methiodide was even more pronounced on muscimol responses. Maximal responses to GABA and muscimol could still be obtained in the presence of bicuculline methiodide, but higher concentrations were required (Figure 5-3). This indicates that the inhibition by BMI is competitive in nature.

5.2.4 Membrane Voltage Responses and Reversal Potentials

Membrane voltage responses to GABA and muscimol took two forms during intracellular recordings with KAc electrodes. In approximately 65% (9/14) of SON neurons studied, lower concentrations of GABA (10-50 μM) or muscimol (0.1-1 μM) induced moderate decreases of R_{in} (30-60%, ΔG = 1-10 nS) and a hyperpolarization of 2-10 mV (Figures 5-2, 5-5 and 5-6). Higher concentrations induced 80-100% decreases of R_{in} (ΔG = 20-100 nS) and biphasic voltage responses characterized by an initial hyperpolarization of 2-10 mV followed by a depolarization of similar amplitude. In the remaining 35% (4/15) of neurons, GABA appeared to be without effect at the lower concentrations but induced a depolarization at higher concentrations (Figures 5-3, 5-5 and 5-7).

Intracellular current injection revealed a voltage dependence of the hyperpolarizing GABA responses similar to that of the spontaneous and evoked IPSPs. The reversal

potential of the hyperpolarizing GABA response (E_{GABA}) was approximately equal to E_{IPSP} (± 5 mV; Figure 5-6). The reversal potential of the depolarizing GABA response ranged between -33 mV and -55 mV (mean -42 mV; Figures 5-6, 5-7).

5.2.5 Chloride-Dependence of the GABA Response

Similar GABA-induced conductance changes were observed in five recordings using KCl electrodes. However, the voltage dependence of the membrane response was altered such that the E_{GABA} was now -40.0 ± 4.3 mV (range -29 to -55 mV; Figure 5-8). E_{GABA} was in close agreement with the E_{IPSP} (±4 mV). In three neurons recorded with KAc electrodes, E_{GABA} exhibited a dependence upon the concentration of chloride ions in the perfusion medium $[Cl^-]_o$ which was similar to that of E_{IPSP} (Figure 5-8). Reduction of $[Cl^-]_o$ from 134 mM to 10.4 mM induced a positive shift of E_{GABA} by 40-50 mV (Figure 5-9). In contrast with the IPSP-associated conductance change (G_{IPSP}), no dependence of G_{GABA} on $[Cl^-]_o$ was observed.

5.3 Discussion

5.3.1 Identity of Action and Pharmacological Sensitivity

The principal objective of the experiments described in this chapter was to test the hypothesis that GABA may

mediate at least one form of synaptic inhibition, i.e. postsynaptic inhibition, in the SON. For this hypothesis to be true, exogenously applied GABA and synaptically-evoked IPSPs should both elicit similar effects on the membrane properties of SON neurons and both should demonstrate similar sensitivity to a specific antagonist (cf. Werman 1966). In fact, GABA's actions proved to be very similar to those of the IPSPs. Thus GABA: 1) inhibited action potential firing, 2) increased membrane conductance and 3) induced a hyperpolarization in most neurons which reversed near E_{IPSP} and was sensitive to the transmembrane chloride gradient. Therefore, similar to the IPSPs recorded in SON neurons, the effects of GABA appear to result from the activation of a chloride ionic conductance.

An explanation for the insensitivity of the GABA-induced conductance to changes in the $[Cl^-]_o$ can only be speculation at this time. As demonstrated by Takeuchi and Takeuchi (1967), the reduction in GABA-induced conductance under these circumstances depends upon depletion of intracellular chloride. This, in turn, depends upon the membrane's chloride conductivity, and would therefore be hastened by spontaneous chloride-mediated IPSPs, or repeated testing with GABA (cf. Meyer, 1976; Matthews and Wickelgren, 1979; Motozikawa et al., 1969; Newberry and Nicoll, 1985). The three SON neurons, whose responses to GABA in low chloride medium are reported here, displayed few spontaneous

IPSPs (see Figure 5-9) and were tested within 10 minutes of changing the perfusion medium from normal to low chloride. Because the intracellular concentration of chloride may be maintained under these conditions, and an outward flux of chloride ions is required to produce a membrane depolarization, no change in the GABA-induced conductance would be anticipated.

The ability of bicuculline methiodide to antagonize the effects of GABA, as it does the IPSPs, is further evidence for GABA mediation of the IPSPs, and suggests that the chloride ionophore is linked to GABA-A type receptors (See review, Enna and Gallagher, 1983). Biochemical studies suggest that the inhibition by bicuculline methiodide of GABA binding to GABA-A receptors is competitive in nature (Enna, 1977; Mohler and Okada, 1977). Several electrophysiological studies (Simmonds, 1980; Bowery and Brown, 1974; Homma and Rovainen, 1978; Pickles, 1979) indicate that inhibition of GABA actions by bicuculline resembles competitive inhibition because, in the presence of bicuculline methiodide, higher doses of GABA can still evoke maximal responses. This is manifested in the parallel shift of the dose-response curve for GABA induced by bicuculline methiodide in SON neurons (Figure 5-3). Thus, the actions of exogenous GABA are consistent with the hypothesis that GABA is the endogenous neurotransmitter mediating the IPSPs.

Glycine weakly mimicked the effects of GABA on SON

neurons. The relative potency of GABA and glycine was similar to that observed in cerebral cortex although opposite to that observed in spinal cord motoneurons (see Krnjevic et al., 1977). In a given brain region, these differences may be attributed to higher density or affinity of receptors for each of these amino acids, or to higher conductance of the corresponding ionophore. Thus, by ore or a combination of these factors, GABA appears to predominate over glycine in the SON. Although strychnine antagonized the IPSPs (Chapter 4), glycine is not viewed as an important inhibitory neurotransmitter in the SON. The ability of strychnine to reduce responses to GABA (cf. Scholfield, 1982), has not yet been confirmed, but would add support to this contention.

5.3.2 Effects of Muscimol

Muscimol, a powerful GABA-A agonist, was 20 times more potent than GABA in inducing a chloride conductance in the SON. This potency ratio is similar to that observed in the olfactory cortex (Pickles, 1979; Scholfield, 1982; Simmonds, 1980; Brown and Galvan, 1979) and is further evidence that the effects of GABA on SON cells are mediated by GABA-A receptors (Enna and Gallagher, 1983). Biochemical studies indicate a smaller, 3 to 8-fold difference in the affinities of GABA and muscimol for the GABA-A receptor (Snodgrass, 1978; Williams and Risley, 1979; Beaumont et al., 1978;

Mohler and Okada, 1977). Although the reason for this discrepancy has not yet been determined, Brown and Galvan (1979) have speculated that GABA is less accessible to the receptor binding site because of glial uptake (cf. Iversen and Kelly, 1975). Muscimol and bicuculline are poor substrates for the Na-dependent GABA binding site thought to mediate GABA uptake (Johnston et al., 1978). This explains not only the greater potency of muscimol, but the longer duration of responses compared to GABA (Figure 5-2). The greater sensitivity of muscimol to antagonism by bicuculline methiodide (Figure 5-3B,C; see also Scholfield, 1982; Simmonds, 1980) can also be explained on this basis. GABA, at higher concentrations (vs. muscimol) necessary to induce a given conductance change, competes more effectively with bicuculline methiodide for GABA-A binding sites.

This discrepancy in potency ratio could also be the result of differing abilities of GABA and muscimol to activate the receptor-ionophore complex following receptor binding. Mathers and Barker (1981) suggested that muscimol activates a channel having a mean open time twice that of the channel activated by GABA. Pertinent to this discussion is the observation that the slope of the log-log plots of ligand-induced currents as a function of ligand concentration is approximately 1.7 for both GABA and muscimol (Figure 5-4B). This value is similar to that observed in several other systems (Barker and Ransom, 1978;

Akaike et al., 1985; Choi and Fischbach, 1981; Krnjevic et al., 1977) and has been held as evidence that two molecules (of either GABA or muscimol), combine with the receptor to activate the chloride ionophore. This similarity of the slopes for GABA and muscimol argues that differences in ionophore activation kinetics do not result from differences in the stoichiometry of the receptor binding → activation sequence for the two agents. A more likely explanation is that the higher affinity of muscimol for the GABA binding site results from slower dissociation of the muscimol-receptor complex. This decreased rate of dissociation might result in slower channel inactivation kinetics.

5.3.3 Biphasic and Depolarizing Responses to GABA

Perhaps the most perplexing aspect of the results of these experiments is the dichotomy in the data concerning the reversal potential of the membrane voltage response to GABA (E_{GABA}). Approximately 60% of SON neurons responded to low doses of GABA (10-100 μM) and E_{GABA} was very similar to the E_{IPSP}. In the remaining neurons, E_{GABA} was 10-36 mV more positive than the E_{IPSP}, similar to the E_{GABA} or E_{IPSP} observed in SON neurons recorded with KCl electrodes. These cells only responded to concentrations of GABA greater than 100 μM. No other membrane property could

be found that demonstrated a strong correlation with E_{GABA}. In particular, there was no correlation between the strength of the evoked IPSP in a given neuron, and its responsiveness to GABA.

Biphasic responses to GABA have been reported in other CNS neurons (Barker and Ransom, 1978a; Alger and Nicoll, 1982; Andersen et al., 1980) and several explanations of the phenomenon have been offered. Barker and Ransom (1978a), whose data are similar to those presented here, suggested that high doses of GABA cause sufficient Cl^- to enter the neuron, resulting in a reversal of the electrochemical chloride gradient. It is difficult to imagine how this could happen, however, since the flow of Cl^- ions should stop when E_{Cl^-} reaches the membrane potential. However, chloride flux into neurons, and perhaps glia, might concomittantly lower extracellular chloride and reverse the membrane chloride gradient.

Barker and Ransom (1978a) also performed topographical studies of GABA responses and showed that depolarizing responses could be regularly evoked in dendrites. This suggests that the electrochemical chloride ion gradient across the dendritic membrane may be reversed, when compared with the somatic membrane. Alger and Nicoll (1982) made similar observations in pyramidal cells in hippocampal slices, and proposed that hyperpolarizing responses to GABA result from activation of somatic, synaptic receptors, while

depolarizing responses result from the activation of dendritic, extrasynaptic receptors. This hypothesis would explain the present data quite well. Unfortunately, detailed information concerning the organization of GABAergic input(s) to the SON, and the location of GABA receptors on SON neurons are not currently available.

A third explanation, proposed by Krnjevic et al. (1977), is that prolonged exposure to high concentrations of GABA activates Na^+-dependent GABA uptake. This transport may be electrogenic and cause a positive shift in membrane potential due to synport of Na^+ and GABA (which is neutral at pH7). If such a mechanism operates in the SON, it must also be activated by muscimol, since this agent also evokes biphasic responses (Figure 5-2). Also, nipecotic acid, a GABA-uptake inhibitor, might be expected to reduce the depolarizing respones to GABA while prolonging its actions on post-synaptic receptors.

The simple and uniform morphology, the frequent spontaneous IPSPs and the ability to reliably evoke an IPSP should make SON neurons an ideal model system in which to perform detailed studies of GABA-mediated neurotransmission in the mammalian central nervous system.

Figure 5-1 Responses of three SON neurons to GABA, muscimol and glycine. Substances were administered during the interval indicated by the horizontal bars; pulses of hyperpolarizing current were administered every 1-2 seconds to monitor the cell's input resistance. In all figures (except Figure 5-1B$_2$) the full amplitude of action potentials is not shown. A) KAc electrode 1) GABA inhibits action potential firing while inducing a membrane hyperpolarization and decreased input resistance. 2) Muscimol has similar effects which last 2-3 fold longer. B) KAc electrode 1) In another cell, GABA suppressed action potential firing but induced a membrane depolarization. 2) Both responses persisted in the presence of tetrodotoxin (TTX, 10^{-6}M); TTX-insensitive Ca^{++}-dependent action potential firing was inhibited by GABA. C) KCl electrode. Glycine also induced a reduction in input resistance and membrane depolarization, but only with a 10-fold higher concentration.

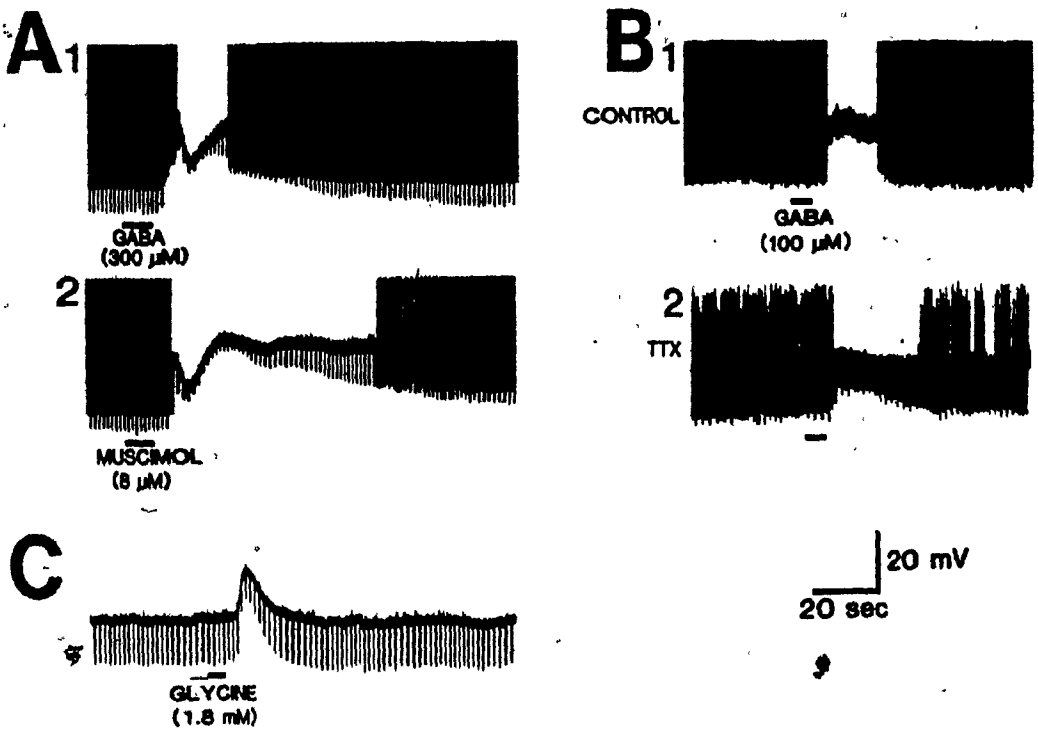
A1
GABA
(300 μM)
2
MUSCIMOL
(6 μM)
B1
CONTROL
GABA
(100 μM)
2
TTX
C
GLYCINE
(1.8 mM)
20 mV
20 sec

Figure 5-2 Chart recordings of the responses of a SON neuron which was sensitive to low doses of GABA and muscimol. The resting membrane potential was -58 to -60 mV throughout; constant-current pulses (70 pA) were administered at 0.5 Hz to monitor input resistance (200-240 MΩ at rest). GABA (A) or muscimol (B) was administered during the period indicated by the bar at the bottom of each series of records at the concentration indicated to the left of each record. Low doses of both substances induced moderate decreases in input resistance accompanied by a hyperpolarization. Higher doses shunted the membrane resistance and induced a biphasic response where an early hyperpolarization was followed by a late depolarization.

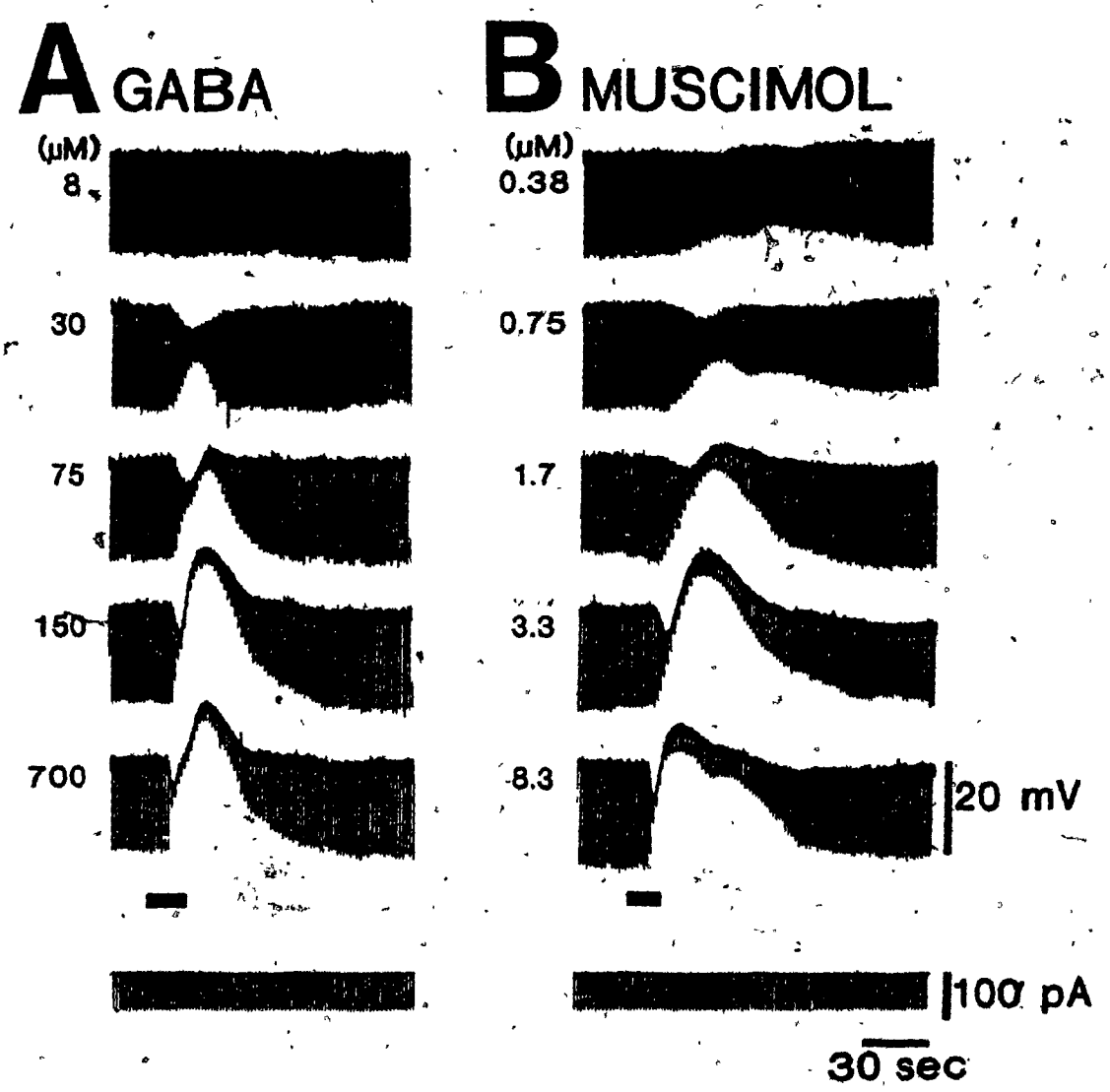
A GABA
(μM)
8
30
75
150
700
B MUSCIMOL
(μM)
0.38
0.75
1.7
3.3
8.3
20 mV
100 pA
30 sec

Figure 5-3 Antagonism by bicuculline methiodide (BMI, 100 μM) of the effects of GABA (A) and muscimol (B). Chart recordings as in Figure 5-2; RMP = -62 to -64 mV throughout; 100 pA constant current pulses indicate that resting input resistance was 240-270 MΩ. Note that for this particular neuron, five to ten-fold higher doses of GABA and muscimol were needed to induce increases in input conductance equivalent to those displayed in the cell in Figure 5-2. The membrane voltage response was primarily depolarizing. Maximal doses of GABA and muscimol increased input conductance by approximately 15 nS. BMI increased the dose of GABA or muscimol necessary to obtain this maximal response. This is illustrated in C) where ΔG is plotted as a function of the concentration of GABA (triangles) or muscimol (diamonds) under either control conditions (filled symbols) or in the presence of BMI (empty symbols). The parallel displacement of the dose-response curve for GABA by BMI indicates that BMI acts as a competitive antagonist.

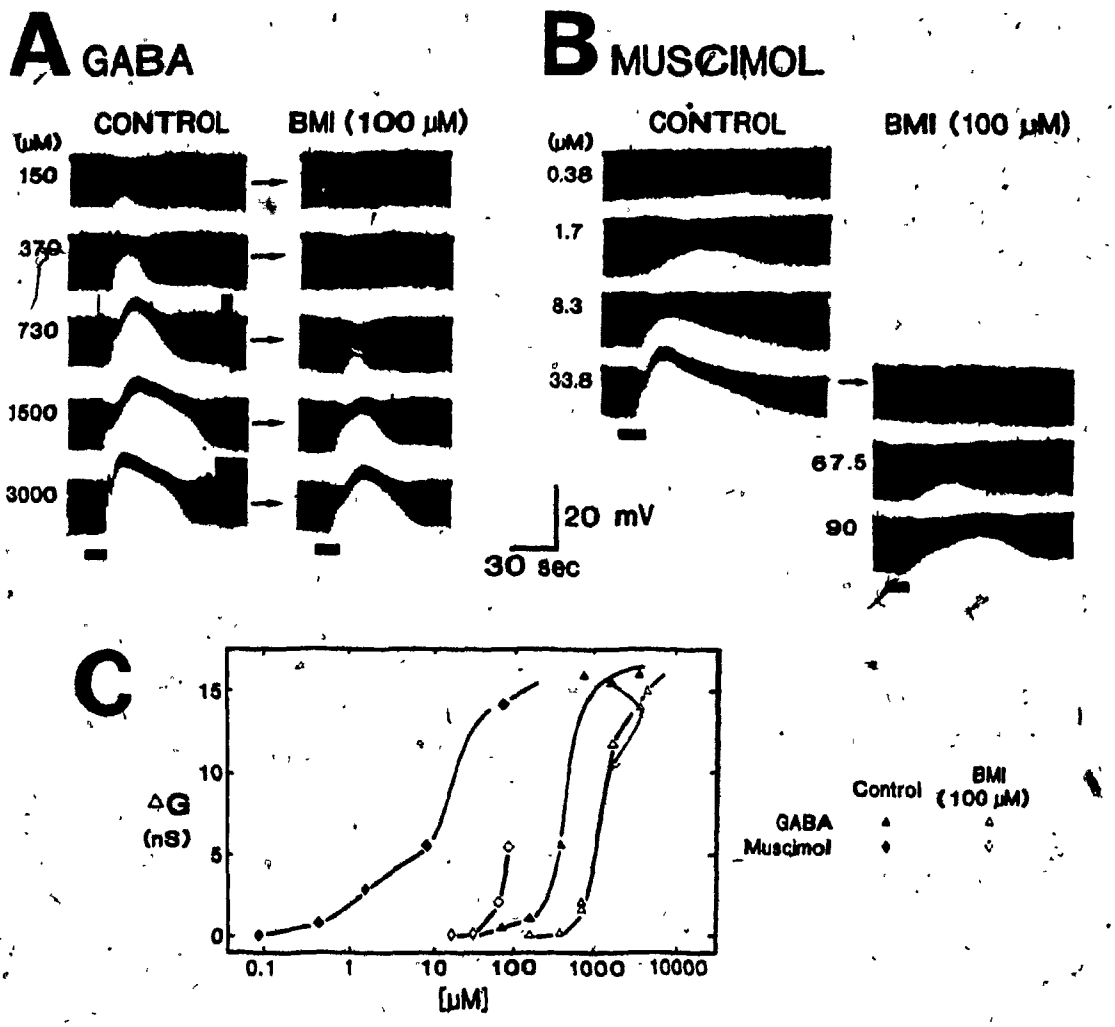
A GABA
CONTROL
BMI (100 μM)
(μM)
150
370
730
1500
3000
B MUSCIMOL
CONTROL
BMI (100 μM)
(μM)
0.38
1.7
8.3
33.8
67.5
90
20 mV
30 sec
C
ΔG
(nS)
15
10
5
0
0.1
1
10
100
1000
10000
[μM]
Control
BMI (100 μM)
GABA
Muscimol

Figure 5-4. Dose-response relationships for the increase in input conductance (ΔG) by GABA (triangles) and muscimol (diamonds) in SON neurons. For individual SON neurons, conductance changes at each concentration of GABA or muscimol, were expressed as a percentage of maximal GABA-induced response in that cell. Data for all cells in this study were then pooled according to the concentration of GABA or muscimol. Each point represents the mean of data obtained from 2-8 SON neurons. A) Semi-log plot reveals sigmoidal dose-response relationship. Muscimol was approximately 20-fold more potent than GABA although maximal concentrations of each drug induced identical conductance changes. B) Log-log plots of the data in A) have critical slopes of 1.7 (GABA) and 1.6 (muscimol). See text for discussion.

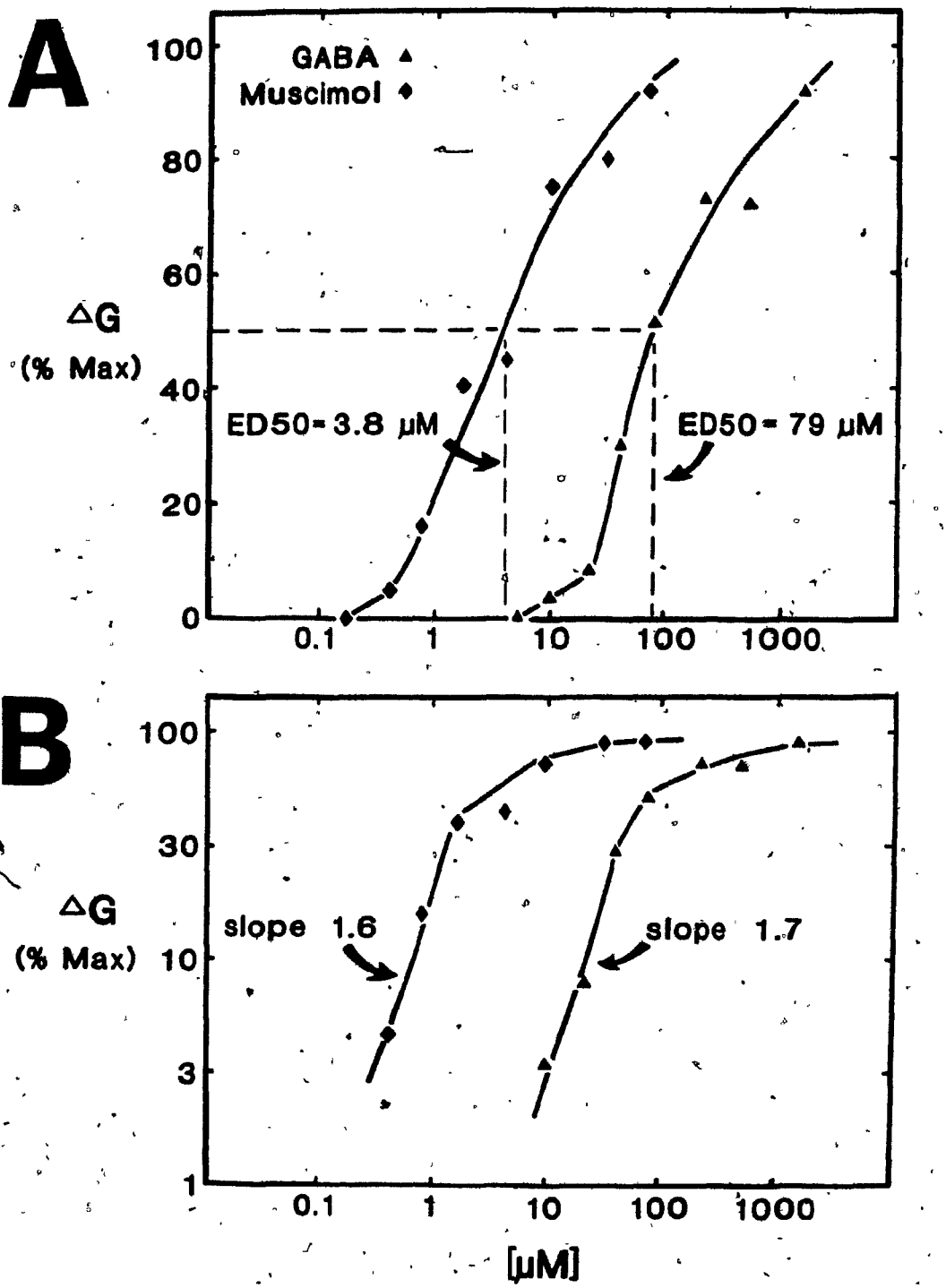
A
GABA ▲
Muscimol ◆
100
80
60
40
20
0
ΔG
(% Max)
ED50= 3.8 μM
ED50= 79 μM
0.1
1
10
100
1000
B
100
30
10
3
1
ΔG
(% Max)
slope 1.6
slope 1.7
0.1
1
10
100
1000
[μM]

Figure 5-5 Differences in the potency of GABA and muscimol on SON neurons whose responses were biphasic (Figure 5-2), or monophasic (depolarizing) (Figure 5-3). The conductance data from Figure 5-4 were divided into two groups based upon the membrane voltage response of the neurons. A) Semi-log plot similar to Figure 5-4A except that the actual induced conductance (ΔG) is plotted. GABA (triangles) and muscimol (diamonds) induced conductance changes ten-fold more potently in cells that responded biphasically (filled symbols) than in those that only depolarized (empty symbols). B) Semi-log plot of the membrane voltage responses (ΔVm) of these neurons. Positive values indicate depolarization; negative values indicate hyperpolarization. Note that neurons that respond biphasically are hyperpolarized by doses of GABA and muscimol 5-10 fold lower than doses that induce a depolarization. Also note that in one SON neuron that was only depolarized by GABA, high doses of muscimol induced a biphasic response.

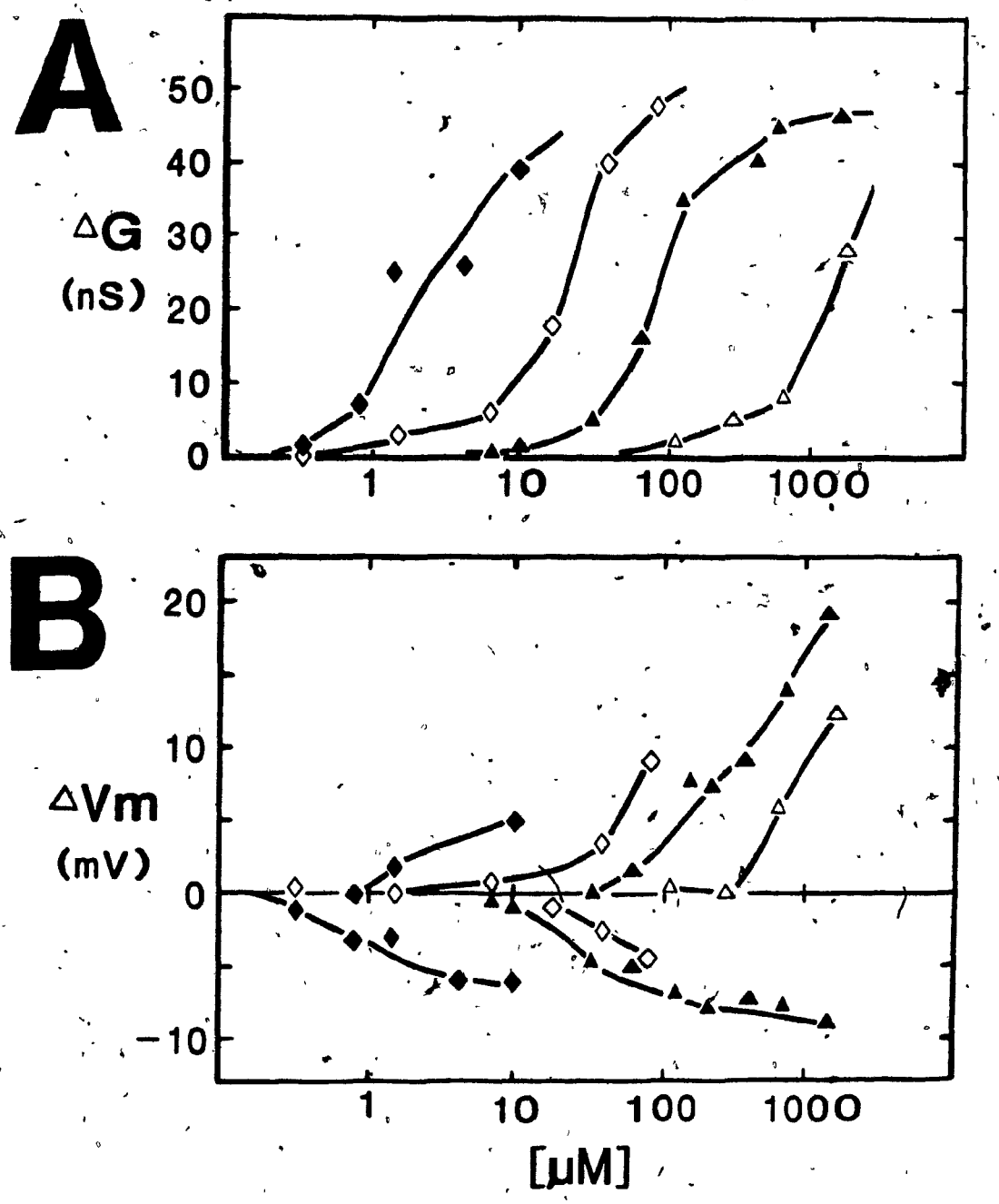
A
ΔG
(nS)
50
40
30
20
10
0
1
10
100
1000
B
ΔVm
(mV)
20
10
0
−10
1
10
100
1000
[μM]
Biphasic
Depolarizing
GABA
Muscimol

Figure 5-6 Voltage-dependence of the hyperpolarization and biphasic responses to GABA and the evoked IPSP in a SON neuron recorded with a KAc electrode. GABA was administered during the period indicated by the bar at 50 μM (A) or 500 μM (B) in order to evoke hyperpolarizing or biphasic responses. The membrane potential (indicated to the left of each record) was adjusted by steady intracellular current injection and the sign and amplitude of the membrane voltage responses (ΔVm) were observed. Similarly in C) the sign and amplitude of the IPSP evoked by electrical stimulation (arrow) of the diagonal band of Broca (Chapter 4) was monitored as the membrane potential was adjusted by intracellular injection of current pulses. D) ΔVm was plotted as a function of membrane potential (Vm). The hyperpolarizing responses to GABA showed a voltage-dependence very similar to that of the evoked IPSP. Both responses reversed near -81 mV. The reversal potential of the depolarizing response to GABA was estimated by extrapolation to be -49 mV.

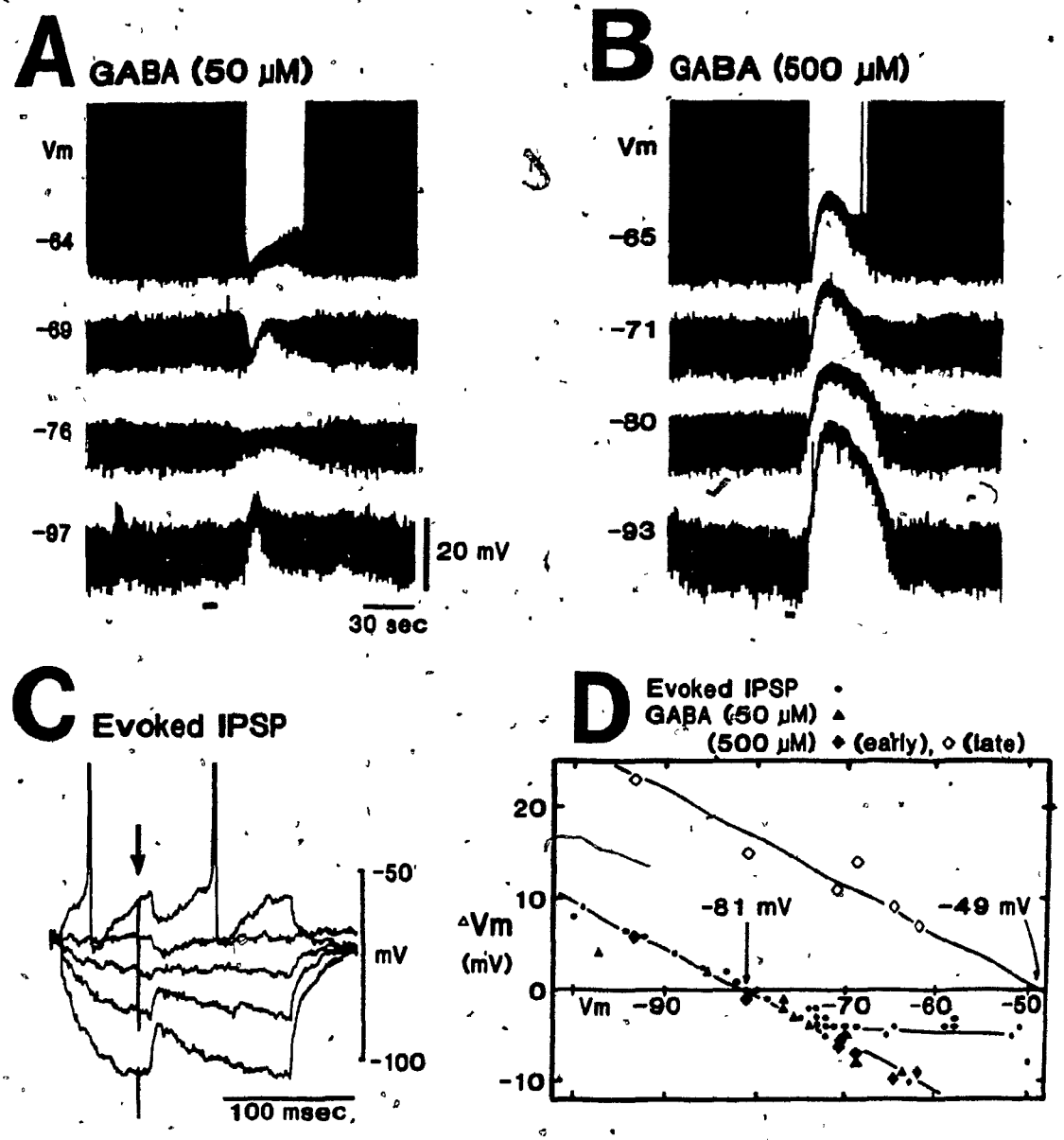
A GABA (50 μM)
Vm
-64
-69
-76
-97
20 mV
30 sec
B GABA (500 μM)
Vm
-65
-71
-80
-93
C Evoked IPSP
-50
mV
-100
100 msec
D Evoked IPSP •
GABA (50 μM) ▲
(500 μM) ◆ (early), ◇ (late)
20
10
0
-10
ΔVm (mV)
-81 mV
-49 mV
Vm -90
-70
-60
-50

Figure 5-7 Voltage-dependence of (A) the depolarizing response to GABA and (B) the evoked IPSP in a SON neuron recorded with a KAc electrode. Same analysis as in Figure 5-6. Note in (C) that the reversal potentials of the GABA and IPSP-induced voltage changes differ by approximately 36 mV.

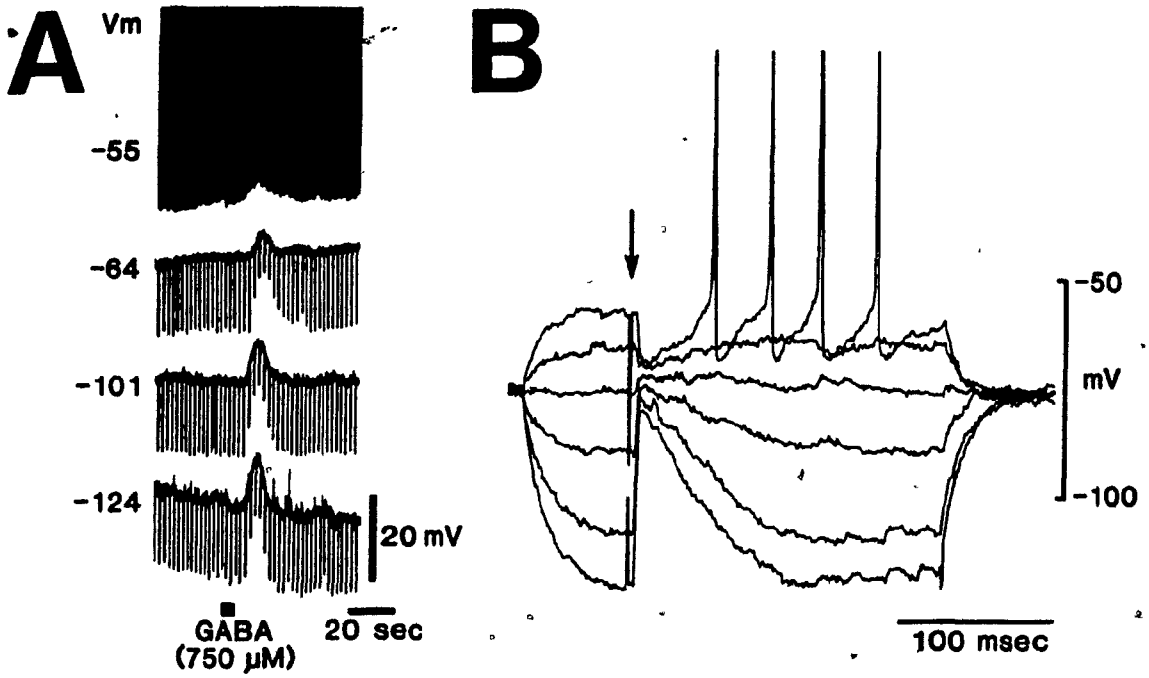
A
Vm
-55
-64
-101
-124
20 mV
GABA
(750 µM)
20 sec
B
-50
mV
-100
100 msec
C
• Evoked IPSP
◦ GABA
ΔVm
(mV)
40
30
20
10
0
Vm
-120
-100
-80
-60
-40
-33 mV
-69 mV

Figure 5-8 Voltage-dependence of the depolarizing response to GABA (A) and the IPSP (B) in a SON neuron recorded with a KCl electrode. Same analysis as in Figure 5-6. Note in C) that the reversal potentials of GABA and IPSP-induced voltage responses are similar.

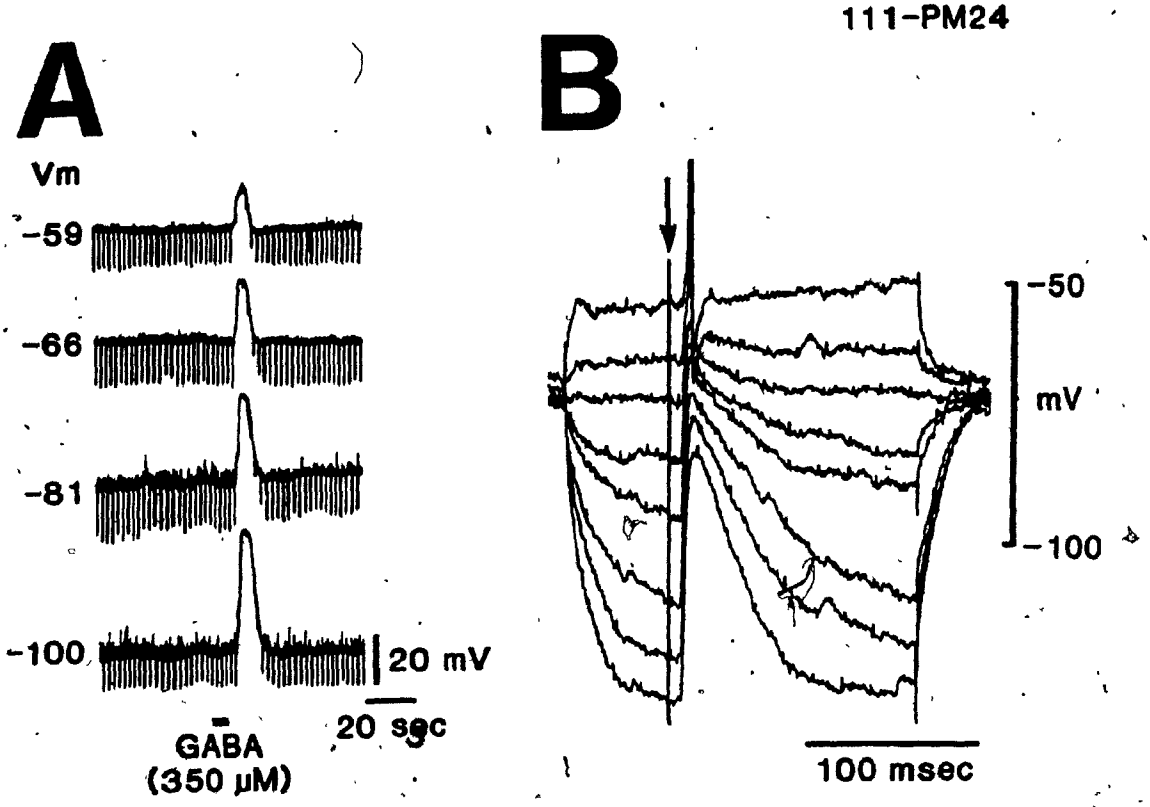
A
Vm
-59
-66
-81
-100
20 mV
20 sec
GABA
(350 μM)
B
-50
mV
-100
100 msec
C
60
40
20
0
ΔVm
(mV)
• Evoked IPSP
○ GABA
-40 mV
-120
-100
-80
-60
-43 mV

Figure 5-9 Dependence of the reversal potential of the GABA-induced voltage responses (E_{GABA}) upon the extracellular concentration of chloride ions. Similar analysis as in Figure 5-6. Responses to GABA were observed in medium containing the normal concentration of chloride (134 mM, A) or in medium containing 10.4 mM Cl^- in which NaCl was replaced by Na Glucuronate (B). C) E_{GABA} was shifted from -63 mV to approximately -10 mV by the reduction of extracellular Cl^-.

115-AM64

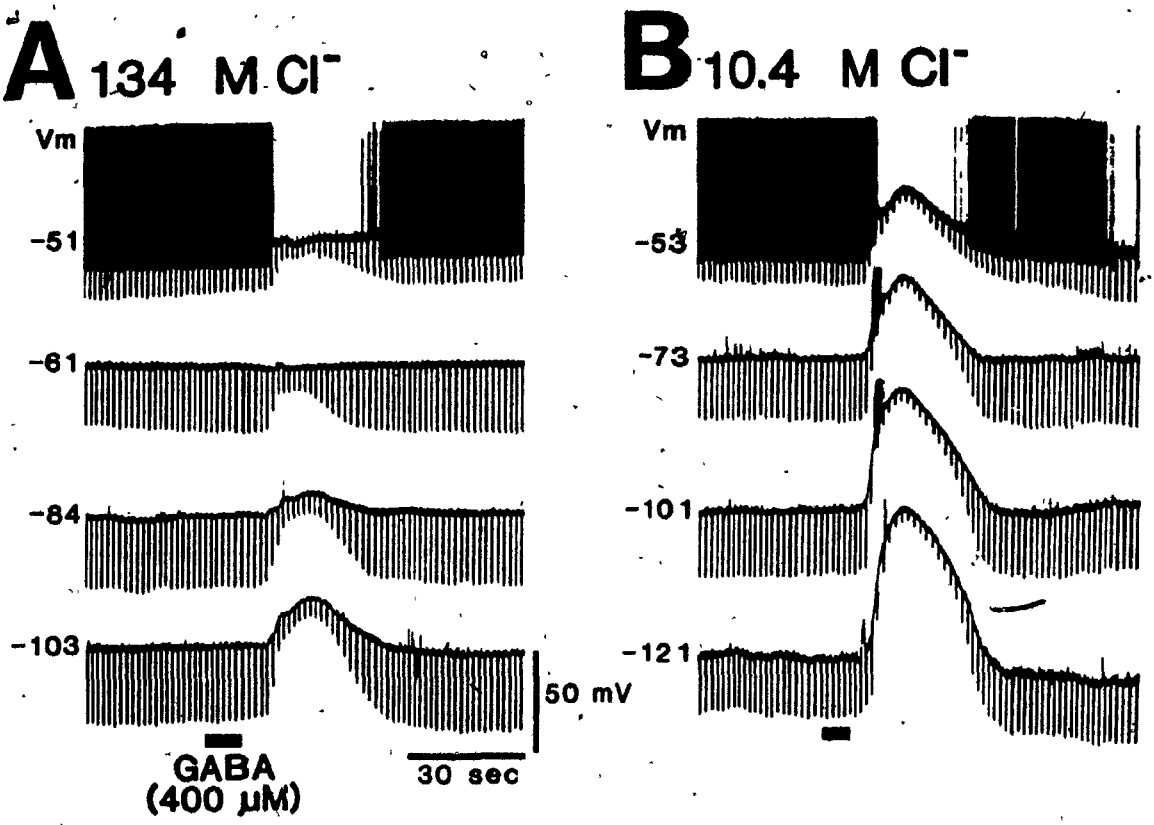
A 134 M Cl⁻
Vm
-51
-61
-84
-103
50 mV
GABA
(400 µM)
30 sec
B 10.4 M Cl⁻
Vm
-53
-73
-101
-121

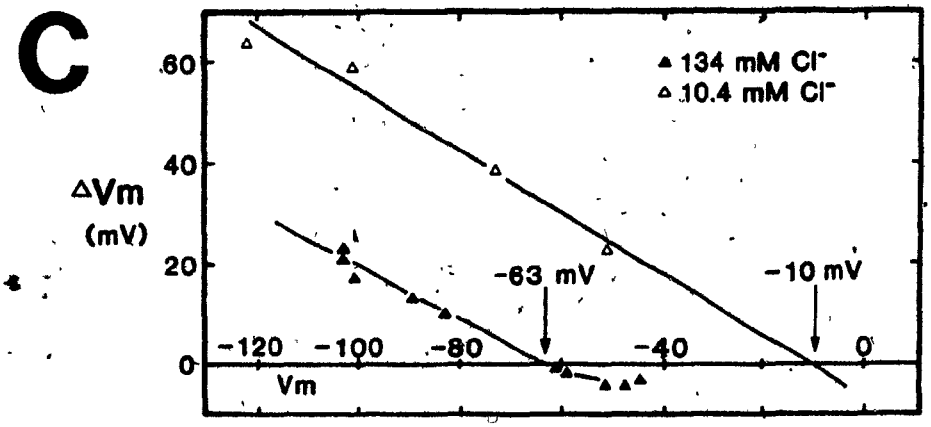
C
▲ 134 mM Cl⁻
△ 10.4 mM Cl⁻
ΔVm
(mV)
60
40
20
0
-63 mV
-10 mV
-120
-100
-80
-40
0
Vm

CHAPTER 6

α-ADRENERGIC ACTIVATION OF SON NEURONS

6-1 Introduction

The SON contains an extremely dense plexus of catecholaminergic fibers (Carlsson et al., 1962) which arises for the most part from norepinephrine-containing somata located in the A1 cell group of the ventrolateral medulla (Swanson et al., 1981). The numerous studies designed to evaluate the influence (ie: facilitatory or inhibitory) of norepinephrine on the release of neurohypophysial hormones have yielded contradictory results and have failed to provide a definitive conclusion (see Chapter 1). In particular, while earlier electrophysiological studies indicate that norepinephrine depresses the firing frequency of SON neurons *in vivo* (Barker et al., 1971; Moss et al., 1971, 1972; Arnauld et al., 1983), recent reports argue to the contrary (Day and Renaud, 1984; Wakerley et al., 1983). Since more precise control of drug concentrations during neuropharmacological tests can be achieved *in vitro*, the experiments reported below used perfused explants of hypothalamus to examine the effects of norepinephrine and analogous compounds on the excitability and membrane properties of SON neurons.

6.2 Results

6.2.1 Adrenergic Effects on Firing Frequency and Pattern

The drug sensitivity of 171 SON neurons (141 recorded extracellularly, 30 intracellularly) in 80 preparations was examined. The spontaneous activity patterns of these cells varied widely from quiescent (<1 Hz) to irregular, continuous or phasic activity. The most consistent response to norepinephrine (10-200 μM) was an increase in excitability observed from 85% of both quiescent and spontaneously active cells. This total includes 13 cells that could be activated antidromically from the pituitary stalk and 7 cells maintained in synaptic isolation in medium containing 15 mM Mg^{++}. Reproducible responses to repeated pressure applications from an adjacent micropipette (Figure 6-1A) indicated no apparent tachyphylaxis.

When added to the perfusion medium, norepinephrine prompted an initial increase in discharge frequency that persisted for as long as several minutes (Figure 6-1B-D). Among silent cells, this could be followed by the appearance of phasic firing (Figure 6-1B). Cells that discharged continuously when initially encountered were seen to show a transition following norepinephrine application to patterned firing which consisted either of a series of brief bursts of 3-15 action potentials (Figure 6-2B), or phasic bursting (Figure 6-1D). Low doses of NE (10 μM) could induce this patterning without much effect on overall firing frequency

(Figure 6-2). Higher doses (30-100 μM) induced a similar bursting pattern of firing, but also increased the overall firing frequency (Figure 6-1B,C).

6.2.2 Effects of Adrenergic Agonists and Antagonists

The α_1-adrenergic agonists methoxamine and phenylephrine (10-200 μM) mimicked the effects of norepinephrine (Figure 6-1B,2,3 & 4). Neither clonidine (10-300 μM, tested on 9 cells), reported to act on α_2-receptors, nor isoproterenol (10-300 μM, tested on 9 cells, Figure 6-2B,C), a β-adrenoreceptor agonist, demonstrated any obvious effect on the firing pattern of SON neurons.

The effect of norepinehrine could be completely blocked by the non-selective α-adrenergic antagonist phenoxybenzamine (1-10 μM, 10 cells, Figure 6-3A) or the selective α_1-antagonist prazosin (10 nM-1 μM; Figure 6-3B, 6-4C). The effects of these two agents were extremely long-lived and reversal of the blockade was obtained only on two occasions. A similar antagonism of the norepinephrine-induced response could be obtained with the predominantly α_2-antagonist yohimbine (3 cells), but this required concentrations in excess of 10 μM (Figure 6-3C).

6.2.3 Adrenergic Effects on Membrane Properties

Norepinephrine, phenylephrine and methoxamine could all induce membrane depolarization associated with the increase

in frequency of action potential firing (Figure 6-4). No consistent change in input resistance was detected (Figure 6-4A). The depolarization induced by norepinephrine was reduced or abolished by prazosin (10-1000 nM; Figure 6-4C). The 5-10 mV depolarizations at resting membrane potentials (-50 to -65 mV) were reduced by membrane hyperpolarization to -90 to -100 mV (Figure 6-5). Further hyperpolarization never reversed the depolarization. It is important to note that this voltage-dependence of the response to norepinephrine and agonists could not be demonstrated as reliably as that of the IPSP (Chapter 4) or the response to GABA (Chapter 5). Nevertheless, in two neurons the norepinephrine-induced depolarization was reduced by increasing the extracellular K^+ concentration (Figure 6-6).

6.2.4 Adrenergic Effects on Action Potentials

Previous studies have indicated that norepinephrine shortens action potentials by reducing inward Ca^{++} currents (Williams and North, 1984; Dunlap and Fischbach, 1981; Galvan and Adams, 1982; Horn and McAfee, 1980). This effect of norepinephrine is probably mediated by α_2-adrenoreceptors since it is mimicked by clonidine (Williams and North, 1984).

SON neurons display calcium-dependent action potentials in the presence of tetrodotoxin (Bourque and Renaud, 1984).

In two experiments, norepinephrine had no effect on the amplitude or duration of these calcium-dependent action potentials (data not shown). This indicates that the calcium-currents underlying action potentials are not modulated by norepinephrine. In contrast, action potential duration was increased 5-50% concomittant with the increased frequency of short interspike intervals (Figure 6-7C; cf. Bourque and Renaud, 1984) during bursting induced by norepinephrine or an agonist. The neuron illustrated in Figure 6-7 responded to methoxamine (30 μM) with a modest increase in firing frequency and action potential duration. Higher doses of norepinephrine or agonists produced greater changes in both parameters.

6.2.5 Adrenergic Effects on "After-Potentials"

Single action potentials or current-evoked bursts in SON neurons are followed by a hyperpolarizing after-potential (Andrew and Dudek, 1984a) that results from the activation of voltage- and calcium- dependent potassium currents (Bourque et al., 1985). The amplitude of these hyperpolarizing potentials was unaffected by norepinephrine and α_1-agonists (Figure 6-7, 6-8; 5 cells). However, α_1-agonists increased the rate of decay of the hyperpolarizing after-potential following single spikes (ie. the gradual depolarization; Figure 6-7D) resulting in shorter interspike intervals (Figure 6-7B$_2$).

A preliminary experiment indicated that the depolarizing after-potential that follows current-evoked bursts of action potentials (Andrew and Dudek, 1984; Bourque, 1984) is also altered in the presence of norepinephrine. As illustrated in Figure 6-8, norepinephrine increased the depolarizing after-potentials 2-fold, independent of its effects on membrane potential.

6.3 Discussion

6.3.1 α_1-Adrenoreceptor-mediated Excitation of SON Neurons

These observations indicate that norepinephrine has a predominantly facilitatory role to enhance the excitability and promote bursting activity in SON neurosecretory neurons, mediated through an α_1-adrenoreceptor mechanism. This is consistent with recently reported *in vitro* observations in rat hypothalamic slices (Wakerly et al., 1983). Such actions are also supported by various *in vivo* studies demonstrating a release of vasopressin by intranuclear (Milton and Paterson, 1974) or intraventricular (Bridges et al., 1976; Kuhn, 1974) norepinephrine injections, and the blockade of norepinephrine-induced vasopressin release by α-adrenoreceptor antagonists (Bridges and Thorn, 1970) or central catecholamine depletion (Miller et al., 1979). However, other observations suggest a predominantly inhibitory role for norepinephrine not only on SON neuronal excitability (Arnauld et al., 1983; Barker et al., 1971;

Sakai et al., 1974), but also on the release of vasopressin (Armstrong et al., 1983; Kimura et al., 1981).

These seemingly contradictory findings may be explained by the presence of functionally different adrenergic receptors on SON neurons, with inhibitory actions mediated by β-adrenoreceptors (Sakai et al., 1974; Barker et al., 1971). Iontophoretically administered norepinephrine, unless carefully controlled, can produce inconstant and excessively high local drug concentrations that may mask any excitatory actions obtained with lower concentrations (Armstrong-James and Fox, 1983). Day et al. (1985) recently showed that pressure ejection of low concentrations of norepinephrine (50-150 μM) in vivo excite SON neurons via α-adrenoreceptors while high concentrations (greater than 1 mM) inhibit via β-adrenoreceptors.

Further support for the present data derives from recent in vivo studies in the rat in which electrical stimulation in the A1 cell group of the ventrolateral medulla, the site of origin of most SON noradrenergic afferents (Sawchenko and Swanson, 1981), was shown to enhance the activity of SON neurosecretory cells (Day and Renaud, 1984). Moreover, in keeping with the anatomical observation that the noradrenergic input is centered predominantly around vasopressin-containing neurons (McNeill and Sladek, 1980; Swanson et al., 1981), this excitation selectively involves the putative vasopressinergic

neurosecretory cells (Day and Renaud, 1984). Similarly, pressure ejection of norepinephrine *in vivo* was more potently excitatory on putatively identified vasopresinergic neurons (Day et al., 1985). The high percentage of SON neurons that demonstrate activation following norepinephrine applications in the present series of experiments may reflect our bias for recordings obtained from the posteroventral parts of the SON, a site rich in vasopressin-containing somata (Swaab et al., 1975a,b; Vandesande and Dierickx., 1975). A definitive answer concerning the selectivity of the norepinephrine action on vasopressinergic neurons electrophysiologically would require additional experiments using a combination of immunocytochemistry and intracellular electrophysiological recordings (Yamashita et al., 1983). However, the experiments described in Chapter 7 examine the purported selectivity of norepinephrine by measuring its effects on secretion of vasopressin and oxytocin.

The location of the α_1-receptor mediating the responses of SON neurons to norepinephrine remains unknown. Experiments with high magnesium indicate that receptors for these actions of norepinephrine are present on SON neurons themselves (ie: post-synaptic) but do not rule out possible effects on local interneurons which might, in turn, synapse with SON neurons.

6.3.2 Mechanism of Action

The strategy employed in Chapters 4 and 5 to determine the mechanism underlying the IPSP and actions of GABA in SON neurons (and also the hyperpolarizing after-potentials in Bourque et al., 1985) was less successful when applied to the mechanism of action of norepinephrine. Norepinephrine had no detectable effect on input resistance. The norepinephrine-induced depolarization could be reduced by membrane hyperpolarization, but was never reversed. Furthermore, this voltage-dependence could not be demonstrated as reliably as that of the IPSPs, GABA responses or the hyperpolarizing afterpotential; perhaps as a consequence of poor voltage control of the active membrane. α_1-Adrenoreceptors may be located on distal dendrites or dendritic spines of SON neurons since the noradrenergic input projects to the ventral part of the SON, an area which is rich in dendrites of neurosecretory neurons (McNeill and Sladek, 1980; Swanson et al., 1981).

Another possible explanation lies with the nature of the α_1-receptor mechanism itself. The amplitude of the α_1-induced depolarization is voltage-dependent in the range -50 to -90 mV, but not at more hyperpolarizing voltages. This suggests that it results, at least in part, from the inactivation of a voltage-dependent K^+ conductance. This hypothesis is supported by the observation that the amplitude of the NE-induced depolarization in SON neurons is

reduced when the concentration of K^+ in the perfusion medium is raised (Figure 6-6; see also Vander Maelen and Aghajanian, 1980).

A recent report (Aghajanian, 1985) suggests that α_1-mediated depolarizations in serotonergic raphé neurons result from the inactivation of a transient K^+ current known as the "A"-current (I_A). Originally described in invertebrate neurons (Connor and Stevens, 1971a), I_A is now known to exist in a number of mammalian neurons as well (see review by Rogawski, 1985). Under voltage clamp, I_A is rapidly activated by voltage steps from holding potentials negative to -70 mV, to potentials of -60 to -40 mV. It manifests itself as an outward current that inactivates within 10-50 ms. Inactivation is removed by a return to a membrane potential negative to -70 mV. I_A can also be demonstrated by similar experiments under current-clamp conditions (Galvan and Sedlmeir, 1984; Dekin and Getting, 1984). The existence of I_A in SON neurons is revealed by such experiments (Figure 6-9). I_A is evident as the "notch" on the rising phase of large depolarizing pulses from membrane potentials negative to -70 mV (Figure 6-9B). I_A inactivates at resting potential, but inactivation is removed in a time- and voltage-dependent manner by hyperpolarizing pulses (Figure 6-9C,D).

Connor and Stevens (1971) predicted that I_A functions primarily in the late part of the interspike interval to

modulate action potential firing frequency. The hyperpolarizing after-potential which follows action potentials reaches sufficiently negative voltages to remove I_A inactivation. During decay of the hyperpolarizing after-potential, I_A switches on and slows the depolarization. This mechanism appears to be operative in modulating the firing of the neuron illustrated in Figure 6-9A. Activation of I_A by the voltage step in Figure 6-9B delays action potential firing. However, this experimental paradigm appears to produce wider swings in the degree of activation and inactivation of I_A, resulting in a repetitive burst firing pattern. This observation may provide an important clue concerning the mechanism of norepinephrine-induced bursting in SON neurons.

The voltage-dependence of I_A would explain the inability to reverse the membrane voltage response to norepinephrine. At membrane potentials negative to -80 mV, I_A is switched off and therefore does not carry inward current. The residual depolarization induced by norepinephrine at membrane potentials of greater than -80 mV is evidence that it also activates an inward current (i.e. Na^+, Ca^{++} or Cl^-) or alters the activity of an electrogenic pump.

An α_1-adrenoreceptor-mediated reduction of I_A in SON neurons would explain the increased rate of decay of the hyperpolarizing after-potential (Figure 6-7D) as well as the

increase in the amplitude of the depolarizing after-potential (Figure 6-8). Summation of the depolarizing after-potential is responsible for the generation of bursts of action potentials in SON neurons (Andrew and Dudek, 1984). Potentiation of the depolarizing after-potential by norepenephrine would induce rapid firing as observed in these experiments. Under appropriate circumstances (as in Figure 6-9B) activation and inactivation of I_A might result in a burst firing pattern. In a manner similar to that proposed for NE, thyrotropin-releasing hormone (TRH) induces burst firing in neurons of the nucleus tractus solitarius by potentiating the depolarizing action potential (Dekin and Getting, 1984). Future studies of the mechanism of action of norepinephrine on SON neurons will focus on a possible modulation of I_A.

Figure 6-1 Ratemeter records of the response of 4 different SON neurons to norepinephrine (NE) or methoxamine (MOXY). In (A), repeated application of NE (100 μM) by pressure ejection (at arrows) from an adjacent micropipette (diameter 10 μm; pressure 30 psi) induces a burst of action potentials that is not mimicked by ejection of perfusion medium (MED) from another pipette channel. For traces (B-D), drugs were applied directly to the perfusion medium (during horizontal solid lines). In B, a previously silent neuron displays a brief burst of enhanced activity, followed by short periods of phasic firing in response to MOXY. In C, a continuously active neuron displays enhanced firing followed by return to baseline control activity following NE application. In D, an initial NE application induces enhanced firing followed by a silent interval and the emergence of a clear phasic activity pattern; a second NE application appears to initiate a phasic burst, with somewhat higher initial firing rate, that is prolonged and is again followed by a period of reduced excitability.

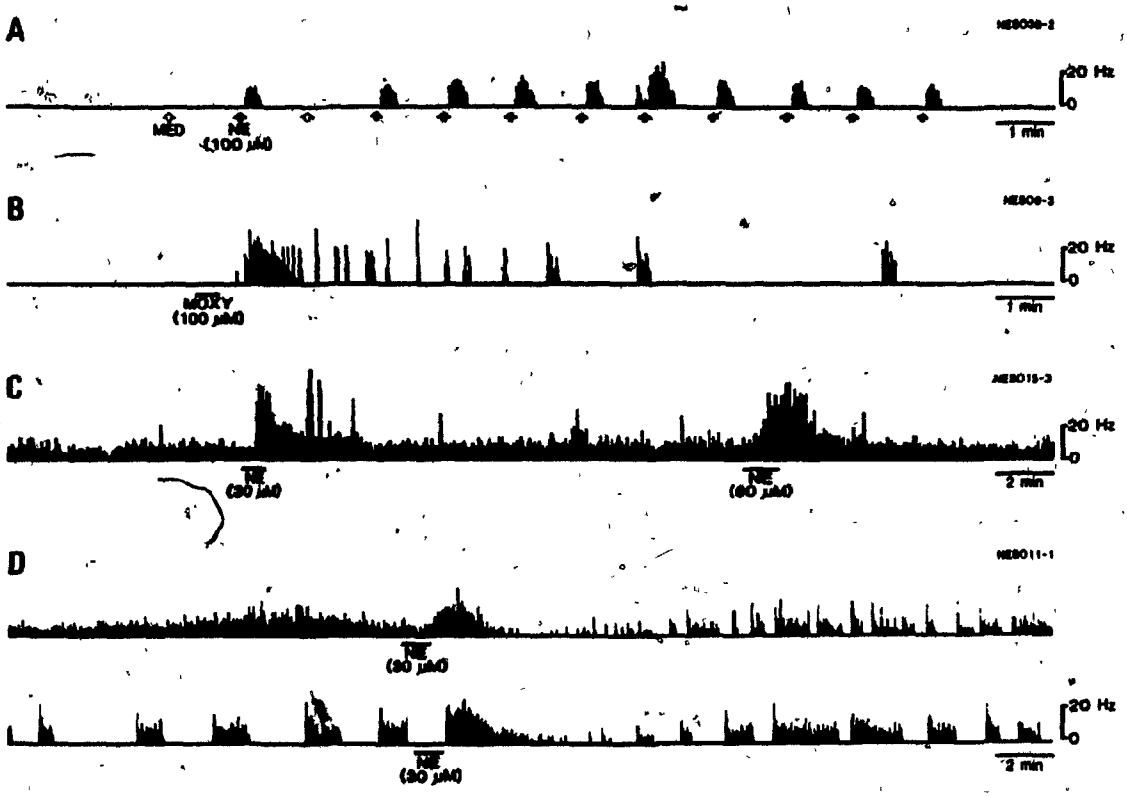
A
MED
NE
(100 µM)
20 Hz
0
1 min
B
MDXY
(100 µM)
20 Hz
0
1 min
C
NE
(30 µM)
NE
(60 µM)
20 Hz
0
2 min
D
NE
(30 µM)
NE
(30 µM)
20 Hz
0
2 min

Figure 6-2 On the left, samples of continuous action potential records plotted on a chart recorder illustrate (A), control activity and (B), patterns of activity obtained immediately after a 60 s application of norepinephrine (NE), methoxamine (MOXY) and isopreterenol (ISO) (10 μM). Note that bursting activity appears only in response to NE and MOXY. In (C), time interval histograms generated during the preceeding control period (separating each drug application) and the period immediately following each drug administration display a shift to the left following NE and MOXY (but not after ISO) applications, without a corresponding change in overall firing frequency (values displayed in the upper right of each histogram).

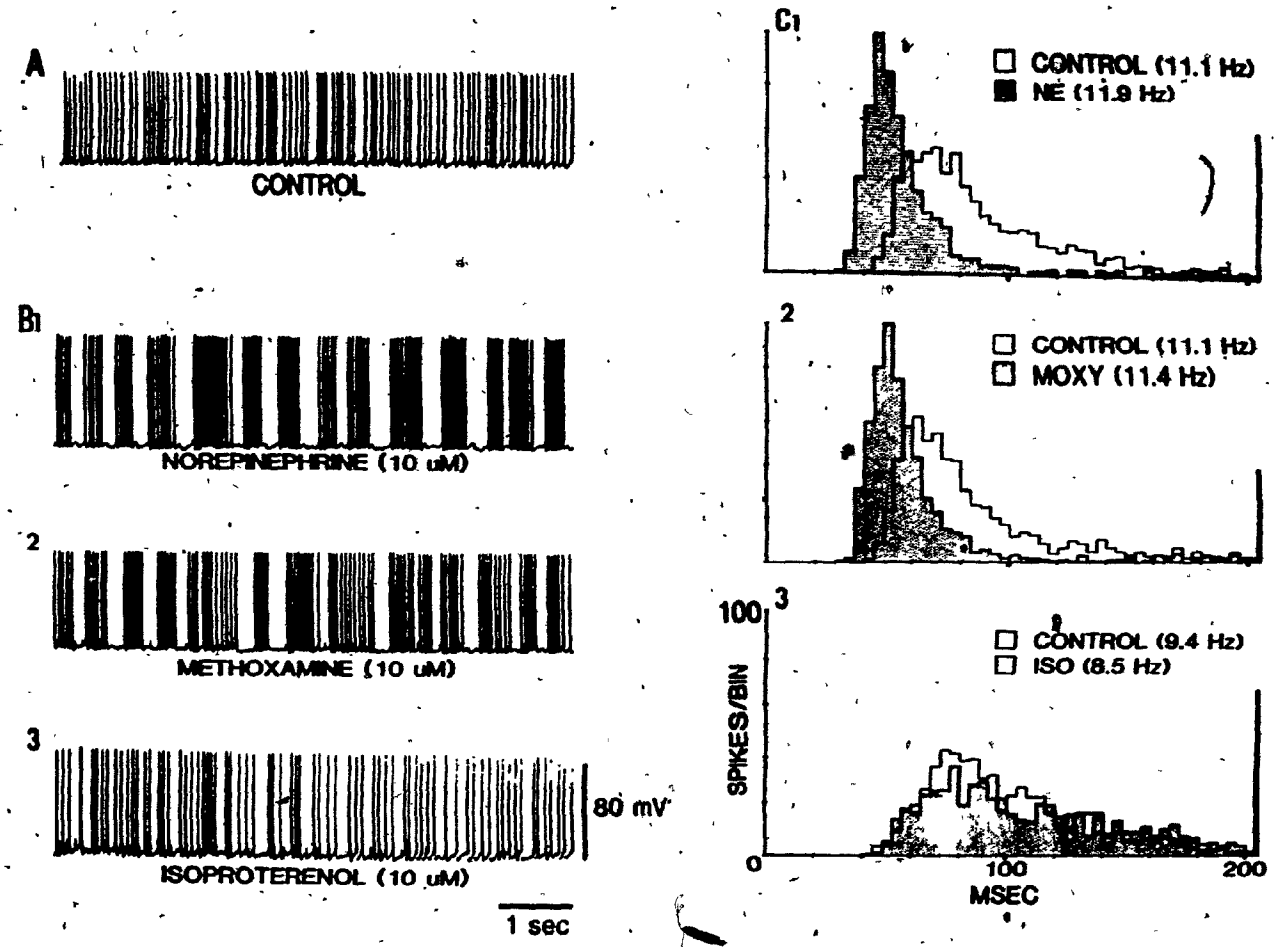
A
CONTROL
B1
NOREPINEPHRINE (10 uM)
2
METHOXAMINE (10 uM)
3
ISOPROTERENOL (10 uM)
80 mV
1 sec
C1
CONTROL (11.1 Hz)
NE (11.9 Hz)
2
CONTROL (11.1 Hz)
MOXY (11.4 Hz)
100
3
CONTROL (9.4 Hz)
ISO (8.5 Hz)
SPIKES/BIN
0
100
200
MSEC

Figure 6-3 Ratemeter records from 3 different SON neurons display the blocking action of α-adrenergic antagonists. All drugs were added directly to the perfusion medium. In (A), phenoxybenzamine induces a reversible blockade at 2 μM. (B,C) illustrate that similar blockade is induced by prazosin, an α_1-antagonist and yohimbine, an α_2-antagonist. Note, however, that prazosin is 1000-fold more potent than yohimbine and that its effects are irreversible during the period of recording.

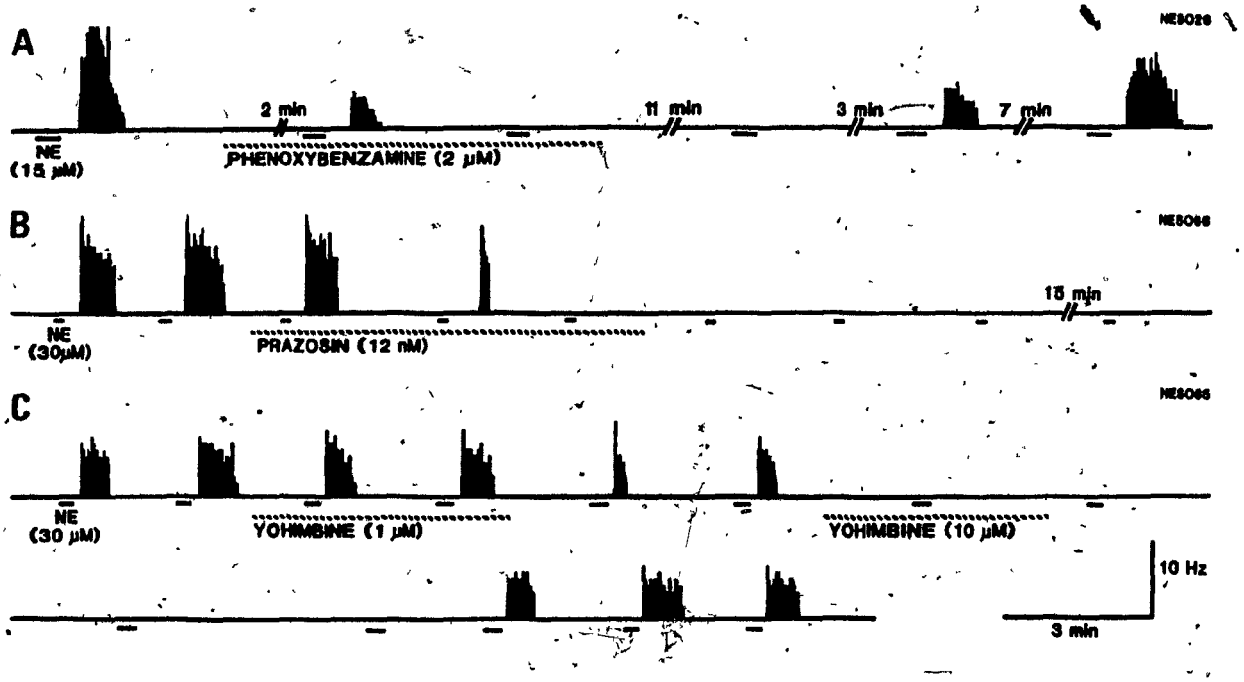
A
2 min
11 min
3 min
7 min
NE
(15 μM)
PHENOXYBENZAMINE (2 μM)
B
15 min
NE
(30μM)
PRAZOSIN (12 nM)
C
NE
(30 μM)
YOHIMBINE (1 μM)
YOHIMBINE (10 μM)
10 Hz
3 min

Figure 6-4. Chart recordings of the responses to norepinephrine (NE) and phenylephrine (PHE) of SON neurons recorded intracellularly. A) The upper records are voltage responses to two separate applications of NE (100 μM) depicted by the horizontal bar. In the upper trace, recorded at resting membrane potential, NE induced a depolarization and action potential firing. The lower trace illustrates the response to NE after a small amount of steady current was applied to hyperpolarize the cell to -65 mv. Constant current pulses, applied to monitor input resistance, indicate that NE had no apparent influence on input resistance. B) Similar depolarizations obtained with PHE (50μM) on another SON neuron. C) Prazosin (50 nM) blocked the effects of NE (100 μM). Recovery of the NE response was obtained after 90 minutes of washout.

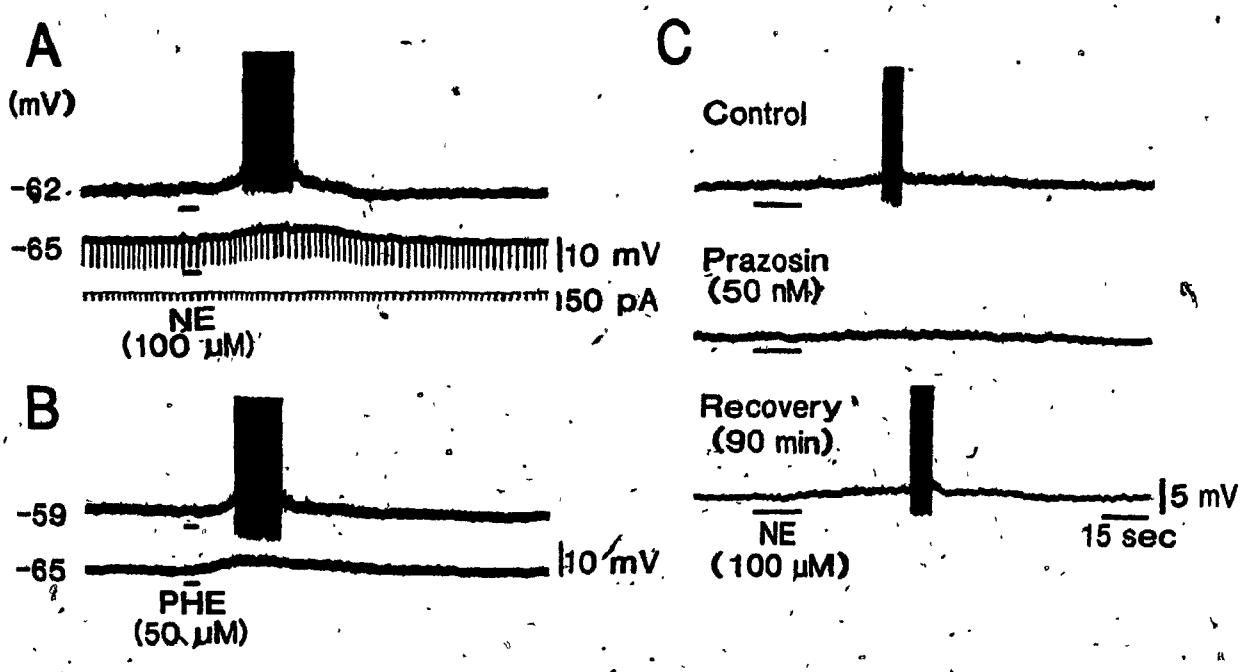
A
(mV)
-62
-65
10 mV
50 pA
NE
(100 µM)
B
-59
-65
10 mV
PHE
(50 µM)
C
Control
Prazosin
(50 nM)
Recovery
(90 min)
5 mV
NE
(100 µM)
15 sec

Figure 6-5 Voltage-dependence of the response to norepinephrine of an SON neuron recorded intracellularly. On the left, chart recordings illustrate the depolarization induced by a brief pulse of norepinephrine (NE; 100 μM). Membrane potential was adjusted by applying the steady hyperpolarizing current indicated to the left of each record. On the right, NE-induced depolarizations are plotted as a function of membrane potential. Depolarizations are expressed as peak amplitude (mV; closed circles) or as the integrated amplitude (mV.sec; open circles).

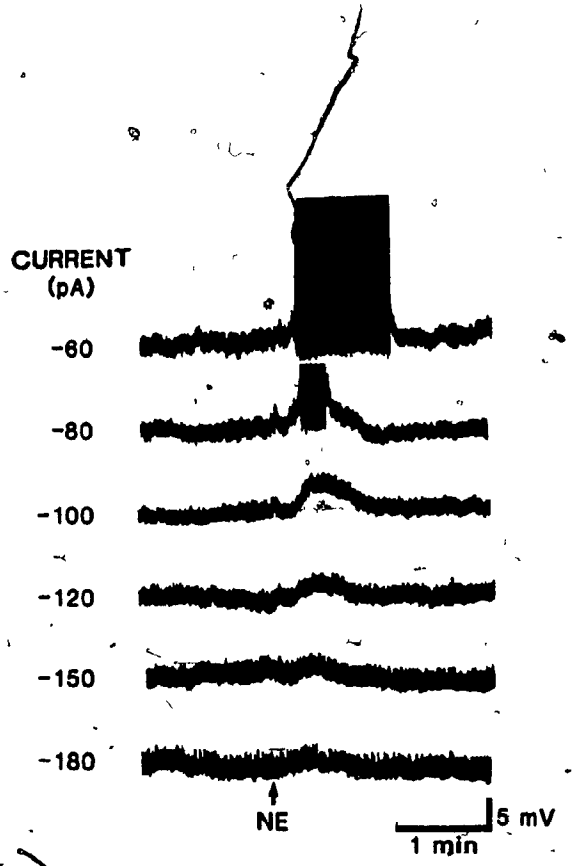
CURRENT
(pA)
-60
-80
-100
-120
-150
-180
NE
5 mV
1 min

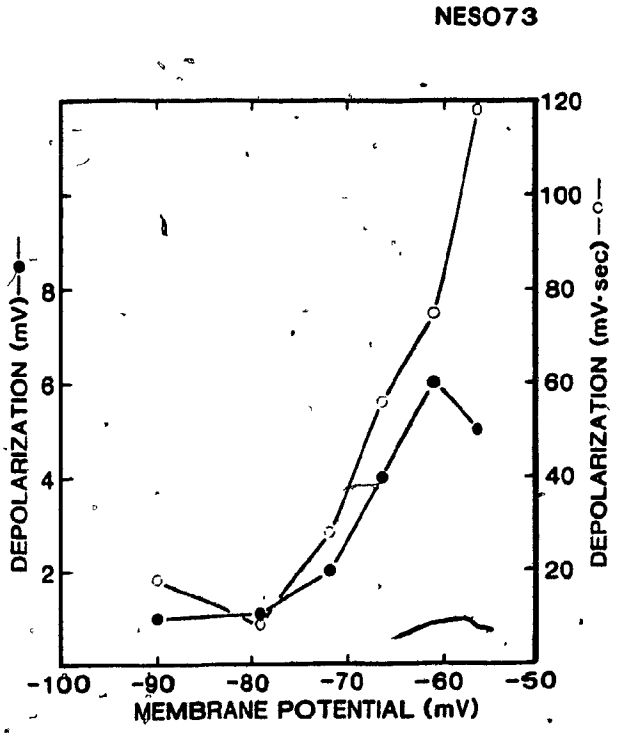
NES073
DEPOLARIZATION (mV)
DEPOLARIZATION (mV·sec)
MEMBRANE POTENTIAL (mV)
2
4
6
8
20
40
60
80
100
120
-100
-90
-80
-70
-60
-50

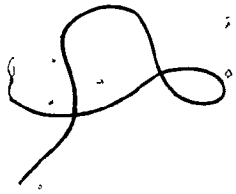

Figure 6-6 Dependence of the norepinephrine (NE)-induced depolarization on the extracellular potassium concentration. A) Chart recordings of the responses to NE (200 μM) of an SON neuron maintained in 2.8 mM K^+. The membrane potential was adjusted as indicated to the left of each record by intracellular injection of hyperpolarizing current. Note that the NE-induced depolarization in this cell is less strikingly voltage-dependent than in the neuron illustrated in Figure 6-5. B) Perfusion with medium containing 7.8 mM K^+ reduces the NE-induced depolarization at all membrane potentials. C) Plot of the NE-induced depolarization as peak amplitude (mV; open symbols) or integrated amplitude (mV.sec; closed symbols) observed in 2.8 mM K^+ (circles) or 7.8 mM K^+ (triangles). The lines were drawn through the points by eye.

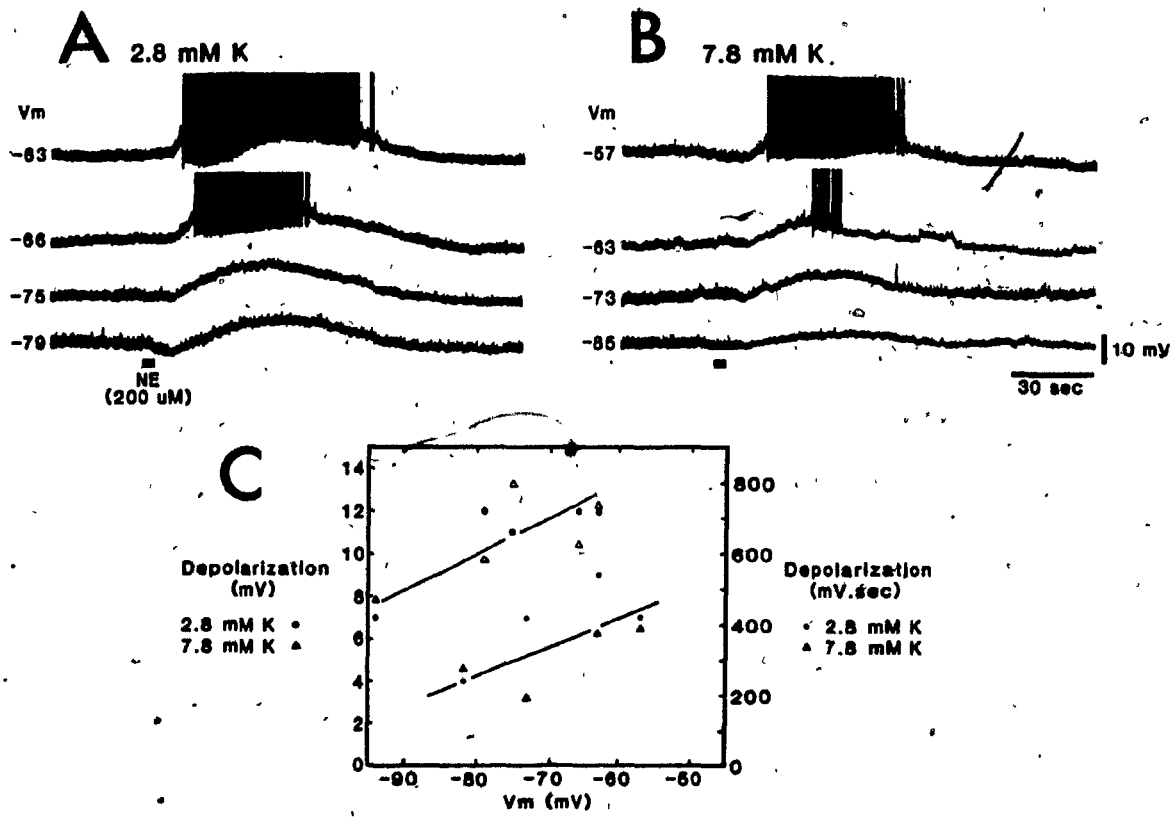
A
2.8 mM K
Vm
-63
-66
-75
-79
NE
(200 uM)
B
7.8 mM K
Vm
-57
-63
-73
-85
10 mV
30 sec
C
Depolarization
(mV)
2.8 mM K
7.8 mM K
14
12
10
8
6
4
2
0
800
600
400
200
0
Depolarization
(mV.sec)
2.8 mM K
7.8 mM K
-90
-80
-70
-60
-50
Vm (mV)

Figure 6-7 Bursting firing pattern induced by methoxamine (MOXY) in a continuously firing SON neuron. A) Ratemeter record of the response to MOXY (30 μM) reveals a slight increase in mean firing rate. B) Slow sweep oscilloscope traces show that the steady firing pattern in the control period (B_1) is converted to a bursting firing pattern in the presence of MOXY (B_2). In C) and D), digital averages of 64 action potentials were obtained during control activity and MOXY-induced bursting. In C), action potential duration was increased slightly by MOXY as a function of the increased frequency of short interspike intervals during bursting (Digitized at 20 kHz). In D), although there was little change in the amplitude of the hyperpolarizing after-potential (HAP), the rate of decay of the HAP was increased during MOXY-induced bursting. Irregularities on the right end of the traces in D) represent action potentials that have been reduced in amplitude by the averaging process (digitized at 2 kHz).

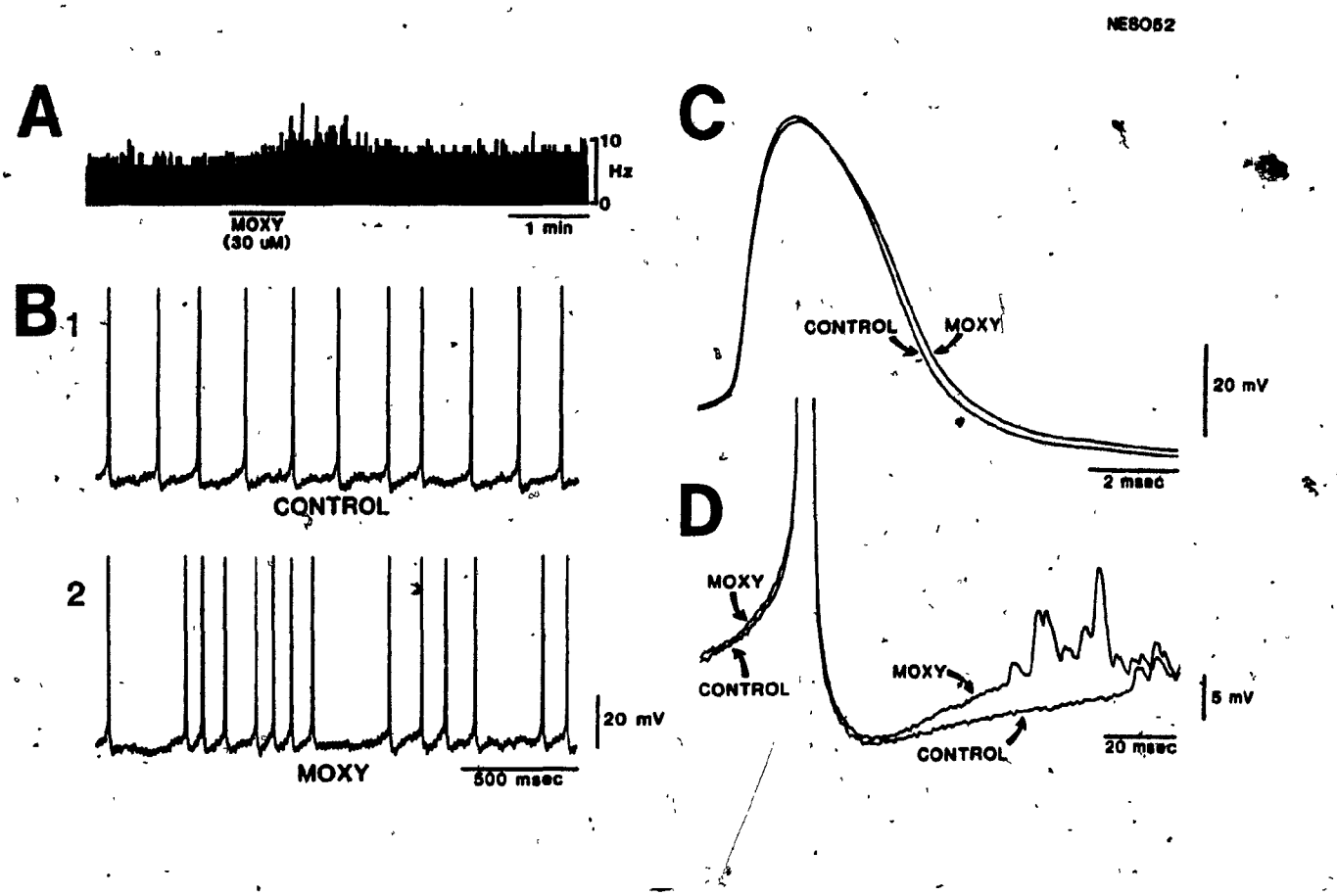
NE8052
A
10
Hz
0
MOXY
(30 uM)
1 min
B
1
CONTROL
2
20 mV
MOXY
500 msec
C
CONTROL
MOXY
20 mV
2 msec
D
MOXY
CONTROL
MOXY
5 mV
CONTROL
20 msec

Figure 6-8 Effects of norepinephrine (NE) on the depolarizing after-potential (DAP) and after-hyperpolarization (AHP) in SON neurons. Top trace (V_m) is a chart record of membrane potential which was held near -60mV by applying 60 pA of hyperpolarizing current (Trace 2,I). Depolarizing pulses (95 pA) applied every 10 seconds (at breaks in Trace I) induced 9-11 action potentials and were followed by an AHP and DAP. DAP amplitude (Trace 3; expressed as peak (mV) or area of depolarization (mV.sec)) was constant under control conditions. HAP amplitude (Trace 4; expressed as peak of hyperpolarization (mV)) varied slightly according to the number of action potentials induced by the depolarizing pulse. Following a brief pulse of NE (100 μM; arrowhead), the membrane potential was maintained at -60 mV prior to each depolarizing pulse by increasing the steady hyperpolarizing current to 75 pA (Trace I). Thus, independent of a change in membrane potential, NE increased the amplitude of the DAP without altering the AHP. The pulses indicated by stars in Trace V_m are expanded at the bottom to illustrate the changes in DAP amplitude.

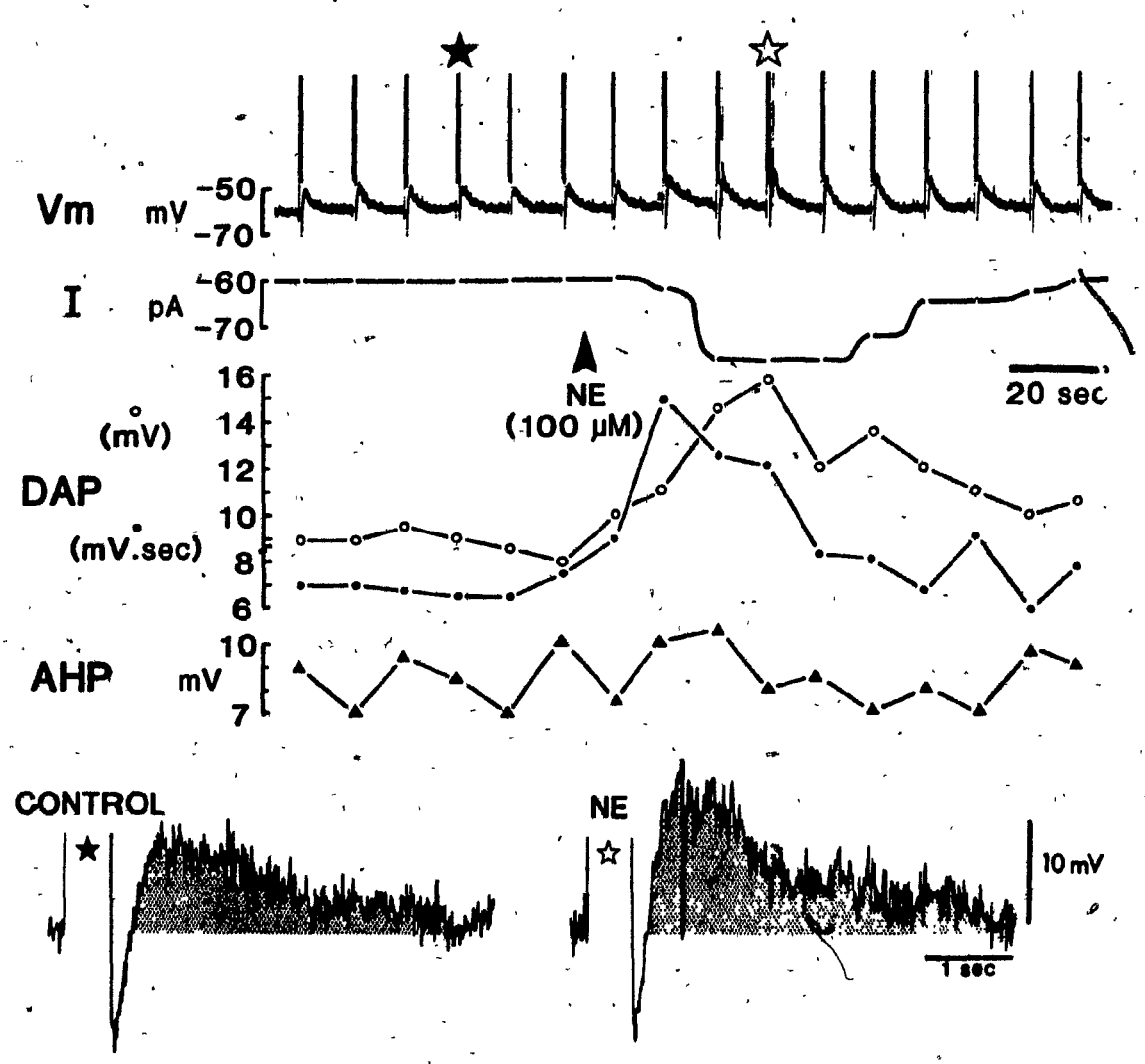
Vm
mV
-50
-70
I
pA
-60
-70
20 sec
NE
(100 µM)
(mV)
DAP
(mV.sec)
16
14
12
10
8
6
AHP
mV
10
7
CONTROL
NE
10 mV
1 sec

Figure 6-9 Evidence of the existence of a transient potassium current (I_A) in current-clamped SON neurons. A) At normal resting membrane potentials (-50 to -65 mV) injection of current pulses induces membrane voltage responses which display monotonic, exponential saturation kinetics (open arrows). Depolarizing pulses induce steady action potential firing at a rate that is proportional to the intensity of the pulse. B) Membrane potential is adjusted to -92 mV by injection of steady hyperpolarizing current. Small depolarizing current pulses induce membrane voltage responses to levels negative to -75 mV which display monotonic, exponential saturation kinetics. Membrane voltage deflections to -70 to -50 mV in response to larger current pulses display a progressively more prominent "notch" (closed arrow) reflecting activation of I_A. Action potential firing is delayed and assumes a bursting pattern. C) Voltage-dependent removal of inactivation of I_A. Inactivation is removed by 200 msec pulses to voltages negative to -70 mV and is near maximal at -90 mV. D) Time-dependent removal of inactivation of I_A. Inactivation is rapidly removed by pulses to -100 mV lasting more than 20 msec and is maximal by 100 msec. In C) and D) numbers indicate the first action potential that follows each pulse. Action potential firing is delayed by activation of I_A.

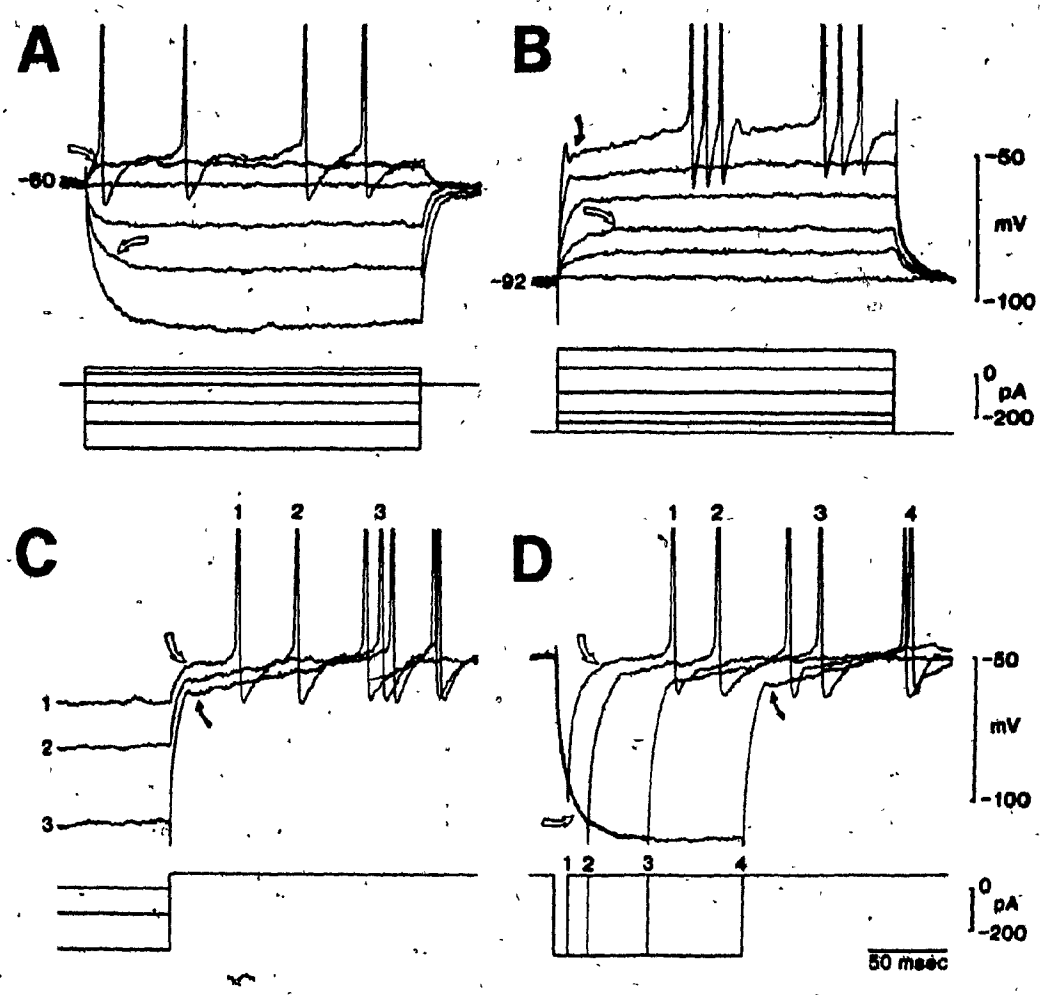
A
B
-60
-92
-50
mV
-100
0
pA
-200
C
D
1
2
3
4
50 msec

CHAPTER 7

NOREPINEPHRINE-INDUCED RELEASE OF VASOPRESSIN AND OXYTOCIN FROM THE HYPOTHALAMIC EXPLANT

7.1 Introduction

The electrophysiological data presented in Chapter 6 indicate that norepinephrine enhances SON neuronal excitability. Moreover, norepinephrine also induces a bursting pattern of action potential firing that is reported to be most efficient for the release of vasopressin and oxytocin from the isolated neurohypophysis (Bicknell and Leng, 1981; Dutton and Dyball, 1979). In combination with evidence obtained *in vivo* to indicate that electrical stimulation of endogenous norepinephrine pathways facilitates the firing of SON vasopressinergic neurons (Day and Renaud, 1984; Day et al., 1984) as does exogenously applied norepinephrine (Day et al., 1985), these data imply that NE is likely to increase rather than reduce (cf. Armstrong et al., 1982) the release of these hormones from perfused hypothalamic explants.

In order to examine this issue, modified hypothalamic explants were prepared as described in section 2.3. Samples of effluent perfusion medium were collected at 1 or 2 minute intervals and vasopressin and oxytocin were measured by radioimmunoassay. Vasopressin-like immunoreactivity

(AVP-LI) and oxytocin-like immunoreactivity (OXY-LI) contained in these experimental samples was identical to the synthetic peptides in competition experiments and high pressure liquid chromatographic (HPLC) analysis (Figure 7.1). Norepinephrine and α-adrenoreceptor agonists and antagonists were added to the perfusion medium at regular intervals in order to evaluate their influence on the release of vasopressin and oxytocin.

7.2 Results

7.2.1 Basal Release of Vasopressin and Oxytocin

Immediately following preparation of the explant, both vasopressin and oxytocin were observed to be released at rates of 10-50 pg/min that declined gradually over the initial 30-50 min. At that point, basal levels of vasopressin released were below the limit of detection of the assay (∓ 2pg/min) while basal levels of oxytocin released varied from undetectable levels (∓ 1 pg/min) to 3 pg/min.

7.2.2 Influence of Norepinephrine on Vasopressin and Oxytocin Release

Norepinephrine (10^{-5}-10^{-3}M) induced a dose-related increase in the release of both vasopressin and oxytocin (Figures 7-2, 7-3). Vasopressin release reached 45 ± 13 pg/min (mean ± SEM) following the addition of 10^{-5}M

norepinephrine and 100-150 pg/min after adding ~ 3 x 10^{-5}M norepinephrine to the perfusion medium (Figure 7-3). Norepinephrine also induced the release of oxytocin up to 6.7 ± 2.5 pg/min using 10^{-5}M norepinephrine and 15-20 pg/min at concentrations ~ 3 x 10^{-5} M. Thus norepinephrine stimulated vasopressin and oxytocin release with similar potencies although 3-20 fold (mean: 5.7-fold) greater amounts of vasopressin were released. Responses to norepinephrine differed quantitatively, but not qualitatively among individual experiments. In each instance the response was prompt and rapidly reversible. During prolonged administration of norepinephrine, vasopressin release peaked rapidly and then dropped to a plateau level which was maintained until the norepinephrine was removed (Figure 7-4). Under these conditions oxytocin release was maintained near its peak level for the duration of the norepinephrine administration. Similarly, repeated administration of norepinephrine evoked vasopressin release in progressively diminishing quantities while oxytocin release was maintained for up to 4 trials (Figure 7-5).

Two lines of evidence argue that an intact neurohypophysial pathway (i.e. pituitary stalk and neurohypophysis) were required in order that vasopressin and oxytocin be released. First, in three experiments in which the hypophyseal stalk was damaged, no release of either

hormone in response to norepinephrine was obtained. Second, the addition of tetrodotoxin (TTX, 10^{-6}M) which blocks sodium channels and the propagation of axonal action potentials, prevented the release of vasopressin and oxytocin induced by norepinephrine (Figure 7-6) in two experiments.

7.2.3 Effects of Adrenoreceptor Agonists and Antagonists

Phenylephrine, an α_1-agonist, stimulated vasopressin and oxytocin release to 40.7 ± 19.6 pg/min and 25.1 ± 22.3 pg/min respectively at 10^{-4} M (3 experiments, Figures 7-3 and 7-7). The response to norepinephrine (1.7×10^{-5} M) was reduced or abolished in the presence of the α-antagonists phentolamine (1.3×10^{-5} M; Figure 7-8) and phenoxybenzamine (10^{-5} M; Figure 7-9) and by the selective α_1-antagonist prazosin (10^{-8}–10^{-6} M; Figure 7-10). In the experiment shown in Figure 7-10, prazosin (10^{-7}M) induced a partially reversible, 70% inhibition of the vasopressin release stimulated by norepinephrine (10^{-5}M). In two separate experiments, when 10^{-5}M norepinephrine and 5×10^{-8}M prazosin were tested, 80-100% reductions of vasopressin release were observed. Complete reversal of the antagonism following their removal was observed in only 1 of 7 experiments with these agents (Figure 7-10).

High concentrations of isoproterenol (3×10^{-4} to 10^{-3} M), a β-agonist, also stimulated the release of vasopressin

in two experiments (data not shown). A possible role of β-adrenoreceptors in the modulation of neurohypophysial hormones was not investigated further.

7.3 Discussion

7.3.1 α-Adrenergic Stimulation of Vasopressin and Oxytocin Release

These observations confirm that norepinephrine can stimulate the release of vasopressin and oxytocin at concentrations identical to those that increase SON electrical activity under similar conditions. Furthermore, the participation of α_1-adrenoreceptors is indicated by the ability of phenylephrine to mimic the actions of norepinephrine and the sensitivity of norepinephrine effects to phentolamine, phenoxybenzamine and prazosin.

These results lend further weight to the hypothesis (Day and Renaud, 1984) that the role of the noradrenergic afferents to SON and paraventricular nucleus is to facilitate the release of the neurohypophysial hormones. As such, these results directly contradict the observations of Armstrong et al., (1982) who reported that norepinephrine depresses both basal and acetylcholine-stimulated release of vasopressin from hypothalamo-neurohypophysial organ cultures. This discrepancy may be due to the fact that their experiments were performed in a static hypothalamic explant system maintained for more than 24 hours. Since this

supressant action was reported to be mediated by α-adrenoreceptors (Armstrong et al., 1982) it is possible that the cellular responses controlled by these receptors differs between acutely perfused and statically cultured hypothalamic explants.

However, Armstrong and coworkers (1982) did observe a small (statistically insignificant) increase in release in response to norepinephrine (10^{-5}M) when medium osmolality was raised from 295 to 315 mOsm/L. While higher doses of norepinephrine were not tested, it is possible that these different responses obtained in the two preparations resulted from differences in a subtle interaction between medium osmolality and norepinephrine. In vivo, vasopressin secretion is stimulated when plasma osmolality exceeds 300 mOsm/L and depressed when it falls below 290 mOsm/L (Dunn et al., 1973). If norepinephrine acts as a modulator, it might be expected to potentiate the actions of osmotic stimuli and further stimulate or depress the release of vasopressin. If this hypothesis is true, the switching point for the osmotic stimuli would appear to have shifted to a level near 305 mOsm/L following several days in culture.

7.3.2 Role of the β-Adrenoreceptor

A role for β-adrenoreceptors is suggested by the ability of high doses of isoproterenol bitartrate (0.3-1mM) to stimulate vasopressin release. However, in vivo

electrophysiological (Barker et al.) 1971; Day et al., 1985) and intracerebral injection studies (Moos and Richard, 1979; BHargava et al., 1972; Tribollet et al., 1978) have indicated that activation of β-adrenoreceptors prompts a reduction in SON neuron activity. It is possible that low basal release of vasopressin from the perfused hypothalamic explant obscures an inhibitory effect of lower doses of isoproterenol. Stimulation of release at much higher doses may be osmotically mediated since 1 mM isoproterenol bitartrate raises the osmolality of the medium by approximately 2 mOsm/L (unpublished observations). Evidently, this matter merits further study.

7.3.3 Does Norepinephrine Stimulate Vasopressin Release Selectively?

Norepinephrine consistently induced the release of 3-20 fold (mean 5.7-fold) more vasopressin than oxytocin. Neural lobe extracts contain similar amounts of vasopressin and oxytocin (approximately 1 µg/gland, Bridges et al., 1976 and unpublished observations) so it is unlikely that the observed differences in release are due solely to differences in availability of the hormones. Electrical stimulation of isolated neural lobes evokes release of vasopressin and oxytocin in variable ratios that range from 19:1 to 1:7 (mean 1.6:1, 16 observations from Bicknell et al., 1982, 1984,; Bicknell and Leng, 1982) indicating that

this stimulus is relatively non-specific. Thus, the apparently selective stimulation of vasopressin release by norepinephrine corroborates electrophysiological observations *in vivo* that tentatively identified vasopressin-secreting neurons are more sensitive than oxytocin neurons to electrical stimulation of the endogenous noradrenergic input from the A1 cell group, or alternatively, application of exogenous norepinephrine (Day and Renaud, 1984; Day et al., 1985). However, all the experiments cited above were performed using male rats. Since norepinephrine is reported to regulate the reflex release of oxytocin during suckling (Tribollet al., 1978; Moos and Richard, 1979) it would be interesting to investigate the effects of norepinephrine on the release of oxytocin from explants obtained from female (primarily lactating) rats.

Although large amounts of vasopressin were released in response to norepinephrine, the response was subject to "fatigue" as vasopressin release declines progressively in the course of sustained (Figure 7-4) or repetitive (Figure 7-5) stimulation with norepinephrine. Smaller amounts of oxytocin were released by norepinephrine, but this level of oxytocin appeared to be continuously maintained (Figures 7-4,7-5). A similar fatigue of electrically-stimulated release from isolated neurohypophyses (Sachs and Haller, 1968; Thorn, 1966; Ingram et al., 1982; Bicknell et al., 1984) may result from depletion of a "readily releaseable

pool" of vasopressin (cf. Sachs et al., 1969; Thorn, 1966). This "pool" may represent newly synthesized hormone which is in physical proximity with the membrane (see Chapter 1.3 and Pickering, 1978). Alternatively, this pool may be more apparent than real, and result from limitations on the movement of Ca^{++} across the plasma membrane (Thorn et al., 1975; Nordmann, 1976) such as the calcium-dependent plateau potentials (Legendre et al., 1982; Theodosis et al., 1983; Bourque et al., in press). Opioid peptides released from the neural lobes during electrical stimulation are reported to reduce oxytocin release (Bicknell and Leng, 1982; Bicknell et al., 1985). This form of presynaptic inhibition may maintain a steady level of oxytocin release by preventing the hormone depletion or calcium current inactivation that causes the fatigue of vasopressin release.

7.3.4 Site of Action of Norepinephrine

Classical concepts of neurosecretory neuronal function hold that the release of vasopressin and oxytocin occurs only in the posterior pituitary while osmotic and synaptic regulation of release occurs primarily at the level of the somata and dendrites in the magnocellular nuclei (Scharrer, 1976). The experiments of Gregg and Sladek (1984) support this theory by showing that, in cultured hypothalamic explants, osmotic stimuli act at the level of the hypothalamus to control the rate of vasopressin release from

the pituitary.

Our observations also support this view in that when propagation of axonal action potentials was blocked, either by damage to the pituitary stalk or by tetrodotoxin (Figure 7-6), the response to norepinephrine and phenylephrine was blocked. This argues that norepinephrine acts at the level of the dendrites or somata of SON and paraventricular nucleus neurons to generate action potentials which are propagated along their axons to signal release of vasopressin and oxytocin from axon terminals in the posterior pituitary. This does not rule out the possibility of "presynaptic" modulation of release in the neural lobe since the opioid antagonist naloxone increases (Bicknell & Leng, 1982; Bicknell et al., 1985) and GABA decreases (Dyball & Shaw, 1979) the electrically-induced release of oxytocin from isolated neural lobes.

Figure 7-1 Verification of the specificity of the vasopressin (AVP) radioimmunoassay. Top: Parallel dilution curves for displacement of ^{125}I-AVP by standard AVP (closed circle) and perfusate (open circle) indicate that perfusate contains genuine AVP. Bottom: Reverse phase HPLC confirms that AVP-LI (AVP-like immunoactivity) in perfusate coelutes with synthetic AVP and is well separated from oxytocin (OXY) and vasotocin (AVT). Gradient was 13-29% acetonitrile (CH_3CN) in 0.1% trifluoroacetic acid (TFA). Analogous results were obtained for the OXY radioimmunoassay.

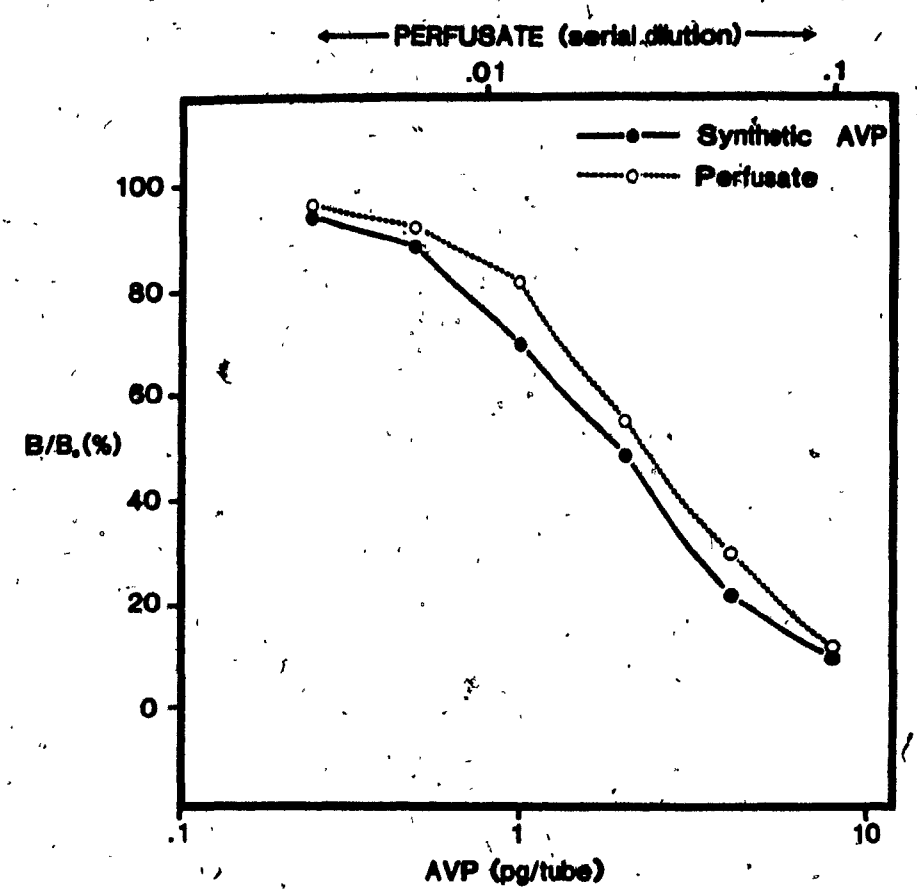
PERFUSATE (serial dilution)
.01
.1
Synthetic AVP
Perfusate
100
80
60
40
20
0
B/B₀(%)
.1
1
10
AVP (pg/tube)

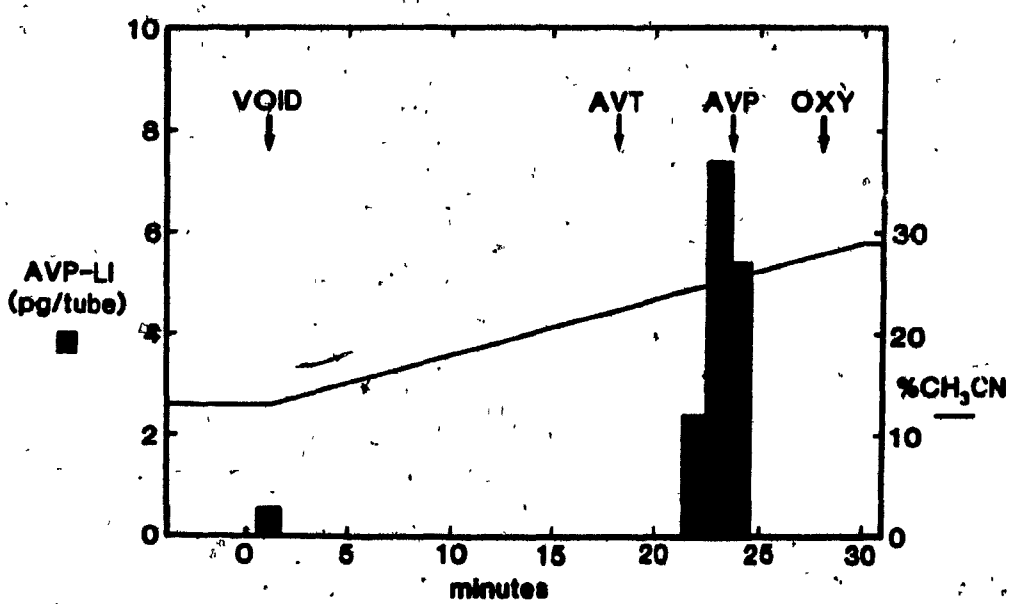
VOID
AVT
AVP
OXY
10
8
6
4
2
0
AVP-LI
(pg/tube)
30
20
10
0
%CH₃CN
0
5
10
15
20
25
30
minutes

Figure 7-2 Effects of norepinephrine (NE, 10^{-6}, 10^{-5}, 10^{-4} M) on the release of vasopressin-like immunoreactivity (AVP-LI) and oxytocin-like immunoreactivity (OXY-LI). Fractions of effluent medium were collected at 1 minute intervals, and NE was applied during the periods indicated by the bars. Note the different scales representing release of AVP-LI and OXY-LI which, in this particular experiment, are in a ratio of approximately 20:1 (at peak responses to NE). Points omitted from the drawing (i.e. from 2-24 mins) represent hormone release below the limit of detection of the radioimmunoassay (∓ 2 pg/min in AVP-RIA and ∓ 1 pg/min in OXY-RIA).

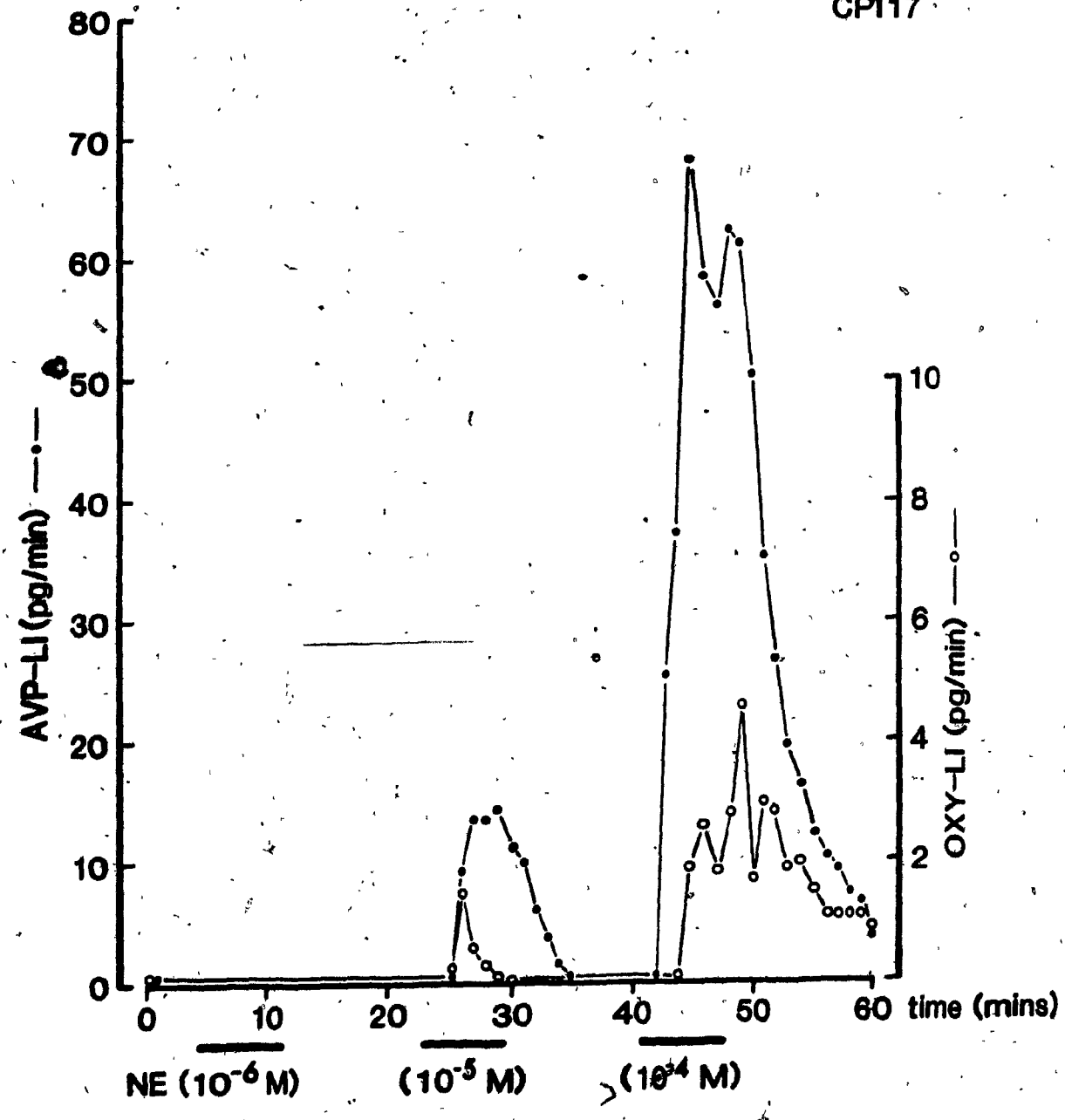
CP117
AVP-LI (pg/min) —•—
OXY-LI (pg/min) —○—
80
70
60
50
40
30
20
10
0
10
8
6
4
2
0
10
20
30
40
50
60 time (mins)
NE (10^{-6} M)
(10^{-5} M)
(10^{-4} M)

Figure 7-3 Dose-response relationship for the release of vasopressin-like immunoreactivity (AVP-LI) and oxytocin-like immunoreactivity (OXY-LI) in response to norepinephrine (NE, 10^{-7} to 10^{-3} M) and phenylephrine (PHE, 10^{-6} to 10^{-3} M). The concentration of NE that caused a half-maximal release of AVP-LI and OXY-LI (ED50) was approximately 20 μM. Note that approximately 5.7-fold more AVP-LI than OXY-LI was released. PHE appears to be less potent than NE but insufficient data was available for estimation of the ED50. Data represent 47 responses in 24 preparations. Each point represents the mean ± SEM of 3 to 15 determinations.

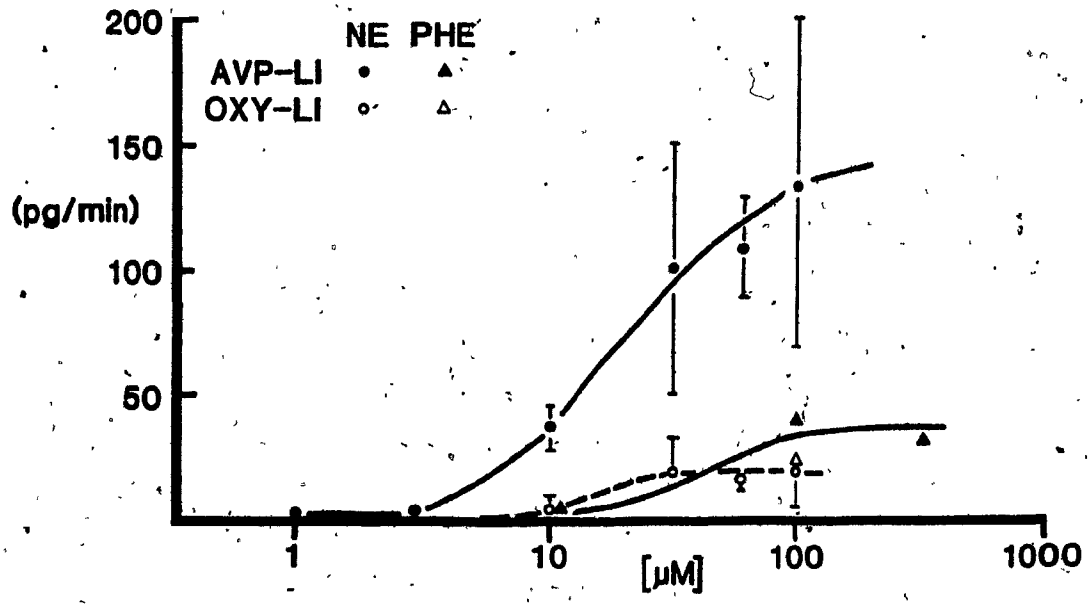
200
150
100
50
(pg/min)
NE PHE
AVP-LI
OXY-LI
1
10
100
1000
[μM]

Figure 7-4 Effects of prolonged administration of NE (3×10^{-5} M) on release of AVP-LI and OXY-LI. In this experiment (and those illustrated in Figures 7-4 and 7-9), collection of effluent medium was begun immediately after preparation of explant. Initially, the first seven fractions (2 minute) were collected at 8 minute intervals. Collection was than continued every 2 minutes for the remainder of the experiment. Administration of NE for 30 minutes induced release of AVP-LI which rose rapidly to peak, but dropped steadily during the final 20 minutes of the pulse and was rapidly reversible when the NE was removed. OXY-LI also rose to a peak which was sustained in the presence of NE, and reversed when NE was removed. A second brief application provoked a prompt but diminished release of both hormones.

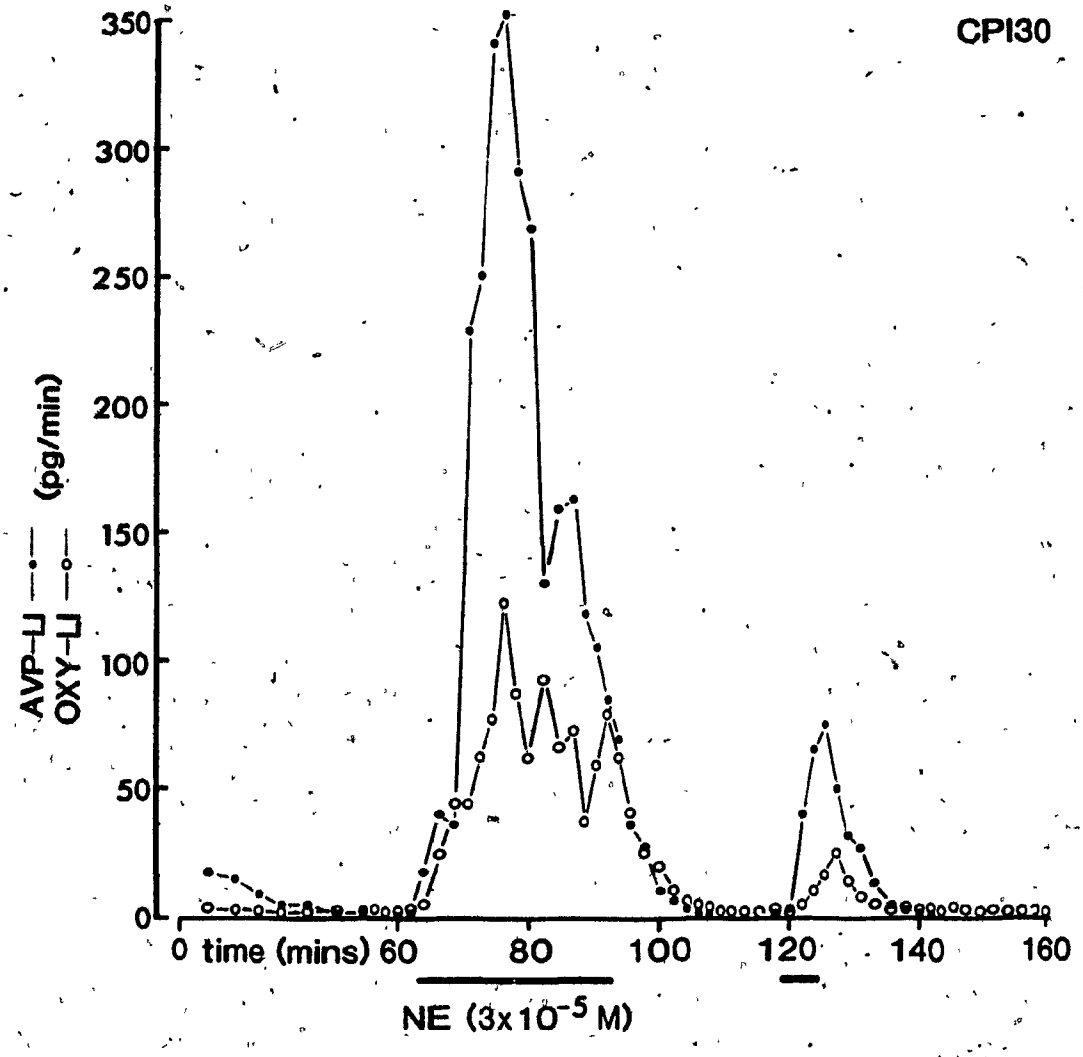
CPI30
350
300
250
200
150
100
50
0
AVP-LI —•— (pg/min)
OXY-LI —○—
0 time (mins) 60
80
100
120
140
160
NE (3x10⁻⁵ M)

Figure 7-5 Effects of repeated administration of NE on release of AVP-LI and OXY-LI. NE (6×10^{-5} M) was applied for 3 minutes at 30 minute intervals. Responses to each administration were similar although the release of AVP-LI declined steadily with each test. The decline in the release of OXY-LI was not as pronounced.

CPI31

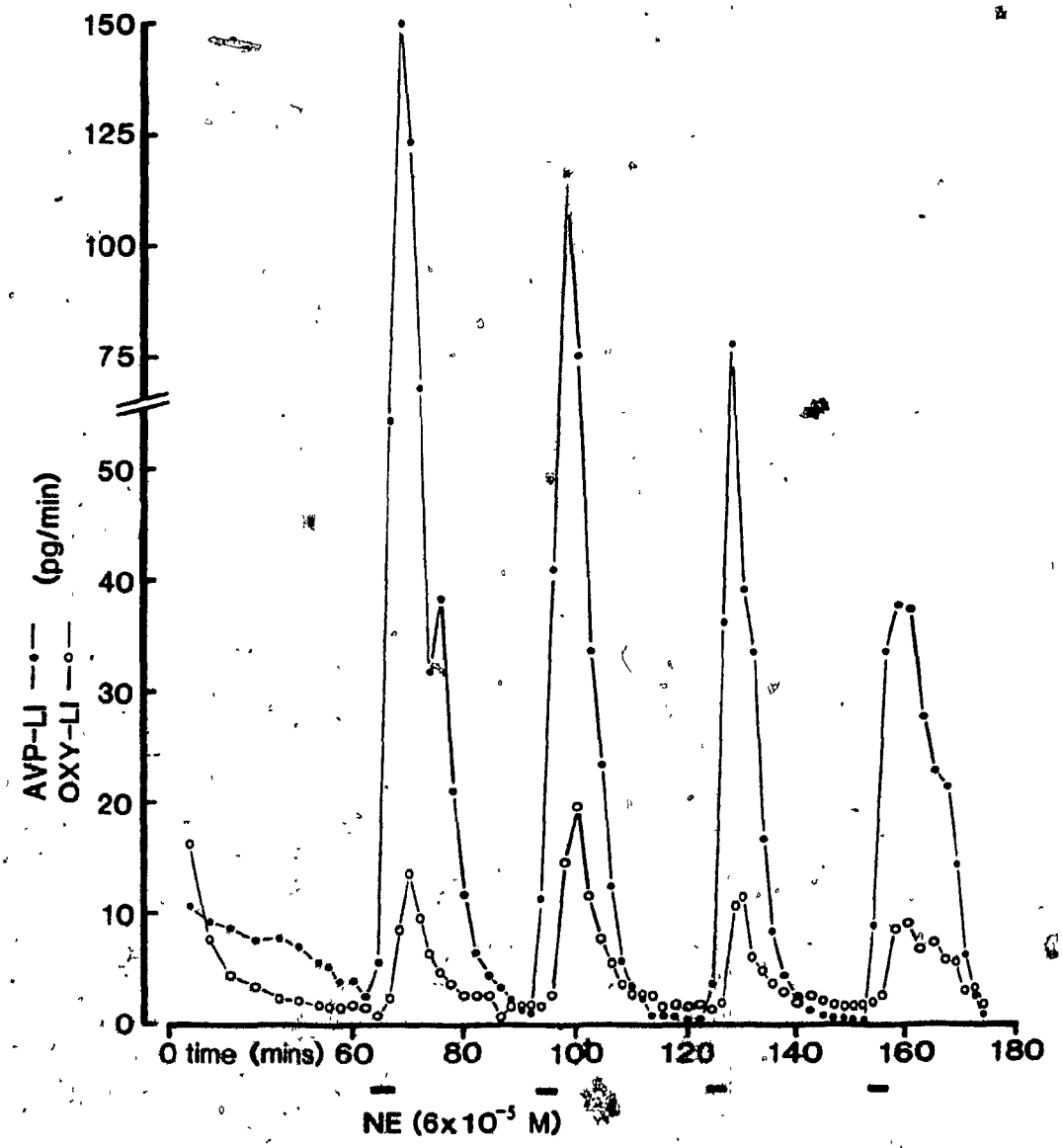
150
125
100
75
50
40
30
20
10
0
AVP-LI —•— (pg/min)
OXY-LI —°—
0 time (mins) 60
80
100
120
140
160
180
NE (6x10⁻⁵ M)

Figure 7-6 Effect of tetrodotoxin (TTX, 10^{-6} M) on the response to repeated doses of NE (6×10^{-5} M). TTX abolished the release of both AVP-LI and OXY-LI in response to NE. Full reversal of the effects of TTX was never observed during the experimental period.

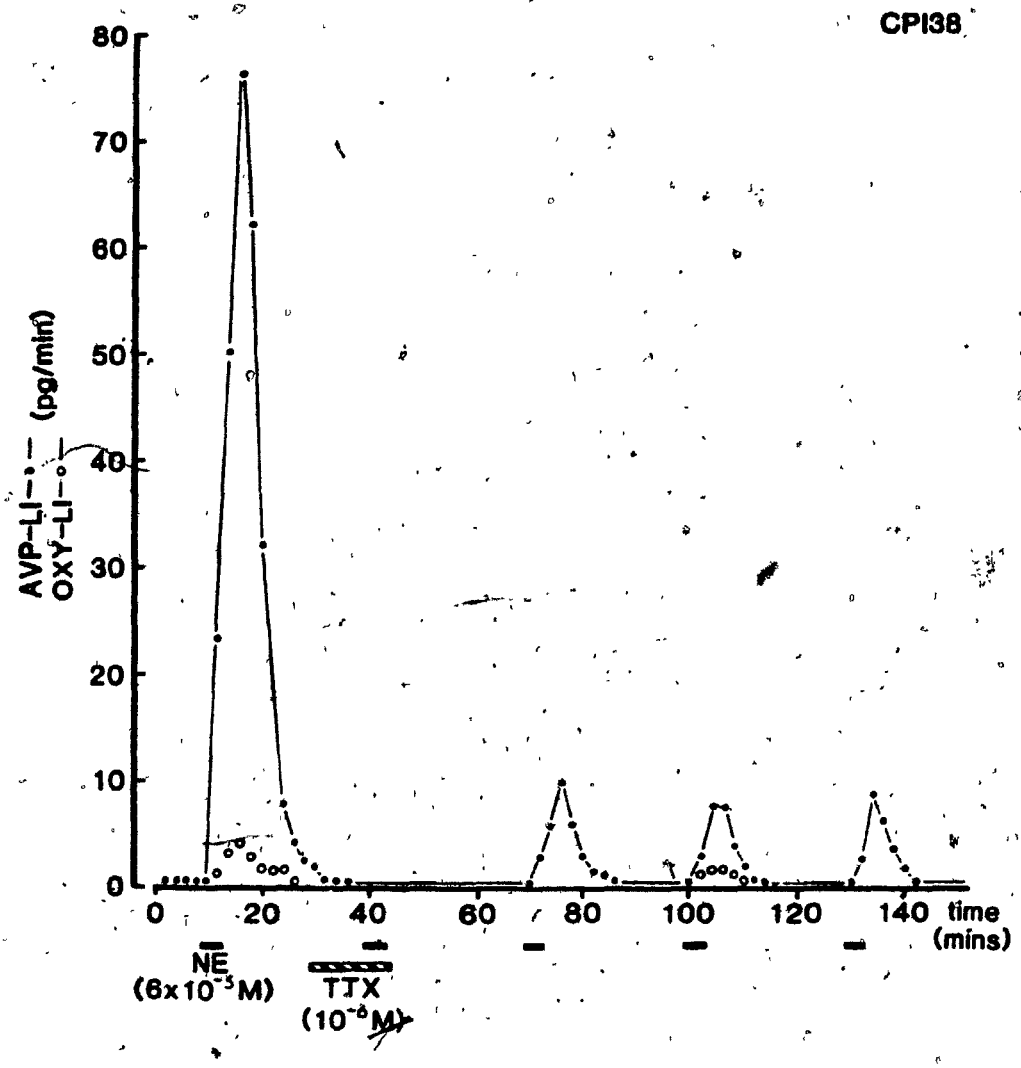
CPI38
AVP-LI-•-- (pg/min)
OXY-LI-°--
80
70
60
50
40
30
20
10
0
0
20
40
60
80
100
120
140
time
(mins)
NE
(6x10⁻⁵M)
TTX
(10⁻⁶M)

Figure 7-7 Effects of phenylephrine (PHE, 10^{-5}, 10^{-4}, 10^{-3} M) on the release of the AVP-LI and OXY-LI. PHE stimulated the release of the hormones less effectively than NE.

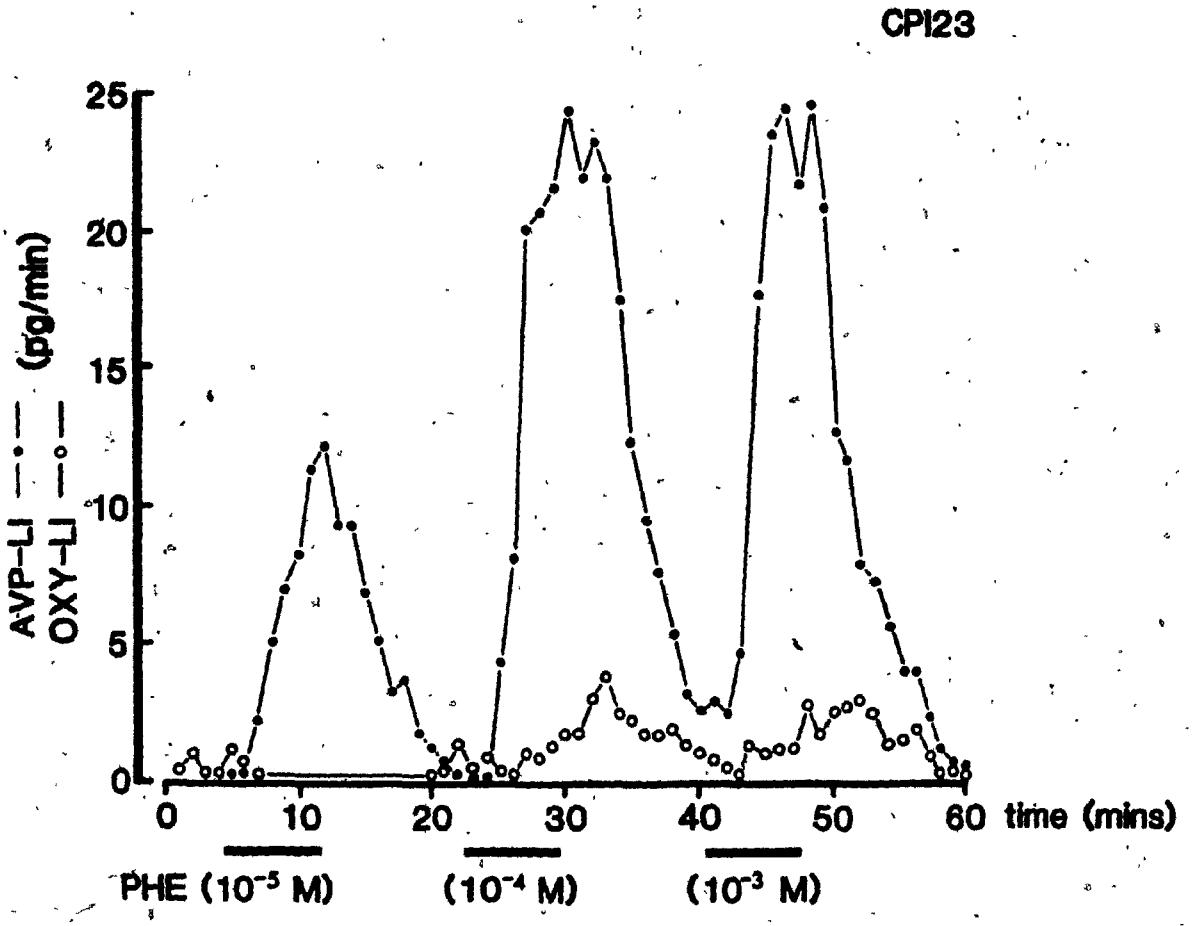
CPI23
AVP-LI —•— (pg/min)
OXY-LI —°—
25
20
15
10
5
0
0
10
20
30
40
50
60 time (mins)
PHE (10^{-5} M)
(10^{-4} M)
(10^{-3} M)

Figure 7-8 Effects of phentolamine (PHEN, 10^{-5} M) on the response to NE (6×10^{-5} M). Phentolamine blocked the NE-induced release of AVP-LI with recovery observed after approximately 50 minutes of washout. In this particular experiment, only small increases in oxytocin levels were detected initially.

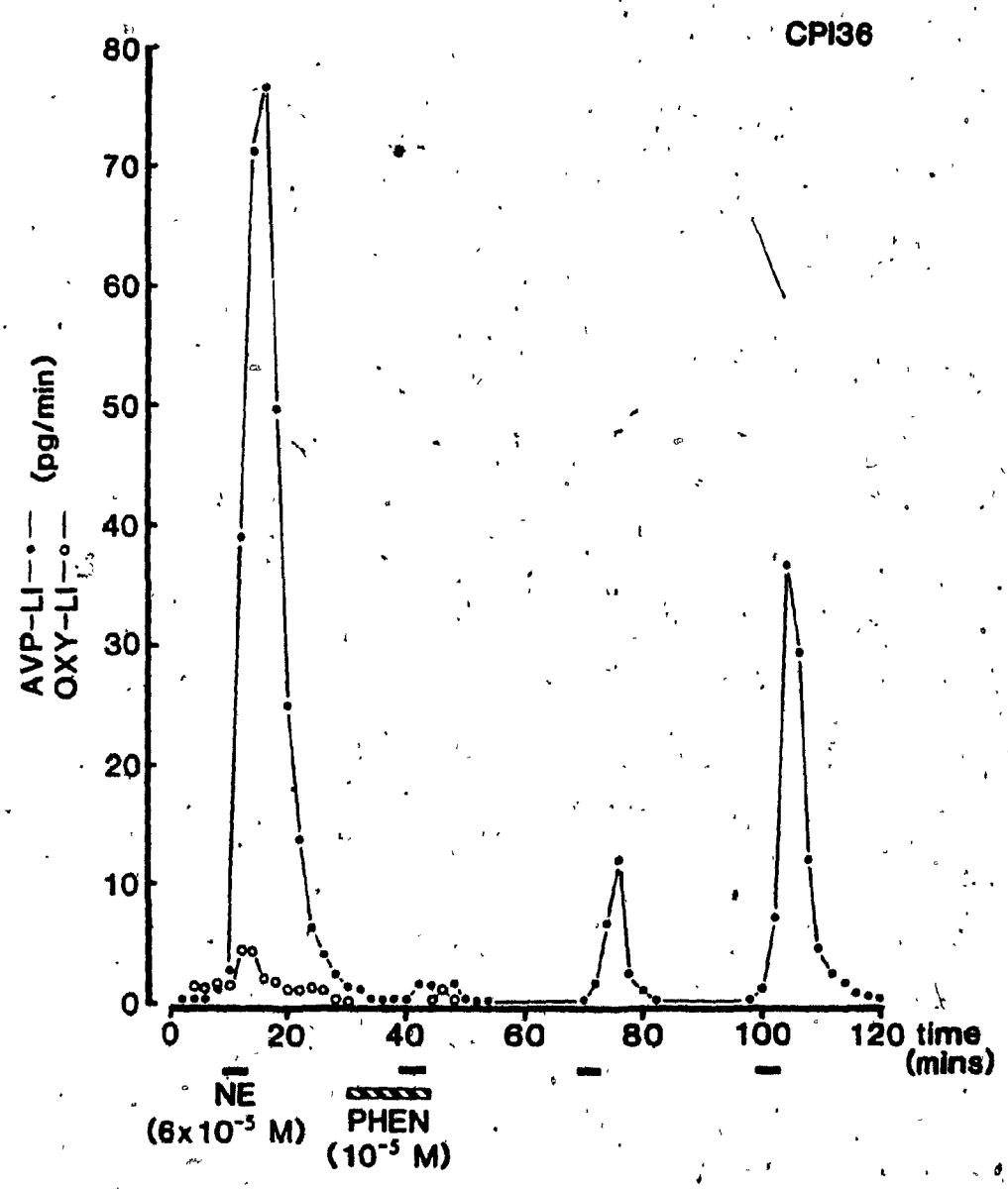
CPI36
AVP-LI—•— (pg/min)
OXY-LI—°—
80
70
60
50
40
30
20
10
0
0
20
40
60
80
100
120 time (mins)
NE
(6x10⁻⁵ M)
PHEN
(10⁻⁵ M)

Figure 7-9 Effect of phenoxybenzamine (PHOXY, 10^{-5} M) on the response to NE (6×10^{-5} M). PHOXY completely abolished the release of AVP-LI in response to NE and markedly reduced the release of OXY-LI. Little reversal of the blockade was observed.

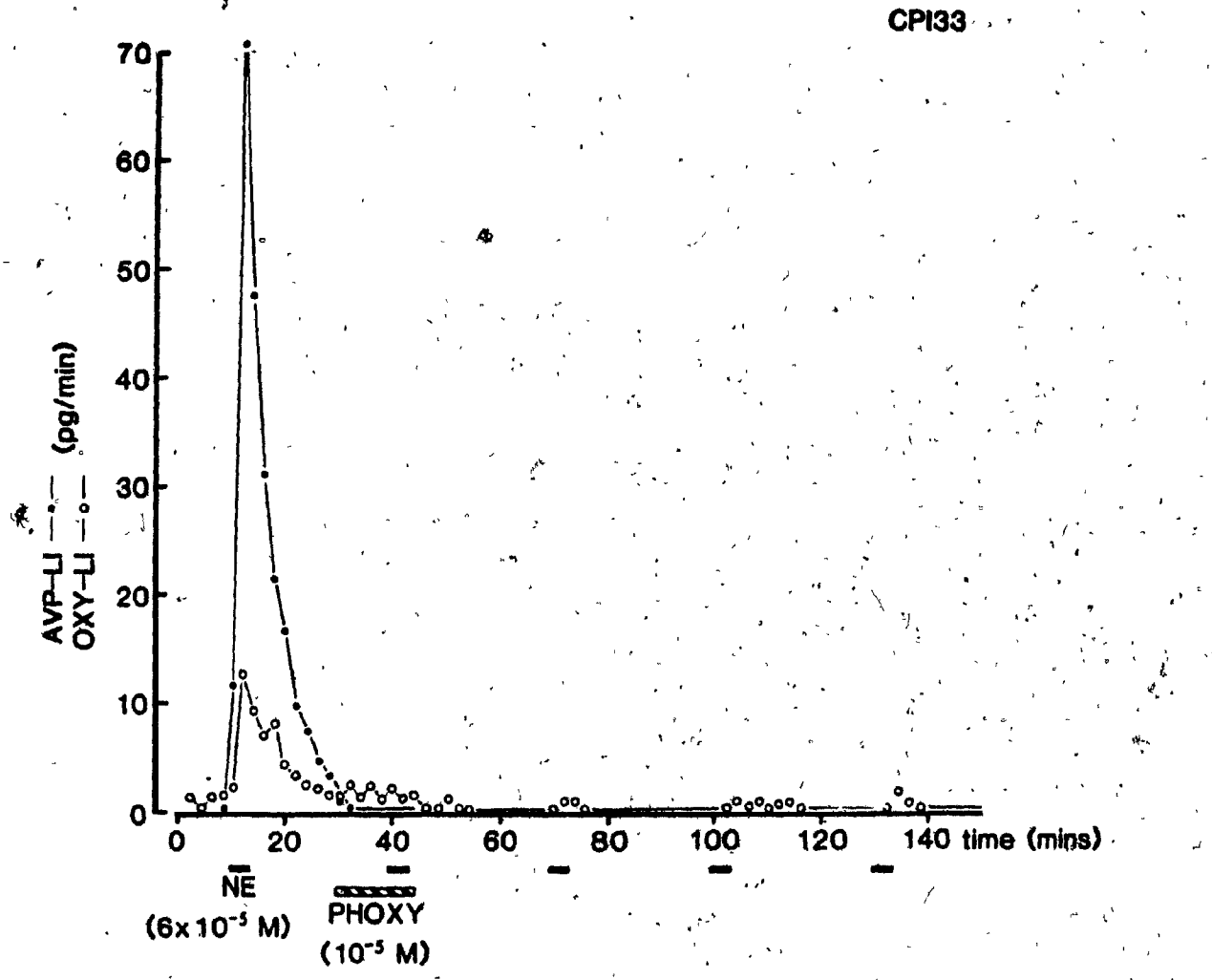
CPI33
AVP-LI —•— (pg/min)
OXY-LI —°—
70
60
50
40
30
20
10
0
0
20
40
60
80
100
120
140 time (mins)
NE
(6x10⁻⁵ M)
PHOXY
(10⁻⁵ M)

Figure 7-10 Effect of prazosin (PRAZ, 10^{-7} M) on the response to NE (6×10^{-5} M). Prazosin reduced the release of AVP-LI in response to NE and completely abolished the NE-induced release of OXY-LI.

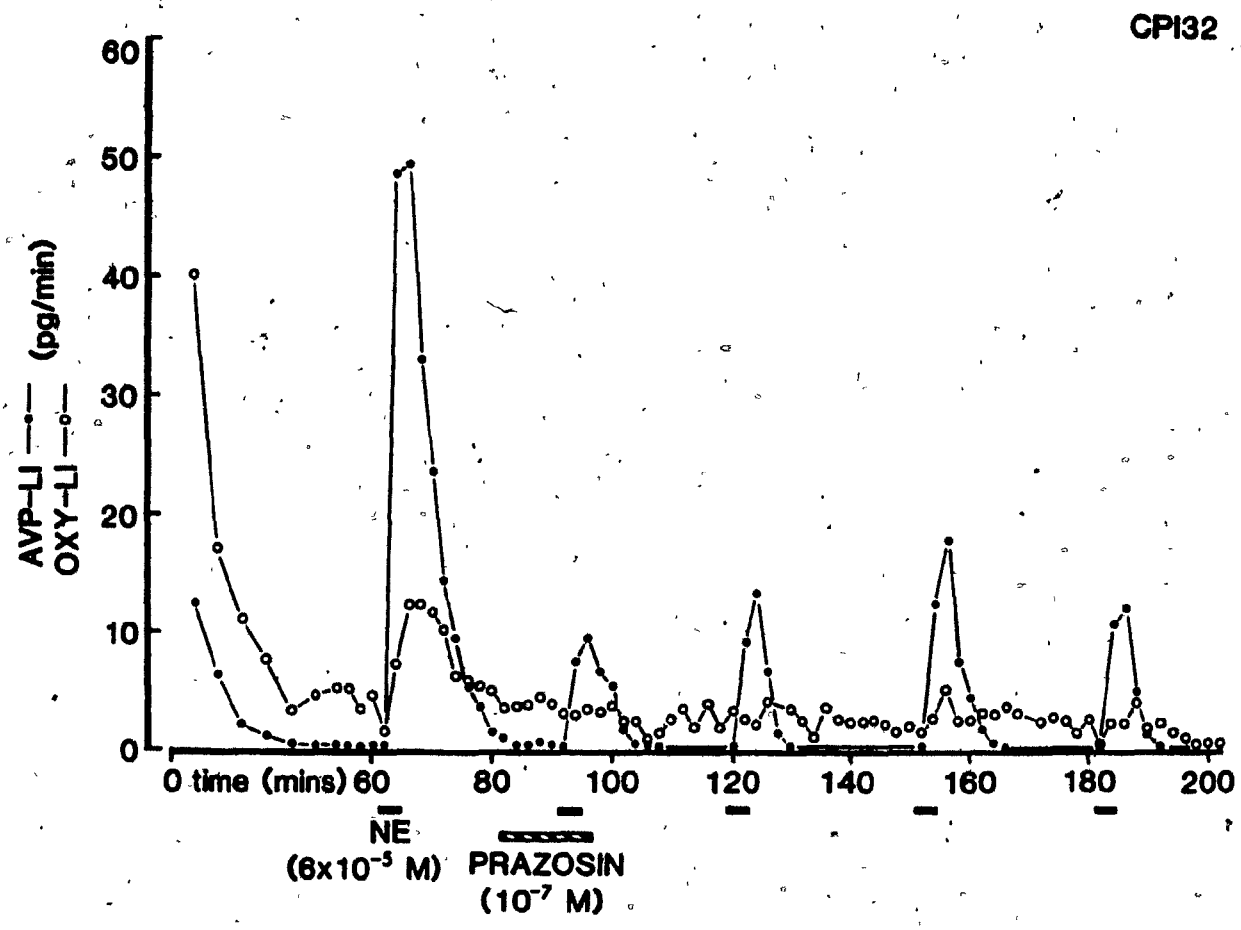
CPI32
AVP-LI —•— (pg/min)
OXY-LI —○—
60
50
40
30
20
10
0
0 time (mins) 60
80
100
120
140
160
180
200
NE
(6x10⁻⁵ M)
PRAZOSIN
(10⁻⁷ M)

CHAPTER 8

GENERAL DISCUSSION

8.1 Conclusions

Three major conclusions can be drawn from the work presented in this thesis.

First, SON neurons are morphologically simple and well suited to the function of synaptic integration. This conclusion derives from a consideration of their morphological and electrical properties (Chapter 3). Their unbranched dendrites, high input resistance and long membrane time-constant are ideal for faithful conduction of synaptic signals to the soma. Moreover, their numerous dendritic spines provide a morphological substrate for complex synaptic modulation and integration.

The second and third conclusions regard the function of potentially important afferent systems to SON neurosecretory neurons. The data presented in Chapters 4 and 5 indicate that SON neurons receive a tonically active inhibitory input mediated by γ-aminobutyric acid (GABA). A large part of this input appears to originate rostral to the third ventricle. Finally, data presented in Chapters 6 and 7 argue that the function of the dense noradrenergic innervation of the SON is to stimulate the electrical activity of SON neurons and the release of vasopressin and

oxytocin from the neurohypophysis.

This Discussion considers the possibility that these two afferent systems participate in the reflex control of release of vasopressin and oxytocin.

8.2 Reflex control of vasopressin release

Secretion of vasopressin is closely regulated by plasma osmolality, CO_2 content, blood pressure and intravascular volume (Dunn et al., 1973; Harris, 1979; Share, 1962; Share and Levy, 1962). An increase in plasma osmolality enhances the electrical activity of SON neurons (Cross and Green, 1959; Brimble and Dyball, 1977) and increases vasopressin secretion (Dunn et al., 1973; Share, 1962). An osmotic stimulus may act directly upon SON neurons (Bourque and Renaud, 1984; Leng, 1980) but may also influence neurons in other sites in the brain (Sladek and Johnson, 1983; Iovino et al., 1983) and in the periphery (Baertschi and Vallet, 1981). Activation of carotid body chemoreceptors by CO_2 infusion also stimulates SON neuronal discharge (Yamashita, 1977; Harris, 1979) and increases vasopressin release (Harris et al., 1975). These all serve to augment the firing of SON neurons. Alternatively SON neuronal activity and vasopressin secretion demonstrate an inverse relationship with blood pressure which is mediated, in part, by carotid body and left atrial baroreceptors (Harris et al., 1975; Harris, 1979; Kannan and Yagi, 1978; Share and Levy, 1962;

Wakerley et al., 1975; Yamashita, 1977). Thus, a reduction of blood volume increases SON neuronal activity (Wakerley et al., 1975) and plasma vasopressin levels (Dunn et al., 1973) while activation of atrial stretch receptors inhibits SON neuronal discharge (Koizumi and Yamashita, 1978).

Participation of A1 noradrenergic neurons in reflex release of vasopressin: The central pathways mediating reflex release of vasopressin are now under investigation (see reviews by Reis et al., 1984; Sawchenko and Swanson, 1982). Primary visceral inputs to the central nervous system entering via the vagal and glossopharyngeal nerves terminate in the nucleus tractus solitarius (NTS; Donoghue et al., 1984; Koizumi and Yamashita, 1978). An important second link in the reflex chain may be mediated by NTS neurons that contain excitatory (substance P or glutamate) or inhibitory (GABA) neurotransmitters and project to noradrenergic (A1 and A6) and adrenergic (C1) cell groups in the medulla and pons (Reis et al., 1984)

It is proposed that noradrenergic neurons of the A1 cell group located in the ventrolateral medulla form a third link in the reflex. Neurons in the ventrolateral medulla respond to cardiovascular stimuli (Caverson et al., 1984). Activation of neurons in the ventrolateral medulla by local application of glutamate (Blessing and Willoughby, 1985b) or focal electrical stimulation (Mills and Wang, 1964a)

stimulates vasopressin release. The latter effect is blocked by intracerebroventricular injection of α-adrenoreceptor antagonists (Mills and Wang, 1964b) indicating the participation of noradrenergic neurons. Lesions of the A1 cell group block the chemoreceptor-induced activation of SON neurons (Banks and Harris, 1984) and interruption of A1 efferents reduce the haemorrhage-induced increase in plasma vasopressin (Lightman et al., 1984). Similarly, inhibition of neurons in the ventrolateral medulla by local application of glycine, GABA, or muscimol, blocks the increased release of vasopressin that follows carotid occlusion (Feldberg and Rocha e Silva, 1981) or haemorrhage (Blessing and Willoughby, 1985a). Furthermore, tonic inhibition of neurons in the ventrolateral medulla appears to maintain circulating vasopressin at its normally low level since application of antagonists of glycine and GABA to the ventral surface of the medulla stimulates vasopressin release (Feldberg and Rocha e Silva, 1978).

This substantial body of evidence suggests that vasopressin release following chemoreceptor activation and/or baroreceptor unloading results from excitation and/or disinhibition of neurons in the ventrolateral medulla. A direct effect of A1 neurons on SON neurons is supported not only by the observations of Mills and Wang (1964b, see above) but also by these observations (Chapters 6 and 7) and the anatomical, electrophysiological and endocrinological

studies described in Chapter 1.4.3. This does not rule out the participation of other neuronal systems and neurotransmitters. For example, Banks and Harris (1984) and Bisset and Chowdrey (1984) have suggested that a cholinergic input to the SON may form a final link in the baroreceptor reflex, in support of an earlier theory by Mills and Wang (1964b).

Reflex inhibition of vasopressin secretion: Removal of a tonic excitation (cf. Wakerley and Noble, 1983) might contribute to the depression of SON neuronal activity and vasopressin secretion that results from baroreceptor activation. However, the consistently rapid baroreceptor responses of SON neurons (Yamashita, 1977; Kannan and Yagi, 1978; Harris, 1979; Koizumi and Yamashita, 1978; Day and Renaud, 1984) might reasonably be expected to result from active inhibition. Furthermore, the increase in rat plasma vasopressin due to dehydration is blocked by stressful stimuli (Mirsky et al., 1954; Keil and Severs, 1976). Intracerebroventricular (I.C.V.) injection of GABA or muscimol lowers, and bicuculline raises, blood pressure and heart rate (Bhargava et al., 1964; Williford et al., 1980). I.C.V. injection of GABA-transaminase inhibitors reduces vasopressin release in response to hypovolaemia (Knepel, 1980). Injection of the glutamate decarboxylase inhibitor, 3-mercaptopropionic acid, increases the hypovolaemia-

induced rise in plasma vasopressin.

Banks and Harris (1984) suggest that the inhibitory response of SON neurons to baroreceptor activation is mediated via noradrenergic A6 neurons of the locus ceruleus. Neurons of the locus ceruleus and sub-ceruleus region alter their activity in response to changes in arterial and atrial pressure (Ward et al., 1980) and destruction of noradrenergic neurons in this area by injection of the selective neurotoxin, 6-hydroxydopamine, abolishes the inhibition of SON neurons provoked by activation of baroreceptors. However, it is unlikely that A6 neurons act directly on SON neurons since: 1) the bulk of evidence indicates that norepinephrine exites SON neurons and stimulates vasopressin release (see chapters 1, 6 and 7), and 2) locus ceruleus contributes only a small portion of the noradrenergic innervation of the SON (Sawchenko and Swanson, 1982).

The data presented in chapter 4 demonstrate that SON neurons receive a powerful inhibitory input from GABA-containing neurons. Evidence from these experiments, when considered along with the literature on the subject (see chapter 4.3), indicate that GABA-containing neurons located adjacent to the SON in the lateral hypothalamus, in the diagonal band of Broca and medial septum or in the amygdala might contribute to this innervation. Electrical stimulation of these regions inhibits SON neurons (chapter

4; Poulain et al., 1980; Cirino and Renaud, 1985; Andrew and Dudek, 1984; Hanamura et al., 1982; Ferreyra et al., 1983). Furthermore, trains of electrical stimuli delivered to the diagonal band of Broca can produce a transient, or indeed prolonged, inhibition of SON neurons that resembles the baroreceptor-evoked inhibition. In addition, repetitive septal stimulation blocks the osmotically-induced increase in SON neuronal activity (Yamashita and Kannan, 1976). Anatomical studies indicate that all these regions receive a substantial noradrenergic innervation from the locus ceruleus (Jones and Moore, 1977) and the parabrachial nucleus (Saper and Loewy, 1980).

I propose, therefore, that the inhibition of SON neurons following baroreceptor activation may result from activation of a GABA-mediated afferent system. As proposed by Banks and Harris (1984), locus coeruleus neurons would form an important link between cardiovascular receptor afferents and the forebrain GABA system that influences SON activity. Figure 8-1 illustrates the features of this hypothesis.

8.3 Reflex control of Oxytocin release

In lactating female mammals, suckling initiates a neuroendocrine reflex that results in oxytocin release from the neurohypophysis and milk ejection. Approximately 10 seconds before milk ejection, oxytocin-secreting neurons of

the SON fire a high-frequency burst of action potentials that causes the sudden release of hormone (see review by Poulain and Wakerley, 1982). Reflex milk ejection can also be elicited by vaginal stimulation or distension, or by stimulation of the proximal stump of the cut vagus nerve (Moos and Richard, 1975). Little is known about the central structures and pathways that mediate (or modulate) reflex oxytocin release although many areas of the brain and several neurotransmitters have been implicated (Poulain and Wakerley, 1982).

Influence of norepinephrine on oxytocin release: One fruitful approach to studying reflex control of oxytocin release has been to determine the effects on milk ejection of central administration of drugs. Relevant to the investigation undertaken in this thesis, injection of α-adrenoreceptor antagonists blocks reflex milk ejection (Moos and Richard, 1975; Tribollet et al., 1978; Clarke et al., 1979). Stimulation of oxytocin release by norepinephrine *in vitro* (chapter 7) may, therefore, be physiologically relevant. The identity of noradrenergic neurons capable of mediating this reflex *in vivo* remain in doubt. The participation of A1 neurons is unlikely in view of their apparently selective innervation of vasopressin neurons (McNeill and Sladek, 1980; Day and Renaud, 1984).

It is worth noting that injection studies also indicate

that cholinergic and dopaminergic receptors mediate stimulatory effects (Moos and Richard, 1975, 1979; Clarke et al., 1979) while β-adrenoreceptors may mediate inhibitory influences (Moos and Richard, 1979; Tribollet et al., 1978). It is possible that norepinephrine also acts on interneurons which, in turn, project to the SON.

Influences of GABA on oxytocin release: The ability of stressful stimuli to interfere with milk ejection (Cross, 1955; Taleisnik and Deis, 1964) is an indication that cortical inhibitory systems modulate the reflex pathway. Lebrun et al. (1983) have shown that reflex milk ejection is delayed or abolished by electrical stimulation of the septum; a procedure known to inhibit SON neurons (Poulain et al., 1980; Cirino and Renaud, 1985). The data presented in chapter 4 indicate that the influences of certain forebrain projections to the SON may be mediated by GABA. Further investigations of the control of oxytocin release may uncover an important inhibitory component mediated by GABA.

Figure 8-1 Block diagram outlining hypothetical pathways mediating reflex control of vasopressin (AVP) secretion. Abbreviations: DBB, diagonal band of Broca; SON, supraoptic nucleus; GABA, γ-aminobutyric acid; NE, norepinephrine; PP, posterior pituitary; A6, noradrenergic cell group of locus ceruleus; A1, noradrenergic cell group of caudal ventrolateral medulla; NTS, nucleus of the tractus solitarius, IX, glossopharyngeal nerve; X, vagus nerve; +, excitatory synapse; −, inhibitory synapse; ±, unknown connection.

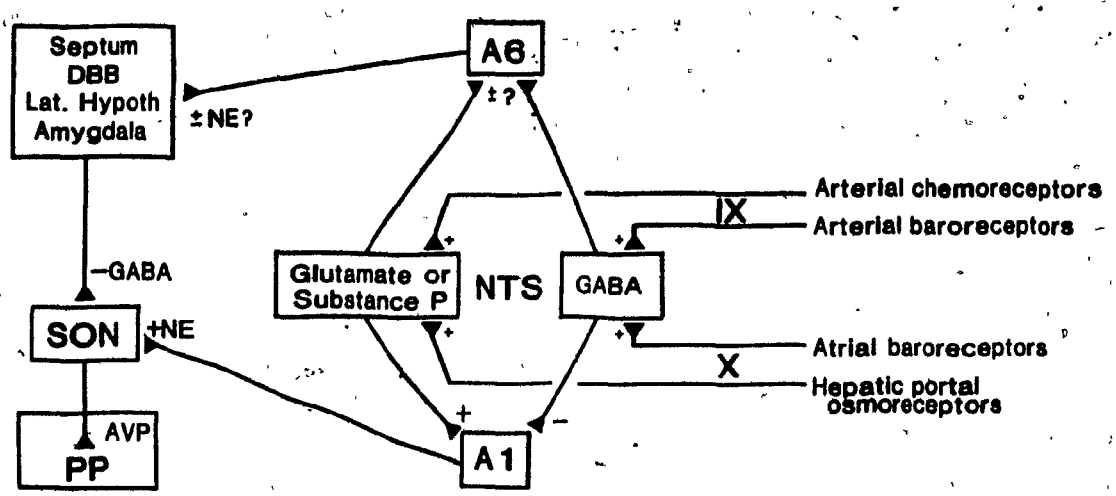
Septum
DBB
Lat. Hypoth
Amygdala
±NE?
A6
±?
Arterial chemoreceptors
IX
Arterial baroreceptors
−GABA
Glutamate or
Substance P
NTS
GABA
SON
+NE
Atrial baroreceptors
X
Hepatic portal
osmoreceptors
AVP
PP
A1

REFERENCES

Abe, H., Inoue, M., Matsuo, T. and Ogata, N. (1983). The effects of vasopressin on electrical activity in the guinea-pig supraoptic nucleus in vitro. J. Physiol. 337;665-685.

Abe, H. and Ogata, N. (1982). Ionic mechanism for the osmotically induced depolarization in neurons of the guinea pig supraoptic nucleus in vitro. J. Physiol. 327;157-17 .

Abrahams, V.C. and Pickford, M. (1956). Observations on a central antagonism between adrenaline and acetylcholine J. Physiol. 131: 712-718.

Adams, P.R. and Brown, D.A. (1975). Actions of γ-aminobutyric acid on sympathetic ganglion cells. J. Physiol. 250:85-120.

Aghajanian, G.K. (1985). Modulation of a transient outward current in serotonergic neurones by α_1-adrenoreceptors. Nature 315:501-503.

Akaike, N., Hattori, K., Inomata, N. and Oomura, Y. (1985). γ-aminobutyric acid and pentobarbitone-gated chloride currents in internally perfused frog sensory neurones. J. Physiol. 360:367-386.

Alger, B.E. and Nicoll, R.A. (1980). Spontaneous inhibitory post-synaptic potentials in hippocampus mechanism for tonic inhibition. Brain Res. 200:195-200.

Alger, B.E. and Nicoll, R.A. (1982). Feed-forward inhibition in rat hippocampal pyramidal cells *in vitro*. J. Physiol. 328:105-123.

Alger, B.E. and Nicoll, R.A. (1982). Pharmacological evidence for two kinds of GABA receptors on rat hippocampal pyramidal cells studied *in vitro*. J. Physiol. 328:125-141.

Alonso, G. and Assenmacher, I. (1981). Radioautographic studies on the neurohypophysial projections of the supraoptic and paraventricular nuclei in the rat. Cell Tissue Res. 219:525-534.

Alonso, G. and Assenmacher, I. (1984). Ultrastructural analysis of the noradrenergic innervation of rat supraoptic nucleus. Neurosci. Letts. 49:45-50. 151-154.

Andersen, P., Dingledine, R., Gjerstad, L., Langmoen, I.A. and Mosfeldt Laussen, A. (1980). Two different responses of hippocampal pyramidal cells to application of gamma-amino butyric acid. J. Physiol. 305:279-296.

Andrew, R.D., MacVicar, B.A., Dudek, F.E. and Hatton, G.I. (1981). Dye transfer through gap junctions between neuroendocrine cells of rat hypothalamus. Science 211:1187-1189.

Andrew, R.D. and Dudek, F.E. (1982). Slow hyperpolarization after repetitive firing of magnocellular neuroendocrine cells in rat hypothalamic slices. Fed. Proc. 41:1534.

Andrew, R.D. and Dudek, F.E. (1983). Burst discharge in mammalian neuroendocrine cells involves an intrinsic regenerative mechanism. Science 221: 1050-1052.

Andrew, R.D. and Dudek, F.E. (1984a). Analysis of intracellularly recorded phasic bursting by mammalian neuroendocrine cells. J. Neurophysiol. 51: 552-566.

Andrew, R.D. and Dudek, F.E. (1984b). Intrinsic inhibition in magnocellular neuroendocrine cells of rat hypothalamus. J. Physiol. 353:171-185.

Andrew, R.D., MacVicar, B.A., Dudek, F.E. and Hatton, G.I. (1981). Dye transfer through gap junctions between neuroendocrine cells of rat hypothalamus. Science 211: 1187-1189.

Armstrong, W.E., Schöler, J. and McNeill, T.H. (1982). Immunocytochemical, Golgi and electron microscopic characterization of putative dendrites in the ventral glial lamina of the rat supraoptic nucleus. Neurosciences 7: 679-694.

Armstrong, W.E, and Sladek, C.D. and Sladek, J.R. (1982). Characterization of noradrenergic control of vasopressin release by the organ-cultured rat hypothalamo-neurohypophysial system. Endocrinology 111:273-279.

Armstrong, W.E., Warach, S., Hatton, G.I. and McNeill, T.H. (1980). Subnuclei in the hypothalamic paraventricular nucleus: A cytoarchitectonic, HRP and immunocytochemical analysis. Neuroscience 5:1931-1958.

Armstrong-James, M. and Fox, K. (1983). Effects of ionophoresed noradrenaline on the spontaneous activity of neurons in rat primary somatosensory cortex. J. Physiol. 335:427-447.

Arnauld, E., Cirino, M., Layton, B.S. and Renaud, L.P. (1983). Contrasting actions of amino acids, acetylcholine, noradrenaline and leucine-enkephalin on the excitability of supraoptic vasopressin-secreting neurons. Neuroendocrinology 36:187-196.

Ascher, P., Kunze, D. and Neild, T.O. (1976). Chloride distribution in aplysia neurones. J. Physiol. 256:441-464.

Aulsebrook, L.H. and Holland, R.C. (1969). Central regulation of oxytocin release with and without vasopressin release. Am. J. Physiol. 216:818-829.

Baertschi, A.J. and Vallet, P.G. (1981). Osmosensitivity of the hepatic portal vein area and vasopressin release in rats. J. Physio. 315:217-230.

Banks, D. and Harris, M.C. (1984). Lesions of the locus ceruleus abolish baroreceptor-induced depression of supraoptic neurones in the rat. J. Physiol. 355:383-398

Barker, J.L., Crayton, J.W. and Nicoll, R.A. (1971). Antidromic orthodromic responses of paraventricular and supraoptic neurosecretory cells. Brain Res. 33; 353-366.

Barker, J.L. and McBurney, R.N. (1979). GABA and glycine may share the same conductance channel on cultured mammalian neurones. Nature 277:234-236.

Barker, J.L. and McBurney, R.N. (1979). Phenobarbitone modulation of postsynaptic GABA receptor function on cultured mammalian neurons. Proc. R. Soc. Lond. B. 206:319-327.

Barker, J.L., McBurney, R.N. and MacDonald, J.F. (1980). Fluctuation analysis of neutral amino acid responses in cultured mouse spinal neurones. J. Physiol. 322:365-387.

Barker, J.L. and Ransom, B.R. (1978a). Amino acid pharmacology of mammalian central neurones grown in tissue culture. J. Physiol. 280:331-354.

Barker, J.L. and Ransom, B.R. (1978b). Pentobarbitone pharmacology of mammalian central neurones grown in tissue culture. J. Physiol. 280:355-372.

Barrett, J.W. and Crill, W.E. (1974). Specific membrane properties of cat motoneurones. J. Physiol. 239; 301-324.

Beaumont, K., Chilton, W.S., Yamamura, H.I. and Enna, S.J. (1978). Muscimol binding in rat brain: association with synaptic receptors. Brain Res. 148:153-162.

Belluzi, O., Sacchi, O. and Wanke, E. (1985) A fast transient outward current in the rat sympathetic neurone studied under voltage-clamp conditions. J. Physiol. 358:91-108.

Bhargava, K.P., Bhattacharya, S.S. and Srimal, R.C. (1964). Central cardiovascular actions of α-aminobutyric acid. Brit. J. Pharmacol. 23:383-390.

Bhargava, K.P., Kulshrestha, V.K. and Srivastava, Y.P. (1972). Central cholinergic and adrenergic mechanisms in the release of antidiuretic hormone. Br. J. Pharmacol. 44:617-627.

Bicknell, R.J., Brown, D., Chapman, C., Hancock, P.D. and Leng, G. (1984). Reversible fatigue of stimulus-secretion coupling in the rat neurohypophysis. J. Physiol. 348:601-613.

Bicknell, R.J., Chapman, C. and Leng, G. (1985). Effects of opioid agonists and antagonists on oxytocin and vasopressin release in vitro. Neuroendocrinol. 41: 142-148.

Bicknell, R.J., Flint, A.P.F. Leng, G. and Sheldrick. E.L (1982). Phasic pattern of electrical stimulation enhances oxytocin secretion from the isolated neurohypophysis. Neurosci. Lett. 30:47-50.

Bicknell, R.J. and Leng, G. (1981). Relative efficiency of neural firing patterns for vasopressin release in vitro. Neuroendocrinol. 33:295-299.

Bioulac, B., Gaffori, O., Harris, M. and Vincent, J.-D. (1978). Effects of acetylcholine, sodium glutamate and GABA on the discharge of supraoptic neurons in the rat. Brain Res. 154:159-162.

Bisset, G.W. and Chowdrey, H.S. (1984). A cholinergic link in the reflex release of vasopressin by hypotension in the rat. J. Physiol. 352:523-545.

Blessing, W.W. and Willoughby, J.O. (1985a) Inhibition of neuronal function in rabbit caudal ventrolateral medulla prevents release of vasopressin in response to hemorrhage. Proc. Australian Neurosci. Soc.

Blessing, W.W. and Willoughby, J.O. (1985b). Excitation of neuronal function in rabbit caudal ventrolateral medulla elevates plasma vasopressin. Proc. Australian Neurosci. Soc.

Bourque, C.W. (1984). Membrane properties of rat supraoptic nucleus neurons *in vitro*. Ph.D. Thesis, McGill University, Montreal, Quebec.

Bourque, C.W., Brown, D.A. and Renaud, L.P. (1986). Ba++ ions induce prolonged depolarizations in neurosecretory neurons of the adult rat supraoptic nucleus. J. Physiol. (submitted).

Bourque, C.W., Randle, J.C.R., and Renaud, L.P. (1985). A calcium-dependent potassium conductance in rat supraoptic neurosecretory cells. J. Neurophysiol. (in press).

Bourque, C.W. and Renaud, L.P. (1983). A perfused *in vitro* preparation of rat hypothalamus for electrophysiological studies on neurosecretory neurons. J. Neurosci. Methods 7:203-214.

Bourque, C.W. and Renaud, L.P. (1984). Activity patterns and osmosensitivity of rat supraoptic neurones in perfused hypothalamic explants. J. Physiol. 349:631-647.

Bourque, C.W. and Renaud, L.P. (1985a). Calcium-dependent action potentials in rat supraoptic neurosecretory neurones recorded *in vitro*. J. Physiol. 363:419-428.

Bourque, C.W. and Renaud, L.P. (1985b). Activity-dependence of action potential duration in rat supraoptic neurosecretory neurones recorded *in vitro*. J. Physiol. 363:429-439.

Bowery, N.G. and Brown, D.A. (1974). Depolarizing action of γ-aminobutyric acid and related compounds on rat superior cervical ganglia *in vitro*. Br. J. Pharmacol. 50:205-218.

Bridges, T.E., Hillhouse, E.W. and Jones, M.T. (1976). The effect of dopamine on neurohypophysial hormone release *in vivo* and from the rat neural lobe and hypothalamus *in vitro*. J. Physiol. 260:647-666.

Brimble, M.J. and Dyball, R.E.J. (1977). Characterization of the responses of oxytocin and vasopressin-secreting neurones in the supraoptic nucleus to osmotic stimulation. J. Physiol. 271:253-271.

Brimble, M.J., Dyball, R.E.J. and Forsling, M.L. (1978a) Oxytocin release following osmotic activation of oxytocin neurones in the paraventricular and supraoptic nuclei. J. Physiol. 287:69-78.

Brimble, J.J., Haller, E.W. and Wakerley, J.B. (1978b). Supraoptic and paraventricular units in slices incubated in iso- or hypertonic medium. J. Physiol. 287:38.

Brody, M.J. and Johnson, A.K. (1980). Role of the anteroventral third ventricle (AV3V) region in fluid and electrolyte balance, arterial pressure regulation and hypertension. In: Frontiers in Neuroendocrinology vol. 6. Ganong, W.F. and Martini, L. (eds.) Raven Press, New York, pp 249-292.

Brown, D.A. and Galvan, M. (1979). Responses of the guinea-pig isolated olfactory cortex slice to γ-aminobutyric acid recorded with extracellular electrodes. Br. J. Pharmacol. 65:347-353.

Brownstein, M.J., Russel, J.T. and Gainer, M. (1980). Synthesis, transport and release of posterior pituitary hormones. Science 207:373-378.

Carithers, J., Bealer, S.L., Brody, M.J. and Johnson, A.K. (1980). Fine structural evidence of degeneration in supraoptic nucleus and subfornical organ of rats with lesions in the anteroventral third ventricle. Brain Res. 201:1-12.

Carithers, J., Bealer, S.L. and Johnson, A.K. (1984). The effects of transverse cuts caudal to the preoptic recess on the hypothalamo-neurohypophyseal neurosecretory system. Brain Res. 305:247-257.

Carithers, J., Dellmann, H.D., Bealer, S.L., Brody, M.J. and Johnson, A.K. (1981). Ultrastructural effects of anteroventral third ventricle lesions on supraoptic nuclei and neural lobes of rats. Brain Res. 220:13-29.

Carlsson, A., Falck, B. and Hillarp, N.A. (1962). Cellular localization of brain monoamines. Acta Physiol. Scand. 56:1-27.

Caverson, M.M., Ciriello, J. and Calaresu, F.R. (1984). Chemoreceptor and baroreceptor inputs to ventrolateral medullary neurons. Am. J. Physiol. 247:R872-R879.

Choi, D.W., Farb, D.H. and Fischbach, G.D. (1981) GABA-mediated synaptic potentials in chick spinal cord and sensory neurons. J. Neurophysiol. 45:632-643.

Choi, D.W. and Fischbach, G.D. (1981). GABA conductance of chick spinal cord and dorsal root ganglion neurons in cell culture. J. Neurophysiol. 45:605-620.

Cirino, M. and Renaud, L.P. (1985). Influence of lateral septum and amygdala stimulation on the excitability of hypothalamic supraoptic neurons. An electrophysiological study in the rat. Brain Res. 326:357-361.

Clarke, G., Fall, C.H.D., Lincoln, D.W. and Merrick, L.P. (1978). Effects of cholinoceptor antagonists on the suckling-induced and experimentally evoked release of oxytocin. Br. J. Pharmacol. 63:519-527.

Clarke, G., Lincoln, D.W. and Merrick, L.P. (1979). Dopaminergic control of oxytocin release in lactating rats. J. Endocrinol. 83:409-420.

Clarke, G., Wood, P., Merrick, L.P. and Lincoln, D.W. (1979). Opiate inhibition of peptide release from the neurohypophysial terminals of hypothalamic neurons. Nature 282:746-748.

Cobbett, P. and Hatton, G.I. (1984). Dye coupling in hypothalamic slices: Dependence on *in vivo* hydration state and osmolality of incubation medium. J. Neuroscience 4:3034-3038.

Connor, J.A. and Stevens, C.F. (1971a) Voltage clamp studies of transient outward membrane current in gastropod neural somata. J. Physiol. 213:21-30.

Connor, J.A. and Stevens, C.F. (1971b). Prediction of repetitive firing behaviour from voltage clamp data on an isolated neurone soma. J. Physiol. 213:31-53.

Cross, B.A. (1955). Neurohormonal mechanisms in emotional inhibition of milk ejection. J. Endocrinology 12:29-37.

Cross, B.A., Dyball, R.E.J., Dyer, R.G., Jones, C.W., Lincoln, D.W., Morris, J.F. and Pickering, B.T. (1975). Endocrine neurones. Rec. Prog. Horm. Res. 31:243-294.

Cross, B.A. and Green, J.D. (1959). Activity of single neurons in the hypothalamus: Effect of osmotic and other stimuli. J. Physiol. 148:554-569.

Curtis, D.R., Duggan, A.W., Johnston, G.A.R. and McLennan, H. (1971a) Antagonism between bicuculline and GABA in the cat brain. Brain Res. 33:57-73.

Curtis, D.R., Duggan, A.W., Felix, D. and Johnston, G.A.R. (1971b). Bicuculline, an antagonist of GABA and synaptic inhibition in the spinal cord of the cat. Brain Res. 32:69-96.

Day, T.A., Randle, J.C.R. and Renaud, L.P. (1985). Opposing alpha- and beta-adrenergic mechanisms mediate dose-dependent actions of noradrenaline on supraoptic vasopressin neurons *in vivo*. Brain Res. (in press)

Day, T.A. and Renaud, L.P. (1984). Electrophysiological evidence that noradrenergic afferents selectively facilitate the activity of supraoptic vasopressin neurons. Brain Res. 303:233-240.

DeFeudis, F.V., Madtes, P. and Gervas-Camacho, J. (1977). Binding of glycine and γ-aminobutyric acid to synaptosomal fractions of 6 regions of the feline brain; effects of strychnine. Experientia 33:340-343.

Dekin, M.S. and Getting, P.A. (1984). Firing pattern of neurons in the nucleus tractus solitarius: modulation by membrane hyperpolarization. Brain Res. 324:180-184.

Dekin, M.S., Richerson, B.B. and Getting, P.A. (1985). Thyrotropin-releasing hormone induces rhythmic bursting in neurons of the nucleus tractus solitarius. Science 229:67-69.

Donoghue, S., Felder, R.B., Jordan, D. and Spyer, K.M. (1984). The central projections of carotid baroreceptors and chemoreceptors in the cat: A neurophysiological study. J. Physiol. 347:397-409.

Douglas, W.W. (1963). A possible mechanism of neurosecretion: Release of vasopressin by depolarization and its dependence on calcium. Nature 197: 81.

Douglas, W.W. (1968). Stimulus-secretion coupling: the concept and clues from chromaffin and other cells. Brit. J. Pharmacol. 34: 452-477.

Douglas, W.W. and Poisner, A.M. (1964). Stimulus-secretion coupling in a neurosecretory organ: the role of calcium in the release of vasopressin from the neurohypophysis. J. Physiol. 172: 1-18.

Dreifuss, J.J., Harris, M.C. and Tribollet, E. (1976). Excitation of phasically firing hypothalamic supraoptic neurones by carotid occlusion in rats. J. Physiol. 257: 337-35 .

Dreifuss, J.J., Kalnins, I., Kelly, J.S. and Ruf, K.B. (1971). Action potentials and release of neurohypophyseal hormones in vitro. J. Physiol. 215: 805-817.

Dreifuss, J.J. and Kelly, J.S. (1972). Recurrent inhibition of antidromically identified rat supraoptic neurones. J. Physiol. 220: 87-103.

Dunlap, K. and Fischbach, G.D. (1978) Neurotransmitters decrease the calcium component of sensory neurone action potentials. Nature 276: 837-839.

Dunlap, K. and Fischbach, G.D. (1981) Neurotransmitters decrease the calcium conductance activated by depolarization of embryonic chick sensory neurons. J. Physiol. 317:519-535.

Dunn, F.L., Brennan, T.J., Nelson, A.E. and Robertson, G.L. (1973). The role of blood osmolality and volume in regulating vasopressin secretion in the rat. J. Clin. Invest. 52: 3212-3219.

Dutton, A. and Dyball, R.E.J. (1979). Phasic firing enhances vasopressin release from the rat neurohypophysis. J. Physiol. 290: 433-440.

Du Vigneaud, V. (1956). Hormones of the posterior pituitary gland: oxytocin and vasopressin. The Harvey Lectures 50: 1-26.

Dyball, R.E.J. and Kemplay, S.K. (1982). Dendritic trees of neurones in the supraoptic nucleus. Neurosci. 7: 223-230.

Dyball, R.E.J. and Koizumi, K. (1969). Electrical activity in the supraoptic and paraventricular nuclei associated with neurohypophyseal hormone release. J. Physiol 201; 711-722.

Dyball, R.E.J. and Shaw, F.D. (1979). Inhibition by GABA of hormone release from the neurohypophysis in the rat. J. Physiol. 289:78P-79P.

Eccles, J.C. (1961). Membrane time constants of cat motoneurons and time courses of synaptic action. Exp. Neurol. 4:1-22.

Eckert, R. and Chad, J. (1984). Inactivation of Ca++ channel. Prog. Biophys. Molec. Biol. 44:215-267.

Enna, S.J. and Gallagher, J.P. (1983). Biochemical and electrophysiological characteristics of mammalian GABA receptors. Int. Rev. Neurobiol. 24:181-212.

Enna, S.J. and Snyder, S.H. (1977). GABA receptor binding in frog spinal cord and brain. J. Neurochemistry 28:857-860.

Feldberg, W. and Rocha e Silva, M. (1978). Vasopressin release produced in anaesthetized cats by antagonists of γ-aminobutyric acid and glycine. Br. J. Pharmacol. 62:99-106.

Feldberg, W. and Rocha e Silva, M. (1981). Inhibition of vasopressin release to carotid occlusion by γ-aminobutyric acid and glycine. Br. J. Pharmacol. 72: 17-24.

Felten, D.L. and Cashner, K.A. (1979). Cytoarchitecture of the supraoptic nucleus. A Golgi study. Neuroendocrinology 29:221-230.

Ferreyra, A., Kannan, H. and Koizumi, K. (1983). Influences of the limbic system on hypothalamo-neurohypophysial system. Brain Res. 264:31-45.

Finley, K.M. (1939). The capillary beds of the paraventricular and supraoptic nuclei of the hypothalamus. J. Comp. Neurol. 71: 1-19.

Gahwiler, B.H. and Dreifuss, J.J. (1980). Transition from random to phasic firing induced in neurons cultured from the hypothalamic supraoptic area. Brain Res. 193: 415-425.

Gallagher, J.P., Higashi, H. and Nishi, S. (1978). Characterization and ionic basis of GABA-induced depolarizations recorded in vitro from cat primary afferent neurones. J. Physiol. 275:263-282.

Gallagher, J.P., Nakamura, J. and Shinnick-Gallagher, P. (1983). The effects of temperature, pH and Cl^- pump inhibitors on GABA responses recorded from cat dorsal root ganglia. Brain Res. 267:249-259.

Galvan, M. and Adams, P.R. (1982) Control of calcium current in rat sympathetic neurons by norepinephrine. Brain Res. 244:135-144.

Galvan, M. and Sedlmeir, C. (1984). Outward currents in voltage-clamped rat sympathetic neurones. J. Physiol. 356:115-133.

Ginsborg, B.L. (1973). Electrical changes in the membrane in junctional transmission. Biochem. Biophys. Acta. 300: 289-317.

Gold, M.R. and Martin, A.R. (1984). γ-Aminobutyric acid and glycine activate Cl^- channels having different characteristics in CNS neurons. Nature 308:639-641.

Gregg, C.M. and Sladek, C.D. (1984). A compartmentalized, organ-cultured hypothalamo-neurohypophysial system for the study of vasopressin release. Neuroendocrinology 38:397-402.

Haller, E.W., Brimble, M.J. and Wakerley, J.B. (1978). Phasic discharge in supraoptic neurones recorded from hypothalamic slices. Exp. Brain Res. 33:131-134.

Hanamura, M., Shibuki, K. and Yagi, K. (1982). Amygdalar inputs to ADH-secreting supraoptic neurones in rats. Exp. Brain Res. 48:420-428.

Harris, M.C. (1979). Effects of chemoreceptor and baroreceptor stimulation on the discharge of hypothalamic supraoptic neurones in rats. J. Endocrinology 82; 115-125.

Harris, M.C., Dreifuss J.J. and Legros, J.J.. (1975). Excitation of phasically firing supraoptic neurones during vasopressin release. Nature 258:80-82.

Harris, M.C., Ferguson, A.V. and Banks, D. (1984). The afferent pathway for carotid body chemoreceptor input to the hypothalamic supraoptic nucleus in the rat. Pflugers Arch. 400:80-87.

Hatton, G.I. (1982). Phasic bursting activity of rat paraventricular neurones in the absence of synaptic transmission. J. Physiol. 327:273-284.

Hatton, G.I., Armstrong, W.E. and Gregory, W.A. (1978). Spontaneous and osmotically-stimulated activity in slices of rat hypothalamus. Brain Res. Bull. 3:497-508.

Hatton, G.I., Ho, Y.W. and Mason, W.T. (1983). Synaptic activation of phasic bursting in rat supraoptic nucleus neurones recorded in hypothalamic slices. J. Physiol. 345:297-317.

Heap, P.F., Jones, C.W., Morris, J.F. and Pickering, B.T. (1975). Movement of neurosecretory product through the anatomical compartments of the neural lobe of the pituitary gland. Cell Tissue Res. 156:483-497.

Herring, P.T. (1908). The histological appearance of the mammalian pituitary body. Quant. J. Exp. Physiol. 1:121-159.

Hillman, H.H., Campbell, W.J. and McIlwain, H. (1963). Membrane potential in isolated and electrically stimulated mammalian cerebral cortex: effects of chlorpromazine, cocaine, phenobarbitone and protamine on the tissues electrical and chemical responses to stimulation. J. Neurochem. 10:325-339.

Hodgkin, A.L. and Huxley, A.F. (1952a). A quantitative description of membrane current and its application to conduction and excitation in nerve. J. Physiol. 117; 500-544.

Hodgkin, A.L. and Huxley, A.F. (1952b). Currents carried by sodium and potassium ions through the membrane of the giant axon of Loligo. J. Physiol. 116; 449-472.

Hodgkin, A.L. and Huxley, A.F. (1952c). The dual effect of membrane potential on sodium conductance of the giant axon of Loligo. J. Physiol, 116; 497-506.

Hodgkin, A.L., Huxley, A.F. and Katz, B. (1952). Measurment of current-voltage relations in the membrane of the giant axon of Loligo. J. Physiol. 116; 424-448.

Homma, S. and Rovainen, C.M. (1978). Conductance increases produced by glycine and γ-aminobutyric acid in lamprey interneurons. J. Physiol. 279:231-252.

Horn, J.P. and McAfee, D.A. (1980). Alpha-adrenergic inhibition of calcium-dependent potentials in rat sympathetic neurons. J. Physiol. 301:191-204.

Ifft, J.D., McCarthy, L. (1974). Somatic spines in the supraoptic nucleus of the rat hypothalamus. Cell. Tiss. Res. 148; 203-211.

Ingram, C.D., Bicknell, R.J., Brown, D. and Leng, G. (1982). Rapid fatigue of neuropeptide secretion during continual electrical stimulation. Neuroendocrinol. 35; 424-428.

Iovino, M., Poenari, S. and Annunziato, L. (1983). Basal and thirst-evoked vasopressin secretion in rats with electrolytic lesions of the medio-ventral septal area. Brain Res. 258:123-126.

Iovino, M. and Steardo, L. (1984). Vasopressin release of central and peripheral angiotensin II in rats with lesions of the subfornical organ. Brain Res. 322:365-368.

Ishida, A. (1967). The effect of tetrodotoxin on the calcium-dependent link in stimulus-secretion coupling in neurohyophysis. Jap. J. Physiol. 17:308-320.

Ishikawa, S.E., Saito, T. and Yoshida, S. (1980). The effect of osmotic pressure and angiotensin II on arginine vasopressin release from guinea pig hypothalamo- neurohypophyseal complex in organ culture. Endocrinol. 106:1571-1578.

Ishikawa, T. and Koizumi, K. (1975). A study of hypothalamic neurosecretory cells of bullfrogs in vitro. J. Physiol. 253:1-19.

Ishikawa, T., Koizumi, K., and Brooks, C. McC. (1966). Electrical activity recorded from the pituitary stalk of the cat. Am. J. Physiol. 210:427-431.

Ito, S., Iwanaga, T., Yui, R., Yamaguchi, K., Hanna, H., Kamoi, K., and Shibata, A. (1981). Presence of α-neo-endorphin-like immunoreactivity in the posterior lobe of the pituitary gland. Life Sci. 29:1457-1461.

Iversen, L.L. and Kelly, J.S. (1975). Uptake and metabolism of γ-aminobutyric acid by neurones and glial cells. Biochem. Pharm. 24:933-938.

Iversen, L.L., Iversen, S.D. and Bloom, F.E. (1981). Opiate receptors influence vasopressin release from nerve terminals in rat neurohypophysis. Nature 284:350-351.

Jhamandas, J.H. and Renaud, L.P. (1985). Influence of anteroventral third ventricle (AV3V) stimulation on the excitability of hypothalamic supraoptic neurosecretory neurons. Soc. Neurosci. Abstr., Vol. 11, Part 2, p. 1235.

Johnston, G.A.R., Kennedy, S.M.E., and Lodge, D. (1978). Muscimol uptake, release and binding in rat brain slices. J. Neurochemistry 31:1519-1523.

Jones, B.E., and Moore, R.Y. (1977). Ascending projections of the locus coeruleus in the rat. II Autoradiographic study. Brain Res. 127:23-53.

Kandel, E.R. (1964). Electrical properties of hypothalamic neuroendocrine cells. J. Gen. Physiol. 47; 691-717.

Kandel, E.R. (1976). Cellular basis of behaviour. W.H. Freeman and Company, San Francisco.

Kannan, H. and Yagi, K. (1978). Supraoptic neurosecretory neurons: evidence for the existence of converging inputs from carotid baroreceptors and osmoreceptors. Brain Res. 145:385-390.

Katz, B. and Miledi, R. (1967a). The timing of calcium action during neuromuscular transmission. J. Physiol. 189; 535-544.

Katz, B. and Miledi, R. (1967b). A study of synaptic transmission in the absence of nerve impulses. J. Physiol. 192; 407-436.

Katz, B. and Miledi, R. (1968). The role of calicum in neuromuscular facilitation . J. Physiol. 195; 481-492.

Keil, L.C. and Severs, W.B. (1976). Reduction in plasma vasopressin levels of dehydrated rats following acute stress. Endocrinology 100:30-38.

Kelly, J.S. and Dreifuss, J.J. (1970). Antidromic inhibition of identified rat supraoptic neurones. Brain Res. 22: 406-409.

Kent, C. and Williams, M.A. (1974). The nature of hypothalamo-neurohypophyseal neurosecretion in the rat. A study of light and electron microscope autoradiography. J. Cell Biol. 60:554-570.

Kimura, T., Share, L., Wang, B.C. and Crofton, J.T. (1981). The role of central adrenoreceptors in the control of vasopressin release and blood pressure. Endocrinology 108:1829-1836.

Knepel,W., Nutto, D., and Hertting, G. (1980). Evidence for the involvement of a GABA-mediated inhibition in the hypovolaemia-induced vasopressin release. Pflugers Arch. 388:177-183.

Knepel, W., Nutto, D. and Hertting, G. (1982). Evidence for inhibition by β-endorphin of vasopressin release during foot shock-induced stress in the rat. Neuroendocrinology 34:353-356.

Koizumi, K. and Yamashita, H. (1972). Studies of antidromically identified neurosecretory cells of the hypothalamus by intracellular and extracellular recordings. J. Physiol. 221; 683-705.

Koizumi, K. and Yamashita, H. (1978). Influence of atrial stretch receptors on hypothalamic neurosecretory neurones. J. Physiol. 285; 341-358.

Krnjevic, K. (1974). Chemical nature of synaptic transmission in vertebrates. Physiol. Rev. 54:518-540.

Krnjevic, K., Puil, E. and Werman, R. (1977). GABA and glycine actions on spinal motoneurons. Can. J. Physiol. Pharmacol. 55:658-669.

Krogsgaard-Larsen, D. and Johnston, G.A.R. (1975). Inhibition of GABA uptake in rat brain slices by nipicotic acid, various isoxazoles and related compounds. J. Neurochem. 25:797-802.

Krogsgaard-Larsen, P., Johnston, G.A.R., Curtis, D.R., Game, C.J.A., and McCullough, R.M. (1975). Structure and biological activity of a series of conformationally restrictd analogues of GABA. J. Neurochem. 25:803-809.

Kuhn, E.R. (1974). Cholinergic and adrenergic release mechanism for vasopressin in the male rat: A study with injections of neurotransmitters and blocking agents into the third ventricle. Neuroendocrinology 16:255-264.

Lafarga, M., Hervas, J.-P., Crespo, D. and Villegas, J. (1980). Ciliated neurons in supraoptic nucleus of rat hypothalamus during neonatal period. Anat. Embryol. 160:29-38.

Land, H., Grez, M., Ruppert, S., Schmale, H., Rebbein, M., Richter, D. and Schutz, G. (1983). Deduced amino acid sequence from the bovine oxytocin-Neurophysin I precursor cDNA. Nature 302:342-344.

Land, H., Schutz, G., Schmale, H., and Richter, D. (1982). Nucleotide sequence of cloned cDNA encoding bovine arginine vasopressin-neurophysin I precursor. Nature 295:299-303.

Lebrun, C.J., Poulain, D.A. and Theodosis, D.T. (1983). The role of the septum in the control of the milk ejection reflex in the rat: Effects of lesions and electrical stimulation. J. Physiol. 339:17-31.

Legendre, P., Cooke, I.M. and Vincent, J.D. (1982). Regenerative responses of long duration recorded intracellularly from dispersed cell cultures of fetal mouse hypothalamus. J. Neurophysiol. 48; 1121-1141.

Leng, G. (1980). Rat supraoptic neurones: The effects of locally applied hypertonic saline. J. Physiol. 304; 405-414.

Leng, G. and Dyball, R.E.J. (1983). Intercommunications in the rat supraoptic nucleus. Quant. J. Exp. Physiol. 68:493-504.

Leng, G. and Dyball, R.E.J. (1984). Recurrent inhibition: a recurring misinterpretation. Q. Jl. Exp. Physiol. 69:393-395.

Leontovich, T.A. (1969). The neurons of the magnocellular neurosecretory nuclei of the dog's hypothalamus. J. Hirnforsch. 11; 499-517.

Leranth, C., Zaborszky, L., Marton, J. and Palkovits, M. (1975). Quantitative studies on the supraoptic nucleus in the rat. I. Synaptic organization. Exptl. brain Res. 22; 509-523.

Lightman, S.L., Todd, K., and Everitt, B.J. (1984). Ascending noradrenergic projections from the brainstem: Evidence for a major role in the regulation of blood pressure and vasopressin secretion. Exp. Brain Res. 55:145-151.

Lincoln, D.W. and Wakerley, J.B. (1974). Electrophysiological evidence for the activation of supraoptic neurones during the release of oxytocin. J. Physio. 242; 533-554.

Lincoln, D.W. and Wakerley, J.B. (1975). Factors governing the periodic activation of supraoptic and paraventricular neurosecretory cells during suckling in the rat. J. Physiol. 250; 445-461.

Lind, R.W., Swanson, L.W. and Gauten, D. (1984). Angiotensin II immunoreactivity in the neural afferents and efferents of the subfornical organ of the rat. Brain Res. 321:209-215.

Lind, R.W., Van Hoesen, G.W. and Johnson, A.K. (1982). An HRP study of the connections of the subfornical organ of the rat. J. Comp. Physiol. 210:265-277.

Llinas, R., Baker, R. and Precht, W. (1974). Blockage of inhibition by ammonium acetate action on chloride pump in cat trochlear motorneurons. J. Neurophysiol. 37:522-533.

LuQui, U.J. and Fox, C.A. (1976). The supraoptic nucleus and the supra-opticohypophyseal tract in the monkey (Macaca mulatta). J. Com. Neurol. 168; 7-40.

Lux, H.D. (1971). Ammonium and chloride extrusion: Hyperpolarizing synaptic inhibition in spinal motoneurons. Science 173:555-557.

Lux, H.D., Loracher, C. and Neker, E. (1970). The action of ammonium on postsynaptic inhibition of cat spinal motoneurons. Exp. Brain Res. 11:431-447.

MacVicar, B.A., Andrew, R.D., Dudek, F.E. and Hatton, G.I. (1982). Synaptic inputs and action potentials of magnocellular neuropeptidergic cells: Intracellular recording and staining in slices of rat hypothalamus. Brain Res. Bull. 8: 87-93.

Mangiapane, M.L. Thrasher, T.N., Keil, L.C., Simpson, J.B., and Ganong, W.F. (1983). Deficits in drinking and vasopressin secretion after lesions of the nucleus medianus. Neuroendocrinology 37:73-77.

Martin, R., Geis, R., Holl, R., Schafer, M., and Voigt, K.H. (1983). Co-existence of unrelated peptides in oxytocin and vasopressin terminals of rat neurohypophysis: immunoreactive methionine^{5}-enkephalin-, leucine^{5}-enkephalin-, and cholecystokinin-like substances. Neuroscience 8:213-227.

Mason, W.T. (1980). Supraoptic neurones of rat hypothalamus are osmosensitive. Nature 287:154-157.

Mason, W.T. (1983a). Excitation of dopamine of putative oxtocinergic neurons in the rat supraoptic nucleus in vitro: Evidence for two classes of continuously firing neurons. Brain Res. 267:113-121.

Mason, W.T. (1983b). Electrical properties of neurons recorded from the rat supraoptic nucleus in vitro. Proc. R. Soc. Lond. 217: 141-161.

Mason, W.T., Ho, Y.W., Eckenstein, F. and Hatton, G.I. (1983). Mapping of cholinergic neurons associated with rat supraoptic nucleus: Combined immunocytochemical and histochemical identification. Brain Res. Bull. 11:617-626.

Mason, W.T., Ho, Y.W. and Hatton, G.I. (1984). Axon collaterals of supraoptic neurones: anatomical and electrophysiological evidence for their existence in the lateral hypothalamus. Neuroscience 11:169-182.

Mason, W.T., Ingram, C.D., Bicknell, R.J. and Waring, D.W. (1984). Intracellular recordings from normal pituitary cells: regulation of electrical events leading to hormone release by hypophysiotropic peptides. 7th Int. Congr. Endocrinol. Abstracts. Excerpta-Medica, Amsterdam. S-205.

Mathers, D.A. and Barker, J.L. (1980). (-) Pentobarbital opens ion channels of long duration in cultured mouse spinal neurons. Science 209:507-509.

Mathers, D.A. and Barker, J.L. (1981). GABA and muscimol open ion channels of different lifetimes on cultured mouse spinal cord cells. Brain Res. 204:242-247.

Matthews, G. and Wickelgren, W.O. (1979). Glycine, GABA and synaptic inhibition of reticulospinal neurons of lamprey. J. Physiol. 293:393-415.

McAfee, D.A. and Yarowsky, P.J. Calcium-dependent potentials in the mammalian sympathetic neurone. J. Physiol. 290:507-523.

McBurney, R.N. and Barker, J.L. (1978). GAGA-induced conductance fluctuations in cultured spinal neurones. Nature 274:596-597.

McKellar, S. and Loewy, A.D. (1982). Efferent projections of the A1 catecholamine cell group in the rat: An autoradiographic study. Brain Res. 241:11-29.

McNeill, T.H. and Sladek, J.R. (1980). Simultaneous monoamine histofluoresence and neuropeptide immunocytochemistry: "Correlative distribution of catecholamine varicosities and magnocellular neurosecretory neurons in the rat supraoptic and paraventricular nuclei". J. Comp. Neurol. 193:1023-1033.

Mendelsohn, J.A.O., Quirion, R., Saavedra, J.M., Aquilera, G., and Catt, K.J. (1984). Autoradiographic localization of angiotensin II receptors in rat brain. Proc. Natl. Acad. Sci. 81:1575-1579.

Meyer, D.K. and Brownstein, M.J. (1980). Effect of surgical deafferentation of the supraoptic nucleus on its choline acetyltransferase. Brain Res. 193:566-569.

Meyer, D.K., Oertel, W.H., and Brownstein, M.J. (1980). Deafferentation studies on the glutamic acid decarboxylase content of the supraoptic nucleus of the rat. Brain Res. 200:165-168.

Meyer, H. and Lux, H.D. (1974). Action of ammonium on a chloride pump. Pflugers Arch. 350:185-195.

Meyer, H. (1976). The different actions of chloride and potassium on postsynaptic inhibition of an isolated neurone. J. Exp. Biol. 64:477-487.

Miles, R., and Wong, R.K.S. (1984). Unitary inhibitory synaptic potentials in the guinea pig hippocampus in vitro. J. Physiol. 356:97-113.

Millan, M.J., Millan, M.H. and Herz, A. (1983). Contribution of the supraoptic nucleus to brain and pituitary pools of immunoreactive vasopressin and particular opioid peptides, and the interrelationships between these in the rat. Neuroendocrinology 36:310-319.

Miller, T.R., Handelman, W.A., Arnold, P.E., McDonald, K.M., Molinoff, P.B. and Schrier, R.W. (1979). Effect of central catecholamine depletion on the osmotic and nonosmotic stimulation of vasopressin (antidiuretic hormone) in the rat. J. Clin. Invest. 64:1599-1607.

Mills, E. and Wang, S.C. (1964a). Liberation of antidiuretic hormone: location of ascending pathways. Am. J. Physiol. 207:1399-1404.

Mills, E. and Wang, S.C. (1964b). Liberation of antidiuretic hormone: pharmacologic blockade of ascending pathways. Am. J. Physiol. 207:1405-1410.

Milton, A.S., and Paterson, A.T. (1973). Intracranial injections of 6-hydroxydopamine (6-OH-DA) in cats: effects on the release of antidiuretic hormone. Brain Res. 61:423-427.

Milton, A.S. and Paterson, A.T. (1974). A microinjection study of the control of antidiuretic hormone release by the supraoptic nucleus of the hypothalamus in the cat. J. Physiol. 241:607-628.

Mirsky, R.R., Stein, M., and Paulisch,G. (1954). The secretion of an antidiuretic substance into the circulation of rats exposed to noxious stimuli. Endocrinology 54:491-505.

Miselis, R.R., Shapiro, R.E. and Hand, P.J. (1979). Subfornical organ efferents to neural systems for control of body water. Science 205; 1022-1025.

Mohler, H. and Okada, T. (1978). Properties of γ-aminobutyric acid receptor-binding with (+)-[^{3}H]bicuculline methiodide in rat cerebellum. Mol. Pharmacol. 14:265-265.

Moos, F. and Richard, P. (1975). Role de la noradrenaline et de l'acetylcholine dans la liberation d'oxytocine induite par des stimulations vaginale, vagale et mammaire. J. Physiol. (Paris) 70:315-332.

Moos, F. and Richard, P. (1979). The inhibitory role of β-adrenergic receptors in oxytocin release during suckling. Brain Res. 169:595-599.

Moos, F. and Richard, P. (1979b). Effects of dopaminergic antagonists and agonists on oxytocin release induced by various stimuli. Neuroendocrinology 28:138-144.

Moss, R.L., Dyball, R.E.J., and Cross, B.A. (1971). Responses of antidromically identified supraoptic and paraventricular units to acetylcholine, noradrenaline and glutamate applied iontophoretically. Brain Res. 35:573-575.

Moss, R.L., Urban, I., and Cross, B.A. (1972). Microelectrophoresis of cholinergic and aminergic drugs on paraventricular neurons. Am. J. Physiol. 223:310-318.

Motokizawa, F., Reuben, J.P. and Grundfelt, H. (1969). Ionic permeability of the inhibitory postsynaptic membrane of lobster muscle fibers. J. Gen. Physiol. 54:437-461.

Murphy, A.D., Hadby, R.D., and Kater, S.B. (1983). Axotomy-induced parallel increases in electrical and dye-coupling between identified neurons of Helisoma. J. Neurosci. 3:1422-1429.

Nagai, T., McGeer, P.L. and McGeer, E.G. (1983). Distribution of GABA-T-intensive neurons in the rat forebrain and midbrain. J. Comp. Neurol. 218:220-238.

Negoro, H. and Holland, R.C. (1972). Inhibition of unit activity in the hypothalamic paraventricular nucleus following ahtidromic activation. Brain Res. 42: 385-402.

Negoro, H., Visessuwan, S. and Holland, R.C. (1973). Inhibition and excitation of units in paraventricular nucleus after stimulation of the septum, amygdala and neurohypophysis. Brain Res. 57:479-483.

Newberry, N.R. and R.A. Nicoll. (1985). Comparison of the action of baclofen with γ-aminobutyric acid on rat hippocampal cells in vitro. J. Physiol. 360:161-185.

Nicoll, R.A., Eccles, J.C., Oshima, T., and Rubia, F. (1975). Prolongation of hippocampal inhibitory postsynaptic potentials by barbiturates. Nature 258:625-627.

Nordmann, J.J. and Labouesse, J. (1981). Neurosecretory granules: evidence for an aging process within the neurohypophysis. Science 211:595-597.

Nordmann, J.J. (1976). Evidence for calcium inactivation during hormone release in the rat neurohypophysis. J. Expl. Biol. 65:669-683.

Nordmann, J.J. and Dreifuss, J.J. (1972). Hormone release evoked by electrical stimulation of rat neurohypophyses in the absence of action potentials. Brain Res. 45: 604-607.

Ogata, N. and Matsuo, T. (1984). Pharmacological characterization of the magnocellular neuroendocrine cells of the guinea pig supraoptic nucleus in vitro. J. Neuropharm. 23:1215-1218.

Okamoto, K., Kimura, H. and Sakai, Y. (1984). Miniature synaptic potentials recorded intracellularly from purkinje cell dendrites in guinea-pig cerebellar slices. Brain Res. 311:281-287.

Oldfield, D.J., Hou-Yu, A., and Silverman, A.-J. (1985). A combined electron microscopic HRP and immunocytochemical study of the limbic projections to rat hypothalamic nuclei containing vasopressin and oxytocin neurons. J. Comp. Neurol. 231:221-231.

Olsson, K. (1969). Studies on central regulation of secretion of antidiuretic hormone (ADH) in the goat. Acta. Physiol. Scand. 77:465-474.

Palade, G. (1975). Intracellular aspects of protein synthesis. Science 189:347-358.

Palay, S.L. (1961). Structural peculiarities of the neurosecretory cells in the preoptic nucleus of the goldfish, Carassius auratus. Anat. Rec. 139:263.

Palkovits, M., Brownstein, M.J. and Zamir, N. (1983). Immunoreactive dynorphin and α-neo-endorphin in rat hypothalamo-neurohypophyseal system. Brain Res. 278:258-261.

Panula, P., Renuelta, A.V., Cheney, D.L., Wu, J.-Y., and Casta, E. (1984). An immunohistochemical study on the location of GABAergic neurons in rat septum. J. Comp. Neurol. 222:69-80.

Perez de la Mora, M., Porrani, L.D., Tapia, R., Teran, L., Palacios, R., Fuxe, K., Hokfelt, T., and Ljungdahl, A. (1981). Demonstration of central γ-aminobutyrate-containing nerve terminals by means of antibodies against glutamate decarboxylase. Neuroscience 6:875-895.

Perlmutter, L.S., Tweedle, L.D., and Hatton, G.I. (1984). Neuronal/glial plasticity in the supraoptic dendritic zone: dendritic bundling and double synapse formation at parturition. Neuroscience 13:769-779.

Peterson, R. (1965). Synapses in the rat supraoptic nucleus. Anat. Rev. 151:399.

Pickering, B.T. (1978). The neurosecretory neurone: A model system for the study of secretion. Essays Biochem. 14:45-81.

Pickering, B.T. and Swann, R.W. (1983). Biosynthesis and processing of neurophypophysial hormones. Pharmacol. Ther. 22:143-161.

Piggott, S.M., Kerkut, G.A. and Walker, R.J. (1977). The actions of picrotoxin, strychnine, bicuculline and other convulsants and antagonists on the response to acetylcholine, glutamic acid and γ-aminobutyric acid on Helix neurones. Comp. Biochem. Physiol. 57C:107-116.

Pickles, H.G. (1979). Presynaptic γ-aminobutyric acid responses in the olfactory cortex. Br. J. Pharm. 65:223-228.

Pittman, Q.J., Hatton, J.D. and Bloom, F.E. (1981). Spontaneous activity in perfused hypothalamic slices: Dependence on calcium content of perfusate. Exp. Brain Res. 42:49-52.

Poulain, D.A., Ellendorff, F. and Vincent, J.D. (1980). Septal connections with identified oxytocin and vasopressin neurones in the supraoptic nucleus of the rat. An electrophysiological investigation. Neuroscience 5:379-387.

Poulain, D.A., Lebrun, L.J. and Vincent J.D. (1981). Electrophysiological evidence evidence for connections between septal neurones and the supraoptic nucleus of the hypothalamus of the rat. Exp. Br. Res. 42: 260-268.

Poulain, D.A. and Wakerley, J.B. (1982). Electrophysiology of hypothalamic magnocellular neurones secreting oxytocin and vasopressin. Neuroscience 7(4): 773-808.

Poulain, D.A., Wakerley, J.B. and Dyball (1977). Electrophysiological differentiation of oxytocin- and vasopressin-secreting neurones. Proc. R. Soc. B. 196: 367-384.

Powell, E.W. and Rorie, D.K. (1967). Septal projections to nuclei functioning in oxytocin release. Am. J. Anat. 120: 605-610.

Preston, R.J., Bishop, G.A., and Kitai, S.T. (1980). Medium spiny neuron projection from the rat striatum: an intracellular horseradish peroxidase study. Brain Res. 183:253-254.

Rall, W. (1959). Branching dendrite trees and motoneuron membrane resistivity. Expt. Neurol. 1:491-527.

Rall, W. (1960). Membrane potential transients and membrane time constant of motoneurons. Expt. Neurol. 2:503-532.

Rall, W. (1967). Distinguishing theoretical synaptic potentials computed for different soma-dendritic distribution of synaptic input. J. Neurophysiol. 30:1138-1168.

Randle, J.C.R., Bourque, C.W. and Renaud, L.P. (1984a). α-adrenergic activation of rat hypothalamic supraoptic neurons maintained in vitro. Brain Res. 307: 374-378.

Ranson, B.R. and Barker, J.L. (1976). Pentobarbital selectively enhances GABA-mediated post-synaptic inhibition in tissue cultured mouse spinal neurons. Brain Res. 114: 530-535.

Reaves, T.A., Cumming, R., Libber, M.T. and Hayward, J.N. (1982). A technique combining intracellular dye-marking immunocytochemical identification and ultrastructural analysis of physiologically identified single neurons. Neurosci. Letts. 29:195-199.

Reaves, T.A., Hou-yu, A, Zimmerman, E.A. and Hayward, J.N. (1983). Supraoptic neurons in the rat hypothalamo-neurohypophysial explant: double-labelling with Lucifer yellow injection and immunocytochemical identification of vasopressin-and neurophysin-containing neuroendocrine cells. Neurosci. Letts.37:137-142.

Reaves, T.A., Hou-yu, A, Zimmerman, E.A. and Hayward, J.N. (1983). Supraoptic neurons in the rat hypothalamo-neurohypophysial explant: double-labelling with Lucifer yellow injection and immunocytochemical identification of vasopressin-and neurophysin-containing neuroendocrine cells. Neurosci. Letts.37:137-142.

Rechardt, L. (1969). Electron microscopic and histochemical observations on the supraoptic nucleus of normal and dehydrated rats. Acta Physiol. Scand. Suppl. 329: 1-79.

Reis, D.J., Granata, A.R., Joh, T.H., Ross, C.A., Ruggiero, D.A., and Park, D.H. (1984). Brainstem catecholamine mechanisms in tonic and reflex control of blood pressure. Hypertension 6:7-15.

Renaud, L.P. (1983). Role of neuropeptides in the regulation of neural excitability. In: Basic Mechanisms of Neuronal Hyperexcitability. A.R.Liss, Inc., New York, p.323-360.

Renaud, L.P., Bourque, C.W., Day, T.A., Ferguson, A.V. and Randle, J.C.R. (1984). Electrophysiology of mammalian hypothalamic supraoptic and paraventricular neurosecretory cells. In: The Electrophysiology of the secretory cell. A.M. Poisner and J. Trifaro, eds. Elsevier. Amsterdam.

Renaud, L.P., Day, T.A., Randle, J.C.R. and Bourque, C.W. (1985). In-vivo and in-vitro electrophysiological evidence that central noradrenergic pathways enhance the activity of hypothalamic vasopressinergic cells. In: Water Balance and Antidiuretic Hormone. R. Schier, ed., Raven Press, New York. (In press).

Renaud, L.P., Rogers J. and Sgro, S. (1983) Terminal degeneration in supraoptic nucleus following subfornical organ lesions: ultrastructural observations in the rat. Brain Res. 275:365-368.

Rogawski, M.A. (1985). The A-current: how ubiquitous a feature of excitable cells is it? Trends in Neuroscience, p.214-219.

Sachs, H. and Haller E.W. (1968). Further studies on the capacity of the neurohypophysis to release vasopressin. Endocrinology 83:251-262.

Sachs, H., Fawcett, P, Takabatake, Y. and Portanova, R. (1969). Biosynthesis and release of vasopressin and neurophysin. Rec. Prog. Horm. Res. 25; 447-491.

Sachs, H., Share, L., Sinchak, O. and Carpi, A. (1967). capacity of the neurohypophysis to release vasopressin. Endocrinology 81:755-770.

Sakai, K.K., Marks, B.H., George, J.M. and Koestner, A. (1974). The isolated organ-cultured supra-optic nucleus as a neuropharmacological test system. J. Pharm. Exp. Therap. 190:482-491.

Salzberg, B.M., Obaid, A.L., Senseman, D.M. and Gainer, H. (1983). Optical recording of action potentials from vertebrate nerve terminals using potentiometric probes provides evidence for sodium and calcium components. Nature 306:36-40.

Saper, C.B. and Loewy, A.D. (1980). Efferent connections of the parabrachial nucleus in the rat. Brain Res. 197: 291-317.

Sawchenko, P.E. and Swanson, L.W. (1982). The organization of noradrenergic pathways from the brainstem to the paraventricular and supraoptic nuclei in the rat. Brain Res. Rev. 4:275-325.

Sawchenko, P.E., Swanson, L.W. and Vale, W.W. (1984). Corticotropin releasing factor co-expression within distinct subsets of oxytocin-, vasopressin-, and neurotensin-immunoreactive neurons in the hypothalamus of the male rat. Brain Res. (In press).

Scharrer, E. (1962). Electron microscopy of neurosecretory cells in the preoptic nucleus of the toadfish (Opsanus tau). Biol. Bull. 123: 461-462.

Scholfield, C.N. (1978a). A depolarizing inhibitory potential in neurones of the olfactory cortex in vitro. J. Physiol. 275: 547-447.

Scholfield, C.N. (1978b). A barbiturate induced intensification of the inhibitory potential in slices of guinea-pig olfactory cortex. J. Physiol. 275: 559-566.

Scholfield, C.N. (1980). Convulsants antagonize inhibition in the olfactory cortex slice. Naunyn-Shmiedelberg's Arch Pharmacol. 314:29-36.

Scholfield, C.N. (1982). Antagonism of α-aminobutyric acid and muscimol by picrotoxin, bicuculline, strychnine, bemigride, leptazol, D-tubocurarine and theophylline in the isolated olfactory cortex. Naunyn-Shmiedelberg's Arch Pharmacol. 318:274-280.

Sgro, S., Ferguson, A.V. and Renaud, L.P. (1984). Subfornical organ-supraoptic nucleus connections: An electrophysiologic study in the rat. Brain Res. 303: 7-13.

Share, L. (1962). Vascular volume and blood level of antidiuretic hormone. Am. J. Physiol. 202: 791-794.

Share, L. and Levy, M.N. (1962) Cardiovascular receptors and blood titer of antidiuretic hormone. Am. J. Physiol. 203:425-428.

Sherlock, D.A., Field, P.M. and Raisman, G. (1975). Retrograde transport of horseradish peroxidase in the magnocellular neurosecretory system of the rat. Brain Res. 88:403-414.

Shibuki, K. (1984). Supraoptic neurosecretory cells: synaptic inputs from the nucleus accumbeus in the rat. Exp. Brain Res. 53:341-348.

Silverman, A.J. and Zimmerman, E.A. (1983). Magnocellular neurosecretory system. Ann. Rev. Neurosci. 6; 357-380.

Silverman, A.J., Goldstein, R. and Gadde, C.A. (1980). The ontogenesis of neurophysin-containing neurons in the mouse hypothalamus. Peptides 1 (Suppl.1): 27-44.

Simmonds, M.A. (1980). Evidence that bicuculline and picrotoxin act at separate sites to antagonize α-aminobutyric acid in rat cuneate nucleus. Neuropharmacology 19:39-45.

Sladek, C.D. and Johnson, A.K. (1983). Effect of anteroventral third ventricle lesions on vasopressin release by organ-cultured hypothalamoneurohypophyseal explants. Neuroendo. 37:78-84.

Sladek, C.D. and Knigge, K.M. (1977a). Cholinergic stimulation of vasopressin release from the rat hypothalamo-neurohypophyseal system in organ culture. Endocrinol. 101:411-420.

Sladek C.S. and Knigge K.M. (1977b). Osmotic control of vasopressin release by rat hypothalamo-neurohypophyseal explants in organ culture. Endocrinology 101: 1834-1838.

Snodgrass, S.R. (1978). Use of ^{3}H-muscimol for GABA receptor studies. Nature 273:392-394.

Sofroniew, M.V .and Glasmann, W. (1981). Golgi-like immunoperoxidase staining of hypothalamic magnocellular neurons that contain vasopressin, oxytocin or neurophysin in the rat. Neuroscience 6:619-643.

Sokol, H.W., Zimmerman, E.A., Sawyer, W.H. and Robinson, A.G. (1976). The hypothalamo-neurohypophyseal system system of the rat: Localization and quantification of neurophysin by light microscopic immunocytochemistry in normal rat and in Brattleboro rats deficient in vasopressin and a neurophysin. Endocrinology 98: 1176-1188.

Stewart, W.W. (1978). Functional connections between cells as revealed by dye-coupling with a highly fluorescent naphthalimide tracer. Cell 14:741-759.

Stutinsky, F. (1974). Morphological and physiological reactions of the supraoptic and paraventricular nuclei. from: Neurosecretion- The Final Neuroendocrine Pathway. F. Knowles and L. Vollrath 9eds.), VI International Symposium on Neurosecretion, London, (1973); Springer-Verlag, New York (1974); p. 15-23.

Swaab, D.F., Nijveldt, F. and Pool, C.W. (1975a). Distribution of oxytocin and vasopressin in the rat supraoptic and paraventricular nucleus. J. Endocrinology 67: 461.

Swanson, L.W., Sawchenko, P.E., Berod, A., Hartman, B.K., Helle, K.B. and Van Orden, D.E. (1981). An immunohistochemical study of the organization of catecholaminergic cells and terminal fields in the paraventricular and supraoptic nuclei of the hypothalamus. J. Comp. Neurol. 196:271-285.

Swaab, D.F., Pool, C.W. and Nijveldt, F. (1975b). Immunofluorescence of vasopressin and oxytocin in the rat hypothalamo-neurohypophyseal system. J. Neural Transm. 36: 195-215.

Swanson, L.W. and Sawchenko, P.E. (1980). Paraventricular nucleus: A site for the integration of neuroendocrine and autonomic mechanisms. Neuroendocrinol. 31: 410-417.

Swanson, L.W. and Sawchenko, P.E. (1983). Hypothalamic integration: Organization of the paraventricular and supraoptic nuclei. Ann. Rev. Neurosci. 6; 269-324.

Takeuchi, A. and Takeuchi N. (1965). Localized action of gamma-aminobutyric acid on the crayfish muscle. J. Physiol. 177:225-238.

Takeuchi A. and Takeuchi, N. (1967). Anion permeability of the inhibitory post-synaptic membrane of the crayfish neuromuscular junction. J. Physiol. 191:575-590.

Taleisnik, S. and Deis, R.P. (1964). Influence of cerebral cortex in inhibition of oxytocin release induced by stressful stimuli. Am. J. Physio. 207: 1394-1398.

Tappaz, M.L., Brownstein M.J. and Kopin, I.J. (1977). Glutamate decarboxylase (GAP) and α-aminobutyric acid (GABA) in discrete nuclei of hypothalamus and substantia nigra. Brain Res. 125: 109-121.

Tappaz, M.L., Oertel, W.H., Wassef, M. and Mugnaivi, E. (1982). Central GABAergic neuroendocrine regulations: Pharmacological and morphological evidence. Prog. Br. Res. In: Chemical Transmission in the Brain; Buijs, Peret and Swaab (eds). Elsevier, New York. p. 77-96.

Theodosis, D.T. (1985). Oxytocin-immunoreactive terminals synpase on oxytocin neurones in the supraoptic nucleus. Nature 313:682-684.

Theodosis, D.T., Legendre, P., Vincent, J.D. and Cooke, I. (1983). Immunocytochemically identified vasopressin neurons in culture show slow calcium-dependent electrical responses. Science 221:1052-1054.

Thomas, R.C. and Wilson, V.J. (1966). Marking single neurons by staining with intracellular recording microelectrodes. Science 151:1538-1539.

Thompson, A.M. (1982). Responses of supraoptic neurones to electrical stimulation of the medial amygdaloid nucleus. Neuroscience 7:2197-2205.

Thorn, N.A. (1966). In vitro studies of the release mechanism for vasopressin in rats. Acta Endo 53: 644-654.

Thorn, N.A., Russell, J.T. and Vilhardt, H. (1975). Hexosamine, calcium, and neurophysin in secretory granules and the role of calcium in hormone release. Ann. N. Y. Acad. Sci. 248: 202-217.

Thorton, S.N., deBeaurepaire, R., and Nicolaidis, S. (1984). Electrophysiological investigation of cells in the region of the anterior hypothalamus firing in relation to blood pressure and volaemic changes. Brain Res. 299: 1-7.

Tribollet, E., Clake, G., Dreifuss, H. and Lincoln, D.W. (1978). The role of central adrenergic receptors in the reflex release of oxytocin. Brain Res. 142: 69-84.

Tribollet, E., Armstrong, W.E., Dubois-Dauphin, M. Dreius, H. (1985). Extrahypothalamic afferent inputs to the supraoptic nucleus area of the rat as determined by retrograde and anterograde tracing techniques. Neuroscience 15: 135-148.

Urano, A. and Kobayashi, H. (1978). Effects of noradrenaline and dopamine injected into the supraoptic nucleus on urine flow rate in hydrated rats. Exp. Neurol. 60: 140-150.

Vandeputte-Van Messon, G and Peeters, G. (1974). Effects of intraventricular administration of cholinergic drugs on water diuresis in goats. Arch. Int. Pharmacodyn. 211: 80-98.

Vandeputte-Van Messon, G. and Peeters, G. (1975). Effect of intraventricular administration of noradrenaline on water diuresis in goats. J. Endo. 66: 375-383.

Vandeputte-Van Messon, G. and Peeters, G. (1976). Effect of isoproterenol on urinary function in goats. Arch Int. Pharmocodyn. 220:346-347.

Vander Maelen, C.P. and Aghajanian, G.K. (1980). Intracellular studies showing modulation of facial motoneurone excitability by serotonin. Nature 287: 340-341.

Vandesande, F. and Dierickx, K. (1975). Identification of the vasopressin producing and of the oxytocin producing neurons in the hypothalamic neurosecretory system of the rat. Cell. Tiss. Res. 164:153-162.

Vigh-Teichmann, I., Vigh, B. and Aros, B. (1976a). Cerebrospinal fluid-containing neurons, ciliated perikarya and "peptidergic" synapses in the magnocellular preoptic nucleus of teleostean fishes. Cell Tiss. Res. 165:397-413.

Vigh-Teichmann, I., Vigh, B. and Aros, B. (1976b). Ciliated neurons and different types of synapses in anterior hypothalamic nuclei of reptiles. Cell. Tiss. Res. 174:138-160.

Vincent, J.D. and Dufy, B. (1982). Electrophysiological correlates of secretion in endocrine cells. In: Cellular regulation of secretion and release. Acad. Press. p. 107-145.

Wakerley, J.B. and Lincoln, D.W. (1971). Phasic discharge of antidromically identified units in the paraventricular nucleus of the hypothalamus. Brain Res. 25:192-194.

Wakerley, J.B. and Lincoln, D.W. (1973). The milk ejection reflex of the rat: a 20 to 40 fold acceleration in the firing of paraventricular neurones during oxytocin release. J. Endocrinol. 57: 477-493.

Wakerley, J.B. and Noble, R. (1983). Extrinsic control of phasic supraoptic neurones in vitro: burst initiation and termination following brief changes in excitatory drive. Neurosci. Letts. 42: 329-334.

Wakerley, J.B., Noble, R. and Clarke, G. (1983). In vitro studies of the control of pasic discharge in neurosecretory cells of the supraoptic nucleus. The Neurohypophysis: Structure, Function and Control. Prog. Brain Res. 60:53-59.

Wakerley, J.B., Poulain, D.A. and Brown, D. (1978). Comparison of firing patterns in oxytocin and vasopressin-releasing neurones during progressive dehydration. Brain Res. 148:425-440.

Wakerley, J.B., Poulain, D.A., Dyball, R.E.J. and Cross, B.A. (1975). Activity of phasic neurosecretory cells during haemorrhage. Nature 258:82-84.

Ward, D.G., Lefcourt, A.M. and Gann, D.S. (1980). neurons in the dorsal rostral pons process informatoin about changes in venous return and in arterial pressure. Brain Res. 181:75-88.

Watkins, W.B. (1976). Immunocytochemical study of the hypothalamo-neurohypophyseal system. I: Localization of neurosecretory neurons containing neurophysin I and neurophysin II in the domestic pig. Cell Tiss Res. 175:165-181.

Watson, S.J., Akil, H., Fischli, W., Goldstein, A., Zimmerman, E., Nilaver, G., Van Wimersma Greidanus, T.B. (1982). Dynorphin and vasopressin: common localization in magnocellular neurons. Science 216:85-87.

Watson, S.J., Khachaturian, H., Akil, H., Coy, D.H., and Goldstein, A. (1982). Comparison of the distribution of dynorphin systems and enkephalin systems in brain. Science 218:1134-1136.

Weber, E., Roth, K.A., Evans, C.J., Chang, J.K., and Barchas, J.D. (1982). Immunohistochemical localization of dynorphin (1-8) in hypothalamic magnocellular neurons: evidence for absence of pro-enkephalin. Life Sci. 31:1761-1764.

Werman, R. (1966). Criteria for identification of a central nervous system transmitter. Comp. Biochem. Physiol. 18:745-766.

Williams, J.T. and North, R.A. (1984). Catecholamine inhibition of calcium action potentials in rat locus coeruleus neurons. Neuroscience 14:103-109.

Williams, M. and Risley, E.A. (1979). Characterization nof the binding of [^{3}H] muscimol, a potent α-aminobutyric acid agonist, to rat brain synaptosomal membranes using a filtration assay. J. Neurochem. 32:713-718.

Williford, D.J., Di Micco, J.A. and Gillis, R.A. (1980). Evidence for the presence of a tonically active forebrain GABA system influencing central sympathetic outflow in the cat. Neuropharm. 19:245-250.

Willoughby, J.O., Jervois, P.M., Menalue, M.F. and Blessing, W.W. (1985). Stimulation of alpha-adrenoreceptors in the supraoptic nucleus elevates plasma vasopressin in the unanesthetized rat. Proc. Australian Neurosci. Soc. February 1985.

Woods, W.H., Holland, R.C. and Powell, E.W. (1969). Connections of cerebral structures functioning in neurohypophyseal hormone release. Brain Res. 12: 26-46.

Yagi, K., Azuma, T. and Matsuda, K. (1966). Neurosecretory cell: Capable of conducting impulse in rats. Science 154:778-779.

Yamamoto, C. and McIlwain, H. (1966). Electrical activities in thin sections from the mammalian brain maintained in chemically defined media in vitro. J. Neurochem. 13: 1333-13443.

Yamashita, H. (1977) Effectc of baro- and chemoreceptor activation on supraoptic nuclei neurons in the hypothalamus. Brain Res. 126:551-556.

Yamashita, H. and Kannan, H. (1976). Interaction of osmotic and neural stimuli on neurosecretory cells of supraoptic nuclei (SON) of the hypothalamus. The Physiologist 19: 418.

Yamashita, H. and Koizumi, K. (1979). Influence of carotid and aortic baroreceptors on neurosecretory neurons in supraoptic nuclei. Brain Res. 170: 259-277.

Yamashita, H., Inenaga, K., Kawata, M. and Sano, Y. (1983). Phasically firing neurons in the supraoptic nucleus of the rat hypothalamus: immunocytochemical and electrophysiological studies. Neurosci. Lett. 37: 87-92.

Yamashita, H., Koizumi, K. and McBrooks, C. (1970). Electrophysiological studies of neurosecretory cells in the cat hypothalamus. Brain Res. 20: 462-466.

Yulis, C.R., Peruzzo, B. and Rodriguez, E.M. (1984). Immunocytochemistry and ultrastructure of the neuropil located ventral to the rat supraoptic nucleus. Cell Tiss. Res. 236:171-180.

Zaborsky, L., Leranth, C., Makara, G.B. and Palkovits, M. (1975). Quantitative studies on the supraoptic nucleus in the rat. II. Afferent fiber connections. Exp. Brain Res. 22:525-540.